La protéine de stress Hsp27 / HspB1, une cible de choix en thérapie anti-cancéreuse

Benjamin Gibert

N° d'ordre 70-2010 Année 2010

THESE

Présentée devant l'UNIVERSITE CLAUDE BERNARD LYON 1

Pour l'obtention du

DIPLOME DE DOCTORAT

(Arrêté du 7 août 2006)

Présentée et soutenue publiquement le 25 mai 2010

Par **Benjamin GIBERT**

La protéine de stress Hsp27/HspB1, une cible de choix en thérapie anti-cancéreuse

JURY

Pr André-Patrick ARRIGO
Dr Chantal DIAZ
Dr Carmen GARRIDO
Pr Germain GILLET
Dr Patrick MEHLEN
Pr Michel MORANGE

UNIVERSITE CLAUDE BERNARD - LYON 1

Président de l'Université	**M. le Professeur L. Collet**
Vice-président du Conseil Scientifique	M. le Professeur J-F. Mornex
Vice-président du Conseil d'Administration	M. le Professeur G. Annat
Vice-président du Conseil des Etudes et de la Vie Universitaire	M. le Professeur D. Simon
Secrétaire Général	M. G. Gay

COMPOSANTES SANTE

Faculté de Médecine Lyon Est – Claude Bernard	Directeur : M. le Professeur J. Etienne
Faculté de Médecine Lyon Sud – Charles Mérieux	Directeur : M. le Professeur F-N. Gilly
UFR d'Odontologie	Directeur : M. le Professeur D. Bourgeois
Institut des Sciences Pharmaceutiques et Biologiques	Directeur : M. le Professeur F. Locher
Institut des Sciences et Techniques de Réadaptation	Directeur : M. le Professeur Y. Matillon
Département de Formation et Centre de Recherche en Biologie Humaine	Directeur : M. le Professeur P. Farge

COMPOSANTES SCIENCES ET TECHNOLOGIE

Faculté des Sciences et Technologies	Directeur : M. Le Professeur F. Gieres
UFR Sciences et Techniques des Activités Physiques et Sportives	Directeur : M. C. Collignon
Observatoire de Lyon	Directeur : M. B. Guiderdoni
Institut des Sciences et des Techniques de l'Ingénieur de Lyon	Directeur : M. le Professeur J. Lieto
Institut Universitaire de Technologie A	Directeur : M. le Professeur C. Coulet
Institut Universitaire de Technologie B	Directeur : M. le Professeur R. Lamartine
Institut de Science Financière et d'Assurance	Directeur : M. le Professeur J-C. Augros
Institut Universitaire de Formation des Maîtres	Directeur : M R. Bernard

REMERCIEMENTS

REMERCIEMENTS :

Je remercie les membres de mon jury d'avoir accepté d'évaluer ces travaux de thèse.

Je remercie l'ensemble du CGMC pour l'ambiance chaleureuse qui y règne. Je remercie plus particulièrement les membres de mon équipe, nouveaux comme anciens, avec qui j'ai pu avoir beaucoup d'interactions aussi bien professionnelles que personnelles.

Je remercie tous mes amis qui m'ont permis de vivre dans la bonne humeur ce qui n'a pas forcement permis d'optmimiser ma carrière professionnelle.

Je remercie plus particulièrement mes parents, mon frère et ma famille qui m'ont toujours apporté un soutien sans faille lors de mes études ou en dehors...

SOMMAIRE

SOMMAIRE

LISTE DES ABREVIATIONS

ABREVIATIONS :

17AAG: 17- AllylAmino-17-demethoxyGeldanamycin

ADN : Acide DésoxyriboNucléique

ADP: Adénosine Di-Phosphate

AIF: Apoptosis Inducing Factor

AMPc: Adénosine Mono-Phosphate Cyclique

ANT: Adenine Nucléotide Translocator

Apaf-1: Apoptotic Protease Activating Factor 1

APC: Antigen Presenting Cell

ARN: Acide RiboNucléique

ARNm: Acide RiboNucléique Messager

ASK1: Apoptosis signal-regulating kinase 1

ATG: Autophagy related genes

ATP: Adénosine Tri-Phosphate

Bag-1: Bcl2-associated athanogene 1 protein

Bcl2: B-cell lymphoma 2

BSA: Bovine Serum Albumin

Cdc37: Cell division control protein 37

Cdk-4: Cyclin dependant kinase 4

CHIP: Carboxy terminus of Hsc70 Interacting Protein

CMA: Chaperone Mediated Autophagy

CMH: Complex Majeur d'Histocompatibilité

DAPK: Death-Associated Protein Kinase

Daxx: Dead domain Associated protein 6

DAPI: 4'-6' DiAmino-2-PhénylIndole

DD: Death Domain

DED: Death Effector Domain

DISC: Death Inducing Signaling Complex

FANCC: Fanconi ANemia Complementation group C gene product

FasL: Fas Ligand

Grp78/75: Glucose related protein 78 and 75

G6P: Glucose 6-Phosphate

G6PDH: Glucose-6-Phosphate Deshydrogenase

GFAP: Glial Fibrillary Acidic Protein

GFP: Green Fluorescent Protein

Gy: Gray

HDAC 6: Histone Deacethylase 6

HIF-1: Hypoxia-Inducible Factor-1

Hsc70: Heat Shock Cognate 70

HSE: Heat Shock Element

HSF: Heat Shock Factor

HSP: Heat Shock Protein

HSR1: Heat Shock RNA-1

IL: Interleukin

IRF-1: Interferon Regulatory Factor 1

MAPK: Mitogen-Activated Protein Kinase

MAPKAPK2: Mitogen-Activated Protein Kinase-Activated Protein Kinase 2

Mdm2: Double Minute 2 protein

MK2 : seconde nomenclature de la MAPKAPK2

MMP9 : Matrix MetalloProteinases 9

Msp : Microtubule associated mini-spindles

mTOR: mamalian Target Of Rapamycin

NF-κB: Nuclear Factor κB

NK: Natural Killer

PA: Peptide Aptamer

PBS: Phosphate Buffer Saline

PCR: Polymerase Chain Reaction

PKB: Protein Kinase B

PP2A: Protein Phosphatase 2A

p53: protein 53

RLO: Radicaux Libres Oxygénés

RIP-1: Receptor Interacting Protein-1

SDS- PAGE: Sodium Dodecyl Sulfate PolyAcrylamide Gel Electrophoresis

sHsp: small Heat Shock Protein

shRNA: small hairpin RNA

siRNA: small interfering RNA

SMN: Survival Motor Neuron

STAT: Signal Transducers and Activators of Transcription

TAK1: TGFbeta Activated Kinase 1

TCP-1: T Complexe Polypeptide 1

TRX: Thioredoxine

TAP: Transporters Associated with Antigen Processing

TLR: Toll Like Receptor

TNFα: Tumor Necrosis Factor α

TUNEL: TdT-mediated dUTP Nick End Labelling

TRAIL: Tumor Necrosis Factor-Related Apoptosis- Inducing Ligand

ODFP : sperm Outer Dense Fiber Protein

VDAC : Voltage Dependent Anion Channel

RESUME

ECOLE DOCTORALE BMIC

Centre de Génétique Moléculaire et Cellulaire
UMR5534
Bât Mendel
16, Rue Dubois
69622 Villeurbanne

RESUME : La protéine de stress Hsp27/HspB1, une cible de choix en thérapie anti-cancéreuse

Hsp27 appartient à la famille des protéines dites de survie comme Bcl2 ou la survivine. C'est une protéine anti-apoptotique qui subit une dérégulation de son expression dans de nombreux types tumoraux. Elle est caractérisée comme étant une cible thérapeutique majeure. Au cours de ma thèse, j'ai isolé des peptides stabilisés, dit aptamères, capables d'inhiber fonctionnellement les activités anti-apoptotiques et tumorigènes d'Hsp27. Ces aptamères perturbent la biochimie structurale de Hsp27 et induisent le blocage du cycle cellulaire *in vivo*. Parallèlement à cette étude, j'ai caractérisé les effets de la déplétion de Hsp27 sur la formation de métastases et de tumeurs osseuses. J'ai aussi montré que la modification du taux de Hsp27 induisait la dégradation de différentes protéines, dites clientes, comme la caspase3, HDAC6 et STAT2.

ABSTRACT: The stress protein HSP27/HspB1, a well therapeutic target in cancer therapies

Hsp27 belongs to the class of survival proteins like Bcl2 or survivin. This protein was well categorized as a major anti apoptotic protein as displaying a high level of expression in lot of tumor types. Moreover, Hsp27 is referenced as a major therapeutic target in cancer. During my PhD, I characterized stable peptides called aptamers, which functionally blocked Hsp27 antiapoptotic and tumorigenic properties. These aptamers disrupted biochemical and structural states of Hsp27 and promoted cell cycle arrest in xenografts. In the same time, I have characterized the effect of Hsp27 depletion in metastasis establishment and bone marrow tumor growth. I have shown that targeting level of Hsp27 induced degradation of several of its client proteins like caspase3, HDAC6 and STAT2.

INTRODUCTION BIBLIOGRAPHIQUE

INTRODUCTION GENERALE :

La cancérisation apparaît comme un processus multifactoriel et pluri-étapes. Depuis la première altération de la cellule, jusqu'à l'invasion de l'organisme, une multitude de protagonistes de la cancérisation vont se distinguer. La caractérisation de ces protagonistes peut permettre d'augmenter les connaissances fondamentales, mais aussi de cibler plus spécifiquement des facteurs récurrents de la cancérisation et ainsi élargir le champ des perspectives thérapeutiques.

L'agressivité tumorale est caractérisée par une résistance aux différents traitements anticancéreux connus, et apparaît comme un élément important de la prolifération cancéreuse. En levant cette résistance, il semble possible de perturber le développement cancéreux voire de l'inhiber.

Les protéines de choc thermique (Heat shock proteins) jouent dans leur grande majorité un rôle cytoprotecteur (Lindquist et Craig, 1986). Dans des conditions physiologiques normales, les Hsp protègent les cellules contre différents types de stress et permettent de ce fait, à l'organisme, de survivre dans des conditions défavorables. Dans le cas d'une cellule cancéreuse, la présence des Hsp, en protégeant la cellule, favoriserait l'échappement tumoral en permettant sa survie malgré les différents traitements utilisés en cancérologie (Ciocca et Calderwood, 2005). Cette hypothèse expliquerait pourquoi les Hsp s'accumulent souvent au cours des différents stades de tumorigenèse, et pourquoi leur expression devient constitutive dans de nombreux carcinomes. Les Hsp participeraient à l'agressivité tumorale et leur inhibition pourrait donc être bénéfique pour de futurs traitements. Il semble ainsi acquis que les Hsp sont des cibles thérapeutiques majeures en cancérologie. On peut cependant se demander si la forte expression des Hsp est une cause ou une conséquence de la cancérisation.

Au cours de ma thèse, j'ai analysé et de caractérisé les effets du ciblage de la petite protéine de stress Hsp27/HspB1 par différentes techniques conduisant soit à son inhibition fonctionnelle soit à l'inhibition de sa synthèse. J'ai ainsi montré que le ciblage d'Hsp27 permettait de sensibiliser des cellules cancéreuses à différents traitements chimio et radio-thérapeutiques à la fois sur des lignées tumorales conservées en laboratoire mais aussi sur des xénogreffes réalisées chez la souris. Par ailleurs, j'ai montré que la déplétion de Hsp27 entrainait la dégradation de plusieurs de ses protéines interactrices dites clientes qui jouent des rôles pivots dans la prolifération et l'apoptose des cellules cancéreuses.

A-PRESENTATION DES PROTEINES DE CHOC THERMIQUE :

A-1. Les protéines de stress, des protéines ubiquistes et universelles

Les protéines de choc thermique ont été décrites comme une classe de protéines subissant une modification de leur niveau d'expression en réponse à différents changements néfastes de l'environnement générant un stress cellulaire : choc thermique, carences nutritives, infections virales, agents chimiques divers (Lindquist et Craig, 1988). Cette réponse est qualifiée d'universelle car elle est présente chez les bactéries, les végétaux et les eucaryotes supérieurs. Les protéines de stress sont classées en deux groupes distincts suivant leur poids moléculaire: les petites Hsp ou sHsp et les grandes de poids moléculaire supérieur à 40kDa (Table 1).

Elles sont dans tout les cas des protéines ubiquistes majoritairement impliquées dans la régulation de l'homéostasie cellulaire, la conformation et la dégradation protéique.

A-1.1. Les Hsp de haut poids moléculaire

Le groupe des Hsp de haut poids moléculaire contient 5 familles classées en fonction de leur poids moléculaire, de leur localisation sub-cellulaire ainsi que de leur homologie de séquence protéique (Table 1).

A-1.1.1. Hsp110

Chez les mammifères, deux Hsp composent cette famille: Hsp105 et Hsp110. Ils possèdent des caractéristiques structurales très proches de celle des membres de la famille Hsp70, avec un domaine capable de lier et d'hydrolyser l'ATP.

Chez la souris l'expression des Hsp110 est très importante dans le cerveau mais est constitutive dans tous les tissus de l'organisme (Lee-Yoon, 1995). Son expression est fortement inductible lors d'un stress thermique et elle est par exemple transloquée dans le nucléole où elle va participer à la protection de l'assemblage des ribosomes lors d'un stress thermique. Elle est ainsi fortement impliquée dans la résistance à l'hyperthermie et agit comme chaperon moléculaire en agissant de concert avec d'autres Hsp (Oh *et al.*, 1997).

Famille	Membres	Poids moléculaire
sHsp	HspB1 (Hsp27) HspB2 HspB3 HspB4 (αA-cristalline) HspB5 (αB-cristalline) HspB6 (Hsp20) HspB7 (cvHsp) HspB8 (Hsp22) HspB9 HspB10 (ODF)	De 12 à 43 kDa
Hsp47	Hsp47	47 kDa
Chaperonine	Hsp60	60 kDa
Hsp70	Hsc70 (Hsp73) Hsc70-t (Hsp70-hom) Hsp70.1 Hsp70.2 Hsp70.3 mtHsp70 (Grp75; mortalin) Bip (Grp78)	De 66 à 78 kDa
Hsp90	Hsp90α (Hsp86) Hsp90β (Hsp84) Grp94 TRAP1	De 83 à 90 kDa
Hsp110	Hsp105 Hsp110	De 100 à 110 kDa

Table 1: *Les familles de protéines de choc thermique humaines*

A-1.1.2 Hsp90

Les Hsp les plus étudiées chez l'homme sont les deux isoformes Hsp90α et β. Ce sont les Hsp constitutives les plus abondantes dans les cellules de mammifères qui peuvent représenter jusqu'à 2% des protéines solubles (Welch et Feramisco, 1982).

Ces deux isoformes possèdent trois domaines distincts : la partie N-terminal correspondant au domaine de liaison à l'ATP, le domaine central formant la zone de liaison aux polypeptides cibles, enfin le domaine C-terminal est nécessaire pour la dimérisation de la protéine. Cette dimérisation est par exemple nécessaire pour la translocation dans le noyau après un choc thermique (Prodromou *et al.*, 2000).

Hsp90 possède la capacité de se lier de manière stable avec des protéines essentielles dans les voies de transduction des signaux, des facteurs de transcription et des protéines du cycle cellulaire. Elle a la faculté de protéger de nombreuses protéines contre une dégradation par le protéasome et a permis de faire émerger le concept de protéines clientes. En effet, en s'associant avec une cible elle permet sa stabilisation et sa non dégradation ce qui augmente ainsi sa demi-vie (Whitesell et Lindquist, 2005 ; Da Rocha Dias *et al.*, 2005).

A-1.1.3. Hsp70

La famille Hsp70 est composée de 8 membres possédant une très grande homologie structurale. Tous les membres de la famille présentent deux domaines fonctionnels conservés: l'extrémité C-terminal responsable de la liaison aux polypeptides cibles et la partie N-terminal, responsable de l'activité ATPasique (Hunt et Morimoto, 1985). Chaque membre de la famille possède une localisation sub-cellulaire qui lui est propre ainsi que des fonctions spécifiques. Des formes constitutives comme Hsc70 sont ubiquitaires et ne subissent pas d'élévation de leur expression en réponse au stress. Elles participent au repliement constitutif des polypeptides naissants et à leur adressage vers les différents compartiments cellulaires. Elles interviennent lors du contrôle qualité des protéines en dirigeant les polypeptides altérés ou mal repliés vers une dégradation (Wickner *et al.*, 1999).

Les isoformes inductibles en cas de stress sont Hsp70.1 et Hsp70.3. Lors d'un choc thermique, ces protéines migrent dans le noyau et participent notamment à la maintenance de l'assemblage des ribosomes. Dans le cytoplasme, elles se lient aux polypeptides dénaturés afin d'éviter leurs agrégations et ainsi protéger les cellules de dommages irrémédiables (Lindquist et Craig, 1988).

Certains membres ont un rôle dans le développement des spermatozoïdes comme Hsp70.2 qui semble jouer un rôle essentiel dans la progression en méiose des cellules germinales mâles (Dix *et al.*, 1997). Les protéines Grp75 et Grp78 sont présentes respectivement dans les mitochondries et la lumière du réticulum endoplasmique où elles participeraient à la translocation et au repliement des polypeptides transloquées dans les différentes organites, de manière ATPasique (Kudo *et al.*, 2008 ; Dollins *et al.*, 2007).

A-1.1.4. Hsp60/Chaperonine

Hsp60 est synthétisée dans le cytosol puis subit une translocation dans la mitochondrie. Elle possède une structure tridimensionnelle très spécifique formée de deux bagues heptamériques formant un cylindre creux. Son rôle est de catalyser l'association de complexes oligomériques en facilitant le repliement des monomères. Elle est essentielle pour l'assemblage des protéines importées dans la mitochondrie (Ostermann *et al.*, 1989).

A-1.1.5. Hsp47

Hsp47 est trouvée en grande quantité dans le réticulum endoplasmique et son expression est concomitante de la synthèse de tous les types de collagènes. En effet, elle serait essentielle lors de la maturation des pro-collagènes en collagène actif. Chez la souris invalidée pour ce gène, les collagènes de type I ne présentent pas de structure quaternaire en triple hélice. Les collagènes de type IV sont également touchés. L'invalidation de ce gène conduit à une mortalité à un stade de 11 jours de développement embryonnaire chez la souris (Makareeva et Leikin, 2007 ; Nagai et al., 2000).

A-1.2. Les petites protéines de stress

Les petites Hsp ou sHsp (small Hsp) forment le deuxième groupe de protéines de stress humaines et regroupent les protéines de faible poids moléculaires (Table 1). Elles sont moins conservées au cours de l'évolution mais présentent un domaine fonctionnel commun nommé α-cristallin (De Jong *et al.*, 1993). Ce sont des protéines ubiquitaires ATP indépendantes, au nombre de 10 chez les mammifères (Taylor et Benjamin, 2005). Elles présentent des profils d'expression très différents dans tout l'organisme (Table 2).

Nomenclature	Désignations alternatives	Localisation
HspB1	Hsp27	Ubiquitaire
HspB2	MKPB	Musculaire
HspB3		Musculaire
HspB4	αA-cristalline	Oculaire
HspB5	αB-cristalline	Ubiquitaire
HspB6	Hsp20	Ubiquitaire
HspB7	cvHsp	Musculaire
HspB8	Hsp22	Ubiquitaire
HspB9		Testiculaire
HspB10	ODFP	Testiculaire

Table 2 : *Distribution tissulaire des petites protéines de stress*

A-1.2.1. HspB1/Hsp27

Hsp27/HspB1 est la petite protéine de stress la plus étudiée. Elle est codée par un gène présent sur le chromosome 7 et est exprimée dans tout l'organisme. Ce n'est pas un chaperon moléculaire au sens strict du terme puisqu'elle est incapable de reconformer sous forme native des protéines dénaturées. Elle aurait un rôle de réservoir de conformation lorsque le système de reconformation arrive à saturation. Elle possède la faculté de former des structures quaternaires de haut poids moléculaire en s'oligomérisant (Arrigo *et al.*, 2009). Comme pour toutes les petites Hsp, sa structure tridimensionnelle est responsable de sa fonction moléculaire. Elle est formée de 205 acides aminés et possède dans son extrémité N-terminal un domaine nommé WDPF essentiel à son oligomérisation (Bova *et al.*, 2000).

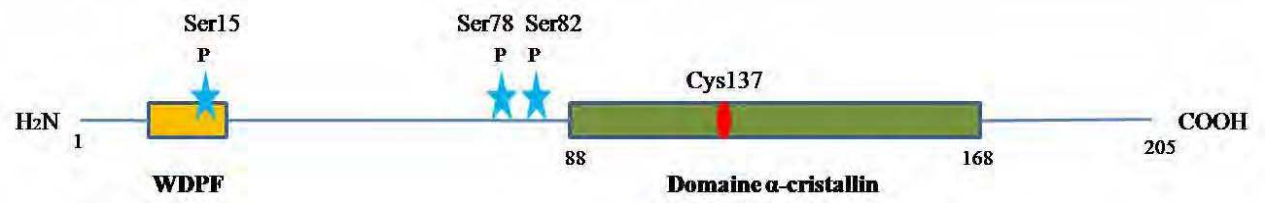

Figure 1 : *Structure générale de la protéine HspB1/Hsp27 (D'après Bova, 2000 ; Diaz Latoud, 2005 ; Landry, 1992)*

Hsp27 peut être phosphorylée sur trois résidus sérines en position 15, 78 et 82 (Figure 1). La voie principale de phosphorylation de Hsp27 est la voie de la p38MAPK associée à la kinase MAPKAK2 ou MK2 (Landry *et al.*, 1992). Dans certaines conditions, il a été montré que l'isoforme δ de la PKC pouvait être une autre voie de phosphorylation pour Hsp27 (Maizels *et al.*, 1998).

Cette phosphorylation est essentielle pour les modulations de la structure oligomérique de la protéine. Ainsi, il apparait que la phosphorylation de Hsp27 lors d'un stress comme le choc thermique permettrait la dissociation rapide des formes de haut poids moléculaire (Arrigo *et al.*, 2009). Par ailleurs, le résidu formé par l'unique cystéine en position C137 permettrait la dimérisation de la protéine, pierre angulaire d'une oligomérisation fonctionnelle (Diaz-Latoud *et al.*, 2005).

Récemment il a été montré que des mutations dans le gène *hspB1* pouvaient induire des neuropathies chez l'homme (Table 3). Ainsi, la neuropathie héréditaire distale des neurones moteurs de type 2B et la maladie de Charcot-Marie-Tooth type 2F seraient liées à des mutations majoritairement dans le domaine α-cristallin d'Hsp27 (Evgrafov *et al.*, 2004 ; Kijima *et al.*, 2005). Ces deux types de maladie provoquent une dégénération prématurée des axones. Ces invalidations fonctionnelles renforcent l'idée que Hsp27 possède une fonction biochimique très corrélée à sa structure moléculaire.

A-1.2.2. HspB4/αA-cristallin

HspB4 est la composante essentielle du cristallin des mammifères et n'est trouvée que dans les yeux. HspB4 possède des propriétés très particulières vis-à-vis de la lumière, liées à sa structure quaternaire encore mal comprise. Elle est phosphorylée sur un résidu sérine en position S122. Sa phosphorylation est dépendante de l'AMPc *via* la PKA, mais il a été montré que l'αA-cristallin, tout comme l'αB-cristallin, pouvait être une autokinase (Kantorow et Piatigorsky, 1998).

Elle est considérée comme un chaperon moléculaire et protègerait les filaments d'actine des agressions liées aux UVA et B. Comme pour Hsp27 il existe des mutations responsables de maladies génétiques chez l'homme (Table 3). Ces mutations dominantes sont responsables de différents types de cataractes (Graw, 2009).

A-1.2.3. HspB5/ αB-cristalline

HspB5 est avec HspB1 le second membre le plus étudié de la famille des sHsp. Elle est le plus souvent retrouvée associée aux microfilaments et aux filaments intermédiaires. Elle protègerait ces différents réseaux contre une pléiade de stress de type oxydatifs, thermiques, UV… On la retrouve associée aux lamellipodes des cellules en cours de migration, mais elle intervient aussi dans de nombreux mécanismes impliquant le réarrangement du cytosquelette d'actine. Son interaction avec l'actine est régulée par sa phosphorylation sur le résidu S59 (Singh *et al.*, 2007). Elle a aussi une affinité très particulière pour les microfilaments tels que la GFAP, la desmine, la vimentine et la périphérine. HspB5 préviendrait leur agrégation dans des conditions normales et pathologiques (Hagemann *et al.*, 2009 ; Song *et al.*, 2008).

Des mutations de HspB5 provoquant des altérations majeures du cytosquelette ont été caractérisées ce qui provoque des syndromes allant de la myopathie myofibrillaire, à la cardiomyopathie et la cataracte (Table 3). La première mutation découverte pour cette protéine nommée R120G, combine la somme de ces trois maladies chez l'homme. Elle a pour origine une accumulation de desmine dans les cellules musculaires qui vont dégénérer (Vicart *et al.*, 1998). Dans le cœur, l'accumulation du mutant R120G engendrerait un stress dit « réducteur » qui provoquerait une hypertrophie cardiaque (Rajasekaran *et al.*, 2007). Toutefois, il semble que le niveau d'expression du mutant soit responsable des effets moléculaires observés et il apparait que HspB5 module aussi négativement le stress oxydatif (Shin *et al.*, 2009).

Gène muté	Transmission	Phénotype
HspB1/Hsp27	Dominante	Neuropathie héréditaire distale des neurones moteurs de type 2B
	Dominante	Charcot-Marie-Tooth type 2F
HspB4/αA-cristalline	Récessive	Cataracte congénitale
	Dominante	Cataracte nucléaire
	Dominante	Cataracte précoce périphérique
	Dominante	Cataracte zonulaire centrale avec des opacité nucléaires
	Dominante	Cataracte nucléaire avec iris colombama et microphtalmie
HspB5/ αB-cristalline	Dominante	Myopathie myofibrillaire
	Dominante	Cardiomyopathie
	Dominante	Cataracte
HspB6/Hsp20	Dominante	Cardiomyopathie
HspB8/Hsp22	Dominante	Neuropathie héréditaire distale des neurones moteurs type 2A
	Dominante	Charcot-Marie-Tooth type 2L

Table 3 : *Les maladies génétiques ayant pour origine une mutation dans les gènes codant les sHsp (d'après : Graw, 2009 ; Evgrafov et al., 2004 ; Kijima et al., 2005 ; Ferrer et Olivié, 2008 ; Hu et al., 2007 ; Nicolaou et al., 2008).*

A-1.2.4. HspB8/Hsp22

Le rôle exact de Hsp22 n'est pas encore totalement élucidé mais il a été mis en évidence qu'elle est capable de supprimer des structures de type amyloïde et de contrôler la synthèse des protéines en modulant la phosphorylation de eIF2-alpha (Carra *et al.,* 2005 ; Carra *et al.*, 2009). Elle possède aussi une fonction dans la macro-autophagie. En effet, son activité chaperon permettrait la reconnaissance des protéines altérées. Cette interaction chaperon/substrat favoriserait le recrutement de la protéine adaptatrice Bag-3 qui permettrait de déclencher la machinerie autophagique (Carra *et al.*, 2008).

Des mutations altérant sa séquence génétique ont été identifiées avant même de connaitre son rôle biologique exact (Table 3). En effet, des mutations ponctuelles dans le gène *hsp22* seraient à l'origine de neuropathies héréditaires distales des neurones moteurs de type 2A et maladies de Charcot-Marie-Tooth type 2L (Hu *et al.*, 2007).

A-1.2.5. Les autres membres des sHsp

A l'exception de HspB6/Hsp20, les autres membres de la famille des sHsp ont été très peu étudiés. Hsp20 protègerait les cellules du muscle cardiaque en condition de stress oxydatif lors d'une ischémie. Ainsi, elle stabiliserait la phosphorylation de Akt ce qui permettrait la survie des cardiomyocites (Fan *et al.*, 2008). Des mutations de Hsp20 ont été mises en évidence dans des cardiomyopathies (Table 3) (Nicolaou *et al.*, 2008). De même, un polymorphisme dans le gène *cvHsp* (HspB7) serait à l'origine d'une recrudescence du nombre d'attaques cardiaques chez l'homme (Matkovich *et al.*, 2010).

HspB2 et B3 sont des protéines uniquement musculaires participant au mécanisme de différenciation des myoblastes. Elles interagiraient directement avec HspB1 et B5 pour restructurer le cytosquelette d'actine. (Sugiyama *et al.*, 2000). HspB9 et B10 ne sont présentes que dans les testicules mais aucune étude n'a pour l'instant été réalisée pour la caractérisation fonctionnelle de ces protéines.

A-2. L'induction de la réponse au stress :

La réponse au choc thermique a été découverte en 1962 par Ritossa, qui a caractérisé une transcription anormale de certains loci sur les chromosomes polytènes de glandes salivaires de drosophiles.

L'induction de l'expression des gènes codant les protéines de stress s'effectue suite à la trimérisation de facteurs de transcription spécifiques nommés HSF (Heat Shock Factor). Chez l'homme ces HSF sont au nombre de quatre et possèdent des profils d'expression différents. Les HSF sont constitutivement liés à certaines Hsp ubiquistes. Lors d'un stress, la liaison entre les Hsp et les HSF est déstabilisée. En effet, l'affinité entre les résidus hydrophobes des protéines dénaturées et les Hsp est plus importante que celle entre les Hsp et les HSF, ce qui entraîne la libération des HSF dans le cytosol (Tang *et al.*, 2005). Leur trimérisation puis leur phosphorylation permet leur migration dans le noyau et leur liaison aux séquences consensus nommées HSE (Heat Shock Element) localisées sur tous les promoteurs des gènes de choc thermique (Figure 2).

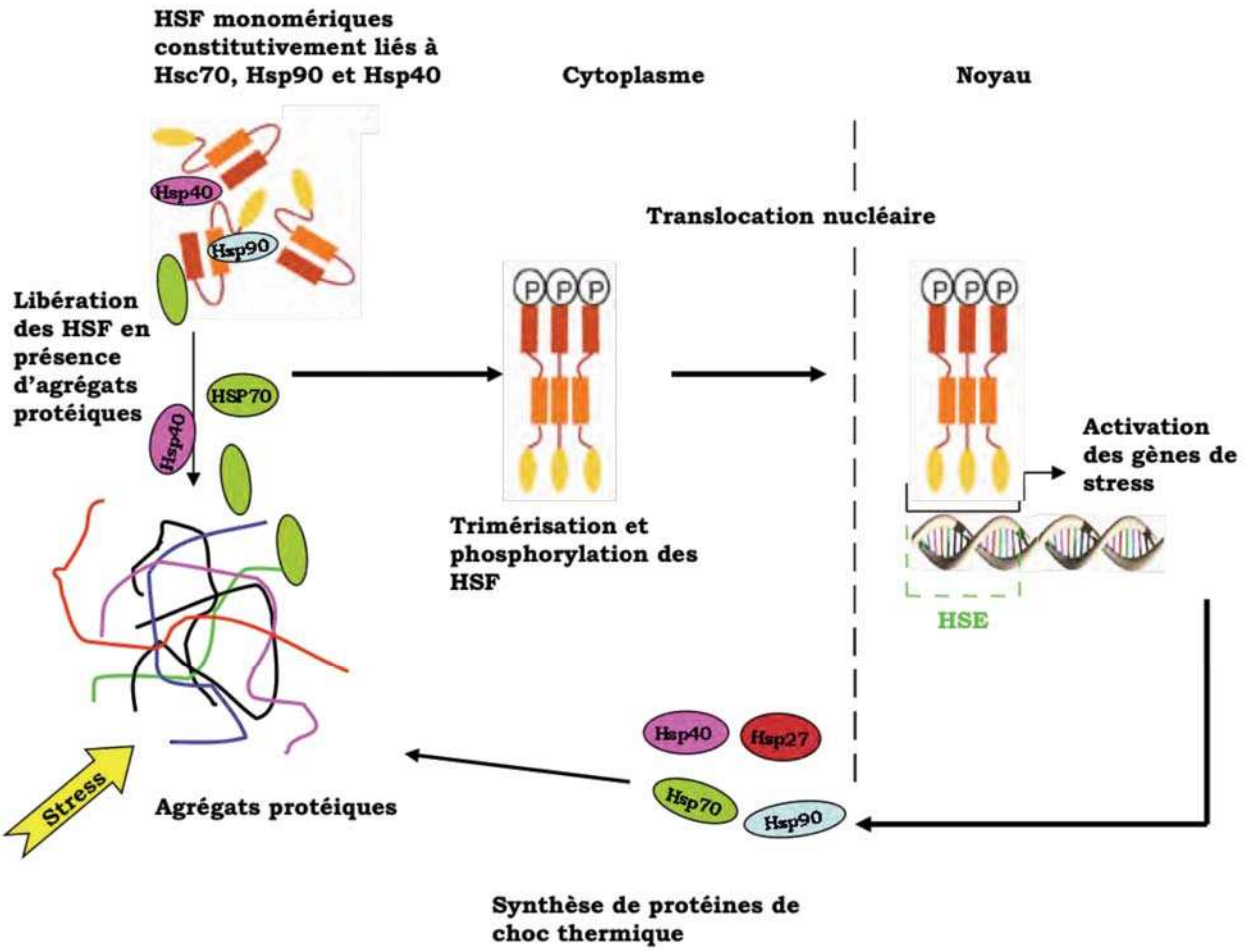

Figure 2 : *La présence d'agrégats protéiques est reconnue par Hsc70 et Hsp90, des chaperons résidents de la cellule non stressée. La liaison formée entre les protéines de stress et les protéines dénaturées est plus stable que celle avec le facteur de transcription HSF. Celui-ci est donc relâché, phosphorylé puis trimérisé. Il migre ensuite dans le noyau où il interagit avec les motifs HSE, localisés dans les promoteurs des gènes codants les Hsp. La grande quantité des HSP produites permet de reconformer les protéines altérées et d'interagir négativement avec HSF, en le maintenant à nouveau inactif dans le cytoplasme, ce qui explique la réversibilité du phénomène.*

Dans des conditions physiologiques normales, les gènes codants les HSF sont exprimés constitutivement. En outre, leur taux d'expression ne varie que très peu lors d'une stimulation par un choc thermique. Il existe cependant, des facteurs de transcription différents en fonction du type de réponse : ainsi HSF-2 induirait la synthèse des Hsp exprimées constitutivement, alors qu'HSF-1 serait l'initiateur de la réponse aux différents stress.

Les rôles de HSF-3 et 4 ne sont pas clairement encore élucidés. L'inactivation d'HSF-3 réduit drastiquement la survie cellulaire après choc thermique (Tanabe *et al.*, 1998). HSF-4 est lui aussi

impliqué dans la réponse au stress. Il a surtout été caractérisé dans l'œil où des mutations de son domaine de liaison à l'ADN sont à l'origine de cataractes congénitales (Bu *et al.*, 2002).

Il a été montré qu'un ARN non codant constitutivement exprimé chez l'homme nommé HSR1 (Heat shock RNA-1) interagissait directement avec HSF-1 et un facteur d'élongation de la transcription eEF1A. Ce complexe ribonucléique est responsable de l'activation de HSF-1. Une inhibition de HSR1 par siRNA rend impossible la réponse au choc thermique ce qui thermo-sensibilise les cellules (Shamovsky *et al.*, 2007). Par ailleurs, il a été mis en évidence que l'acétylation de HSF-1 est responsable de son activité et que la déacétylase de classe III SIRT-1 qui était à l'origine de cette modification d'activité (Westerheide *et al.*, 2009).

Les protéines de stress les plus fortement produites en réponse au choc thermique sont Hsp27 et Hsp70, cependant leurs cinétiques d'activation sont différentes, Hsp70 étant exprimée beaucoup plus rapidement que Hsp27 (Ananthan *et al.*, 1986). Il a été montré récemment que la transcription de Hsp70 était favorisée par une perte rapide des nucléosomes en condition de stress ce qui facilite l'accessibilité de l'ADN pour l'ARN polymerase II (Petesch et Lis, 2008).

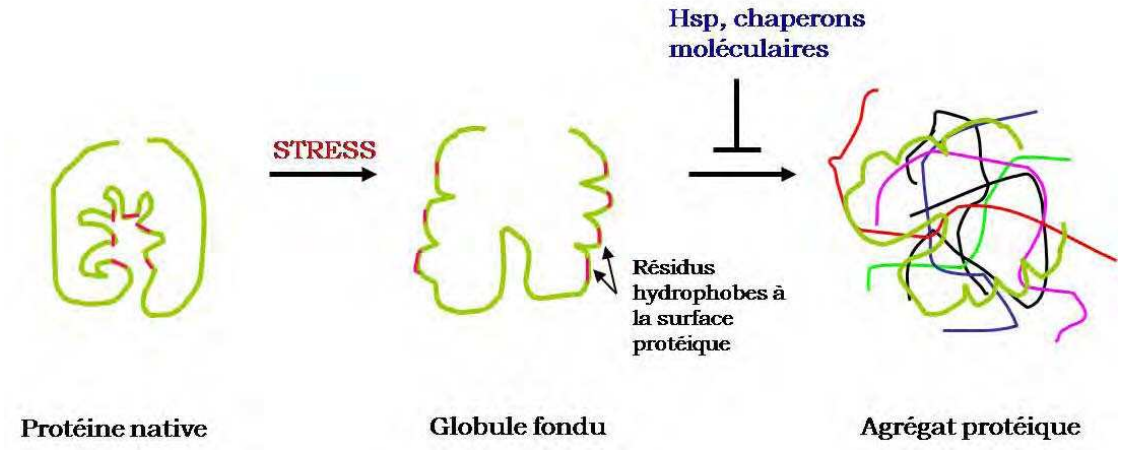

Figure 3 : *En condition de stress, la structure tridimensionnelle des protéines peut être déstabilisée ce qui induit l'exposition de résidus hydrophobes à la surface du polypeptide. Cette présentation donne lieu à la formation d'un intermédiaire de conformation nommé globule fondu (molten globule).*
Les Hsp, par leur fonction chaperon, reconnaissent et reconforment les régions hydrophobes des polypeptides altérés et inhibent la formation d'agrégats protéiques létaux pour la cellule.

A-3. Les gardiennes de l'intégrité cellulaire:

A-3.1. Rôle de chaperons moléculaires

En conditions physiologiques normales, un rôle des Hsp constitutives (de type Hsc70) est de se lier aux polypeptides néo-synthétisés et de catalyser leur maturation conformationnelle. De nombreux chaperons non inductibles et cofacteurs dits résidents, sont nécessaires à la synthèse des polypeptides et participent au contrôle qualité des protéines mais n'appartiennent pas à la famille des protéines de choc thermique. Les Hsp endogènes interviennent aussi lors des translocations protéiques dans les différents compartiments cellulaires. Ainsi, le dimère Hsp40/Hsp60 va conformer les protéines pénétrant dans la mitochondrie par les pores matriciels (Ostermann *et al.*, 1989).

En conditions de stress, il est établi que l'élévation du niveau d'expression des protéines de choc thermique a pour origine la déstabilisation des structures protéiques, matérialisée par la présence de globules fondus (molten globules ; figure 3). Ces protéines endommagées possèdent des résidus hydrophobes exposés à leur surface. Elles peuvent s'accumuler et former des agrégats insolubles létaux pour la cellule. La présence de globules fondus entraîne la synthèse de nombreux chaperons moléculaires qui ont pour rôle soit de reconformer ces protéines, soit lorsque la

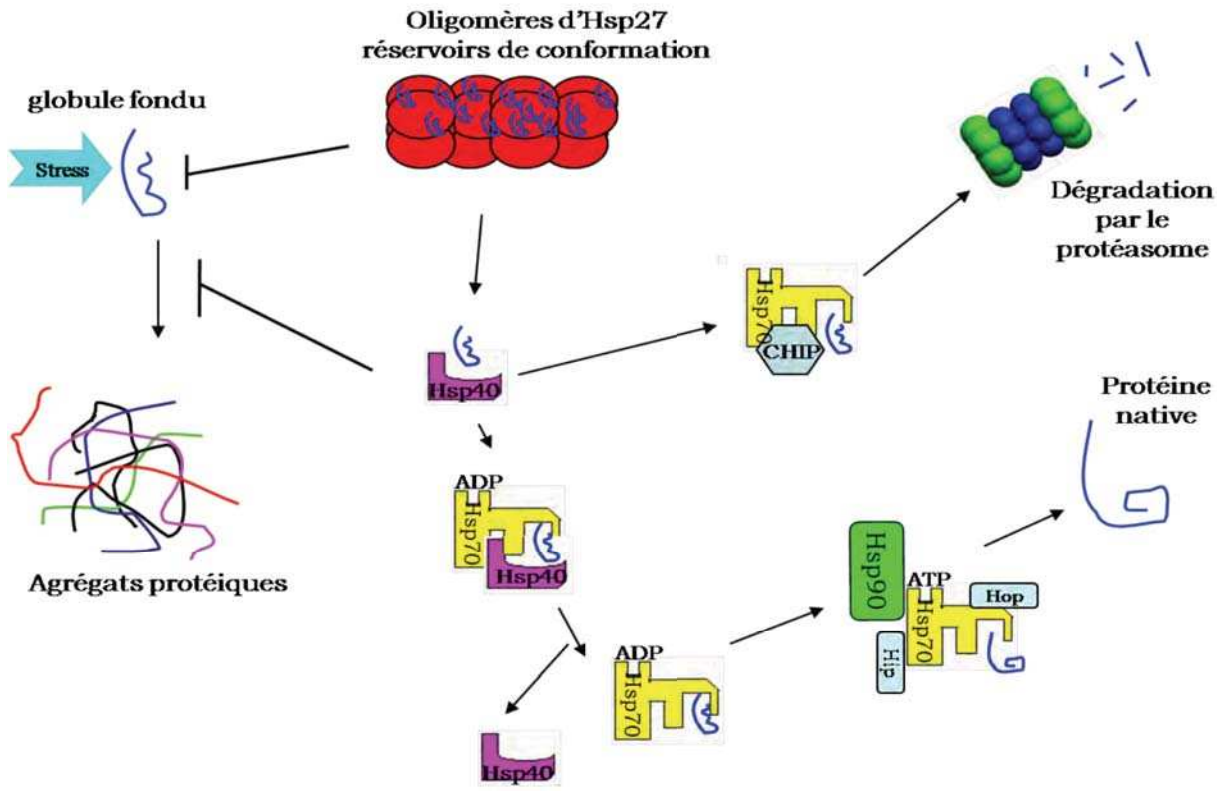

Figure 4: *Au cours d'un stress, les agrégats protéiques formés présentent à leur surface des zones hydrophobes. Celles-ci sont reconnues par Hsp40 qui, via son domaine J, forme un complexe avec la protéine Hsp70. Celle-ci, sous sa forme liant l'ADP, englobe la protéine substrat dans son domaine de liaison peptidique. La renaturation de la protéine substrat par Hsp70 nécessite des co-chaperons tels que Hip, Hop et Hsp90.*
Dans certaines conditions les atteintes conformationnelles des protéines sont trop importantes et la cellule, via la protéine CHIP, peut diriger ces protéines vers la voie de dégradation par le protéasome 26S.
Dans des conditions ou le système est saturé par un afflux massif de protéines à reconformer, un stockage transitoire est effectué par des structures oligomériques formées par les Hsp de faible poids moléculaire de type Hsp27 et α cristallines.

reconformation est impossible, de les envoyer vers une dégradation par le protéasome 26S *via* l'ubiquitination (Arrigo, 2005).

Les Hsp jouent donc des rôles prépondérants dans la reconformation des protéines altérées dans ces conditions de stress et préviennent l'apparition d'agrégats protéiques. La détection des globules fondus est réalisée par Hsp40 qui se lie à certains résidus hydrophobes exposés à la surface des protéines endommagées. Hsp40 est le cofacteur adaptateur qui permet le recrutement des véritables protéines chaperons comme Hsp70. Celle-ci prévient l'agrégation des protéines altérées et permet, *via* l'hydrolyse d'ATP, de reconformer les protéines dans une structure tridimensionnelle adéquate. Enfin, les sHsp forment des oligomères qui jouent un rôle de stockage et empêchent la saturation du système des chaperons (figure 4).

Hsp90 forme des complexes stables avec des protéines intervenant principalement dans la transduction des signaux cellulaires ou dans la régulation du cycle cellulaire. On lui dénombre de très nombreux interacteurs qui peuvent se regrouper en trois principales classes : des protéines kinases, des facteurs de transcription ainsi que des protéines de structure cellulaire. Son activité chaperon et de séquestration permet aussi d'augmenter la demie vie de certaines de ces protéines mutantes. Hsp90 a donc aussi pour rôle de « masquer » un grand nombre de mutations induisant une déstabilisation des structures protéiques ce qui peut être létal pour la cellule. Ce phénomène a aussi des implications sur l'évolution des organismes et des génomes. En effet, il favorise la conservation de mutations pourtant délétères d'une génération à une autre sans que cela affecte directement l'organisme. Hsp90 fournirait donc un second contrôle de l'expression génique au niveau protéique (Rutherford et Lindquist, 1998. Queitsch *et al.*, 2002).

A-3.2. Bases moléculaires de la conformation protéique

Une grande énigme concentre actuellement beaucoup d'efforts de recherches. Elle consiste à comprendre le déroulement du repliement correct des protéines ou « protein folding ». Les structures protéiques sont d'une très grande variété. Le repliement des polypeptides implique la création de structures secondaires et de superstructures régulières. La structure secondaire, formée par les hélices alpha et les feuillets bêta, constitue l'élément de base des conformations protéiques. Ces deux structures sont stabilisées par des liaisons hydrogène. La structure tertiaire correspond à la création de liaisons covalentes sous la forme de ponts disulfures entre des résidus cystéine, ou la formation de clusters métalliques. La formation de la structure quaternaire implique l'assemblage de sous-unités déjà repliées. Peu avant d'occuper leur conformation native énergiquement favorable, les molécules peuvent passer par un état intermédiaire de globule fondu. C'est souvent cet évènement qui est régit par les Hsp et par les autres chaperons (Bukau *et al.*, 2006).

Sans évènement extérieur, le nombre de conformations d'une chaîne polypeptidique de n acides aminés, susceptibles d'adopter s structures secondaires, est s^n. Le nombre de conformations protéiques, par exemple pour un polypeptide de n = 100 acides aminés et s = 13 structures secondaires, est un temps théorique de 10^{85} secondes ou 3.10^{17} siècles. Un processus du repliement s'opérant selon une recherche au hasard de la structure de plus basse énergie la plus stable est donc absolument impossible d'un point de vue cinétique et totalement incompatible avec la vie. C'est le paradoxe de Levinthal (Levinthal, 1968).

Les chaperons moléculaires ont pour but d'abaisser les temps de structuration moléculaire des protéines. Les chaperons sont en mesure d'isoler les protéines les unes des autres, ce qui fait que leur repliement n'est pas interrompu par les interactions avec les autres protéines. Les études de la cinétique du repliement ont montré l'existence de structures intermédiaires instables. Ces intermédiaires ont une demi-vie très courte et sont très délicats à identifier. Un très grand nombre de co-chaperons intervient dans la structuration protéique. Ces co-chaperons reconnaissent chacun un type de substrat donné et permettent de l'isoler du reste de la cellule puis de le présenter aux chaperons moléculaires capables de reconformer de manière ATP lytique les protéines sous forme native. Ainsi, les protéines de la famille Bag, composée de six membres, jouent un rôle essentiel dans différents processus permettant de présenter des protéines cibles à la famille Hsp70 (Takayama et Reed, 2001).

Les protéines de la famille Hsp70 sont les plus étudiées pour leur activité chaperon, en particulier l'homologue procaryote DnaK. Les mécanismes de moteurs moléculaires permettant la reconformation protéique sont encore mal compris (Mayer et Bukau, 2005). Il a été montré que l'activité ATPasique responsable de la modification protéique était dépendante des ions $Mg2^{+}$ et K^{+}. La fixation de l'ADP se fait dans une poche hydrophobe de liaison à l'adénosine. C'est sous cette forme liant l'ADP que Hsp70 englobe alors la protéine dénaturée dans son domaine peptidique. Le remplacement de l'ADP par une molécule d'ATP va permettre la renaturation de la protéine cible ainsi que sa libération concomitante à hydrolyse de L'ATP. Ce sont des co-chaperons comme Bag-1 qui augmentent la déstabilisation de la forme ATP du complexe Hsc70/Hsp70-substrat et permettent le relarguage de ce dernier (Takayama et Reed, 2001).

La renaturation de la protéine substrat par Hsp70 nécessite la participation d'autres co-chaperons tels que Hip et Hop (figure 4). Hip est considérée comme antagoniste du relargage des protéines par compétition avec Bag-1, et en stabilisant la forme Hsp70-ADP (Kanelakis *et al.*, 2000). Hop est une protéine essentielle pour le recrutement de Hsp90 sur le complexe Hsc70/Hsp70-substrat (Scheufler *et al.*, 2000). Hsp90 aurait des rôles multiples dans tous les mécanismes moléculaires conduisant à des destructurations moléculaires telles que l'export des organelles (Wang *et al.*, 2006). Certains polypeptides nécessitent une étape ultérieure de repliement par la protéine eucaryote TCP-1 ring complex qui est associée avec les membranes de l'appareil de Golgi (Willison *et al.,* 1989). Hsp60 est l'analogue mitochondrial de TCP-1.

Enfin, certains polypeptides trop altérés sont envoyés vers une dégradation par le protéasome 26S *via* la protéine CHIP (Carboxy terminus of Hsc70 Interacting Protein) et son activité E3-ubiquitine ligase (Qian *et al.*, 2006).

Les protéines de stress participent donc à de nombreux processus physiologiques de maintien de l'homéostasie cellulaire. Elles interviennent de manière pléiotrope dans de nombreuses régulations dépendantes des conditions environnementales. Dans des situations défavorables, lorsque l'intégrité cellulaire est menacée les Hsp tentent d'inhiber ces phénomènes de stress cellulaire potentiellement létaux. Ainsi, les protéines de stress tentent de prévenir la mort cellulaire et interviennent à différents niveaux des cascades effectrices conduisant à la mort d'une cellule.

B-LES HSP ET LE BLOCAGE DE LA MORT CELLULAIRE :

Les Hsp appartiennent à la grande famille des protéines de survie (comme Bcl2 ou la survivine). L'une des fonctions majeures des Hsp est donc leur rôle cytoprotecteur. Il a été établi que les Hsp inhibent un grand nombre de mécanismes conduisant à la mort cellulaire. Ainsi, les Hsp exercent leur action, des récepteurs aux effecteurs, en modulant l'activité de différents composants la voie de transduction des signaux *via* les kinases et les facteurs de transcription.

B-1. L'inhibition de l'activité des récepteurs de mort :

B-1.1. L'apoptose

Le terme apoptose désigne une mort cellulaire programmée (Kerr *et al.*, 1972). L'origine génétique de l'apoptose et les premiers composants moléculaires ont été découverts grâce à des travaux menés chez le nématode *Caenorhabditis elegans*, notamment par la mise en évidence de protéases actives lors de l'apoptose : les caspases (Hengartner et Horvitz, 1994).

L'apoptose est un processus fondamental tant au cours du développement que pour l'homéostasie générale d'un organisme. L'apoptose induit de nombreux changements morphologiques de la cellule comme la condensation nucléaire, le clivage de l'ADN et de protéines nécessaires au maintien de l'intégrité cellulaire ainsi que le remodelage de la membrane plasmique avec la présence de corps apoptotiques (Figure 5). Deux voies de signalisation majeures conduisent à l'apoptose : la voie des récepteurs de mort dite extrinsèque et la voie mitochondriale ou intrinsèque.

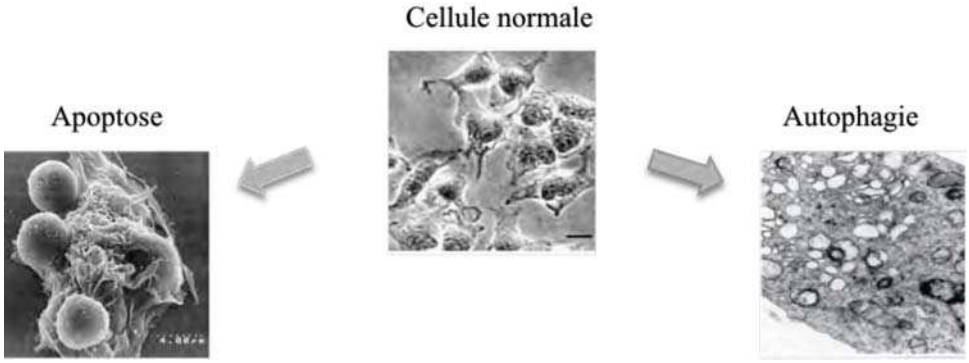

Figure 5 : *Les différents types de morts cellulaires génétiquement actives, l'apoptose et l'autophagie. Lors de l'apoptose la membrane cellulaire va bourgeonner et former des corps apoptotiques. Les phosphatidylsérines présentes dans le feuillet interne de la membrane plasmique sont externalisées. L'autophagie correspond à une auto-protéolyse avec accumulation de vacuoles autophagiques et destruction d'organites. (D'après Golstein et Kroemer, 2007; www.erudit.org)*

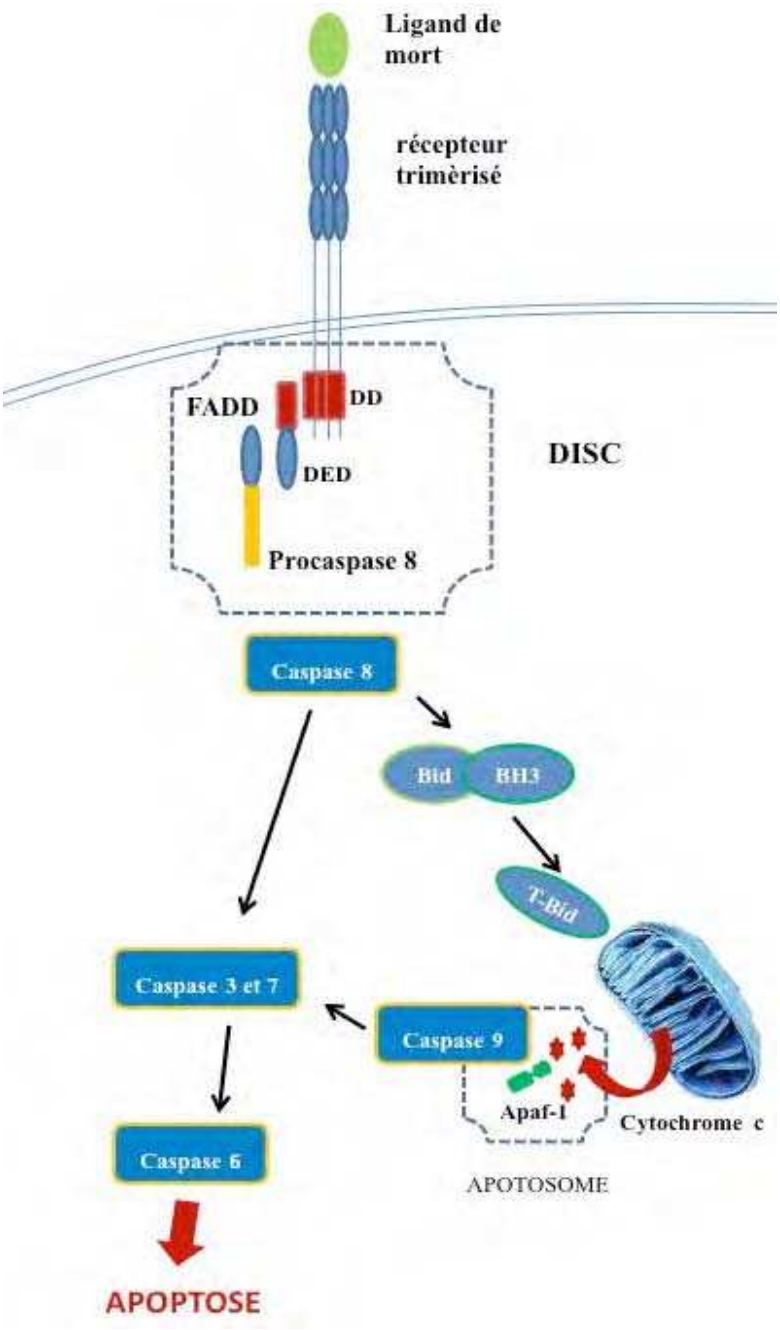

Figure 6 : *Schéma de la voie des récepteurs de mort. Le ligand active la trimérisation du récepteur, ce qui permet le recrutement de la protéine adaptatrice FADD. Le clivage de la procaspase 8 va initier la chaine d'activation des caspases.*
DD : Death Domian ; DED : Death Effector Domain.

B-1.2. Les récepteurs de mort

De nombreux stimuli sont capables d'induire l'apoptose. Toutefois, il existe une famille de récepteurs spécialisés dans l'induction, ce sont les récepteurs de mort. Ces récepteurs sont le plus souvent impliqués dans la réponse immunitaire qu'elle soit anti-tumorale ou anti-pathogène. Ils

sont les effecteurs du système immunitaire. Les récepteurs de mort jouent un rôle prépondérant dans la cytotoxicité des lymphocytes T et permettent l'élimination d'une cellule cible par activation d'un processus apoptotique.

La majorité des récepteurs de mort appartient à la grande famille des récepteurs du Facteur Nécrosant des Tumeurs (TNF-R). Les membres de la famille impliqués dans la mort cellulaire sont Fas/APO-1 (CD95), TNF-R1, et les récepteurs au ligand TRAIL (Tumor Necrosis Factor-Related Apoptosis- Inducing Ligand) formés par les récepteurs DR3, 4, 5 et 6. La mort induite par ces récepteurs est dépendante de l'activation de certaines caspases (Enari *et al.*, 1995).

Les récepteurs de mort possèdent dans leur partie intracytoplasmique, une région conservée d'environ 80 acides aminés appelée domaine de mort (Death Domain, DD). La stimulation du récepteur Fas par son ligand va induire la trimérisation du récepteur et le recrutement par l'intermédiaire de son domaine de mort cellulaire, d'un certain nombre de protéines impliquées dans la transduction du signal apoptotique. La protéine adaptatrice FADD est essentielle au déclenchement de la voie de transduction. FADD présente la particularité de posséder, en plus de son DD, un DED (Death Effector Domain). Le domaine DED est nécessaire et suffisant pour induire l'activation de l'apoptose. C'est le recrutement des caspases initiatrices 8 et 10 par FADD qui permet le déclanchement de la cascade apoptotique avec l'activation de la capase 3 exécutrice (Figure 6). Le complexe formé par le récepteur, les protéines adaptatrices et la caspase initiatrice est appelé DISC (Death Inducing Signaling Complex). Dans certains types cellulaires, une apoptose mitochondriale peut être activée par le clivage de la protéine de la famille BH3 Bid en t-Bid (Luo *et al.*, 1998 ; *cf.* B-2.1.1.).

Dans certaines conditions, TNF-R1 recrute également FADD, par l'intermédiaire d'une autre protéine adaptatrice TRADD. Cette dernière peut aussi interagir avec le DD de la serine/thréonine kinase RIP, qui selon les circonstances, peut induire l'activation de la voie NF-κB et la survie ou l'apoptose. RIP est également associée aux récepteurs aux ligands Fas et TRAIL (Jin et El-Deiry, 2006).

B-1.3. Protection engendrée par les protéines de stress

Certaines Hsp sont capables de réguler négativement l'apoptose induite par la stimulation de récepteurs pouvant induire une mort cellulaire active. Ainsi, Hsp27 protège contre la mort induite par l'activation du complexe Fas/FasL. La protéine Daxx se lie à la partie intracellulaire de

ce récepteur. Elle est nécessaire pour le recrutement des kinases transductrices de cette voie comme Ask-1. La rétention de Daxx par Hsp27 prévient son interaction avec le récepteur, et inhibe donc la mort induite par Fas (Mehlen *et al.*, 1996 ; Charrette *et al.*, 2000). De même, Hsp70 prévient la mort induite par Fas en amont de la voie d'apoptose dépendante de la mitochondrie (Clemons *et al.*, 2005).

Il est aussi remarquable de constater qu'une stimulation pro-apoptotique induite par le ligand Fas induit des changements du statut de très nombreuses protéines de stress, qui se traduit par une augmentation de leur synthèse pour Hsp27 et Hsp70 ou une modification de leur phosphorylation pour Hsp90 et 110 (Gerner *et al.*, 2000). Il a été mis en évidence que le facteur de transcription HSF-1 était activé lors de cette stimulation pro-apoptotique (Schett *et al.*, 1999).

Hsp70 exerce également une protection contre la mort induite par le Tumor Necrosis Factor α (TNFα) mais aucune interaction directe avec le récepteur au TNF n'a été démontrée (Jäättelä *et al.*, 1992). Le TNFα augmente l'activité de protéines phosphatases conduisant à l'inactivation transitoire de HSF-1, inhibant ainsi l'induction de Hsp70 ce qui favorise l'entrée en apoptose (Schett *et al.*, 2003). De plus, il apparait que Hsp70 interagit directement avec la protéine FANCC, un anti-apoptotique majeur de la lignée hématopoïétique. La formation de ce complexe permet de protéger des cellules hématopoïétiques contre le TNFα, l'IFNγ mais aussi contre d'autres stress cytotoxiques comme la présence d'ARN double brins (Pang *et al.*, 2001).

De même, les petites protéines de stress αB-cristallin et Hsp27 procurent une résistance à l'action cytotoxique du TNFα (Mehlen *et al.*, 1995). Il apparait que Hsp27 est un médiateur important de la réponse inflammatoire induite par la synthèse d'IL-1 et d'IL-10 ce qui permet, par un mécanisme dépendant de la sérine/thréonine kinase TAK1, une activation des voies de survie cellulaire comme la voie NFκB (Alford *et al.*, 2007 ; Omori *et al.*, 2006). Hsp90 participe à ce mécanisme en stabilisant directement la même kinase TAK1 lors de traitements par ces cytokines (Shi *et al.*, 2009).

Les Hsp sont également impliquées dans la protection contre la mort induite par le ligand TRAIL. L'αB-cristallin protège de cette mort en bloquant l'activation de la caspase 3 (Kamradt *et al.*, 2005). Il a aussi été mis en évidence que la déplétion de Hsp27 sensibilise des cellules de lignées pulmonaires soumises à une mort induite par cette même mort (Zhuang *et al.*, 2009).

Les grandes Hsp interviennent dans la mort induite par le ligand TRAIL. Ainsi, Hsp90α a la particularité de se lier de manière ATP dépendante à la forme courte de la protéine FLIP et de la

stabiliser. Cette liaison empêche la formation du death-inducing signaling complex (DISC) ce qui inhibe la mort induite par les récepteurs au ligand TRAIL (Panner *et al.*, 2005).

B-2. L'inhibition des effecteurs de la mort cellulaire :

Quelles que soient les origines de la mort cellulaire, les protéines de stress sont impliquées dans de nombreux mécanismes moléculaires conduisant à la survie des cellules. Ainsi, des phénomènes génétiquement actifs comme l'activation des caspases ou des gènes de la machinerie autophagique, ou des phénomènes fortuits comme l'agrégation protéique d'un prion, sont des cibles moléculaires de choix pour les Hsp.

B-2.1. La voie apoptotique mitochondriale :

B-2.1.1. L'apoptose mitochondriale

L'apoptose mitochondriale ou voie intrinsèque forme la seconde grande voie d'apoptose mise en évidence. D'une manière surprenante, c'est la mitochondrie qui joue un rôle primordial dans la régulation de l'apoptose.

En effet, la phase effectrice de l'apoptose comporte l'ouverture de pores dans la membrane externe des mitochondries. Ce mécanisme est régit par de nombreuses molécules pro-apoptogènes comme Bax et Bak. Ces molécules sont constitutivement liées aux membres anti-apoptotiques de la famille BH3 comme Bcl2. Les signaux générateurs de l'apoptose sont encore mal compris mais il est reconnu que la perte d'interaction entre les membres anti-apoptotiques et les membres de la famille BH3 pro-apoptotiques qui permet l'oligomérisation de ces derniers sur la membrane plasmique et la formation des pores. Le pore mitochondrial est un canal constitué au niveau de la membrane externe par la protéine VDAC (Voltage Dependent Anion Channel) et au niveau de la membrane interne par la cyclophiline-D et l'ANT (Adenine Nucléotide Translocator). Il a été mis en évidence que Bax interagissait directement avec VDAC et ANT (Shimizu *et al.*, 1999). Il semble que le complexe Bax/Bak puisse induire un changement de conformation du canal VDAC afin de former un pore permettant le passage des différentes molécules apoptogènes (Figure 7). La formation de ce pore a pour conséquence première la chute du potentiel mitochondrial nommé $\Delta\Psi m$.

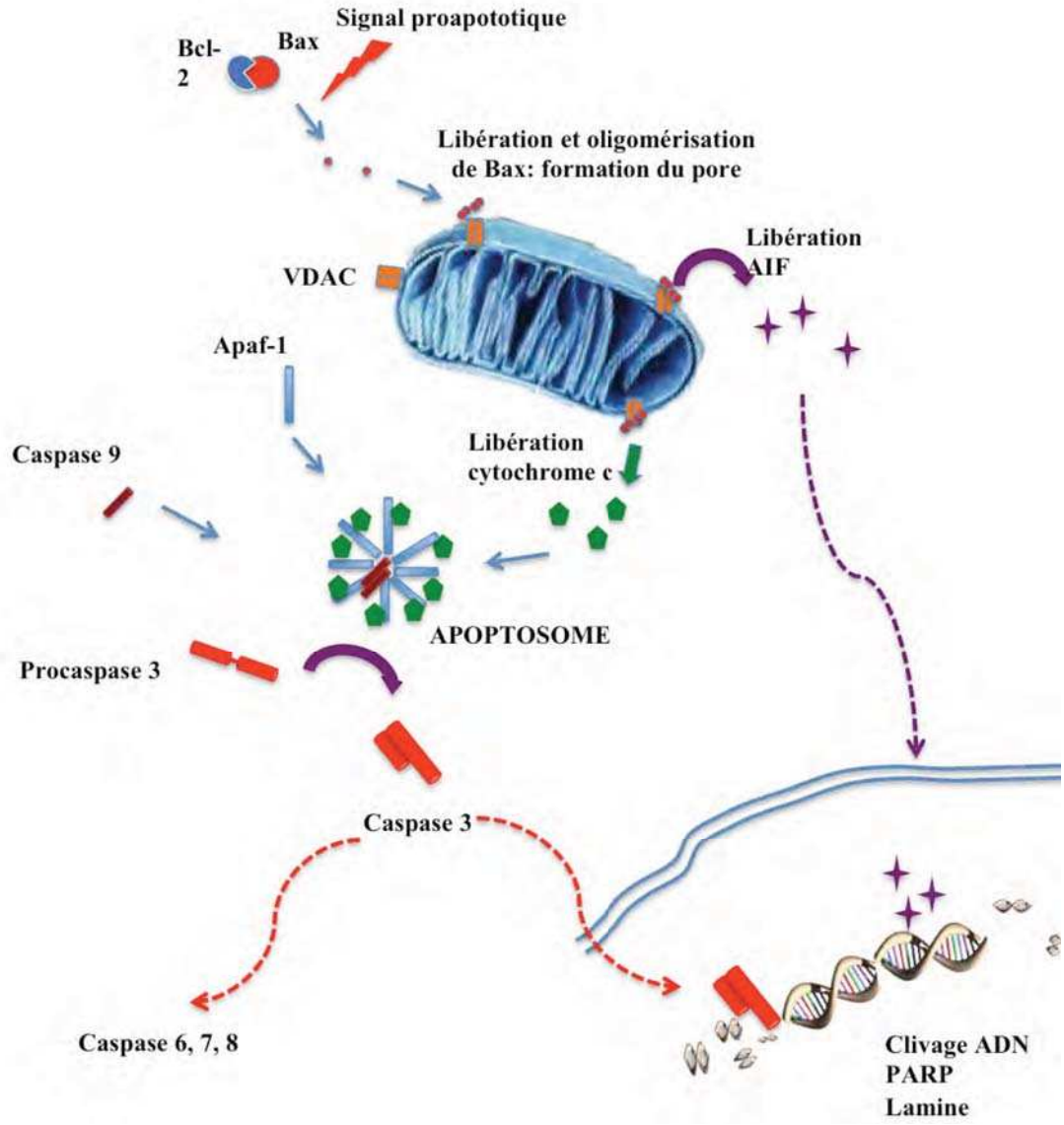

Figure 7 : *La libération de Bax va permettre son oligomérisation et la formation de pores sur la membrane mitochondriale. Le cytochrome c va s'échapper de la mitochondrie pour former l'apoptosome et permettre l'activation des caspases exécutrices. AIF sort aussi de la mitochondrie, migre dans le noyau où il va engendrer des modifications délétères sur l'ADN.*

Le relargage massif de molécules apoptogènes comme le cytochrome *c* et AIF (Apoptosis Inducing Factor), va être l'événement primordial pour la mort cellulaire. Le cytochrome *c*, en présence d'ATP, a la propriété de se lier à Apaf-1 (Apoptotic Protease Activating Factor-1) pour former un complexe supra moléculaire nommé apoptosome. Ce complexe est capable d'induire le clivage de la pro-caspase 9 en caspase 9 active (Li *et al.*, 1997), qui va ensuite permettre l'activation de la capasse 3 exécutrice. Celle-ci va déclencher la phase effective de l'apoptose par clivage des substrats essentiels à la vie cellulaire comme les lamines, PARP-1 et l'ADN.

Par ailleurs AIF, localisé dans l'espace intermembranaire de la mitochondrie est, après sa libération dans le cytosol, transloqué vers le noyau où il engendre la condensation de la

chromatine et des lésions à l'ADN. La voie AIF est indépendante des caspases et ne nécessite aucun intermédiaire pour provoquer l'apoptose nucléaire (Susin *et al.*, 1999).

La voie des récepteurs de mort est connectée à l'apoptose mitochondriale. En effet, la protéine pro-apoptotique Bid est directement clivée par la caspase 8. Son fragment C- terminal ou t-Bid permet la libération du cytochrome *c* (Luo *et al.*, 1998). Ce mécanisme serait un moyen d'amplifier le signal apoptotique issu des récepteurs de mort. Tous les types de cellules ne sont pas sensibles à ce mécanisme et ce serait le taux endogène de caspase 8 qui serait responsable de l'activation ou de la rétention de la sortie de cytochrome *c* (Luo *et al.*, 1998).

B-2.1.2. Mécanismes moléculaires du blocage induit par les Hsp

Les Hsp interagissent directement avec les protéines exécutrices de la mort cellulaire. Ainsi, on peut identifier des cibles communes effectrices de la cascade apoptotique.

L'apoptosome est une cible commune pour Hsp27, 70 et 90 qui bloquent la formation de ce complexe. Les mécanismes moléculaires de cette inhibition ne sont pas clairement élucidés. Toutefois, il a été montré que Hsp27 intervient spécifiquement dans cette voie mitochondriale dépendante des caspases. Une interaction entre Hsp27 et le cytochrome *c* a été démontrée lorsque celui-ci est relâché de la mitochondrie. Cette interaction inhiberait la formation de l'apoptosome (Bruey *et al.*, 2000). Hsp70, à l'instar de Hsp90, pourrait interagir avec Apaf-1 pour inhiber la formation de l'apoptosome (Beere *et al.*, 2000). Cependant, des travaux plus récents ont remis en cause cette interaction et laissent penser que Hsp70 possèderait plutôt un rôle inhibiteur du relargage du cytochrome *c* en amont de la mitochondrie (Steel *et al.*, 2004). Néanmoins, Hsp70 se lie directement à AIF et inhibe sa fonction pro-apoptotique (Ravagnan *et al.*, 2001).

Une autre étude a montré que Hsp27 pourrait interférer avec l'activation de la procaspase 3 en s'associant directement avec la protéase inhibant ainsi son clivage en caspase 3 active (Pandey *et al.*, 2000). De même, Hsp70 interagit aussi avec le mécanisme d'activation des caspases, lors de l'apoptose mais également au cours de processus liés au développement (Ribeil *et al.*, 2007).

Enfin, il a aussi été montré que Hsp27 interagissait avec l'actine, permettant sa stabilisation puisque le cytosquelette subit de profondes altérations lors de l'apoptose. Cette

inhibition en amont du déclenchement de l'apoptose provoque le blocage de la sortie du cytochrome *c* mitochondrial (Paul *et al.*, 2002).

B-2.2. La mort cellulaire indépendante des caspases.

B-2.2.1. L'autophagie

L'autophagie est à la fois un mécanisme de survie et de mort cellulaire. Elle participe à la dégradation des agrégats protéiques et des organites. C'est un processus de survie enclenché principalement pendant les périodes de jeun cellulaire. Sa distinction avec l'apoptose est souvent délicate. Le mécanisme autophagique a lieu sans activation des caspases mais par intervention des protéines ATG (Autophagy related genes), les protéines Beclin-1 et Bcl2, les voies mTOR (mamalian target of rapamycin) et PI3Kinase de classe III (Levine et Kroemer, 2008). L'autophagie est souvent caractérisée par la présence de vacuoles autophagiques caractéristiques (Figure 5).

Il a été mis en évidence que Hsp70 intervient négativement lors de l'autophagie cellulaire. En effet, elle possède une affinité pour certains lipides et permet l'inhibition de la perméabilisation de la membrane lysosomiale (Kirkegaard *et al.*, 2010). La protéine Hsp70 se concentre dans les lysosomes et les vésicules d'exocytose, uniquement lorsque la cellule présente une expression membranaire externe de la cathepsine D. Cette libération de la protéase dans la matrice extracellulaire serait à l'origine du caractère invasif des tumeurs et de l'angiogenèse. La fonction de Hsp70 serait d'inhiber les possibles fuites de ces vésicules dans le cytosol (Nylansted *et al.*, 2004).

Par ailleurs, toute la machinerie des chaperons est nécessaire pour la transduction des protéines altérées dans le lysosome (Agarraberes et Dice, 2001). Il a été démontré que 30% des protéines de certains tissus comme le foie ou les reins en condition de privation de nutriments, étaient dégradées par un mécanisme nommé l'autophagie médiée par les chaperons ou CMA (Chaperone Mediated Autophagy). D'une manière surprenante, toutes les protéines dégradées par cette protéolyse contiennent le motif peptidique KFERQ. C'est ce motif qui est reconnu par Hsc70. Ce complexe est ensuite transloqué vers la matrice lysosomiale pour y être dégradé par des protéases (Agarraberes *et al.*, 1997)**.**

Concernant les petites Hsp, seule HspB8 a été montrée comme faisant partie de la machinerie autophagique. Elle interagit directement avec la protéine Bag3 et aurait pour rôle la reconnaissance des substrats agrégés comme des agrégats de polyglutamine de la maladie de Huntington (Carra *et al.*, 2008).

Par ailleurs, il a été montré que de protéines clientes de Hsp90 pouvaient être dégradées par la voie autophagique. En effet, un peptide issu d'un domaine d'une toxine permet le décrochage et la dégradation autophagique de certaines cibles de Hsp90 (Shen *et al.*, 2009).

B-2.2.2. Maladies neuro-dégénératives et prions

Les protéines de stress jouent un rôle central dans les maladies neuro-dégénératives et la formation des structures amyloïdes de type prion car elles sont le pivot de lutte contre l'agrégation protéique.

Ainsi, tout le système des chaperons est activé pour lutter contre ce type de dérèglements moléculaires. Ce sont essentiellement les propriétés moléculaires de chaperons stricts et de détection des polypeptides altérés qui sont mises en jeu dans ces mécanismes.

La protéine Tau est une protéine associée aux microtubules des axones neuronaux, qui contrôle la mise en place des différentes isoformes de tubuline ainsi que leur phosphorylation. Dans le cas de la maladie d'Alzheimer et d'autres tauopathies, elle est surexprimée, hyper phosphorylée, et possède une forte tendance à s'autoagréger. Pratiquement toutes les protéines de stress sont impliquées dans des mécanismes moléculaires modulant l'activité de Tau. Ainsi, Hsp70 et 90 se lient directement à Tau, augmentent sa solubilité et son association aux microtubules et diminuent son agrégation en condition pathologique (Dou *et al.*, 2003). Les petites protéines de stress interviennent dans ces processus et sont surexprimées dans ces conditions pathologiques. Cependant, leur rôle n'est pas complètement élucidé car si Hsp27 semble de manière surprenante augmenter la phosphorylation de Tau, à l'inverse l'αB-cristallin diminuerait cette phosphorylation (Björkdahl *et al.*, 2008).

Les Hsp sont aussi modulées dans le cas de la maladie de Parkinson caractérisée par l'accumulation de l'α-synucléine qui s'agrège et où Hsp70 joue un rôle pivot (Huang *et al.*, 2006). A l'identique, les petites Hsp interviennent et inhibent l'agrégation de nombreuses altérations des

protéines du cytosquelette comme le GFAP (Glial Fibrillary Acidic Protein) dans la maladie d'Alexander (Hagemann *et al.*, 2009).

Des études sur le rôle des Hsp dans la formation de structures amyloïdes de type prion ont été réalisées chez la levure. Les homologues des Hsp humaines jouent un rôle essentiel pour lutter contre la propagation des prions. Ainsi, Hsp104, 70 et 40 agissent de concert pour inhiber à la fois la formation, la diffusion et l'élimination du prion sup35 de levure (Shorter et Lindquist, 2008).

B-3. Les voies de transduction des signaux

B-3.1 La modulation de kinases

Les Hsp possèdent la faculté d'interagir avec des kinases dont le rôle est central dans différentes voies de transduction de signaux, fréquemment altérées lors de cancers. Ainsi, Hsp90 stabilise la protéine kinase RIP-1 (qui relie les récepteurs de mort à la voie de survie NF-κB). En absence de Hsp90, RIP-1 est dégradée et la voie NF-κB inactivée, ceci conduit à une sensibilisation à la mort induite par la cytokine TNFα. Hsp90 interagit et stabilise également la DAPK (Death-Associated Protein Kinase) qui s'associe lors d'une stimulation pro-apoptotique aux domaines de morts de certains récepteurs. Hsp90 inhibe sa dégradation en prévenant le recrutement de la co-chaperone CHIP, responsable de son ubiquitination et de sa dégradation (Zhang *et al.*, 2007).

Ce rôle anti-apoptotique peut aussi être médié par la capacité d'Hsp90 à interférer avec l'une des voies majeures de survie cellulaire, la voie Akt/PKB (Sato *et al.*, 2000). En effet, l'interaction d'Hsp90 avec la phosphoprotéine Akt/PKB protège cette dernière de sa déphosphorylation par la protéine phosphatase PP2A, et contribue ainsi à l'inhibition de la voie apoptotique mitochondriale en bloquant l'activation de la caspase 9. Hsp27 interagit également avec Akt et module ses fonctions. Ainsi, la rétention de Hsp27 dans un complexe formé par Akt, la p38 MAPK et la MAPKAPK2 provoquerait un blocage de la voie de survie Akt, engendrant ainsi une apoptose massive. Inversement, la phosphorylation de Hsp27 et sa libération par le complexe permettraient d'amplifier le signal de survie. Ce mécanisme serait l'une des bases du contrôle de l'apoptose ou de la survie des neutrophiles (Rane *et al.*, 2003).

Hsp70 est un régulateur négatif de la kinase Ask-1 impliquée dans le maintien de l'équilibre redox en réponse aux RLO ou en réponse au stress du réticulum endoplasmique (Park *et al.*, 2002). Cette kinase permet l'activation des voies de réponse au stress telles que la voie de la p38MAPK et la voie de la c-Jun N-terminal kinase (JNK).

B-3.2 Le cycle et la division cellulaire

B-3.2.1 Modulation directe du cycle

Hsp90 joue aussi un rôle prépondérant dans le cycle cellulaire en modulant l'activité de nombreuses kinases directement impliquées dans le cycle.

Ainsi, Hsp90 se lie à Cdk-4 (cyclin dependant kinase 4) ce qui agit directement sur le relarguage de la cycline-D. La fonction chaperon d'Hsp90 permet une stabilisation du complexe Cdk4/cycline D lors de la phase G_1. Ce complexe serait déstabilisé pour permettre l'entrée en phase S (Zhao *et al.*, 2004). Les régulations du cycle cellulaire s'effectuent grâce à l'action d'un autre co-chaperon, la protéine Cdc37. Celle-ci se lie à un domaine protéique spécifique des Cdk nommé boite G (G-box). Il semble que l'implication de Hsp90 dans le cycle cellulaire soit l'une des bases de l'effet des traitements anti-cancéreux ciblant cette protéine de stress. Ainsi, cibler Hsp90 par des inhibiteurs chimiques provoque la dégradation de ses interacteurs comme cdc2 and cdc25c ce qui entraine un blocage du cycle en phase G_2/M (García-Morales, 2007).

De même, Cdk11 p110, un autre membre de la super famille des Cdk interagit directement avec la cycline L, impliquée principalement dans la régulation de l'épissage des pré-ARNm. Ainsi, la kinase Cdk11 p110, un substrat des caspases lors de l'apoptose, est stabilisé par Hsp90. Ce mécanisme permettrait de bloquer l'entrée en apoptose et empêcherait l'arrêt du cycle cellulaire lié à un épissage incorrect des pré-ARNm (Mikolajczyk et Nelson, 2004)

Par ailleurs, il a été montré que Hsp27 permet la dégradation de la protéine p27 kip1 ce qui permet l'entrée en phase S des cellules stressées (Parcellier *et al.*, 2006). De plus, Hsp27 permet une levée de la sénescence cellulaire induite par traitement chimique en modulant la régulation p53 dépendante, de la protéine p21 (O'Callaghan-Sunol *et al.*, 2007).

B-3.2.2 Hsp et mitose

Les protéines de stress jouent également un rôle dans les mécanismes moléculaires de la division cellulaire. En effet, Hsp70 est une protéine présente dans les centrosomes en condition normale et les protègent aussi en condition de stress. Sa présence permet d'éviter des déstructurations pouvant provoquer des divisons anormales (Hut *et al.*, 2005). De plus, il apparait que la forme mitochondriale de Hsp70 (mtHsp70) permet le recrutement de p53 au niveau des centrosomes. L'inhibition de cette interaction par des formes mutantes empêche leur duplication et ne permet donc pas la division cellulaire (Ma *et al.*, 2006).

Hsp90 permet le recrutement du complexe cycline B/Msp (Microtubule associated mini-spindles) au niveau des fuseaux mitotiques. Hsp90 ne joue cependant aucun rôle pour la stabilité de ce même complexe qui est un évènement clef de la division cellulaire (Basto *et al.*, 2007).

Sp1 a été décrite comme étant un co-chaperon de Hsp90. Les protéines de la famille Polo sont impliquées dans l'organisation des centrosomes et interagissent directement avec Sp1. Des mutants de la protéine Sp1 perturbent la division cellulaire et bloquent les cellules dans un état quiescent de prométaphase. D'une manière remarquable, des cellules possédant des mutations de Hsp90 présentent le même phénotype de défaut de formation des centrosomes (Martins *et al.*, 2009).

B-4. <u>Facteurs de transcription:</u>

L'interaction la plus étudiée entre les Hsp et des facteurs de transcription est celle conduisant à la rétention cytoplsamique des facteurs HSF en abscence de stress (*cf.* A-2.). Cependant, les Hsp stabilisent également d'autres facteurs de transcription impliqués dans différents mécanismes moléculaires.

B- 4.1. Le suppresseur de tumeur p53

Les Hsp sont impliquées dans la modulation des activités de facteurs de transcription clefs dans la régulation de la balance entre survie cellulaire et apoptose.

Ainsi Hsc70, Hsp90 et un complexe de protéines agissant en tant que co-chaperons interagissent avec la protéine suppresseur de tumeur p53 (King *et al.*, 2001). On remarque aussi que cette affinité est augmentée en condition de stress, ce qui préviendrait l'inactivation de p53

par dénaturation thermique (Muller *et al.*, 2004). Le recrutement de la protéine CHIP par le complexe de chaperons permet une dégradation de p53. Ce mécanisme constituerait une alternative à la dégradation de p53 contrôlée par la protéine Mdm2 (Esser *et al.*, 2005).

Comme mentionné précédemment, Hsp90 possède aussi la faculté de « chaperonner » certains mutants non fonctionnels. Ainsi, Hsp90 interagit avec le mutant p53-R175H qui a un effet dominant négatif sur p53. En inhibant sa dégradation, Hsp90 favoriserait les disfonctionnements du cycle cellulaire et permettrait ainsi l'échappement tumoral. Cependant, il a été montré que l'affinité entre les Hsp et les mutants de p53 est diminuée. En effet, les Hsp reconnaissent une structure protéique déterminée et celle-ci est souvent altérée chez les mutants. Il n'y aurait donc pas de rétention systématique des mutants de p53 par Hsp90 (King *et al.*, 2001). Cependant, les interactions entre les nombreux mutants de p53 et Hsp90 semble un élément primordial de la transformation cellulaire aboutissant à un phénotype malin et l'implication réelle des Hsp lors de ces processus.

B-4.2. Les autres facteurs de transcriptions

Ainsi, Hsp70 et 90 collaborent dans la régulation du facteur de transcription IRF-1 (Interferon Regulatory Factor 1). Ce dernier active la transcription de gènes impliqués dans la réponse à l'hypoxie, à des infections pathogènes et à des dommages à l'ADN. Le gène codant IRF-1 est un suppresseur de tumeur et sa déplétion entraine une recrudescence de cancers de l'œsophage et de leucémies. Inhiber Hsp90 et 70 empêche les activités transcriptionnelles de ce facteur ce qui potentialise des traitments à l'interferon. Par ailleurs, Hsp90 augmente la demi-vie de IRF-1 et permet son accumulation nucléaire mais pas cytoplasmique (Narayan *et al.*, 2009).

De même, Hsp27 possède la faculté d'interagir et de stabiliser le facteur de transcription STAT3 (Signal Transducers and Activators of Transcription 3), dérégulé dans de très nombreux cancers. C'est un activateur transcriptionnel des gènes codant deux anti-apoptotiques majeurs que sont BCL-XL et la survivine. Il a été prouvé dans des cellules de prostate qu'une déplétion en Hsp27 favorisait la dégradation de STAT3 ce qui impliquerait que d'autres Hsp possèderaient des protéines clientes comme Hsp90 (Rocchi *et al.*, 2005).

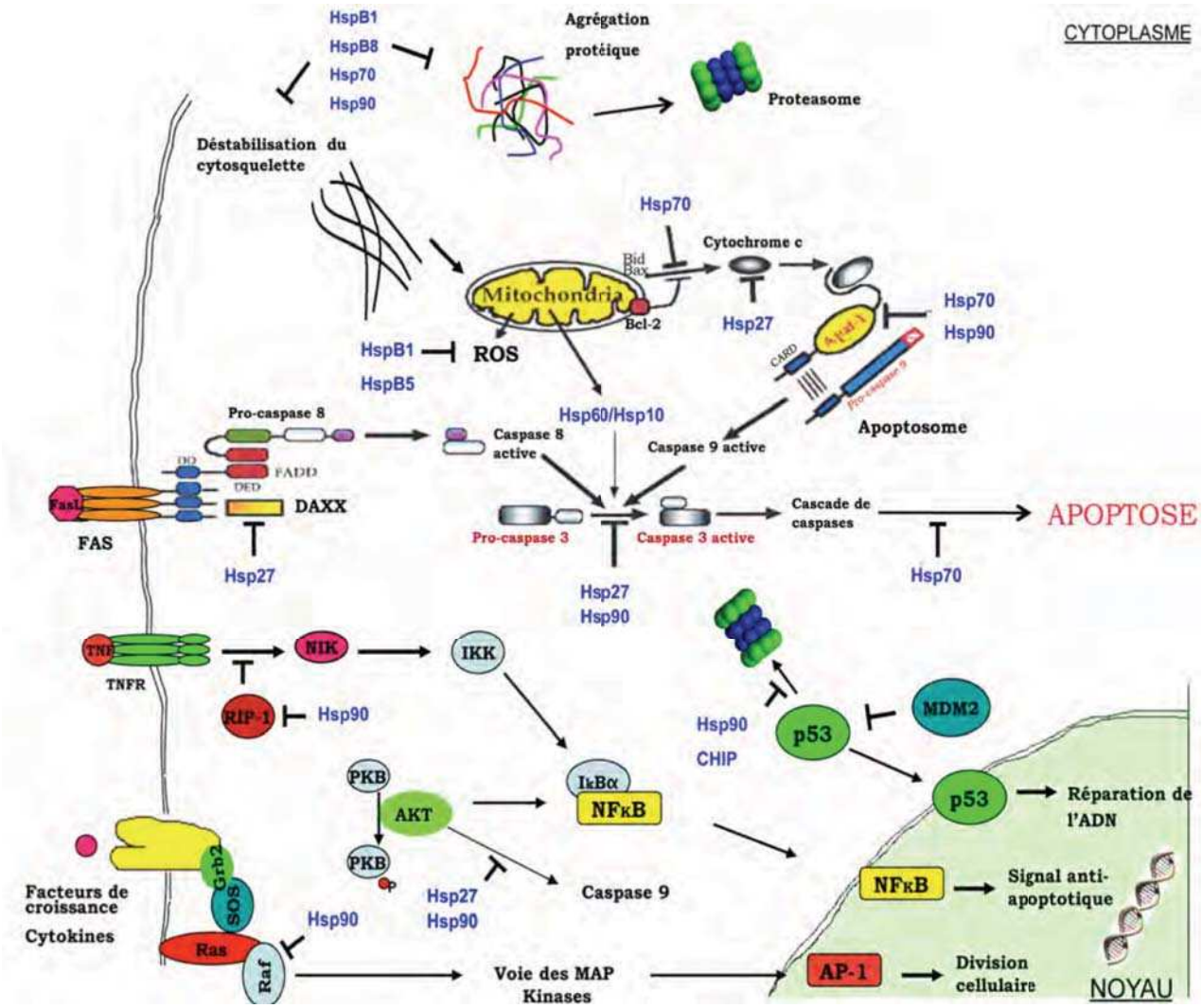

Figure 9: *Schéma récapitulatif des interactions des Hsp avec les différentes voies de mort cellulaire. La grande diversité ainsi que le grand nombre de cibles inhibées rend compte des nombreuses implications des Hsp dans la cytoprotection.*

La pluralité des cibles des Hsp est autant d'exemples du rôle central qu'elles occupent dans les différents processus de maintien de l'homéostasie cellulaire et notamment dans la balance entre la mort de la cellule et sa survie (Figure 9). Ainsi, grâce aux Hsp, une cellule pourrait survivre malgré différentes mutations et se diriger vers un état de malignité.

C-LES HSP ET LA CANCERISATION :

Le blocage du processus apoptotique par les Hsp peut permettre à la cellule de survivre à différentes altérations comme des mutations oncogéniques. Celles-ci, en s'accumulant vont altérer le fonctionnement de la cellule et participer à la transformation, jusqu'à un état prolifératif puis cancéreux.

C-1. Les Hsp et l'échappement tumoral

C-1.1. Hsp et transformation tumorale

Les Hsp sont impliquées dans l'inhibition de la mort cellulaire mais il est envisageable que le maintien en vie d'une cellule possédant des lésions, notamment des inactivations d'oncogène, ne soit pas l'unique mécanisme permettant la transformation d'une cellule. Les Hsp interviendraient de manière active et donc directement dans les mécanismes menant à la cancérisation.

HSF-1 a été montré comme possédant intrinsèquement un potentiel oncogénique chez la souris. En effet, des souris invalidées pour le gène *hsf-1*, présentent une diminution importante du nombre de tumeurs induites après traitement par un carcinogène puissant (Dai *et al.*, 2007). Il semble donc établi que ses cibles transcriptionnelles sont des molécules à fort potentiel oncogénique. HSF-1 fait donc aussi potentiellement des cibles thérapeutiques majeures, car l'inhiber revient à bloquer la synthèse de la majeure partie des Hsp.

Le phénomène de rétention de mutants d'oncogènes comme ceux de la protéine p53 par Hsp90 semble aussi être un phénomène central dans le passage à l'état transformé (*cf.* B-4.1.). Ce phénomène serait potentiellement en adéquation avec la théorie de transformation cancéreuse par étape de type Weinberg (Hahn *et al.*, 1999).

C-1.2. Rôle cytoprotecteur des Hsp en thérapie anti-cancéreuse

Outre ces phénomènes actifs de passage à l'état cancéreux, il apparait que les protéines de stress sont impliquées de manière plus passive *via* leur accumulation en réponse au stress, dans la survie des cellules tumorales.

C-1.2.1. La chimiothérapie

Lors d'un traitement chimio-thérapeutique, les cellules cancéreuses subissent un stress important engendré par l'agent utilisé. Ainsi, il a été montré que les protéines de stress protègent les cellules contre l'action de nombreux inducteurs d'apoptose et de drogues anticancéreuses. Il est cependant remarquable de constater que le stress engendré par des traitements comme le cisplatine et l'adryamicine provoque l'accumulation des Hsp dans les cellules cancéreuses. La protection engendrée par les Hsp est donc amplifiée lors de la tumorigènèse (Ciocca et Calderwood, 2005). L'apparition des protéines anti-apoptotiques est donc un mécanisme clef de la prolifération et de l'agressivité tumorale.

Il est à noter que l'immense majorité des études, réalisées à ce jour, concernent seulement trois Hsp : Hsp27, 70 et 90. En effet, les autres protéines de stress agissent plutôt comme cofacteurs de ces principales Hsp mais de récentes études tendraient à montrer qu'elles possèdent également un fort potentielle oncogénique (Moyano *et al.*, 2006).

Les Hsp protègent la cellule tumorale contre différentes drogues utilisées en chimiothérapie en bloquant la mort cellulaire. Hsp27 inhibe ainsi la mort induite par des agents comme l'étoposide, un inhibiteur de la topoisomérase 2, qui lui même inhibe la synthèse de Hsp27 lors de traitement de cancers ovariens et utérins (Tanaka *et al.*, 2004). L'inactivation du protéasome par le bortezomib conduit à l'accumulation de protéines mal conformées ; Hsp27 et Hsp70 inhibent cette accumulation et favorisent la survie de celles tumorales traitées par cet inhibiteur (Chauhan *et al.*, 2004 ; Voorhees *et al.*, 2007). Hsp27 protège contre la mort induite par le cisplatine (agent intercalant), en favorisant l'activation de la voie PI3Kinase/Akt et l'activité d'une enzyme détoxifiante des RLO la thioredoxine réductase (Zhang et Shen, 2007). Hsp70 inhibe la mort de cellules cancéreuses du pancréas traitées au quercetin (Aghdassi *et al.*, 2007). De manière identique, Hsp70 procure une forte résistance de cellules de tumeurs mammaires au traitements par la gemcitabine et le topotecan, respectivement un antimétabolite et un inhibiteur mitotique (Sliutz *et al.*, 1996). Hsp70 et Hsp27 agiraient de concert pour favoriser la survie après

traitement par la doxorubicine, une molécule génératrice de RLO (Karlseder *et al.*, 1996 ; Venkatakrishnan *et al.*, 2006).

De même, Hsp90 joue un rôle central dans la cytoprotection. En effet, elle a été décrite comme bloquant de nombreux agents anticancéreux comme les agents progestatifs et le taxol. De plus, l'inhibition d'Hsp90, en perturbant le signal de survie Akt, potentialiserait largement ce traitement (Saulit *et al.*, 2003).

C-1.2.2. La radiothérapie

L'expression des Hsp est également fortement accrue en réponse à l'action de rayonnements ionisants comme ceux utilisés en radiothérapie. La présence des Hsp semble inversement corrélée à l'efficacité de la réponse aux traitements et semble être à l'origine d'une forte radiorésistance (Miyazatui *et al.*, 2005). Il semble donc possible à partir de biopsies, de prédire la future réponse d'un patient à la radiothérapie et ainsi de proposer un traitement adéquat. Dans ce contexte, notre laboratoire en collaboration avec une équipe de l'Hôpital Lyon-Sud a montré qu'Hsp27 était un modulateur négatif de la mort induite par les rayonnements γ, pour des cancers des voies aériennes supérieures (Aloy *et al.*, 2007).

Hsp70 protège aussi contre les rayonnements ionisants de type γ en agissant de concert avec Hsp40 et les protéines de la famille Bag, en s'externalisant de la cellule ce qui module l'activité de cellules Natural Killers (Gehrmann *et al.*, 2005 ; *cf.* C-2.2.)

L'ensemble de ces données indique que les Hsp interviennent dans la survie des cellules cancéreuses. Les Hsp comme toutes les protéines anti-apoptotiques jouent donc un rôle important dans la résistance aux traitements, et donc un rôle central dans l'agressivité tumorale.

C-1.3 Les Hsp et l'agressivité tumorale

Les protéines de stress jouent un rôle important dans le blocage du processus apoptotique et dans la cytoprotection, ce qui induit directement leur implication dans l'échappement tumoral. Il a par exemple, été montré chez le rat que la seule présence de Hsp27 et de Hsp70 dans deux lignées issues du même cancer du côlon pouvait induire des formes progressives (présence) ou régressives (absence) de formation de tumeur, une fois ces cellules réinjectées dans un animal syngénique (Garrido *et al.*, 1998).

Organe touché	Hsp	Implications	Organe touché	Hsp	Implications
CANCER SEIN	Hsp27	suspicion d'agressivité corrélation avec le récepteur aux estrogènes	REIN	Hsp70	Favorable pour la survie
CANCER SEIN	Hsp70	Faible différenciation ; métastases. Mauvais pronostique	MELANOME	Hsp27	Forte expression
CANCER SEIN	Hsp90	Baisse survie	MELANOME	Hsp60	Forte expression
CANCER OVAIRE	Hsp27	Baisse survie	MELANOME	Hsp70	Expression faible corrélée avec le stade clinique
CANCER OVAIRE	Hsp70	Pas de corrélation avec la survie	LEUCEMIE	Hsp27	Prédictif de la réponse à la chimiothérapie
CANCER OVAIRE	Hsp90	Pas de corrélation avec la survie	VESSIE	Hsp27	Faible expression dans tumeurs radiosensibles
CANCER OVAIRE	Hsp60	Quand surexprimée meilleur pronostique	VESSIE	Hsp70	Expression corrélée au grade . Baisse survie
PANCREAS	Hsp90	Surexprimée	OESOPHAGE	Hsp27	Pronostique favorable
FOIE	Hsp27	surexprimée dans les hépatomes	OESOPHAGE	Hsp70	Pronostique favorable Faible expression corrélée avec bonne réponse
FOIE	Hsp70	marqueur des stade précoces	COLORECTAL	mtHsp70	pronostique sombre quand surexprimée
ESTOMAC	Hsp27	Baisse survie quand surexprimée	PROSTATE	Hsp27	Faible pronostique
ESTOMAC	Hsp70	Pas de corrélation avec la survie	PROSTATE	Hsp60	pas de corrélation avec la survie

Table 4 : *Implications de Hsp dans le pronostic et la pathologie cancéreuse. (D'après Ciocca et Calderwood, 2005 ; Koga et al. ; Tian et al., 2007 ; Gehrmann et al., 2005).*

De plus, on retrouve des taux significativement plus élevés de Hsp27 dans de très nombreux types de tumeurs. Le traitement n'explique souvent pas à lui seul la présence des Hsp, car on les retrouve dans de très nombreux types tumoraux non encore médicalisés. Ainsi, il apparaît qu'une forte accumulation de Hsp27 semble néfaste dans des cancers comme ceux de l'ovaire, de l'estomac, du poumon ou de la prostate. À l'inverse, un fort taux d'expression de Hsp27 semble bénéfique pour un nombre bien plus restreint de carcinomes tels que les cancers de l'œsophage et de l'endomètre (Ciocca et Calderwood, 2005). Hsp27 serait aussi une protéine

favorisant à l'apparition de métastases (Tian *et al.*, 2007). Les premières études montrent que la MMP-9, une métalloprotéinase essentielle pour le clivage de protéines matricielles et l'invasion, est régulée négativement lorsque Hsp27 est déplétée (Bausero *et al.*, 2006).

Le taux d'αB-cristallin serait corrélé à un pronostic sombre dans des cancers du sein, où il serait favorable à la formation d'acini, une lésion pré-invasive (Moyano *et al.*, 2006)

De même, Hsp90 possède des propriétés contradictoires selon le type de cancers, néanmoins sa présence semble largement défavorable. Par exemple, la présence d'Hsp90 induit un pronostic néfaste lors d'un hépatocarcinome. En effet, Hsp90 aurait la capacité de « chaperonner » les protéines oncogéniques HER-2/neu et p53 mutées et d'inhiber leur dégradation par le protéasome, protégeant ainsi des cellules contenant de graves altérations. Par ailleurs, Hsp90 possèderait la propriété de stabiliser le facteur d'hypoxie HIF-1. Celui-ci est sécrété massivement dans des cellules en condition de privation d'oxygène. Dans des modèles de tumeurs hépatiques ou de tumeurs de la vessie, inhiber chimiquement Hsp90 permet de réduire drastiquement l'invasion tumorale, mais aussi de prévenir l'angiogenèse ainsi que la formation de métastases (Koga *et al.*, 2007).

À l'inverse, la fonction chaperon de Hsp90 permet le maintien d'un état plus mature du récepteur à la progestérone, ce qui freine une perte trop drastique de l'état différencié et rend les tumeurs moins agressives et plus sensibles aux agents progestatifs synthétiques, dans le cas d'un cancer de l'endomètre (Saha *et al.*, 2004).

Enfin, Hsp70 joue des rôles variables dans différents types de cancers. Sa présence est bénéfique pour le pronostic cancéreux dans des tumeurs comme celles de l'œsophage, du pancréas, du rein et défavorable dans de très nombreux cancers comme ceux de l'estomac, de l'endomètre et de l'utérus (Ciocca et Calderwood, 2005).

Ce rôle ambivalent des Hsp ne va cependant pas à l'encontre du rôle important qu'elles possèdent dans la cytoprotection et l'agressivité tumorale. Il est donc important de connaître les rôles des Hsp dans les différents types de cancers pour évaluer si leur inhibition présentera un avantage thérapeutique lors d'un traitement anticancéreux.

C-1.4. Le diagnostique cancéreux

Les Hsp ne semblent pas être de bons marqueurs du diagnostic des pathologies cancéreuses. Il n'a en effet pas été établi de corrélation directe entre le niveau d'expression des protéines de choc thermique et le stade de différenciation tumorale : cancer bien délimité, avec envahissement ganglionnaire, métastatique, et plus généralement pas de lien direct avec la classification TNM. Il existe tout de même quelques exceptions Hsp27 serait un marqueur diagnostic pour des cancers de la prostate résistant aux androgènes et Hsp70 serait un marqueur important dans les cancers du foie (Cornford *et al.*, 2000 ; Di Tommaso *et al.*, 2009).

Il est cependant possible de prédire la future réponse aux traitements émise par les patients en regardant les niveaux d'expression des Hsp et de toutes les autres protéines de survie (Miyazatui *et al.*, 2005). Les Hsp seraient donc assimilables à des facteurs pronostics mais ne permettant pas le diagnostic réel, sans doute lié au fait de l'hétérogénéité de leur faculté d'induction.

C-2. <u>Ciblage thérapeutique des Hsp:</u>

C-2.1. L'inhibition des Hsp

Il est certain qu'inhiber les protéines de stress semble être une stratégie pertinente pour des thérapies anti-cancéreuses. De plus, les cellules normales n'expriment que très peu les Hsp inductibles, leur ciblage n'entrainerait donc qu'une faible toxicité et une spécificité de ciblage de la tumeur.

C-2.1.1. Les inhibiteurs chimiques de Hsp90

La découverte d'un antibiotique naturel, inhibiteur de la fonction chaperon d'Hsp90 : la geldanamycine et d'un homologue stable moins hépatotoxique, le 17-AAG ou tanespimcycin (17-allylamino-17-demethoxygeldanamycine) permet d'envisager dès à présent un ciblage thérapeutique de cette Hsp. Des études cliniques de phase II sont d'ailleurs actuellement réalisées aux Etats-Unis et en Grande-Bretagne (Hostein *et al.*, 2000 ; Banerji *et al.*, 2005).

Parallèlement, de nombreuses recherches ont été initiées dans le but de trouver des homologues encore plus stables et moins toxiques et de développer d'autres molécules de la

famille des benzoquinones telles que l'herbimycine A et l'ansamycine. Toutes ces molécules possèdent la même faculté de bloquer le domaine de liaison à l'ATP de Hsp90 (Miyata, 2005).

Le 17-AAG a été utilisé pour le traitement de différents types de cancers comme ceux de l'ovaire, de l'estomac et les différents cancers gastriques pour déterminer les différents niveaux de toxicité supportables par les patients.
Il est acquis dans la littérature que l'effet du 17-AAG est lié à la fonction d'Hsp90 dans des voies d'activation de kinases (Banerji *et al.*, 2005). Lors des différentes études réalisées, les auteurs ont souligné les diminutions des niveaux intra-cellulaires de nombreuses oncoprotéines des familles telles que Erb, Ras ou Akt, suite à une déstabilisation engendrée par l'inhibition fonctionnelle de la protéine chaperon. Après traitement par le 17-AAG, entraînant une déplétion rapide des kinases Raf-1 et Cdk-4, on observe une surexpression de Hsp70 chez de nombreux patients, ce qui conduit à penser que les cellules cancéreuses s'adaptent en permanence à leur environnement extérieur en utilisant les différentes voies de prolifération disponibles. Des inhibiteurs de Hsp90 n'induisant pas l'activation des HSF sont d'ailleurs recherchés dans le but de réduire l'activation d'autres Hsp en réponse à l'inhibition d'une première. Par ailleurs, il a été démontré que la présence de Hsp90 dans la mitochondrie était spécifique des cellules tumorales. Trouver des inhibiteurs spécifiques de cette forme s'avère une piste sérieuse pour abaisser la toxicité des composés ciblant Hsp90 (Kang *et al.*, 2007).

Il semblerait que le ciblage de Hsp90 par ces composés chimiques induise un blocage du cycle cellulaire. Les effets moléculaires restent à affiner car ils apparaissent contradictoires selon les lignées utilisées mais soulignent la complexité du rôle joué par Hsp90. En effet, une étude montre que l'effet du 17-AAG est corrélé à un blocage du cycle cellulaire pendant la phase G_2/M, lié à la surexpression de la protéine du rétinoblastome Rb dans trois des quatre lignées de cancer du côlon testées (Hostein *et al.*, 2000). Or, une autre montre que l'arrêt du cycle cellulaire à lieu pendant la phase G_1 sur des lignées pulmonaires (Srethapakdi *et al.*, 2000). De ce fait, elles ne permettent pas de caractériser totalement les effets induits par les traitements. Il reste néanmoins évident que la compréhension des effets cliniques du 17AAG et de ses dérivés en cours de développement, est très importante pour déterminer avec quels autres médicaments les inhibiteurs de Hsp90 pourront être combinés.

Il semble aussi qu'inhiber lors d'un traitement, la fonction d'une protéine jouant un rôle aussi central que Hsp90 puisse perturber certaines voies et entraîner à long terme des effets négatifs sur les patients. Ainsi, il a été montré que l'inhibition de Hsp90 pouvait induire la

dégradation de la kinase suppresseur de tumeurs LKB1 ce qui pourrait potentiellement entraîner l'apparition de polypes. La caractérisation des effets à long terme de l'inhibition de Hsp90, semble donc aussi très importante pour ajuster au mieux les futurs traitements (Nony *et al.*, 2003).

Récemment un nouvel inhibiteur est venu compléter la gamme des inhibiteurs de Hsp90. Il s'agit d'un amide resorcinylic isoxazole nommé NVP-AUY922, qui permet d'inhiber à la fois la croissance tumorale mais aussi l'angiogenèse et la formation de métastases issues de xénogreffes induites chez la souris (Eccles *et al.*, 2008). Ce composé est actuellement en test pour des essais cliniques de phase I, mais malheureusement les premières limites sont déjà apparues puisque son utilisation engendre l'induction de Hsp70. Un autre composé le 2-aminothieno[2,3-d]pyrimidine qui entre en compétition avec la boite ATPasique de Hsp90, inhibe la croissance de xénogreffes chez la souris. Ce composé fournira une grande facilité d'utilisation pour les patients et le transport de la molécule dans le système sanguin car il est soluble dans l'eau (Brough *et al.*, 2009). Dernièrement, il a été montré que le PU-H71, permettait de traiter des lymphomes B en déstabilisant l'interaction entre l'oncogène Bcl6 et Hsp90. Cette nouvelle molécule est un dérivé de base purique et permet la dégradation de Bcl6 dans des lymphomes où elle est chroniquement activée (Cerchietti *et al.*, 2009).

C-2.1.2. Les inhibiteurs chimiques de Hsp70

Récemment des inhibiteurs chimiques de Hsp70 ont été caractérisés. Une équipe a montré que le 2-phenylethynesulfonamide ou PES se liait sélectivement à la forme inductible de Hsp70 et non à sa forme constitutive Hsc70 (Leu *et al.*, 2009). Ce composé chimique a été découvert après un crible chimique centralisé sur le déclenchement d'une apoptose mitochondriale induite par activation de la voie p53. Il a pour action de déstabiliser l'interaction entre Hsp70 et p53 mais aussi de moduler l'interaction entre Hsp70 et certains de ses co-chaperons. Cette drogue augmente aussi l'autophagie, ce qui induit un effet délétère sur la survie de cellules cancéreuses. De plus, ce composé semble utilisable en thérapie anticancéreuse puisqu'il augmente la survie de souris modèles de lymphome (Leu *et al.*, 2009).

D'autres molécules chimiques sont en cours de développement mais les études sont encore sommaires pour connaître leur réel potentiel thérapeutique. Par exemple, le VER-155008, un dérivé de l'adénosine se lie avec la boite ATPase de Hsp70 et permet de sensibiliser des lignées

cancéreuses à l'apoptose. Ce composé mime l'effet des inhibiteurs de Hsp90 puisque les protéines clientes de Hsp90 sont dégradées (Massey *et al.*, 2010).

C-2.1.3. Les méthodes alternatives

A ce jour aucun inhibiteur chimique n'a été identifié pour Hsp27, ce qui laisse un large champ d'investigations ouvert. L'une des difficultés majeures dans la création de nouvelles molécules ciblant Hsp27 est le fait qu'il n'a pas été réalisé de cristallographie de cette protéine à l'état oligomérique, une structure clef régulant sa fonction protectrice et anti-apoptotique.

Des stratégies alternatives se développent pour fournir de nouvelles molécules anticancéreuses. Ainsi, deux types de méthodes se développent essentiellement basées sur les stratégies antisens et les inhibitions par des peptides compétiteurs et ceci pour toutes les protéines de stress (figure 10).

Inhiber Hsp70 par des stratégies basées sur l'interférence ARN permet d'inhiber la survie de cellules cancéreuses. D'une manière surprenante inhiber les mêmes membres de la famille avec ces stratégies permet une synergie très importante pour la mort cellulaire. Il est à noter que dans une étude, Hsp70-2 montrée pour être impliquée dans la spermatogenèse, est aussi étudiée en temps que cible thérapeutique puisque surexprimée dans les tumeurs (Rohde *et al.*, 2005). De même, le ciblage concomitant de Hsp70 et Hsc70 inhibe les activités de Hsp90. Il est remarquable de constater que cette inhibition semble spécifique des cellules cancéreuses (Powers *et al.*, 2008).

Une nouvelle génération de stratégies antisens est aussi en train d'émerger. Elle est basée sur des petits ARN stabilisées et moins sensibles à l'action de ribonucléases. Des groupements 2' O-Methoxy ethyl/ methyl sont ajoutés aux extrémités 3' et 5' de la structure de base de l'antisens. En plus d'une demi-vie augmentée ces oligonucléotides présentent une affinité plus forte vis-à-vis de leur cible. Pour Hsp27, l'OGX-427 développé par la société OncoGenex (Canada) a été montré comme efficace lors d'études précliniques sur des cancers de la prostate, de la vessie et du carcinome tête et cou (Snoek *et al.*, 2009 ; Hatchity *et al.*, 2009 ; Mastui *et al.*, 2009).

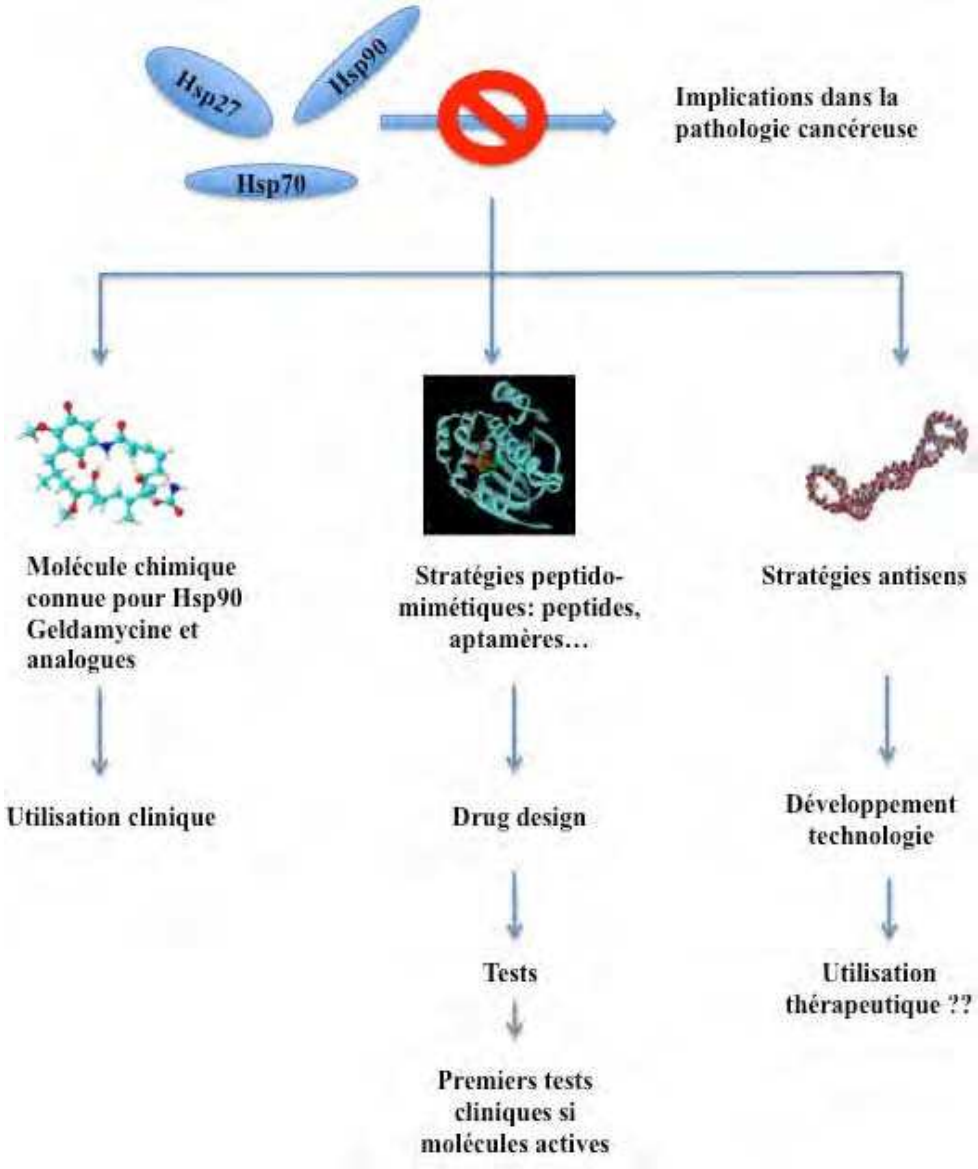

Figure 10 : *Schéma des stratégies de ciblage développées pour inhiber les protéines de stress. La principale contrainte réside dans le facteur temps du développement de drogues inhibant spécifiquement une cible, pour les Hsp qui ne possèdent pas d'inhibiteurs naturels.*

D'autres stratégies consistent à isoler des molécules possèdant un effet peptido-mimétiques. Ainsi, la Shepherdine est un peptide conçu pour inhiber la boite ATPase de Hsp90. Ce composé a pour origine un peptide issu de la séquence polypeptidique de la survivine, cliente de Hsp90. Il permet le décrochage des autres protéines clientes de la protéine de stress. Cette molécule ne semble pas être cytotoxique pour les cellules normales comme les progéniteurs hématopoïétiques (Plescia *et al.*, 2005). Sur le même modèle, une étude a permis d'isoler un heptapeptide inhibiteur des activités tumorigéniques de Hsp27. Ce peptide correspond à la zone d'interaction restreinte entre Hsp27 et la kinase PKC δ (Kim *et al.*, 2007).

C.2.2. Hsp et immunité

C-2.2.1. Hsp et système immunitaire

Différentes études démontrent une implication des Hsp dans certains mécanismes de la réponse immunitaire. Il a été montré que Hsp70 joue un rôle de cargo moléculaire lors de la présentation des peptides du complexe majeur d'histocompatibilité (CMH) à la surface cellulaire. En effet, elle s'associe aux peptides antigéniques issus de la dégradation par le protéasome et les guide dans le réticulum endoplasmique où ils sont maturés et associés aux récepteurs du CMH grâce aux transporteurs TAP (Transporters associated with Antigen Processing). De même, Hsp90 participe à la formation des molécules du CMH de classe II (Houlihan *et al.*, 2009).

Ces récepteurs subissent alors une présentation à la surface cellulaire où ils seront reconnus par le système immunitaire.

C-2.2.2. Hsp et vaccination

Dans les carcinomes de stade avancé, certaines anomalies cellulaires engendrent des dérèglements induisant le relargage dans la matrice extracellulaire de Hsp70 couplée à certains peptides antigéniques (Gong *et al.*, 2010). Ce mécanisme est une des bases de la présentation croisée (cross-presentation) des antigènes où des peptides du soi sont présentés en étant associés aux récepteurs du CMH (Massa *et al.*, 2005). Les protéines de stress extracellulaires fourniraient donc aussi un signal de danger qui engendrerait le déclenchement du système immunitaire (figure 10).

Ainsi, le relargage des complexes Hsp70/peptide serait à l'origine d'une amplification de la réponse immunitaire ciblant la tumeur. L'utilisation de Hsp70 comme adjuvant dans des vaccins pourrait induire une inhibition de la croissance tumorale en favorisant le système immunitaire et la présentation croisée des antigènes (Ciupitu *et al.*, 2002 ; Massa *et al.*, 2004 ; Murshid *et al.*, 2008 ; Gong *et al.*, 2010).

Toutefois, les mécanismes moléculaires de cette action sont encore assez méconnus. Le complexe Hsp70/peptide, qu'il soit présenté à la surface cellulaire, relargué par les cellules cancéreuses ou apporté par le vaccin, serait reconnu par des récepteurs comme les TLR (Toll Like

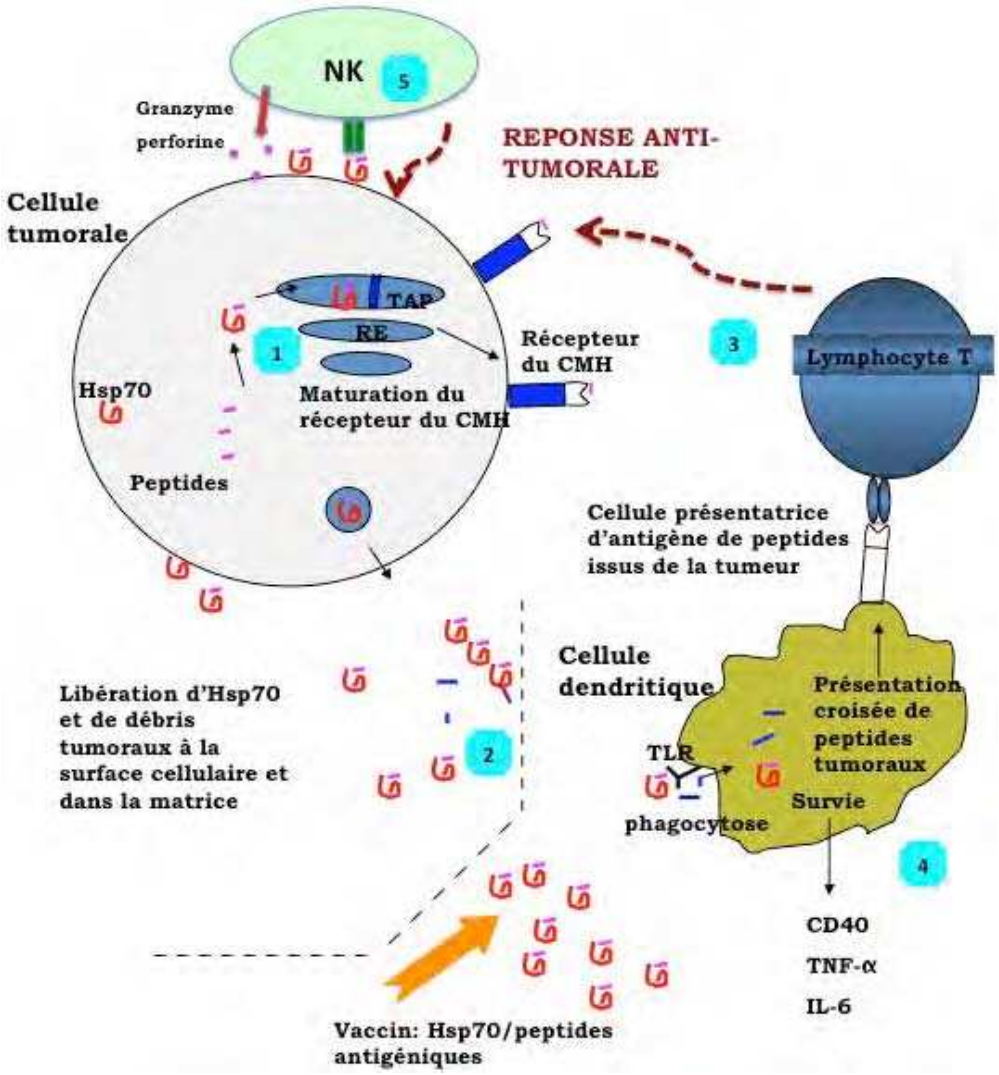

Figure 11 : *1. Hsp70 participe au guidage des peptides antigéniques issus de la dégradation par le protéasome. Elle permet leur association, avec l'aide des transporteurs TAP, aux récepteurs du CMH de classe I.*
2. Dans une cellule cancéreuse, le complexe Hsp70/peptide est relâché dans la matrice extracellulaire. Ce complexe est reconnu par des récepteurs TLR d'une cellule dendritique ce qui va induire sa phagocytose. On a alors une présentation croisée en tant que peptide antigénique.
3. La reconnaissance de l'antigène par un lymphocyte T va activer toute la réponse immunitaire ce qui va induire l'activation de la réponse anti-tumorale.
4. La liaison du complexe peptide/Hsp70 va aussi induire un signal de survie chez la cellule dendritique entraînant la synthèse de facteurs amplificateurs de la réponse immune.
5. Les celles NK reconnaissent directement les Hsp extracellulaires et vont directement cibler ces cellules via leur système lytique granzyme et perforine.
(D'après Massa et al., 2005 ; Murshid et al., 2008 ; Chen et al., 2009 ; Javid et al., 2009 ; Gong *et al.*, 2010*).*

Receptors) 2 et 4 des cellules dendritiques (Chen *et al.*, 2009). La liaison entre ce complexe et le récepteur activerait la voie de survie NF-κB. Cette dernière provoquerait la synthèse de nombreux facteurs nécessaires à la réponse immunitaire telles que CD40, IL-6, TNF-α… Tous ces agents sont des initiateurs de la réponse immune et permettraient d'amplifier la réponse anti-tumorale

préexistante. On aurait aussi une phagocytose de débris issus de la nécrose des cellules cancéreuses qui pourrait activer une réponse immune anticancéreuse (Javid *et al.*, 2009).

Il semble enfin que les complexes Hsp/peptides pourraient être internalisés et présentés à la surface de cellules dendritiques (Massa *et al.*, 2005). Cette présentation permettrait la reconnaissance de ces peptides antigéniques par des lymphocytes T cytotoxiques et fournirait ainsi des épitopes spécifiques des cellules cancéreuses. Il semblerait aussi que la présence des protéines de stress et plus particulièrement de Hsp70, soit importante pour activer les cellules NK (Natural Killer), les cellules de l'immunité innée qui ne nécessitent pas de présentation d'antigènes spécifiques (Zeng *et al.*, 2006) (figure 11).

CONCLUSION- PERSPECTIVES

Les protéines de stress, du fait de leur rôle de chaperons moléculaires, jouent un rôle majeur dans le maintien de l'homéostasie cellulaire. En conditions de stress, ce rôle est renforcé car la cellule subit des altérations diverses qui peuvent conduire à sa mort. Les Hsp participent activement à la cytoprotection et favorisent donc parfois la sauvegarde d'anomalies, qui en s'accumulant peuvent participer à la cancérisation.

Si l'on considère ce phénomène comme un processus multi-étapes, on peut penser que la présence de protéines protectrices favorise l'échappement tumoral. D'ailleurs, il semble que le niveau d'expression des Hsp soit plus important au fur et à mesure de la cancérisation, et qu'il augmente en réponse aux différents traitements (Ciocca et Calderwood, 2005).

Les grands espoirs engendrés par les inhibiteurs d'Hsp90 suggèrent que les différentes Hsp peuvent être considérées comme des cibles thérapeutiques anticancéreuses accessibles. Il reste cependant à affiner les études sur les mécanismes moléculaires de cytoprotection des Hsp, à découvrir des inhibiteurs de Hsp27 et 70 et à progresser au niveau de l'étude des inhibiteurs de Hsp90 déjà existants.

Il apparaît aussi que les Hsp, comme toutes les protéines anti-apoptotiques, peuvent être utilisées dans le pronostic cancéreux. Des prédictions de radio et de chimiorésistance pourraient être envisagées en testant le niveau d'expression des protéines de survie, ce qui donnerait lieu à une thérapie personnalisée pour chaque patient et chaque type de cancer.

PROJETS DEVELOPPES

Au cours de mes travaux de thèse, j'ai tenté d'analyser les effets du ciblage de Hsp27 comme thérapie anticancéreuse. En effet, cette protéine appartient à la famille des protéines anti-apoptotiques et inhibe la mort cellulaire. Elle est surexprimée dans de très nombreux types tumoraux et forme une cible thérapeutique majeure. Au laboratoire, nous avons caractérisé les effets du ciblage de Hsp27 par deux stratégies distinctes.

D'une part, nous avons identifié, isolé et caractérisé des aptamères peptidiques, peptides stabilisés capables d'inhiber les fonctions d'une protéine cible par compétition d'interaction. Ces aptamères permettent d'inhiber les activités tumorigènes de Hsp27, à la fois dans des lignées cellulaires mais aussi dans des xénogreffes réalisées chez la souris Nude.

La stratégie des aptamères permet d'isoler une structure peptidique de base capable de se lier et d'inhiber une cible de manière spécifique. Le but est de modéliser cette structure et de réaliser un crible informatique de « drug design » afin d'isoler des structures chimiques proches de celle du peptide précédemment caractérisé. Des études commencent à être réalisées avec les aptamères comme outil moléculaire de ciblage. Ainsi, une étude a permis de cibler par des aptamères certains mutants de p53 mais pas la protéine sauvage et de modéliser ces structures (Guida *et al.*, 2008).

D'autre part, nous avons analysé les effets de la déplétion de Hsp27 dans plusieurs lignées cancéreuses. La diminution constitutive du taux de Hsp27 dans des lignées cancéreuses permet de ralentir la prolifération cellulaire. Nous avons également caractérisé l'effet de la déplétion de Hsp27 sur l'établissement de métastases spécifiques de l'os. Ainsi, nous avons pu mettre en évidence que cette stratégie anti-sens permettait d'inhiber la formation de métastases après injection de lignées directement dans le sang des animaux. Parallèlement à cette étude nous avons réalisé des xénogreffes directement dans le tibia des animaux pour analyser la croissance de tumeurs dans les mêmes conditions de facteurs de croissances. Il apparait d'une même manière que la baisse du taux de Hsp27 entraine une inhibition de la croissance tumorale. Ces résultats sont à mettre en corrélation avec les résultats que nous avons obtenus pour les tumeurs réalisées dans l'étude de caractérisation des aptamères où l'interférence ARN formait un contrôle positif.

Enfin, nous avons pu montrer que la déplétion de Hsp27 de manière stable dans des lignées cancéreuses induit la dégradation de protéines clefs importantes dans différents mécanismes

cellulaires. Ces protéines sont la caspase 3, le facteur de transcription STAT2 et l'histone deacétylase HDAC6. Hsp27 par son activité chaperon permettrait leur stabilisation et augmenterait leur demi-vie de manière très significative. Ce mécanisme moléculaire n'avait été jusqu'alors mis en évidence que pour Hsp90.

MATERIEL ET METHODES

MATERIEL ET METHODES

1. Double hybride de levures

Afin de visualiser les interactions existant entre Hsp27 et ses interacteurs (les PA ou les formes mutantes de Hsp27) nous avons utilisé la technique du double hybride de levures (Fields et Song, 1989). Les souches de levures sélectionnées possèdent un génome haploïde de type a /α. La mise en présence des deux souches (= *mating type*), permet de réaliser leur conjugaison, et les deux protéines appât/proie sont produites dans ces conjugants. L'expression concomitante des deux protéines dans les levures, va permettre de tester leur interaction. Ainsi, lors d'une interaction appât/proie, la reconstitution du transactivateur transcriptionnel LexA/B42 va induire l'activation de l'expression du gène rapporteur codant la β-galactosidase (Fields et Song, 1989).

1.1. Vecteurs de double hybride utilisés

Les vecteurs utilisés sont pEG202 (= vecteur appât) et pJG4-5 (= vecteur proie). Ces vecteurs pEG202 et pJG4-5 possèdent respectivement le gène codant une enzyme participant à la synthèse de l'Histidine et du Tryptophane. Un autre vecteur pJK103, contient la séquence codant le rapporteur Lac Z sous contrôle de l'opérateur LexA, sensible au transactivateur LexA/B42. Par ailleurs, ce vecteur contient le gène permettant la synthèse de l'Uracile. Les vecteurs sont amplifiés après transformation de bactéries DH5α (Invitrogen). Le plasmide est extrait et purifié à l'aide d'un kit midi-prep (Genelute plasmid midi-prep kit, Sigma).Transformation et conjugaison

1.2. Transformation et conjugaison

Cette étape consiste à introduire les vecteurs d'expression dans les levures. Les levures des souches d'intérêts sont préalablement culottées (5000rpm, 1min). Ce culot est repris dans 1ml de TE 1X pH 7.5 stérile. Après centrifugation, le culot est repris dans 250 µL d'une solution d'acétate de lithium à 100 mM, TE1X. 1µg de chaque plasmide et 10µg d'ADN dénaturé de sperme de saumon sont ajoutés à la suspension. Enfin, 600 µL d'une solution LiAc/40% PEG sont additionnés à la suspension avant incubation de 30 min à 30°C.

Après addition de 70 µL de DMSO, un choc thermique de 7 min est réalisé à 42°C. Les levures sont ensuite lavées puis étalées sur milieu sélectif. Les transformants sont sélectionnés sur des milieux dépourvus de l'acide aminé dont le vecteur incorporé dirige la synthèse.

1.3. Milieux utilisés et tests d'auto-activation de l'appât

Toutes les souches de levures utilisées présentent un génome défectif pour les gènes *trp1*, *his3*, et *ura3*. Par ailleurs, les gènes *leu2* et *ade2* sont placés dans le génome sous contrôle de l'opérateur LexA. Leur expression est donc conditionnée par la reconstitution du transactivateur transcriptionnel.

Les souches 226α et 210a sont utilisées pour le crible de la banque. Une conjugaison de souches a et α est effectuée en testant à chaque fois l'interaction entre un vecteur appât pEG202 et un vecteur proie pJG45. La souche 226α a préalablement été transformée avec le vecteur pJK103 contenant le gène codant le rapporteur LacZ, sous contrôle de l'opérateur LexA. La conjugaison est réalisée sur milieu riche YAPD. Les conjugants sont répliqués à l'aide de velours stériles sur trois milieux sélectifs différents. Seules vont se développer les levures possédant chacun des trois plasmides.

Les milieux de sélection utilisés sont nommés :- SD-U-H-W ; le sucre est le dextrose ; le milieu est dépourvu en Histidine, Uracile et Tryptophane.

- SD-U-H-W+X-Gal ; le sucre est le dextrose ; le milieu est dépourvu en Uracile, Histidine, Tryptophane supplémenté en X-Gal.

- G/R –U-H-W +X-Gal ; les sucres sont le galactose et le raffinose, le milieu est dépourvu en Uracile, Histidine et Tryptophane supplémenté en X-Gal.

Les résultats d'interactions sont analysés sur le milieu G/R-U-H-W+X-Gal, en effet la synthèse de la fusion B42-proie est sous contrôle du promoteur minimal Gal. Le milieu SD-U-H-W+X-Gal sert de témoin négatif car seule l'interaction entre l'appât et la proie induit la synthèse de β-Galactosidase. Le milieu SD-U-H-W sert de contrôle positif de croissance.

Les tests d'autoactivation de l'appât, de pénétrance du phénotype et de détermination du bruit de fond ont également été réalisés. Cette première étude a permis de mettre au point le système double hybride de criblage des banques d'aptamères c'est-à-dire de choisir les souches de levures et les gènes rapporteurs à utiliser pour optimiser le crible avec l'appât Hsp27.

1.4. Crible de la banque

Une suspension de levure de souche MB226α, préalablement transformée avec le vecteur rapporteur pJK103 et le vecteur appât pEG202-Hsp27, est mise en culture sur la nuit. Les levures de la souche MB210a constituant les deux banques d'aptamères, sont synchronisées en phase G1

après décongélation. La conjugaison s'effectue sur la nuit et les colonies sont étalées sur milieu sélectif GR-UHW+XGal. Les clones se développant et exprimant la β-galactosidase sont ainsi isolés et repiqués.

Les plasmides codant les aptamères sont extraits par lyse des levures et extraction Phenol-Chloroforme. L'ADN plasmidique contenu dans la phase aqueuse est précipité à l'éthanol. Le culot est séché puis repris dans 40µl de TE (10mM Tris ; 1mM EDTA). Les plasmides sont amplifiés grâce à la transformation de bactéries MH3 préalablement rendues compétentes.

1.5. Clonage des formes mutantes de Hsp27

Les séquences d'intérêt sont amplifiées par réaction de « Polymerase Chain Reaction » (PCR) pour les différents clonages réalisés. Une ADN polymérase possédant une activité *proof-reading* (pfx Invitrogen) ainsi que des amorces spécifiques d'Hsp27 contenant un site de restriction pour les enzymes XhoI ou EcoRI en leur extrémité 5', sont utilisées pour cette amplification. Ces sites de restriction permettent le clonage de la région amplifiée dans les différents vecteurs appâts et proies. Une fraction aliquoté du produit d'amplification est déposée sur gel d'agarose 1.2% pour vérifier que l'amplification a bien été réalisée.

Un gradient de température de 0.5°C pour les 10 premiers cycles est réalisé lors de l'amplification des fragments. 30 cycles, comprenant chacun : une dénaturation de 30 secondes à 94°C, une phase d'élongation de 1 minute à 55°C et une phase d'hybridation à 68°C pendant 1 minute, sont réalisés.

Le produit d'amplification PCR est purifié (PCR extraction Kit, QIAGen), puis digéré par les enzymes de restriction EcoRI et XhoI. Après digestion, l'insert est purifié sur gel d'agarose 1,2% et extrait de l'agarose (QIAquick Gel Extraction Kit, QIAGen). Enfin, l'insert est lié aux différents vecteurs utilisés. Ces derniers sont ensuite séquencés (Genome Express, Meylan).

2. Culture cellulaire

2.1. Milieux de culture et lignées cellulaires

Les cellules utilisées sont des fibroblastes de cancer du col de l'utérus de type HeLa, des cellules SQ20B de carcinome tête et cou (head and neck cancer), des cellules BO2 issues de la lignée métastatique de tumeur mammaire MDA-MB231 et des cellules de carcinome de sein MCF-7. Les cellules sont cultivées, à 37°C sous 5% de CO_2, dans un milieu Dulbeco's Modified Eagle Medium (DMEM, Gibco), contenant 10% de sérum de veau fœtal (SVF), 0,05% d'antibiotique (pénicilline, streptomycine) et 0,04% d'anti-fongique (fungizone).

2.2. Transfections transitoires

Les cellules HeLa sont ensemencées à raison de $1,5x10^6$ cellules par boîtes de culture de 100mm de diamètre. Chaque transfection est réalisée par addition sur les cellules de 7µg de vecteur ADN et de 50µl de Lipofectamine (Invitrogen) selon le protocole du fabriquant, en présence de milieu sans sérum pendant 3 heures (Optimem Gibco). Les différents tests sont effectués 48 heures après transfection.

2.3. Lignées stables

Les lignées stables ont été obtenues après transfection des vecteurs pSUPER-Neo-Sh27, pSUPER-Ms-Sh27, pSUPER-Neo-Sc27, par isolement clonale à raison de 3 clones indépendants par lignée (*cf.* mat et met 4.2.)

3. Analyse de la mort cellulaire

3.1. Détermination de la mort cellulaire par coloration au cristal violet

Les cellules transfectées par les différents aptamères sont ensemencées 24h après transfection, en plaque 96 puits à raison de $7,5x10^4$ cellules/puits. Les cellules sont traitées par la staurosporine, un inhibiteur de kinases (Sigma), ajoutée au milieu de culture pendant 12 heures.

Le milieu est éliminé ainsi que les cellules mortes non adhérentes par simple retournement de la plaque de culture. Les cellules adhérentes sont colorées par 30µl d'une solution de cristal

violet 5%, méthanol 20%. Les densités optiques sont lues en plaques (appareil Victor™, PerkinElmer) après dissolution par une solution de citrate de sodium 5%, méthanol 50%, pH 4,2.

3.2. Cytométrie en flux

Les cellules HeLa sont préalablement traitées, 48h après transfection, par différentes concentrations de staurosporine pendant 6 heures. Les cellules sont récoltées par trypsination et centrifugation. Après lavage au PBS, les cellules sont reprises dans 200µl de tampon contenant l'Annexin-V couplé au FITC (AbC306FI, AbCys) et incubées 10 minutes à l'obscurité. Après centrifugation, les cellules sont reprises dans 400µl de tampon contenant l'iodure de propidium.
Les mesures d'incorporation, de l'iodure de propidium et de l'Annexin-V, sont effectuées au cytomètre de flux avec les filtres FL1 et FL3.

3.3. Activation des caspases exécutrices 3 et 7

Les cellules sont ensemencées, 24h après transfection, en plaques 96 puits à raison de $1x10^5$ cellules/puits. Les cellules sont traitées, pendant 4h, par différentes concentrations de staurosporine. Le milieu est éliminé par retournement de la plaque de culture. Les cellules sont ensuite incubées pendant 30min, en présence de 10µl/puits de tampon caspases Glo 3/7 assay (Promega). L'activation des caspases effectrices 3 et 7 est révélée par émission luminescente à 485nm.

Une coloration par le cristal violet est réalisée en parallèle, dans les mêmes conditions de traitement, pour uniformiser les quantités de cellules déposées entre les échantillons.

3.4. Mort clonogénique

La mort clonogénique après irradiation est déterminée après des irradiations comprises entre 0.5 et 8 Gy. Les cellules sont remises à incuber durant un temps correspondant à 6 divisions cellulaires, ce qui forme des colonies théoriques de 64 cellules. Après un lavage au PBS, les cellules sont colorées au Giemsa, 30 min. Les valeurs expérimentales permettent de définir une courbe à partir de l'équation mathématique ou ($SF= \exp [-\alpha \times D - \beta \times D^2]$.

SF représente la fraction survivante et D représente la dose d'irradiation administrée. Cette courbe permet de définir la fraction de survie à 2 Gy ou SF2, qui est considérée comme un index de radio sensibilité.

3.5. Immunohistochimie

3.5.1. TUNEL

La fragmentation de l'ADN pour les coupes tumorales paraffinées est analysée par la technique TUNEL (TdT-mediated dUTP Nick End Labelling) avec le kit Dead End Fluorimetric TUNEL System, selon le protocole du fabriquant (Promega, France). Après traitement au xylème et réhydratation dans un gradient alcoolique, les coupes sont fixées au PFA 4%. Les cellules sont perméabilisées avec une solution de protéinase K (20µg/ml) et incubées en atmosphère humide et absence de lumière, en présence d'une solution de dUTP-isothiocyanate de fluorescéine (FITC) et de terminale transférase 1h, 37°C. La réaction est arrêtée par ajout du tampon SSC 2X. Les lames sont montées en VECTASHILED™ après rinçage au PBS, puis examinées au microscope à fluorescence.

3.5.2. Prolifération, Ki67.

Les coupes paraffinées sont traitées au xylème et un démasquage antigénique est effectué dans une solution tampon à 0.1 mol/L EDTA pH7.4 ; 95°C, 10min. L'activité peroxydase endogène est bloquée par traitement à l'eau oxygénée H202, 0.3%. Après lavage au PBS, les lames sont incubées dans une solution d'anticorps monoclonal de souris anti-Ki67 (Clone MIB-1, DAKO). L'anticorps secondaire est un Ig de chèvre couplé à la peroxydase de Rainford ($1/100^{ème}$). Après lavage au PBS, la révélation de la peroxydase est effectuée par ajout d'une solution de 3.3'-diaminobenzidine (Sigma, France), suivie d'une contre coloration à l'hematoxyline. Les lames sont montées en VECTASHILED™. L'index de prolifération est déterminé par le pourcentage de cellules positives pour le marqueur Ki67 par rapport au nombre total de cellules dans 20 champs aléatoires.

4. <u>Biologie moléculaire</u>

4.1. Western Blot

Les protéines sont séparées par électrophorèse sur gel d'acrylamide-bis acrylamide. Après migration les protéines sont transférées sur membrane de nitrocellulose (Schleicher & Schuell) sur

Protéine reconnue	Origine	Fabricant
Actine	Mouse	Chemicon MAB1511R
Akt-1	Mouse	Santa CruzSc-5298
P-Akt (ser473)	Rabbit	Santa Cruz Sc-7985-R
Bax (N-20)	Rabbit	Santa Cruz Sc-493
Bcl-2	Mouse	Santa Cruz Sc-509
Bcl-xl (H-5)	Mouse	Santa Cruz Sc-8392
Caspase-3	Mouse	Alexis ALX-804-305
Cyclin-D1	Mouse	Santa Cruz Sc-246
Cyclin-D3	Mouse	Santa Cruz Sc-6283
HA-tag	Mouse	Santa Cruz Sc-7392
HDAC-6 (H-300)	Mouse	Santa Cruz Sc-11420
Hsp27	Mouse	Stressgen SPA-800
Hsp70	Mouse	Stressgen SPA-820
Mcl-1	Mouse	Santa Cruz Sc-12756
Myc-tag	Rabbit	Sigma C 3956
p27 (M-197)	Rabbit	Santa Cruz Sc-776
Stat-2 (C-20)	Rabbit	Santa Cruz Sc-476
Survivin (D-8)	Mouse	Santa Cruz Sc-17779
Thioredoxine	Rabbit	Santa Cruz Sc-801
Alpha-tubuline	Rabbit	Cell Signaling #2144

Table 5 : *Récapitulatif des anticorps utilisés lors des différentes études.*

la nuit à 25V, dans une solution de Tris-Glycine 0,5X –Ethanol 20%. Une étape de saturation dans du T-TBS (20mM Tris ; 0,137 mM ; pH 7,6) Tween 0,1%, Lait Ecrémé 5%, est suivie d'une incubation avec un anticorps primaire (Table 6). Après trois rinçages au T-TBS les membranes sont incubées avec un anticorps secondaire couplé à la peroxydase. La révélation est réalisée par addition du substrat de l'enzyme (système de chimioluminescence ECL, Amersham) et exposition sur film (Kodak).

Nom	Numéro	Séquence
ShRNA27	Oligo A	5'ACCGCTGCAAAATCCGATGAGACTTCCTG TCATCTCATCGGATTTTGCAGCTTTTTC 3'
	Oligo B	5' TGCA GAAAAA GCTGCAAAATCCGATGAGA TGACAGGAAG TCTCATCGGATTTTGCAGC 3'
MsRNA27	Oligo A	5' ACCGACCAATGATGGTGTGGTG CTTCCTGTCA CACCACACCATCATTGGTC TTTTTC 3'
	Oligo B	5' TGCA GAAAAA GACCAATGATGGTGTGGTG TGACAGGAAG CACCACACCATCATTGGTC 3'
ScRNA27	Oligo A	5' ACC GAGTGCTGACGAGTGCGAG CTTCCTGTCA CTCGCACTCGTCAGCACTC TTTTTC 3'
	Oligo B	5' TGCA GAAAAA GAGTGCTGACGAGTGCGAG TGACAGGAAG CTCGCACTCGTCAGCACTC 3'
ShHDAC6	Oligo A	5 ' ACC GTTCCCCGCTCTATCCCCAAT CTTCCTGTCA ATTGGGGATAGAGCGGGGAAC TTTTTC 3'
	Oligo B	5' TGCA GAAAAA GTTCCCCGCTCTATCCCCAAT TGACAGGAAGATTGGGGATAGAGCGGGGAAC 3'
MsHDAC6	Oligo A	5 ' ACC GTCACCCGCTCTATACCAAAT CTTCCTGTCA ATTTGGTATAGAGCGGGTAGC TTTTTC 3'
	Oligo B	5' TGCA GAAAAA GTCACCCGCTCTATACCAAAT TGACAGGAAGATTTGGTATAGAGCGGGTAGC 3'
ScHDAC6	Oligo A	5 ' ACC CTCTCCCGCTATTTCCGCTTA CTTCCTGTCA TAAGCGGAAATAGCGGGAGAG TTTTTC 3'
	Oligo B	5' TGCA GAAAAA CTCTCCCGCTATTTCCGCTTA TGACAGGAAG TAAGCGGAAATAGCGGGAGAG 3'

Table 6 : *Séquences des brins matrices nécessaires à la construction des shARN.*

4.2. Constructions de ShARN

Les vecteurs utilisés pour construire les ShARN sont les vecteurs pSuper-Neo et pSh-puro. Deux oligonucléotides synthétiques sont hybridés et clonés dans les différents vecteurs (Table6). Les constructions stables sont obtenues par isolement clonal à raison de trois clones par boite de culture cellulaire pour chaque transfection réalisée. Les lignées sont maintenues en présence de puromycine (12µg/ml pour B02) et de Neomycine (10µg/ml pour les cellules HeLa ; 12 µg/ml pour MCF-7 et SQ20B).

4.3. Immunofluorescences

Les cellules sont transfectées et incubées sur lamelles de verre. Après 3 rinçages au PBS froid, les cellules sont fixées au PFA 4% ; 15 min, puis perméabilisées au Triton X-100, 0.1%.

Après lavage, les lamelles sont incubées dans la solution contenant l'anticorps primaire dans du PBS X, 2% BSA ; RT. Les cellules sont lavées 3 fois 5min au PBS, puis incubées dans la solution d'anticorps secondaires en absence de lumière. Le montage lames/lamelles est réalisé en Mowiol (Sigma).

4.4. Chromatographie d'exclusion-diffusion

Les cellules ($3x10^7$) sont lavées au PBS 1x froid puis grattées. Après centrifugation, le culot est repris dans 1ml de tampon TEM froid (20mM Tris-HCl pH 7,4 ; 20mM NaCl ; 5mM MgCl2 ; 0,1mM EDTA) + 0,1% de Triton X100. Après incubation dans la glace pendant 15min, les cellules sont lysées à l'aide d'un Potter puis centrifugées à 4°C pendant 10min à 14 000rpm. Le surnageant est déposé sur une colonne de Sépharose CL-6B (1cm x 100cm) (Pharmacia) équilibrée avec du tampon TEM. L'efflux est récolté à l'aide d'un collecteur en différentes fractions contenant des protéines et des complexes protéiques de poids moléculaire décroissant. L'analyse se fait par Western-blot après la précipitation des protéines et ajout de tampon d'échantillon 2x (62,5mM Tris-HCl pH 6,8 ; 1% SDS ; 0,1M dithiotreitol ; 10% glycérol et 0,01% bleu de bromophénol). Les colonnes sont calibrées en utilisant des marqueurs de poids moléculaire : Bleu Dextran (> 2 000kDa), thyroglobuline (660kDa), apoferritine (443kDa), α-amylase (200kDa), albumine (66kDa) et anhydrase carbonique (29kDa).

4.5. Co-immunoprécipitation

4.5.1. Sur fractions de colonne

Les échantillons protéiques issus des fractions de colonne enrichies en protéines d'intérêt sont mélangés avec l'Anticorps Goat Polyclonal anti Hsp27 (Santa-Cruz Biotechnology, INC) et incubés 4h sur une roue tournante à 4°C. Des billes de Protéine-G couplée à l'Agarose (Invitrogen) équilibrées dans du tampon TEM sont ensuite ajoutées aux échantillons qui sont ensuite replacés sur la roue. Après 4h d'incubation, les échantillons sont rincés plusieurs fois dans du tampon TEM puis repris avec du tampon d'échantillon 2x et bouillis pendant 5minutes. Le surnageant est récupéré et le culot est repris dans 50µl d'eau, vortexé puis centrifugé. Le surnageant est ajouté au précédent. Les surnageants récupérés sont ensuite déposés sur gel de polyacrylamide pour une analyse par Western-blot.

4.5.2. Sur lysat cellulaire

Les cellules sont rincées par du PBS 1x froid puis grattées sur la glace dans 1ml de tampon de lyse froid (50mM Hepes pH 7,5, 150mM NaCl, 0,1% Tween 20, 1mM EDTA, 2,5mM EGTA, 10% glycérol, 1mM DTT, 0,1mM PMSF, 10µg/ml d'inhibiteurs de protéases Chymostatin (Sigma), Antipain (FLUKA-BioChemica), Pepstatin (Sigma), Leupeptin (Sigma). Les cellules sont incubées dans la glace pendant 30min et vortexées à intervalles réguliers puis subissent 3 cycles de congélation dans l'azote – décongélation dans un bain marie à 37°C. Après centrifugation à 4°C pendant 20min, le surnageant est séparé en 2 fractions : la fraction "Total", à laquelle on ajoute un volume équivalent de tampon d'échantillon 2x, et la fraction immune dans laquelle 5µL d'anticorps anti-Hsp27 (Goat Polyclonal, Santa Cruz Biotechnology, INC) ont été ajoutés. Après 3h d'agitation sur une roue placée à 4°C, la fraction immune est ajoutée à 100µL de Protéines-G couplées à l'Agarose (Invitrogen) lavées dans du binding buffer (0,01M sodium phosphate pH 7,0, 0,15M NaCl) puis du tampon de lyse. Le mélange est placé sur une roue tournante à 4°C pendant 3h. Après 3 lavages sur la glace dans du tampon de lyse froid, les protéines liées sont éluées comme précédemment décrit. Le culot obtenu après la lyse cellulaire est repris dans 1ml de PBS 1x et 100µl sont prélevés et ajoutés à 100µl de tampon d'échantillon puis bouillis 5min. Les échantillons sont ensuite déposés sur un gel de polyacrylamide et analysés par Western-blot.

5. Analyses *in vivo* :

5.1. Xénogreffes

5.1.1. Etude aptamères

Pour l'étude concernant les aptamères peptidiques les xénogreffes sont réalisées par injection sous cutanée à raison de 3×10^6 de cellules SQ20B. Deux lignées par souris sont injectées sur la face interne de la patte de souris NUDE athymiques femelles de 4 semaines (SWISS-Foxn1^{nu}, Charles river, France). Les anesthésies ont lieu au moment de la greffe par injection intra-péritonéale de kétamine (Ketalar, 80 µg/g, Merial) et xylazine (Rompun, 80 µg/g, Bayer).

5.1.2. Tumeurs osseuses et métastases

Pour étudier la formation de métastases, des cellules B02 (5×10^5 cellules dans 100µL de PBS) sont injectées dans la veine caudale de souris Nude anesthésiées. La croissance tumorale est analysée par injection directe dans la moelle osseuse du tibia droit de chaque souris. La dissémination et le développement tumoral sont visualisés par bioluminescence. L'ostéolyse est analysée par radiographie (films MIN-R2000, Kodak) avec un appareil à rayon-X (MX- 20, Faxitron X-Ray Corporation). La quantification des surfaces de lyse sur radiographies a été réalisée avec une station d'analyse d'image (Visiolab 2000, Biocom).

5.2. Luminométrie

La masse tumorale des animaux métastatiques est mesurée par des techniques d'imagerie non invasive. La fluorescence et la bioluminescence émises par les cellules tumorales sont mesurées sur des appareils d'analyse d'images (FluorImager, Molecular Dynamics et NightOwl B 983 NC100 ; Berthold). Le développement métastatique ainsi que la croissance tumorale sont analysés chaque semaine du protocole. Les surfaces tumorales sont évaluées à l'aide de logiciels pour chaque mesure effectuée (Berthold).

5.3. Radiographie

L'ostéolyse induite par les cellules tumorales est mesurée par radiographie avec un appareil à rayon-X (MX-20, Faxitron X-Ray Corporation). La quantification des plages de lyse osseuse sur les radiographies est réalisée avec une station d'analyse d'image (ExploraNova Morpho). Les résultats ont été analysés avec le logiciel Statview v5.0. Les résultats sont exprimés comme la moyenne ± SD (Standard Deviation) et les différences sont considérées comme statistiquement significatives dès lors que la valeur de *p* est inférieure à 0,05.

5.4. Coupes d'organes

A la fin des protocoles expérimentaux, les pattes arrières des souris métastatiques et non métastatiques sont prélevées, fixées dans une solution de paraformaldéhyde (4% p/v) puis inclues dans une résine plastique de métacrylate de méthyle. Ensuite des coupes de 7µm d'épaisseur sont

réalisées à l'aide d'un microtome HM350S (microm), colorées au trichrome de Goldner et enfin montées sur lamelles.

Les lamelles sont analysées en utilisant une station d'analyse d'image (ExploraNova Bone). La destruction osseuse (BV/TV) est calculée selon le rapport entre le volume osseux trabeculaire et cortical (bone volume ou BV) et le volume tissulaire total (tissu volume ou TV). Le volume métastatique osseux (Tumor burden ou TB) est mesuré par rapport au volume total de tissu mou (Soft tissu volume ou STV).

RESULTATS

PUBLICATION - 1

PUBLICATION 1 - Hsp27 (HspB1) and alphaB-crystallin (HspB5) as therapeutic targets

FEBS Lett. 2007 Jul 31;581(19):3665-74.

Dans cette courte revue, nous envisageons les deux petites protéines de stress Hsp27 et αB-cristallin, en tant que cibles thérapeutiques dans les pathologies cancéreuses. Ces deux petites protéines de stress sont souvent surexprimées dans de nombreux types tumoraux (Ciocca et Calderwood, 2005). Elles interviennent dans de nombreux mécanismes moléculaires et protègent contre la mort cellulaire et en particulier lors de l'apoptose. Ces activités anti-apoptotiques participeraient à la survie des cellules cancéreuses et à leur échappement vis à vis de l'organisme et du système immunitaire. Les mécanismes moléculaires de protection contre la mort cellulaire sont dépendants de la dynamique structurale de Hsp27 et de l'αB-cristallin.

Bien que majoritairement étudiées dans le développement tumoral, ces protéines possèdent aussi des implications dans d'autres pathologies ou la mort cellulaire joue un rôle central comme l'asthme, les myopathies ainsi que les maladies neuro-dégénératives.

FEBS Letters 581 (2007) 3665–3674

Minireview

Hsp27 (HspB1) and αB-crystallin (HspB5) as therapeutic targets

André-Patrick Arrigo[a,*], Stéphanie Simon[a,b], Benjamin Gibert[a], Carole Kretz-Remy[a], Mathieu Nivon[a], Anna Czekalla[a], Dominique Guillet[a], Maryline Moulin[a], Chantal Diaz-Latoud[a], Patrick Vicart[b]

[a] *Laboratoire Stress, Chaperons et Mort Cellulaire, CNRS, UMR5534, Centre de Génétique Moléculaire et Cellulaire, Université Lyon 1, Bat. Gregor Mendel, 16 Rue Dubois, F-69622, Villeurbanne Cedex, France*
[b] *EA 300 Stress et Pathologies du Cytosquelette, UFR de Biochimie, Université Paris 7, Paris, France*

Received 16 February 2007; revised 11 April 2007; accepted 15 April 2007

Available online 24 April 2007

Edited by Robert Barouki

Abstract Hsp27 and αB-crystallin are molecular chaperones that are constitutively expressed in several mammalian cells, particularly in pathological conditions. These proteins share functions as diverse as protection against toxicity mediated by aberrantly folded proteins or oxidative-inflammation conditions. In addition, these proteins share anti-apoptotic properties and are tumorigenic when expressed in cancer cells. This review summarizes the current knowledge about Hsp27 and αB-crystallin and the implications, either positive or deleterious, of these proteins in pathologies such as neurodegenerative diseases, myopathies, asthma, cataracts and cancers. Approaches towards therapeutic strategies aimed at modulating the expression and/or the activities of Hsp27 and αB-crystallin are presented.

Keywords: Hsp27; αB-crystallin; Neurodegenerative diseases; Myopathies; Cancers

1. Hsp27 and αB-crystallin: old and new

Heat shock proteins (Hsps) or stress proteins have in common a stimulated synthesis in response to heat shock or when the environment of a cell becomes deleterious and alters protein folding. In cells exposed to heat shock, Hsps act as molecular chaperones that counteract the formation of aberrantly folded polypeptides and allow their correct refolding during stress recovery. In addition of being expressed in stressed cells, some Hsps show a basal level of constitutive expression and act as in-house chaperone towards several fundamental cellular processes, such as protein intracellular transport, cytoskeletal architecture, mutations masking, translation regulation, intracellular redox homeostasis or protection against spontaneous or stimulated programmed cell death.

Mammalian Hsp27 (HspB1) and αB-crystallin (HspB5) belong to the family of small heat shock proteins (sHsps). In human, 10 different sHsps have been characterized but only few of them, as Hsp27, Hsp22 and αB-crystallin, are true heat shock proteins that display an enhanced synthesis in response to stress. Up until now, the more studied sHsps have been mammalian Hsp27 and αB-crystallin. sHsps are characterized by low molecular masses (12–43 kDa) and a conserved C-terminal domain (the α-crystallin domain, see Fig. 1). sHsps also contain a WDPF domain in their N-terminal part and a non conserved flexible domain which constitutes the C-terminal part of the proteins. sHsps share the property to form globular oligomeric structures that are characterized, in mammalian cells, by molecular masses ranging from 50 to about 700–800 kDa. The dynamic organization of sHsps oligomers appears to be a crucial factor which controls the activity of these proteins. We still do not have a good knowledge of the structural organization of sHsps. This is mainly due to the heterogenous size and dynamic properties of sHsps oligomers and of their ability to form hetero-complexes with other members of the sHsps family. An intriguing property of some sHsps, such as Hsp27 and αB-crystallin, concerns their ability to be phosphorylated and therefore under the control of several transduction pathways. Indeed, both proteins show rapid phosphorylation that modulates their activities in response to a wide variety of stimuli [1,2]. Both proteins have phosphorylated serine sites in the N-terminal part of the polypeptides, in the WDPF domain [2] and close to the α-crystallin domain. Hsp27 is phosphorylated at serines 15, 78 and 82 by mitogen-activated protein kinases associated protein kinases (MAPKAP kinases 2,3) which are themselves activated by phosphorylation by MAP p38 protein kinase [3,4] (see Fig. 1). As Hsp27, αB-crystallin is phosphorylated at three serine site corresponding to residues 19, 45 and 59. At least two pathways are implicated in the αB-crystallin phosphorylation: the MAPKAPK2 kinases are responsible of the phosphorylation of serine 59 while serine 45 appears under the control of p42/p44 MAPKinase. The kinase responsible of the phosphorylation of serine 19 is still not known. Hence, Hsp27 phosphorylation can be modulated by signals as diverse as those mediated by growth factors, differentiating agents, tumor necrosis factor, oxidative stress or heat shock [5,6]. In the case of α-crystallin, a recent study has shown that disorganization of microfilaments or microtubules networks results in the activation of convergent pathways to MAPK p38 [1]. At least in the case of Hsp27, phosphorylation was demonstrated to result in a decrease size of the oligomers [7].

In addition of being overexpressed in stress conditions, Hsp27 and αB-crystallin share the ability of having a tissue/cell

*Corresponding author. Fax: +33 4 72432685.
E-mail address: arrigo@univ-lyon1.fr (A.-P. Arrigo).

0014-5793/$32.00
doi:10.1016/j.febslet.2007.04.033

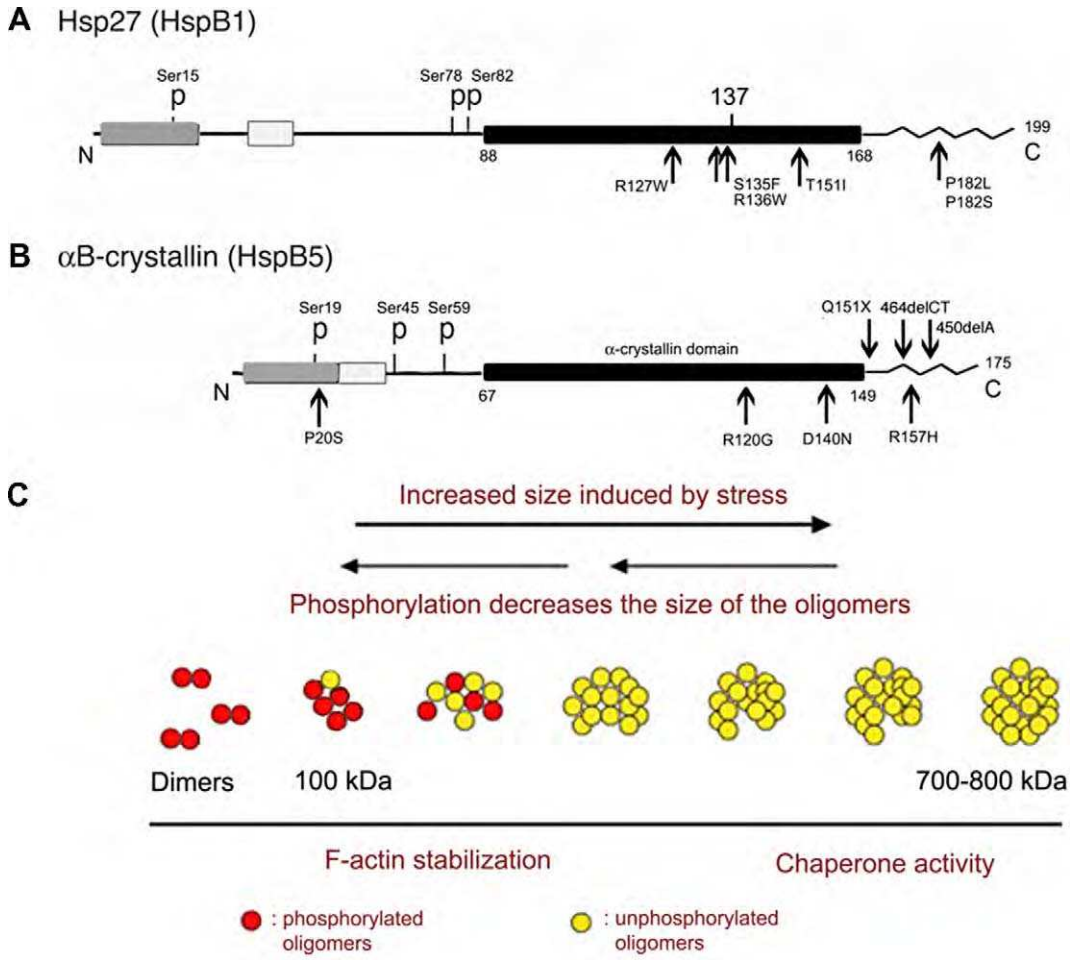

Fig. 1. Properties of human Hsp27 and αB-crystallin. (A) Organization of human Hsp27 and αB-crystallin protein sequences. Light box: conserved region; black box: alpha crystallin domain; gray box: WDPF domain; ΛΛΛΛΛ: flexible domain; P: phosphorylated serine residues. Amino acids are indicated. Position 137 in Hsp27 sequence corresponds to the only cysteine residue in the protein sequence. Its deletion abolishes dimer formation and knocks out Hsp27 protective activity. Positions of point mutations that are responsible of pathologies (see Table 2) are indicated by arrows. 464delCT: frame-shift mutant. The resulting mutant is modified from aa 155 and is truncated of 13 residues compared to wild type protein. 450delA: frame-shift mutant. The resulting mutant is modified from aa160 to aa184. This protein is larger than wild type polypeptide (175aa). (B) Biochemical properties of Hsp27. Stress favors the formation of large oligomers associated with unfolded polypeptides while phosphorylation does the reverse. The system is therefore in equilibrium. The formation of small oligomers may be required to bind unfolded proteins that are then stored at the level of the large oligomers. Phosphorylation may also favor the recycling of the large oligomers. Yellow circles indicate nonphosphorylated Hsp27 and red circle phosphorylated Hsp27. Large non-phosphorylated oligomers of sHsp (>300 kDa) have greater potentiality to protect the cell through their ability to display chaperone activity [6]. In contrast, small unphosphorylated oligomers of Hsp27 may act at the level of F-actin polymerization/depolymerization [32].

specific expression in the absence of stress which can be detected in the healthy adults as well as during the development of the organisms. In mammals, αB-crystallin is a major polypeptide of the eye lens where it is associated with the closely related αA-crystallin (HspB4) to form large hetero-oligomeric structures. In mice and rats, αB-crystallin is also constitutively expressed in tissues with high rates of oxidative metabolism, including, the heart, type I and type IIa skeletal muscle fibers, brain and oxidative regions of the kidney. Hsp27 tissue-specific expression resembles that of αB-crystallin. However, different levels of expression of these two proteins are often detected. The significance of the constitutive expression of these Hsps is probably linked to protection of the cells against stress or to a specific function in a particular tissue. This review summarizes the current knowledge about Hsp27 and αB-crystallin as well as the significance of the overexpression of these polypeptides in several pathological situations. Collectively, these observations lead to the conclusion that Hsp27 and αB-crystallin are major targets for the development of future therapeutic strategies against pathologies as diverse as neurodegenerative diseases, myopathies, asthma, cataracts and cancers.

Analysis of Hsp27 and αB-crystallin oligomers has revealed that these structures are in a dynamic equilibrium. It was then shown that the high molecular weight oligomeric structures formed by Hsp27 and αB-crystallin bear an ATP-independent chaperone activity and that phosphorylation induces modifications in oligomer size and chaperone-like activity [8]. For example, in heat shock treated cells which are prone to accumulate misfolded proteins, the large unphosphorylated oligomers of Hsp27 act as tanks that store misfolded polypeptides until they are either processed for refolding by ATP-dependent chaperones (i.e. Hsp70 and co-chaperones) [9] or degraded by the proteasome [10]. Recent studies of α B-crystallin have revealed that the β3 sequence of the α-crystallin domain (aa

Table 1
Multiple functions of αB-crystallin and/or Hsp27 and the corresponding interactions with (or functional modulation of) protein or peptide targets

Function(s)	Targets
Lens transparency and protection	αA-crystallin and other crystallin proteins
Heart protection	Titin, Hsp20
Cytoskeletal architecture and protection	F-actin Intermediate filament proteins (desmin, vimentin, GFAP, neurofilaments, filensin, phakinin, lamin) Microtubules and microtubule-associated proteins
Apoptosis resistance	Pro-caspase 3, cytochrome *c*, Smac/Diablo, Akt, DAXX, STAT3, Bcl-xs, Bax, P53
Ubiquitin–proteasome system	Fbx4, C8/α7 subunit of 20S proteasome, eIF4F and eIF4G complex, ubiquitin
Cell cycle regulation	Cyclin D1, p27kip1, P53
Redox homeostasis	Glutathione, G6PDH
Protein intracellular transport	Microtubule, SMN, neurofilaments
Stress signalling pathway	P38 cascade, I Kappa B kinase
Hormone signalling pathway	ERb (Estrogen cascade), hGMEB1 (glucocorticoïd hormones cascade)
Unknown nuclear function(s)	SMN, SC35
Unknown cytosolic function(s)	αB-crystallin, Hsp20, Hsp22, Hsp27
Pathological-related misfolded proteins	Desmin, GFAP, neurofilaments, ZASP, filamin C, myotiline, parkin, α-synuclein, prion protein, tau, β-amyloid, huntingtin, serpin, SOD, P150 dynactin, αA-crystallin, αB-crystallin, Hsp20, Hsp22, Hsp27
Virus	NS5A protein from Hepatitis C
Immune response	CD10, β2-microbulin
Unknown function in Sertoli cells	PASS 1
Golgi architecture	GM130

GFAP, glial fibrillary acidic protein; DAXX, death domain-associated protein 6; STAT3, signal transducer and activator of transcription 3; Fbx4, F-box only protein 4; eIF4F, eukaryotic translation initiation factor 4F; eIF4G, eukaryotic translation initiation factor 4G; G6PDH, glucose-6-phosphate dehydrogenase; SMN, survival motor neuron protein; SOD, superoxide dismutase; ER, estrogen receptor; SC35, splicing factor; hGMEB1, human glucocorticoid modulatory element-binding protein 1; NS5A, non-structural protein 5A; ZASP, LIM domain-binding protein 3; PASS 1, protein associated with small stress protein 1. GM130, golgi matrix-protein 130.

73–85) [11] may represent the interacting site with unfolded polypetide targets and the β3-β8-β9 surface of the alpha crystallin core domain may be an interface for complex assembly and chaperone activity [12]. Moreover, the N- and C-termini of human αB-crystallin appear important for the recognition, selection, and solubility of substrate proteins [13]. Hsp27 and αB-crystallin also share the ability to participate in the so-called "protein triage" that occurs in cells recovering from stress or committed to differentiate. Indeed, Hsp27 and αB-crystallin modulate the ubiquitin–proteasome pathway [14,15] (see Table 1) and are essential for proper disassembly–assembly of protein complexes to prevent undesirable interactions and aggregation [16,17]. In this respect, the lack of Hsp27 expression during early differentiation induces aberrant cell differentiation [16] or massive apoptosis [18–20]. Moreover, tissue-specific hetero-oligomeric structures of sHsps have been described [16] suggesting structurally independent sHsps chaperone complexes with distinct molecular targets [21]. Hence, these observations favor the hypothesis that highly modulable sHsp structural networks exist in the cell that rapidly react to cope with tissue-specific stress- or differentiation-induced protein damages and/or protein complexes reorganization.

An intriguing function of Hsp27 and αB-crystallin is the ability to increase the resistance of cells to oxidative injuries [22]. The phenomenon is not restricted to cell cultures and has been observed in whole animals [23]. Hsp27 and αB-crystallin expression correlates with decreased levels of reactive oxygen species (ROS) and nitric oxide ($NO^{\cdot}$) [6,24–26]. Consequently, in cells exposed to oxidative challenges, sHsps expression reduces lipid peroxidation, protein oxidation and F-actin architecture disruption [24–27]. These Hsps also uphold the mitochondrial membrane potential ($\Delta\Psi m$) level [24,28]; a phenomenon which provides the stressed cells with abundant ATP production that favors the activity of chaperones. The antioxidant activity of Hsp27 and αB-crystallin was found to depend on reduced glutathione [25]. The phenomenon probably depends on the upregulation of glucose-6-phosphate dehydrogenase (G6PDH) [23,24] (Table 1), the key enzyme that provides the reducing power of the cell by reducing NADP+ in NaDPH(H)+. In addition, recent results have shown that Hsp27 [29,30] or αB-crystallin (our unpublished information) expression decreases iron intracellular levels; a phenomenon which subsequently interferes with the formation, through iron-dependent Fenton reaction, of the potent macromolecules oxidizing hydroxyl radical (OH^{O}) [26]. As in the case of cells exposed to heat shock, the active form of Hsp27 appears associated with the large unphosphorylated oligomers of the protein [6,31].

Other functions have been assigned to Hsp27 and αB-crystallin that depend on the structural organization of these polypeptides. One example is the control of F-actin cytoskeletal integrity mediated by the small oligomers of Hsp27 [32,33]. This activity plays a crucial role in cells exposed to heat shock or oxidative stress because of the well-known ability of these stress to collapse F-actin cytoskeleton. Hsp27 was also found to regulate neutrophil chemotaxis and exocitosis through actin reorganization [34,35]. Moreover, a decrease in the level of expression of Hsp27 impairs growth and cytoskeletal organization [36]. These observations confirm that these polypeptides are major regulators of actin polymerization-depolymerization process. Moreover, Hsp27 and αB-crystallin also appear to bind and stabilize microtubules [1,37–39]. Taken together with the fact that αB-crystallin is a well known stabilizer of intermediate filaments [40,41], these observations enlighten the major role played by these Hsps in cytoskeletal architecture homeostasis.

Increased cellular resistance to several pro-apoptotic agents or conditions is observed in cells expressing high loads of Hsp27 [42–44]. On the opposite, inhibition of Hsp27 expression

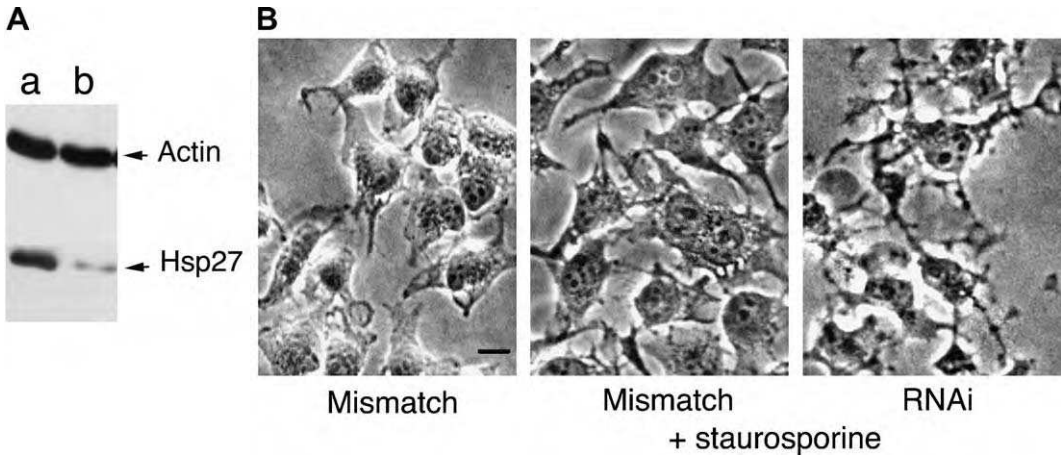

Fig. 2. Anti-apoptotic protective activity of constitutively expressed Hsp27 in HeLa cells. HeLa cells are human cancerous cells of the cervix that constitutively express high levels of Hsp27. These cells were transiently transfected with DNA vectors encoding either mismatch RNA (a) or RNAi Hsp27 sequences (b) (according to [104]). Two days after transfection, cells were either kept untreated or treated for 4 h with 0.2 μM of the kinase inhibitor and apoptosis inducer staurosporine. Hsp27 immunoblots (A) and phase contrast pictures (B) are presented. Note the drastic increase in cell death morphology induced by Hsp27 withdrawal. This leads to the conclusion that Hsp27 enhances the deleterious apoptotic resistance of these cancer cells. Bar: 15 μm.

sensitizes cells to apoptosis [45–48] (see Fig. 2). These phenomena result of the interaction of Hsp27 with several crucial apoptotic factors (see Table 1). For example, towards the intrinsic apoptotic pathway, Hsp27 acts upstream of mitochondria towards the signals that trigger the release of cytochrome *c* [45] or Smac/DIABLO [49] from mitochondria. In this respect, the ability of Hsp27 to protect F-actin network integrity [45] may play a crucial role. Hsp27 also acts down-stream of mitochondria at the level of cytochrome *c* and apoptosome [50]. The third site of action of this protein is at the level of pro-caspase 3 activation [51]. At the level of the Fas receptor pathway, Hsp27 was described to negatively interfere through an interaction with DAXX [52]. Hsp27 also binds and inhibits cellular factors involved in oncogenic signaling pathways, such as signal transducer and activator of transcription-3 (STAT3) [53]. This transcription factor is constitutively active in most tumors and controls the expression of key genes involved in cell transformation or apoptosis inhibition, such as those encoding Bcl-xL and survivin. An other important factor modulated by Hsp27 is Akt [54]. In vivo, Hsp27 anti-apoptotic property has been demonstrated [55,56]. Moreover, the transient expression of Hsp27 during cell differentiation is also related to a protection against apoptosis [18,43,57]. Concerning the structural organization of Hsp27 in cells exposed to apoptotic stimuli, the major information available today is that the large oligomers of Hsp27 inhibit in vitro caspase activation [58], hence suggesting a link with the chaperone activity of the protein.

Concerning αB-crystallin, its overexpression confers protection against a large panel of apoptotic stimuli while its silencing sensitizes cells to apoptosis [20,42,59,60]. Moreover, αB-crystallin negatively regulates apoptosis during myogenic differentiation [20]. Several steps in the apoptotic pathway are modulated by αB-crystallin. This protein has been shown to bind pro-apoptotic Bax, Bcl-x_S and P53 polypeptides (see Table 1) and to prevent their translocation to the mitochondria [61,62]. Downstream of mitochondria, αB-crystallin counteracts the activation of pro-caspase-3. Interestingly, phosphorylation of αB-crystallin at the level of serine 59 appears sufficient to provide maximal protection of cardiomyocytes against apoptosis [63].

2. Protein conformation and inflammation related diseases

In vivo, Hsp27 and αB-crystallin are abundantly produced in response to various types of stress in cardiac and skeletal muscles as well as in the brain. This suggests that, in these organs, these sHsps act as molecular chaperones suppressing the aggregation of specific client polypeptides. For example, transgenic mice overexpressing Hsp27 are strongly protected against myocardial infarction and cerebral ischemia [56,64]. Moreover, αB-crystallin and Hsp27 are often upregulated and accumulate into inclusion bodies in many protein conformation diseases. For instance, αB-crystallin and/or Hsp27 accumulate in Rosenthal fibers of Alexander disease, cortical Lewy bodies, Alzheimer disease plaques, neurofibrillary tangles as well as in synuclein deposit associated to Parkinson disease or myopathy-associated inclusion body [65]. The exact reason for the frequent association of Hsp27 and/or αB-crystallin with these structures is probably linked to the chaperone activity of these sHsps. Indeed, molecular chaperones are known to provide a first line of defence against misfolded, aggregation-prone proteins probably because of their ability to modulate the earliest aberrant protein interactions that trigger pathogenic cascades. For example, it has been reported that sHsps protect against alpha-synuclein [66], huntingtin [26,67,68], amyloid and desmin mutants induced aggregation and/or toxicity.

Other studies have reported that αB-crystallin is present in reactive glia in Creutzfeldt-Jakob disease and a high prevalence of anti-alpha-crystallin antibodies has been described in multiple sclerosis which correlates with severity and activity of the disease. Upregulation of Hsp27 has also been observed in a transgenic model of ALS. The importance of Hsp27 in neuropathologies was further confirmed by the discovery of

Table 2
Mutations in αB-crystallin and Hsp27 and the corresponding pathologies

sHsps	Mutations	Associated pathologies	Ref.
αB-crystallin	R120G	Myofibrillar myopathy, cardiomyopathy, cataract	(1)
	Q151X	Myofibrillar myopathy	(2)
	464delCT	Myofibrillar myopathy	(2)
	R157H	Cardiomyopathy	(3)
	P20S	Cataract	(4)
	D140N	Cataract	(5)
	450delA	Cataract	(6)
Hsp27	R127W	Distal hereditary motor neuropathy	(7)
		Charcot-Marie-Tooth type 2F	(9)
	S135F	Distal hereditary motor neuropathy Charcot-Marie-Tooth type 2F	(7)
	R136W	Charcot-Marie-Tooth type 2F	(7)
	T151I	Distal hereditary motor neuropathy	(7)
	P182L	Distal hereditary motor neuropathy	(7)
	P182S	Distal hereditary motor neuropathy	(10)

Refs: (1) [71]. (2) [72]. (3) [78]. (4) [77] (5) Berry, V. et al. (2001) Am. J. Hum. Genet. 69, 1141–5. (6) Liu, Y. et al. (2006) Invest. Ophthalmol. Vis. Sci. 47, 1069–1075. (7) Evgrafov, O.V. et al. (2004) Nat. Genet. 36, 602–606. (8) Tang, B. et al. (2005) Arch. Neurol. 62, 1201–1207. (9) Liu, X.M. et al. (2005) Zhonghua Yi Xue Yi Chuan Xue Za Zhi. 22, 510–513. (10) Kijima, K., Numakura, C., Goto, T., Takahashi, T., Otagiri, T., Umetsu, K. and Hayasaka, K. (2005) J. Hum. Genet. 50, 473–476.

human mutations in the Hsp27 encoding gene in families associated with inherited peripheral neuropathies [69] and axonal Charcot-Marie-Tooth disease [70] (see Table 2). These motor neuropathies are caused by premature axonal loss, neuronal death and subsequent degeneration. Moreover, the mutations are associated with a decreased ability of Hsp27 to promote neuronal survival compared to the wild type protein. Taken together, these studies suggest that, in animal models of human diseases, Hsp27 and αB-crystallin are potent suppressors of neurodegeneration.

Other protein conformation diseases associated to Hsp27 and/or αB-crystallin expression are myopathies and alcoholic liver diseases characterized by the presence of Mallory bodies. Concerning the myopathies, recent studies have revealed the importance of αB-crystallin towards desmin network (see Table 2). Indeed, one major target of the chaperone activity associated to αB-crystallin appears to be type III intermediate filaments [40,41]. The discovery in 1998 of a missense mutation in αB-crystallin gene, changing arginine 120 to glycine (R120G), responsive of a myofibrillar myopathy associated with cardiomyopathy and cataract [71], confirmed the importance of αB-crystallin in these diseases. Recently, two novel mutations leading to myofibrillar myopathies (Q151X and 464delCT) have been identified in the terminal part of the αB-crystallin coding sequence [72]. At the exception of the report describing the identification of these new mutants, the published studies on αB-crystallinopathies concern the R120G mutant. It is now accepted that αB-crystallinopathies result from the misfolding and progressive aggregation of mutated αB-crystallin to which subsequently associate desmin filaments to form αB-crystallin/desmin/amyloid positive aggresomes [73,74]. These aggregates can by themselves be toxic, inhibiting the ubiquitin–proteasomal system of protein degradation [75] and causing deficits in mitochondrial function [76]. αB-crystallinopathies are a special case of protein conformation disease in which the destabilizing mutations at the origin of the disorder occurs in a molecular chaperone which is itself potentially involved in the protein quality control of the cell. Three mutations in αB-crystallin gene (P20S, 464delCT and D140N) are also responsive for dominant cataract [77] and two mutations (R157H and G154S) for cardiomyopathy [78]. At the biochemical level, mutations in αB-crystallin have been found to modify the properties of αB-crystallin such as its oligomerization and in vitro chaperone-like activity [79] and to increase its affinity to desmin [80]. Moreover, the ability of αB-crystallin to interact with members of the apoptotic cascade, cytoskeletal polypeptides or with the other sHsps may also be modified.

Hsp27 and αB-crystallin are also involved in inflammation diseases. For example, these proteins interferes with TNFα signaling pathway through their ability to protect against oxidative stress [81] and through modulation of TAK-1 activity [82]. An other example is given by the absence of colonic inflammation seen in the majority of individuals infected with the parasite *Entamoeba histolytica* which is related to the ability of Hsp27 to suppress NF-κB activation through an interaction with IKK-α and IKK-β [83]. Moreover, recent reports have shown that Hsp27 is needed for the activation by interleukin (IL)-1 of TAK1 and downstream signalling by p38 MAPK, JNK and their activators (MKK-3, -4, -6, -7) and IKKβ [82]. These observations suggest crucial roles of Hsp27 and αB-crystallin in the control of inflammatory processes. Among pathologies where the anti-oxidative potential of Hsp27 is crucial, one can cite airway inflammation associated with asthma which is characterized by the damage of the bronchial epithelium. In this respect, we have observed that an increased Hsp27 expression in the epithelium of asthmatic subjects generates a protection against the oxidative stress induced by the chronic inflammatory state of this tissue (see Fig. 3) [84].

3. Cancer

High levels of Hsp27 constitutive expression have been detected in several cancer cells, particularly those of carcinoma origin [85,86]. Recently, the number of reports dealing with Hsp27 in cancer pathologies has grown exponentially. In addition to its presence in breast, ovary and colon cancers, Hsp27 has recently been detected in liver, kidney, lung (non-small

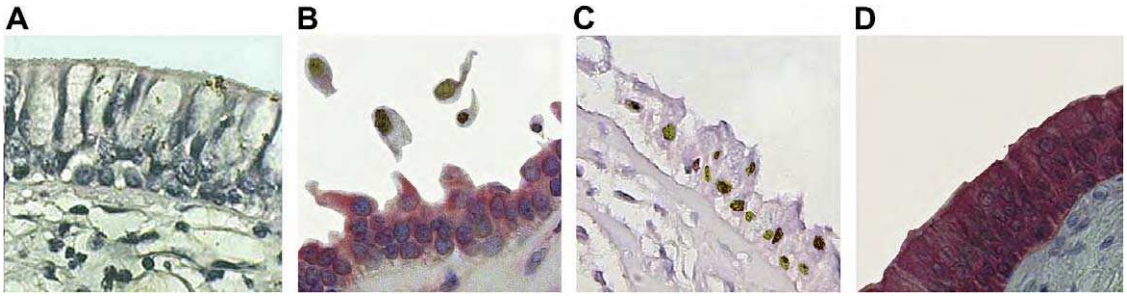

Fig. 3. Beneficial protective effect of Hsp27 expression in bronchial epithelial cells from asthmatic patients. Hsp27 expression and TUNEL immunoreactivity in bronchial epithelial cells of a normal (A) subject and an asthmatic (B–D) patient. Cells that express Hsp27 show a red immunostaining as the result of the Hsp27 immunoreactivity. TUNEL-positive cells are characterized by a brown staining of the nuclei. (A) Area of intact epithelium of a bronchial biopsy taken from a normal subject showing no immunoreactivity for Hsp27 and for TUNEL. (B) Area of damaged epithelium of a bronchial biopsy taken from an asthmatic subject with desquamated epithelial cells which are not immunoreactive for Hsp27 but show a positivity for the TUNEL technique. (C) Wide area of fragile epithelium not immunoreactive for Hsp27 showing a nuclear TUNEL staining of many bronchial epithelial cells. (D) Area of intact epithelium showing a strong immunostaining for Hsp27, and a complete lack of nuclear staining due to the TUNEL technique. These observations support the beneficial role of Hsp27 in asthma. Indeed, desquamative cells are apoptotic and devoid of Hsp27 while cells that express Hsp27 are not apoptotic and do not desquamate. See [84] for further informations.

cells) and prostate cancers. Moreover, experimental approaches performed in rodents have enlightened the tumorigenic potential of Hsp27 expression [87]. Hence, Hsp27 is supposed to increase the ability of some cancer cells to resist to and evade from the apoptotic processes mediated by the immune system. The large oligomers which bear the chaperone-like activity are also responsible for the tumorigenic activity of Hsp27 [58]. Concerning this issue, it cannot be excluded that Hsp27 large oligomers may act as Hsp90 and bind specific client proteins that participate in the tumorigenic and metastatic processes.

αB-Crystallin constitutive expression has been detected in gliomas, prostate cancer, oral squamous cell carcinomas, renal cell carcinomas, head and neck cancer. A normal high level of αB-crystallin has also been detected in basal-like breast carcinomas and preinvasive ductal carcinoma that correlated with poor clinical outcome of the patients. Recently, a pathological role of αB-crystallin has again been reported in breast cancer diseases, hence suggesting that this protein acts as an oncoprotein [88]. Neoplastic changes and invasive properties of breast cells are inhibited by phosphorylation of αB-crystallin [89]. Indeed, serine 59 phosphorylation reduces the oligomerization and anti-apopototic activities of αB-crystallin [90,91]. It can therefore be concluded that, as for Hsp27, the large oligomers of αB-crystallin may contribute to the aggressive behavior of cancer cells. However, the differential expression of αB-crystallin and Hsp27 reported in anaplastic thyroid carcinomas and in brain cancer suggests different involvement of these sHsps in these pathologies [92,93].

The expression of Hsp27 and αB-crystallin is also associated to other problems in cancer biology. First, high levels of Hsp27 are observed in metastatic tissues compared to non metastatic tissues suggesting that this protein plays a key role in metastasis formation [94]. αB-crystallin expression is correlated with lymph node involvement in breast carcinomas resulting in a shorter survival. Second, Hsp27 and αB-crystallin expression is associated with cellular resistance to cytostatic anticancerous drugs used in the clinic [95,96]. In addition, some of these drugs, particularly cisplatin [97], vincristine and colchicine [98] enhance Hsp27 and/or αB-crystallin expression. Collectively, these phenomena impair the efficiency of the clinical treatments using chemotherapeutic agents.

4. Hsp27 and αB-crystallin as therapeutic targets?

Hsp27 and αB-crystallin are potent protective factors of cells in which the disease-causing proteins are prone to aggregate and form large inclusions. In spite of the presence of Hsp27 and/or αB-crystallin, these diseases usually result in excessive cell death (Fig. 4). One therapeutic option could be the enhanced expression of the corresponding wild type protein. Unfortunately, such an approach is not feasible nowadays. Similarly, this approach can not be used to treat pathologies caused by Hsps mutations. Another approach to the development of therapeutic intervention for these diseases has been to identify chemical compounds that reduce the size or number of inclusions. However, recent results suggest that inclusion formation may in fact be beneficial to the cell to get rid of the mutated protein through autophagy [99]. However, inclusion formation or aggregation of metal-binding proteins (such as α-synuclein, Alzheimer β-amyloid peptide, PrP106-126 prion or polyQ mutants of Huntingtin) is a risky process since it can generate deleterious oxidative stress [67,100]. Hence, using available cellular models, studies will have to be performed to identify compounds that promote oxidative stress free inclusion formation as a therapeutic approach for neurodegenerative diseases caused by protein misfolding [101]. These studies will have to test whether compounds (still to be discovered, such as RNA/peptide aptamers or chemical chaperones, see below) that modulate Hsp27 and/or αB-crystallin functions are active towards the deleterious damages induced by these diseases.

In the myopathy and cataract research field, it is reasonable to assume that prevention of the formation of aggregates induced by αB-crystallin myopathy- and cataract-associated mutants may be an efficient strategy to inhibit the development of the disease (Fig. 4). For example, it is well known that the cessation of the expression of αB-crystallin R120G mutant in symptomatic mice improved cardiac function and rescued these animals from premature death [73]. Towards these pathologies, specific peptide/RNA aptamers or chemical chaperones that interfere with the mechanism leading to the aggregation of the mutated αB-crystallin but not with the wild type protein functionality should be researched and tested. A similar approach can be proposed towards the pathologies induced by mutations of Hsp27.

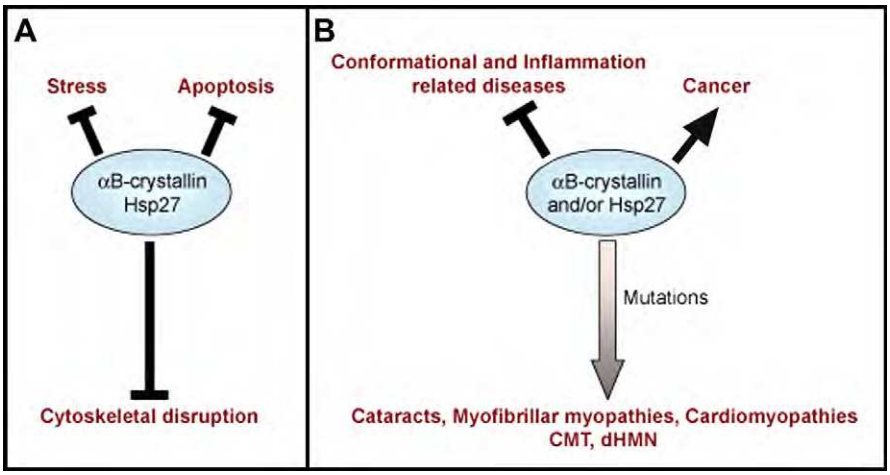

Fig. 4. Role of Hsp27 and αB-crystallin in normal and pathological cells. (A) In normal cells, Hsp27 and/or αB-crystallin participate in cytoskeleton, redox state and protein folding homeostasis. These proteins are also involved in the protection of cells in case of stress. In this respect, these sHsps interfere with spontaneous or induced apoptosis. (B) In pathological cells, Hsp27 and/or αB-crystallin have beneficial effects towards protein conformation and inflammation related diseases. In contrast, these proteins can have pernicious effects through their ability to protect cancer cells against the immune system- or drug-mediated death. Mutations in Hsp27 and/or αB-crystallin are responsive of the development of pathologies such as, cataracts, myofibrillars myopathies, cardiomyopathies, Charcot-Marie-Tooth (CMT) disease and motor-neuronal neuropathies, such as Distal Hereditary motor neuronopathy (dHMN).

Towards inflammation and asthma, compounds that stimulate the anti-oxidative activity of Hsp27 and αB-crystallin should be actively researched. Once again specific peptides or RNA aptamers or drugs that maintain these proteins in the form of large oligomers may stimulate their chaperone and anti-oxidative properties.

In the cancer field, Hsp27 and αB-crystallin have negative activities and should be either eliminated or their activity impaired (Fig. 4). Indeed, up until today, no report has described a positive role of these proteins in cancer cells, such as better tumor antigen-recognition at the cell surface as already shown in the case of Hsp70 [102,103]. Hence, experiments have been performed using anti-sense or nucleotide-based therapies with aim to inhibit Hsp27 and αB-crystallin expression. This approach sensitizes cancer cells to apoptotic inducers [45] and anticancer drugs and reduces the tumorigenic potential of bladder and prostate cancer cells [46,48]. The decrease in tumors aggressivity mediated by second generation of RNAi molecules, such as OGX 437 (Oncogenex Inc.), appears to be linked to loss of the anti-apoptotic protection mediated by Hsp27 [48]. Moreover, the degradation of putative and still unknown tumorigenic and/or metastatic client proteins that may bind Hsp27 should also be considered. As mentioned above, peptide/RNA aptamers or chemical chaperones that bind specific structural organizations of Hsp27 or αB-crystallin could be an alternative approach to reduce the tumorigenic and metastatic activities of these proteins. Similarly aptamers or drugs that modulate the anti-oxidant potential of these proteins (see above) may prove useful to block Hsp27 ability to counteract the killing efficiency of redox state dependent anti-cancer therapeutic drugs, such as 17AAG, or physical challenges such as X-rays irradiation.

5. Conclusions and perspectives

The number of reports that describe the importance of Hsp27 and αB-crystallin in pathologies is increasing exponentially and the need of drugs that modulate the activity of these chaperones is rising fast. The discovery of drugs will be a challenge since the tri-dimensional structures of human Hsp27 and αB-crystallin is still not known because of the difficulty to obtain stable crystals of these oligomeric proteins for X-ray analysis. In spite of these considerations, an astonishing array of strategies to either stimulate the beneficial properties or to affect the pathological roles played by these proteins is fast emerging. For example, the discovery of specific peptides that recognize the oligomeric forms of Hsp27 or αB-crystallin may prove useful to determine the structure of peptido-mimetic compounds leading to the emergence of chemical drugs designated to modulate specific activities of Hsp27 and αB-crystallin and/or which can correct and mask specific mutations in these chaperones. Hence, it is likely that in a near future drugs will be available for clinical trials. In addition, the intense work which is actually performed towards the eight other members of the human small stress family of proteins and the fact that most sHsps interact with each other and form homo- and hetero-oligomeric complexes may lead to the emergence of other interesting therapeutic targets and strategies.

Acknowledgements: Apologies to all those whose work has not been cited due to lack of space and references number limitation. Research in the authors laboratory was supported by the Région Rhône-Alpes (Contract Cible 06 to A.P.A.), the Centre National de la Recherche Scientifique (CNRS), the French Minister of Research, the Association Française contre les Myopathies (AFM Grants #11764 to P.V. and #12594 to A.P.A.) as well as Lyon 1 and Paris 7 Universities. Benjamin Gibert is supported by a doctoral fellowship of the Région Rhône-Alpes (Cible 06). Stéphanie Simon is supported by an AFM post-doctoral fellowship.

References

[1] Launay, N., Goudeau, B., Kato, K., Vicart, P. and Lilienbaum, A. (2006) Cell signaling pathways to alphaB-crystallin following stresses of the cytoskeleton. Exp. Cell Res. 312, 3570–3584.
[2] Theriault, J.R., Lambert, H., Chavez-Zobel, A.T., Charest, G., Lavigne, P. and Landry, J. (2004) Essential role of the

NH2-terminal WD/EPF motif in the phosphorylation-activated protective function of mammalian Hsp27. J. Biol. Chem. 279, 23463–23471, Epub 2004 Mar 21.
[3] Stokoe, D., Engel, K., Campbell, D., Cohen, P. and Gaestel, M. (1992) Identification of MAPKAP kinase 2 as a major enzyme responsible for the phosphorylation of the small mammalian heat shock proteins. FEBS Lett. 313, 307–313.
[4] Rouse, J., Cohen, P., Trigon, S., Morange, M., Alonso-Llamazares, A., Zamanillo, D., Hunt, T. and Nebreda, A.R. (1994) A novel kinase cascade triggered by stress and heat shock that stimulates MAPKAP kinase-2 and phosphorylation of the small heat shock proteins. Cell 78, 1027–1037.
[5] Arrigo, A.P. (1998) Small stress proteins: chaperones that act as regulators of intracellular redox state and programmed cell death. Biol. Chem. 379, 19–26.
[6] Rogalla, T. et al. (1999) Regulation of Hsp27 oligomerization, chaperone function, and protective activity against oxidative stress/tumor necrosis factor alpha by phosphorylation. J. Biol. Chem. 274, 18947–18956.
[7] Kato, K., Hasegawa, K., Goto, S. and Inaguma, Y. (1994) Dissociation as a result of phosphorylation of an aggregated form of the small stress protein, hsp27. J. Biol. Chem. 269, 11274–11278.
[8] Jakob, U., Gaestel, M., Engels, K. and Buchner, J. (1993) Small heat shock proteins are molecular chaperones. J. Biol. Chem. 268, 1517–1520.
[9] Ehrnsperger, M., Graber, S., Gaestel, M. and Buchner, J. (1997) Binding of non-native protein to Hsp25 during heat shock creates a reservoir of folding intermediates for reactivation. EMBO J. 16, 221–229.
[10] McDonough, H. and Patterson, C. (2003) CHIP: a link between the chaperone and proteasome systems. Cell Stress Chaperones 8, 303–308.
[11] Ghosh, J.G., Estrada, M.R., Houck, S.A. and Clark, J.I. (2006) The function of the beta3 interactive domain in the small heat shock protein and molecular chaperone, human alphaB crystallin. Cell Stress Chaperones 11, 187–197.
[12] Ghosh, J.G., Estrada, M.R. and Clark, J.I. (2006) Structure-based analysis of the beta8 interactive sequence of human alphaB crystallin. Biochemistry 45, 9878–9886.
[13] Ghosh, J.G., Shenoy Jr., A.K. and Clark, J.I. (2006) N- and C-Terminal motifs in human alphaB crystallin play an important role in the recognition, selection, and solubilization of substrates. Biochemistry 45, 13847–13854.
[14] Parcellier, A. et al. (2003) HSP27 is a ubiquitin-binding protein involved in I-kappaBalpha proteasomal degradation. Mol. Cell Biol. 23, 5790–5802.
[15] Lin, D.I. et al. (2006) Phosphorylation-dependent ubiquitination of cyclin D1 by the SCF(FBX4-alphaB crystallin) complex. Mol. Cell. 24, 355–366.
[16] Duverger, O., Paslaru, L. and Morange, M. (2004) HSP25 is involved in two steps of the differentiation of PAM212 keratinocytes. J. Biol. Chem. 279, 10252–10260.
[17] Arrigo, A.P. (2005) In search of the molecular mechanism by which small stress proteins counteract apoptosis during cellular differentiation. J. Cell. Biochem. 94, 241–246.
[18] Mehlen, P., Mehlen, A., Godet, J. and Arrigo, A.-P. (1997) hsp27 as a switch between differentiation and apoptosis in murine embryonic stem cells. J. Biol. Chem. 272, 31657–31665.
[19] Mehlen, P., Coronas, V., Ljubic-Thibal, V., Ducasse, C., Granger, L., Jourdan, F. and Arrigo, A.P. (1999) Small stress protein Hsp27 accumulation during dopamine-mediated differentiation of rat olfactory neurons counteracts apoptosis. Cell Death Differ. 6, 227–233.
[20] Kamradt, M.C., Chen, F., Sam, S. and Cryns, V.L. (2002) The small heat shock protein alpha B-crystallin negatively regulates apoptosis during myogenic differentiation by inhibiting caspase-3 activation. J. Biol. Chem. 277, 38731–38736, Epub 2002 Jul 24.
[21] Sugiyama, Y. et al. (2000) Muscle develops a specific form of small heat shock protein complex composed of MKBP/HSPB2 and HSPB3 during myogenic differentiation. J. Biol. Chem. 275, 1095–1104.
[22] Arrigo, A.P. (2001) Hsp27: novel regulator of intracellular redox state. IUBMB Life 52, 303–307.
[23] Yan, L.J., Christians, E.S., Liu, L., Xiao, X., Sohal, R.S. and Benjamin, I.J. (2002) Mouse heat shock transcription factor 1 deficiency alters cardiac redox homeostasis and increases mitochondrial oxidative damage. Embo J. 21, 5164–5172.
[24] Preville, X., Salvemini, F., Giraud, S., Chaufour, S., Paul, C., Stepien, G., Ursini, M.V. and Arrigo, A.P. (1999) Mammalian small stress proteins protect against oxidative stress through their ability to increase glucose-6-phosphate dehydrogenase activity and by maintaining optimal cellular detoxifying machinery. Exp. Cell Res. 247, 61–78.
[25] Mehlen, P., Préville, X., Kretz-Remy, C. and Arrigo, A.-P. (1996) Human hsp27, Drosophila hsp27 and human αB-crystallin expression-mediated increase in glutathione is essential for the protective activity of these protein against TNFα-induced cell death. EMBO J. 15, 2695–2706.
[26] Firdaus, W.J., Wyttenbach, A., Diaz-Latoud, C., Currie, R.W. and Arrigo, A.P. (2006) Analysis of oxidative events induced by expanded polyglutamine huntingtin exon 1 that are differentially restored by expression of heat shock proteins or treatment with an antioxidant. Febs J. 273, 3076–3093.
[27] Préville, X., Gaestel, M. and Arrigo, A.P. (1998) Phosphorylation is not essential for protection of L929 cells by Hsp25 against H2O2-mediated disruption actin cytoskeleton, a protection which appears related to the redox change mediated by Hsp25. Cell Stress Chaperones 3, 177–187.
[28] Paul, C. and Arrigo, A.P. (2000) Comparison of the protective activities generated by two survival proteins: Bcl-2 and Hsp27 in L929 murine fibroblasts exposed to menadione or staurosporine. Exp. Gerontol. 35, 757–766.
[29] Arrigo, A.P., Virot, S., Chaufour, S., Firdaus, W., Kretz-Remy, C. and Diaz-Latoud, C. (2005) Hsp27 consolidates intracellular redox homeostasis by upholding glutathione in its reduced form and by decreasing iron intracellular levels. Antioxid. Redox Signal 7, 414–422.
[30] Chen, H., Zheng, C., Zhang, Y., Chang, Y.Z., Qian, Z.M. and Shen, X. (2006) Heat shock protein 27 downregulates the transferrin receptor 1-mediated iron uptake. Int. J. Biochem. Cell Biol. 38, 1402–1416, Epub 2006 Mar 7.
[31] Mehlen, P., Hickey, E., Weber, L. and Arrigo, A.-P. (1997) Large unphosphorylated aggregates as the active form of hsp27 which controls intracellular reactive oxygen species and glutathione levels and generates a protection against TNFα in NIH-3T3-ras cells. Biochem. Biophys. Res. Commun. 241, 187–192.
[32] Benndorf, R., Hayess, K., Ryazantsev, S., Wieske, M., Behlke, J. and Lutsch, G. (1994) Phosphorylation and supramolecular organization of murine small heat shock protein HSP25 abolish its actin polymerization-inhibiting activity. J. Biol. Chem. 269, 20780–20784.
[33] Mounier, N. and Arrigo, A.P. (2002) Actin cytoskeleton and small heat shock proteins: how do they interact? Cell Stress Chaperones 7, 167–176.
[34] Jog, N.R., Jala, V.R., Ward, R.A., Rane, M.J., Haribabu, B. and McLeish, K.R. (2007) Heat shock protein 27 regulates neutrophil chemotaxis and exocytosis through two independent mechanisms. J. Immunol. 178, 2421–2428.
[35] Singh, B.N., Rao, K.S., Ramakrishna, T., Rangaraj, N. and Rao, Ch.M. (2007) Association of alphaB-crystallin, a small heat shock protein, with actin: role in modulating actin filament dynamics in vivo. J. Mol. Biol. 366, 756–767.
[36] Mairesse, N., Horman, S., Mosselmans, R. and Galand, P. (1996) Antisense inhibition of the 27 kDa heat shock protein production affects growth rate and cytoskeletal organization in MCF-7 cells. Cell Biol. Int. 20, 205–212.
[37] Préville, X., Mehlen, P., Fabre-Jonca, N., Chaufour, S., Kretz-Remy, C., Michel, M.R. and Arrigo, A.-P. (1996) Biochemical and immunofluorescence analysis of the constitutively expressed hsp27 stress protein in monkey CV-1 cells. J. Biosci. 21, 1–14.
[38] Hino, M., Kurogi, K., Okubo, M.A., Murata-Hori, M. and Hosoya, H. (2000) Small heat shock protein 27 (HSP27) associates with tubulin/microtubules in HeLa cells. Biochem. Biophys. Res. Commun. 271, 164–169.
[39] Xi, J.H., Bai, F., McGaha, R. and Andley, U.P. (2006) Alpha-crystallin expression affects microtubule assembly and prevents their aggregation. Faseb J. 20, 846–857.

[40] Bennardini, F., Wrzosek, A. and Chiesi, M. (1992) Alpha B-crystallin in cardiac tissue. Association with actin and desmin filaments. Circ. Res. 71, 288–294.
[41] Djabali, K., de Nechaud, B., Landon, F. and Portier, M.M. (1997) AlphaB-crystallin interacts with intermediate filaments in response to stress. J. Cell Sci. 110, 2759–2769.
[42] Mehlen, P., Schulze-Osthoff, K. and Arrigo, A.P. (1996) Small stress proteins as novel regulators of apoptosis. Heat shock protein 27 blocks Fas/APO-1- and staurosporine-induced cell death. J. Biol. Chem. 271, 16510–16514.
[43] Arrigo, A.P. (2000) sHsp as novel regulators of programmed cell death and tumorigenicity. Pathol. Biol. (Paris) 48, 280–288.
[44] Concannon, C.G., Gorman, A.M. and Samali, A. (2003) On the role of Hsp27 in regulating apoptosis. Apoptosis 8, 61–70.
[45] Paul, C., Manero, F., Gonin, S., Kretz-Remy, C., Virot, S. and Arrigo, A.P. (2002) Hsp27 as a negative regulator of cytochrome C release. Mol. Cell Biol. 22, 816–834.
[46] Rocchi, P., Jugpal, P., So, A., Sinneman, S., Ettinger, S., Fazli, L., Nelson, C. and Gleave, M. (2006) Small interference RNA targeting heat-shock protein 27 inhibits the growth of prostatic cell lines and induces apoptosis via caspase-3 activation in vitro. BJU Int. 28, 28.
[47] Bausero, M.A. et al. (2006) Silencing the hsp25 gene eliminates migration capability of the highly metastatic murine 4T1 breast adenocarcinoma cell. Tumour Biol. 27, 17–26, Epub 2005 Dec 8.
[48] Kamada, M., So, A., Muramaki, M., Rocchi, P., Beraldi, E. and Gleave, M. (2007) Hsp27 knockdown using nucleotide-based therapies inhibit tumor growth and enhance chemotherapy in human bladder cancer cells. Mol. Cancer Ther. 6, 299–308, Epub 2007 Jan 11.
[49] Chauhan, D. et al. (2003) Hsp27 inhibits release of mitochondrial protein Smac in multiple myeloma cells and confers dexamethasone resistance. Blood 102, 3379–3386, Epub 2003 Jul 10.
[50] Bruey, J.M. et al. (2000) Hsp27 negatively regulates cell death by interacting with cytochrome c. Nat. Cell Biol. 2, 645–652.
[51] Pandey, P. et al. (2000) Hsp27 functions as a negative regulator of cytochrome *c*-dependent activation of procaspase-3. Oncogene 19, 1975–1981.
[52] Charette, S.J., Lavoie, J.N., Lambert, H. and Landry, J. (2000) Inhibition of daxx-mediated apoptosis by heat shock protein 27. Mol. Cell Biol. 20, 7602–7612.
[53] Song, H., Ethier, S.P., Dziubinski, M.L. and Lin, J. (2004) Stat3 modulates heat shock 27kDa protein expression in breast epithelial cells. Biochem. Biophys. Res. Commun. 314, 143–150.
[54] Rane, M.J. et al. (2003) Heat shock protein 27 controls apoptosis by regulating akt activation. J. Biol. Chem. 278, 27828–27835.
[55] Brar, B.K., Stephanou, A., Wagstaff, M.J., Coffin, R.S., Marber, M.S., Engelmann, G. and Latchman, D.S. (1999) Heat shock proteins delivered with a virus vector can protect cardiac cells against apoptosis as well as against thermal or hypoxic stress. J. Mol. Cell Cardiol. 31, 135–146.
[56] Latchman, D.S. (2005) HSP27 and cell survival in neurones. Int. J. Hyperthermia. 21, 393–402.
[57] Arrigo, A.-P. (1995) Expression of stress genes during development. Neuropathol. Appl. Neurobiol. 21, 488–491.
[58] Bruey, J.M., Paul, C., Fromentin, A., Hilpert, S., Arrigo, A.P., Solary, E. and Garrido, C. (2000) Differential regulation of HSP27 oligomerization in tumor cells grown in vitro and in vivo. Oncogene 19, 4855–4863.
[59] Kamradt, M.C., Chen, F. and Cryns, V.L. (2001) The small heat shock protein alpha B-crystallin negatively regulates cytochrome c- and caspase-8-dependent activation of caspase-3 by inhibiting its autoproteolytic maturation. J. Biol. Chem. 276, 16059–16063, Epub 2001 Mar 23.
[60] Kamradt, M.C. et al. (2005) The small heat shock protein alpha B-crystallin is a novel inhibitor of TRAIL-induced apoptosis that suppresses the activation of caspase-3. J. Biol. Chem. 280, 11059–11066, Epub 2005 Jan 14.
[61] Mao, Y.W., Liu, J.P., Xiang, H. and Li, D.W. (2004) Human alphaA- and alphaB-crystallins bind to Bax and Bcl-X(S) to sequester their translocation during staurosporine-induced apoptosis. Cell Death Differ. 11, 512–526.
[62] Liu, S., Li, J., Tao, Y. and Xiao, X. (2007) Small heat shock protein alphaB-crystallin binds to p53 to sequester its translocation to mitochondria during hydrogen peroxide-induced apoptosis. Biochem. Biophys. Res. Commun. 354, 109–114.
[63] Morrison, L.E., Hoover, H.E., Thuerauf, D.J. and Glembotski, C.C. (2003) Mimicking phosphorylation of alphaB-crystallin on serine-59 is necessary and sufficient to provide maximal protection of cardiac myocytes from apoptosis. Circ. Res. 92, 203–211.
[64] Efthymiou, C.A., Mocanu, M.M., de Belleroche, J., Wells, D.J., Latchmann, D.S. and Yellon, D.M. (2004) Heat shock protein 27 protects the heart against myocardial infarction. Basic Res. Cardiol. 99, 392–394, Epub 2004 Jul 13.
[65] Muchowski, P.J. and Wacker, J.L. (2005) Modulation of neurodegeneration by molecular chaperones. Nat. Rev. Neurosci. 6, 11–22.
[66] Outeiro, T.F., Klucken, J., Strathearn, K.E., Liu, F., Nguyen, P., Rochet, J.C., Hyman, B.T. and McLean, P.J. (2006) Small heat shock proteins protect against alpha-synuclein-induced toxicity and aggregation. Biochem. Biophys. Res. Commun. 351, 631–638, Epub 2006 Oct 26.
[67] Firdaus, W.J., Wyttenbach, A., Giuliano, P., Kretz-Remy, C., Currie, R.W. and Arrigo, A.P. (2006) Huntingtin inclusion bodies are iron-dependent centers of oxidative events. Febs J. 273, 5428–5441.
[68] Wyttenbach, A., Sauvageot, O., Carmichael, J., Diaz-Latoud, C., Arrigo, A.P. and Rubinsztein, D.C. (2002) Heat shock protein 27 prevents cellular polyglutamine toxicity and suppresses the increase of reactive oxygen species caused by huntingtin. Hum. Mol. Genet. 11, 1137–1151.
[69] Dierick, I., Irobi, J., De Jonghe, P. and Timmerman, V. (2005) Small heat shock proteins in inherited peripheral neuropathies. Ann. Med. 37, 413–422.
[70] Evgrafov, O.V. et al. (2004) Mutant small heat-shock protein 27 causes axonal Charcot-Marie-Tooth disease and distal hereditary motor neuropathy. Nat. Genet. 36, 602–606, Epub 2004 May 02.
[71] Vicart, P. et al. (1998) A missense mutation in the alphaB-crystallin chaperone gene causes a desmin-related myopathy. Nat. Genet. 20, 92–95.
[72] Selcen, D. and Engel, A.G. (2003) Myofibrillar myopathy caused by novel dominant negative alpha B-crystallin mutations. Ann. Neurol. 54, 804–810.
[73] Sanbe, A., Osinska, H., Villa, C., Gulick, J., Klevitsky, R., Glabe, C.G., Kayed, R. and Robbins, J. (2005) Reversal of amyloid-induced heart disease in desmin-related cardiomyopathy. Proc. Natl. Acad. Sci. USA 102, 13592–13597, Epub 2005 Sep 9.
[74] Sherman, M.Y. and Goldberg, A.L. (2001) Cellular defenses against unfolded proteins: a cell biologist thinks about neurodegenerative diseases. Neuron 29, 15–32.
[75] Bence, N.F., Sampat, R.M. and Kopito, R.R. (2001) Impairment of the ubiquitin–proteasome system by protein aggregation. Science 292, 1552–1555.
[76] Maloyan, A., Sanbe, A., Osinska, H., Westfall, M., Robinson, D., Imahashi, K., Murphy, E. and Robbins, J. (2005) Mitochondrial dysfunction and apoptosis underlie the pathogenic process in alpha-B-crystallin desmin-related cardiomyopathy. Circulation 112, 3451–3461.
[77] Liu, M. et al. (2006) Identification of a CRYAB mutation associated with autosomal dominant posterior polar cataract in a Chinese family. Invest. Ophthalmol. Vis. Sci. 47, 3461–3466.
[78] Inagaki, N. et al. (2006) Alpha B-crystallin mutation in dilated cardiomyopathy. Biochem. Biophys. Res. Commun. 342, 379–386, Epub 2006 Feb 8.
[79] Bova, M.P., Yaron, O., Huang, Q., Ding, L., Haley, D.A., Stewart, P.L. and Horwitz, J. (1999) Mutation R120G in alphaB-crystallin, which is linked to a desmin- related myopathy, results in an irregular structure and defective chaperone-like function. Proc. Natl. Acad. Sci. USA 96, 6137–6142.
[80] Perng, M.D., Wen, S.F., van den, I.P., Prescott, A.R. and Quinlan, R.A. (2004) Desmin aggregate formation by R120G alphaB-crystallin is caused by altered filament interactions and is dependent upon network status in cells. Mol. Biol. Cell. 15, 2335–2346, Epub 2004 Mar 5.

[81] Mehlen, P., Préville, X., Chareyron, P., Briolay, J., Klemenz, R. and Arrigo, A.-P. (1995) Constitutive expression of human hsp27, Drosophila hsp27, or human alpha B-crystallin confers resistance to TNF- and oxidative stress-induced cytotoxicity in stably transfected murine L929 fibroblasts. J. Immunol. 154, 363–374.
[82] Alford, K.A., Glennie, S., Turrell, B.R., Rawlinson, L., Saklatvala, J. and Dean, J.L. (2007) HSP27 functions in inflammatory gene expression and TAK1-mediated signalling. J. Biol. Chem. 3, 3.
[83] Kammanadiminti, S.J. and Chadee, K. (2006) Suppression of NF-kappaB activation by *Entamoeba histolytica* in intestinal epithelial cells is mediated by heat shock protein 27. J. Biol. Chem. 281, 26112–26120, Epub 2006 Jul 13.
[84] Merendino, A.M. et al. (2002) Heat shock protein-27 protects human bronchial epithelial cells against oxidative stress-mediated apoptosis: possible implication in asthma. Cell Stress Chaperones 7, 269–280.
[85] Ciocca, D.R. and Calderwood, S.K. (2005) Heat shock proteins in cancer: diagnostic, prognostic, predictive, and treatment implications. Cell Stress Chaperones 10, 86–103.
[86] Calderwood, S.K., Khaleque, M.A., Sawyer, D.B. and Ciocca, D.R. (2006) Heat shock proteins in cancer: chaperones of tumorigenesis. Trends Biochem. Sci. 31, 164–172, Epub 2006 Feb 17.
[87] Garrido, C., Fromentin, A., Bonnotte, B., Favre, N., Moutet, M., Arrigo, A.P., Mehlen, P. and Solary, E. (1998) Heat shock protein 27 enhances the tumorigenicity of immunogenic rat colon carcinoma cell clones. Cancer Res. 58, 5495–5499.
[88] Gruvberger-Saal, S.K. and Parsons, R. (2006) Is the small heat shock protein alphaB-crystallin an oncogene? J. Clin. Invest. 116, 30–32.
[89] Chelouche-Lev, D., Kluger, H.M., Berger, A.J., Rimm, D.L. and Price, J.E. (2004) alphaB-crystallin as a marker of lymph node involvement in breast carcinoma. Cancer 100, 2543–2548.
[90] Webster, K.A. (2003) Serine phosphorylation and suppression of apoptosis by the small heat shock protein alphaB-crystallin. Circ. Res. 92, 130–132.
[91] Moyano, J.V. et al. (2006) AlphaB-crystallin is a novel oncoprotein that predicts poor clinical outcome in breast cancer. J. Clin. Invest. 116, 261–270.
[92] Hitotsumatsu, T., Iwaki, T., Fukui, M. and Tateishi, J. (1996) Distinctive immunohistochemical profiles of small heat shock proteins (heat shock protein 27 and alpha B-crystallin) in human brain tumors. Cancer 77, 352–361.
[93] Mineva, I. et al. (2005) Differential expression of alphaB-crystallin and Hsp27-1 in anaplastic thyroid carcinomas because of tumor-specific alphaB-crystallin gene (CRYAB) silencing. Cell Stress Chaperones 10, 171–184.
[94] Xu, L., Chen, S. and Bergan, R.C. (2006) MAPKAPK2 and HSP27 are downstream effectors of p38 MAP kinase-mediated matrix metalloproteinase type 2 activation and cell invasion in human prostate cancer. Oncogene 16, 16.
[95] Oesterreich, S., Weng, C.-N., Qiu, M., Hilsenbeck, S.G., Osborne, C.K. and Fuqua, S.W. (1993) The small heat shock protein hsp27 is correlated with growth and drug resistance in human breast cancer cell lines. Cancer Res. 53, 4443–4448.
[96] Rocchi, P. et al. (2004) Heat shock protein 27 increases after androgen ablation and plays a cytoprotective role in hormone-refractory prostate cancer. Cancer Res. 64, 6595–6602.
[97] Oesterreich, S., Schunck, H., Benndorf, R. and Bielka, H. (1991) Cisplatin induces the small heat shock protein hsp25 and thermotolerance in Ehrlich ascites tumor cells. Biochem. Biophys. Res. Commun. 180, 243–248.
[98] Kato, K., Ito, H., Inaguma, Y., Okamoto, K. and Saga, S. (1996) Synthesis and accumulation of alphaB crystallin in C6 glioma cells is induced by agents that promote the disassembly of microtubules. J. Biol. Chem. 271, 26989–26994.
[99] Ravikumar, B. et al. (2004) Inhibition of mTOR induces autophagy and reduces toxicity of polyglutamine expansions in fly and mouse models of Huntington disease. Nat. Genet. 36, 585–595, Epub 2004 May 16.
[100] Turnbull, S., Tabner, B.J., Brown, D.R. and Allsop, D. (2003) Copper-dependent generation of hydrogen peroxide from the toxic prion protein fragment PrP106-126. Neurosci. Lett. 336, 159–162.
[101] Bodner, R.A. et al. (2006) Pharmacological promotion of inclusion formation: a therapeutic approach for Huntington's and Parkinson's diseases. Proc. Natl. Acad. Sci. USA 103, 4246–4251, Epub 2006 Mar 6.
[102] Basu, S. and Srivastava, P.K. (2000) Heat shock proteins: the fountainhead of innate and adaptive immune responses. Cell Stress Chaperones 5, 443–451.
[103] Wells, A.D. and Malkovsky, M. (2000) Heat shock proteins, tumor immunogenicity and antigen presentation: an integrated view. Immunol. Today 21, 129–132.
[104] Arrigo, A.P., Firdaus, W.J., Mellier, G., Moulin, M., Paul, C., Diaz-Latoud, C. and Kretz-Remy, C. (2005) Cytotoxic effects induced by oxidative stress in cultured mammalian cells and protection provided by Hsp27 expression. Methods 35, 126–138, Epub 2004 Dec 19.

PUBLICATION - 2

PUBLICATION 2 - Dynamic processes that reflect anti-apoptotic strategies set up by HspB1.

In press, Experimental Cell Research.

Hsp27 est une protéine qui possède la particularité de former des structures de type oligomériques. Ces structures sont encore assez mal décrites dans la littérature mais leur rôle semblerait être la rétention de protéines dénaturées lors de stress. Des études biochimiques ont montré que les formes de plus petites tailles, inférieures à 200kDa, seraient les formes phosphorylées par la MK2 (MAPKAPK2). Trois résidus sérine en position S15, 78 et 82, sont phosphorylés lors d'un stress comme le choc thermique. Cette phosphorylation serait à l'origine de la dissociation des formes de haut poids moléculaire. Ainsi, lors d'un stress se produirait une modification importante des états de phosphorylation de Hsp27 et de sa structure oligomérique.

Les mécanismes structuraux de l'oligomérisation sont eux aussi mal compris. Il est établi que le motif hydrophobe WDPF en position N-terminal est important dans les phénomènes d'oligomérisation. Le domaine α-cristallin serait responsable des associations entre monomères, pièces de bases de l'établissement des structures de haut poids moléculaire. L'établissement de liaison disulfure entre deux résidus cystéine en positon 137 serait responsable de la dimérisation covalente entres deux monomères de Hsp27 (Diaz-Latoud *et al.*, 2005). Cependant, l'inhibiton de cette dimérisation ne conduit pas à l'abolition de la formation des oligomères mais provoque la formation d'oligomères non fonctionnels. Les phosphorylations sont nécessaires pour le maintien de l'intégrité du cytosquelette. Ainsi, Hsp27 interagirait avec l'actine uniquement sous ses formes phosphorylées. Cette interaction serait un élément important pour protéger des altérations du cytosquelette et de la F-actine au cours de l'apoptose et plus généralement du stress. Il a aussi été montré que Hsp27 prévenait les altérations du cytosquelette comme celles induites par les RLO. Ces mécanismes de lutte contre la déstructuration du cytosquelette conduisent à inhiber l'apoptose par inhibition de la sortie du cytochrome *c* mitochondrial.

Dans cette étude nous avons analysé la modulation des différents paramètres structuraux qui régissent la biochimie de Hsp27 tels que son oligomérisation, sa phosphorylation et sa localisation cellulaire. Nous avons ainsi pu montrer que les différents paramètres biochimiques analysés pour Hsp27 étaient très variants suivant le type de stress réalisé.

Nous avons traité des cellules HeLa avec différents inducteurs d'apoptose : un inhibiteur de topoisomérase II, l'étoposide ; une inhibiteur de kinase, la staurosporine ; un inhibiteur de la polymérisation de l'actine, la cytochalasine D et l'anticorps mimant l'action du liguant de mort Fas. Nous avons pu ainsi montrer que la déplétion partielle en Hsp27 provoquait une inhibition de la mort induite par ces composés, en diminuant l'induction de la sortie du cytochrome *c* mitochondrial.

Il apparait que la dispersion spatiale de Hsp27 est largement modifiée après traitement par chacun de ces composés. De plus, cette dispersion semble être profondément corrélée avec les changements du cytosquelette et en particulier de la F-actine. En effet, le cytosquelette subit de profondes modifications après ces traitements proapototiques, et la F-actine semble être redistribuée dans les corps apoptotiques ainsi que dans les « boursouflures des membranes » ou « membranes rufles ». Hsp27 serait présente à la base de ces formations et collaborerait avec l'actine pour l'adhésion de ces structures. Ces modifications de localisation cellulaire sont corrélées avec des changements importants de l'oligomérisation de la protéine. Deux modifications semblent être opérées selon le type d'apoptose induite. En effet, les inducteurs de mort, ciblant plus directement l'actine et sa structure, comme la cytochalasine D et la staurosporine, induisent une phosphorylation rapide et importante corrélant avec une forte diminution du nombre de structures de haut poids moléculaires. Les composés permettant une altération indirecte du cytosquelette comme l'étoposide et le liguant Fas provoquent une oligomérisation importante reliée à un faible taux de phosphorylation.

Dans la majeure partie des études concernant la protéine de stress Hsp27, les phosphorylations étaient analysées dans leur globalité c'est-à-dire en considérant que chacune des trois résidus sérines phosphorylables l'était de la manière identique. Nous avons pu montrer, à l'aide d'anticorps spécifiques de chaque site de phosphorylation, que ces phosphorylations étaient différentielles, en fonction du résidu sérine considéré et des formes oligomériques formées. Par ailleurs, il apparait que des formes phosphorylées sont retrouvées dans les structures de haut poids moléculaires, ce qui complexifie encore la vision de la structure de Hsp27 proposée jusqu'alors. Ainsi, la phosphorylation de la serine en position 82 serait retrouvée dans les petites formes de Hsp27 $\leq$ 150 kDa et les très grandes $\geq$ 400kDa. Celle en position en position 78, serait retrouvée dans les formes moyennes entre 150 et 400 kDa. Enfin, la forme phophorylée de la sérine 15 serait présente uniquement dans les petites formes $\leq$ 150 kDa, et ceci pour les quatre traitements réalisés. De plus, le phénomène semble encore plus complexe puisque dans le cas d'un choc thermique, des phosphorylations de la sérine S15 sont aussi retrouvées dans les très gros oligomères.

La relation structure/fonction est particulièrement importante pour les petites α-cristallines. Le phénomène d'oligomérisation est difficile à appréhender et à étudier du fait de l'importance de l'hétérogénéité des réponses biologiques observées. En outre, on peut imaginer que le système se complexifie encore plus si l'on tient compte du fait que les petites protéines de stress sont capables de former des hétéro oligomères entre elles, par exemple entre Hsp27, l'αB-cristallin et Hsp22. Comprendre ces mécanismes moléculaires d'oligomérisation semble essentiel pour pouvoir cibler ces petites Hsp et inhiber sélectivement leurs activités anti-apoptotiques.

EXPERIMENTAL CELL RESEARCH 316 (2010) 1535–1552

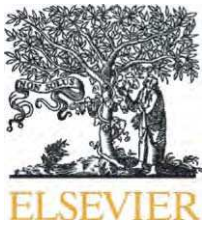

available at www.sciencedirect.com

ScienceDirect

www.elsevier.com/locate/yexcr

Research Article

Dynamic processes that reflect anti-apoptotic strategies set up by HspB1 (Hsp27)

Catherine Paul[a,b,1], *Stéphanie Simon*[a,c,1], *Benjamin Gibert*[a,1], *Sophie Virot*[a], *Florence Manero*[a], *André-Patrick Arrigo*[a,*]

[a]*Laboratoire Stress, Chaperons et Mort Cellulaire, CNRS UMR 5534, Université Claude Bernard Lyon1, Villeurbanne, France*
[b]*EPHE, Immunologie et Immunothérapie des Cancers, CRINSERM U866, Université de Bourgogne, Dijon, France*
[c]*Stress et Pathologies du Cytoskelette, UFR Biochimie, Université Paris 7, Paris, France*

ARTICLE INFORMATION

Article Chronology:
Received 22 October 2009
Revised version received
5 March 2010
Accepted 9 March 2010
Available online 15 March 2010

Keywords:
Hsp27
HspB1
Chaperone
Apoptosis
Oligomerization
Phosphorylation

ABSTRACT

Human HspB1 (also denoted Hsp27) is an oligomeric anti-apoptotic protein that has tumorigenic and metastatic roles. To approach the structural organizations of HspB1 that are active in response to apoptosis inducers acting through different pathways, we have analyzed the relative protective efficiency induced by this protein as well its localization, oligomerization and phosphorylation. HeLa cells, that constitutively express high levels of HspB1 were treated with either etoposide, Fas agonist antibody, staurosporine or cytochalasin D. Variability in HspB1 efficiency to interfere with the different apoptotic transduction pathways induced by these agents were detected. Moreover, inducer-specific dynamic changes in HspB1 localization, native size and phosphorylation were observed, that differed from those observed after heat shock. Etoposide and Fas treatments gradually shifted HspB1 towards large but differently phosphorylated oligomeric structures. In contrast, staurosporine and cytochalasin D induced the rapid but transient formation of small oligomers before large structures were formed. These events correlated with inducer-specific phosphorylations of HspB1. Of interest, the formation of small oligomers in response to staurosporine and cytochalasin D was time correlated with the rapid disruption of F-actin. The subsequent, or gradual in the case of etoposide and Fas, formation of large oligomeric structures was a later event concomitant with the early phase of caspase activation. These observations support the hypothesis that HspB1 has the ability, through specific changes in its structural organization, to adapt and interfere at several levels with challenges triggered by different signal transduction pathways upstream of the execution phase of apoptosis.

Introduction

Heat shock (or stress) proteins (Hsps) are characterized by their stimulated expression when the cellular environment is deleterious, as for example in heat shock conditions [1]. Small Heat shock proteins (sHsps) (20 to 40 kDa) share a C-terminal domain with homology to alpha-crystallin from the vertebrate eye (about 40% of the protein, the alpha-crystallin domain) [2–4], as well as a flexible

* *Corresponding author.* Stress, Chaperons and Cell death Laboratory, CNRS UMR 5534, Claude Bernard University Lyon1, 16 rue Dubois, Bat. Gregor Mendel, 69622 Villeurbanne Cedex, France. Fax: +33 472432385.
E-mail addresses: parrigo@me.com, arrigo@univ-lyon1.fr (A.-P. Arrigo).

Abbreviations: Hsps, Heat shock proteins; sHsps, small Heat shock proteins; PBS, Phosphate buffered saline; DAXX, Death domain-associated protein 6; Akt, murine thymoma viral oncogene homolog; G6PDH, Glucose 6-phosphate dehydrogenase

[1] These authors have equally contributed to the work.

0014-4827/$ – see front matter © 2010 Elsevier Inc. All rights reserved.
doi:10.1016/j.yexcr.2010.03.006

C-terminal tail and a weakly conserved N-terminal domain containing a hydrophobic WDPF motif. sHsp complex heterogeneous oligomerization is linked to the physiology of the cells, the phosphorylation status of sHsps and the potential exposure to stress [3,5–7]. Tetramers assembled from dimers are the building blocks of sHsp multimeric oligomeric complex [8]; a phenomenon controlled by phosphorylation-sensitive interactions in the N-terminal part of sHsps [9].

In human, ten different sHsps have been characterized [10]. One of them, HspB1 (Hsp27) which has been studied for several years, enhances the resistance of cells to the deleterious effects induced by either heat shock [11], oxidative stress [12,13], anti-cancer drugs [14–18] or compounds and/or conditions that trigger apoptosis [19–21]. Concerning the molecular mechanisms underlying sHsp protective activities, it was observed that HspB1 large oligomers, which are in dynamic equilibrium with those of smaller sizes [22], bear *in vitro* ATP-independent «holdase» chaperone activity [23,24]. In cells recovering from heat shock, HspB1 forms large oligomeric structures that store misfolded polypeptides generated by the heat stress. Consequently, the misfolded polypeptides preserve their folding competent state and do not form toxic aggregates [25–27]. Stored misfolded polypeptides are then either processed for refolding by ATP-dependent foldase chaperones (i.e. Hsp70 and co-chaperones) [28] or degraded by the ubiquitin–proteasome [29] and/or autophagy pathways [30]. Small oligomers formed by HspB1 can also sustain cytoskeleton integrity [31–34]. Of interest, HspB1 also targets specific polypeptides and modulates their activity and/or half-life, such as glucose-6-phosphate dehydrogenase (G6PDH), caspase-3, cytochrome c, Daxx, Akt, eIF4G and eIF4E [35–42], but it is not known whether these features require a particular structural organization of HspB1, such as that bearing chaperone activity.

In human cells, HspB1 phosphorylation is catalysed by MAPKAP kinases 2 and 3 [43–45] and/or phosphatases inactivation [46,47] and occurs at three serine sites [15,78,82] localized in the N-terminal part of the polypeptide outside of the alpha-crystallin domain. We and others have described that the stress-induced phosphorylation of HspB1 redistributes the protein in oligomers of small sizes [6,48]. This negatively regulates the chaperone activity of HspB1 and favors the involvement of this sHsp against stress-induced F-actin architecture disruption [49].

Studies performed with non-phosphorylatable or phosphorylated mimicry mutants led to the conclusion that the large unphosphorylated oligomers (>400 kDa) represent the active form of HspB1 responsive of the protection against oxidative stress [6,27]. It has also been reported that the phosphorylation and oligomerization of HspB1 is modulated by reactive oxygen species [50]. The dynamic changes in HspB1 oligomerization and phosphorylation that regulates and/or recycles HspB1 chaperone activity has also been proposed to be involved in the protection against heat and oxidative stress mediated damages to the cytoskeleton [51,52].

Our observations, confirmed by others, have shown that HspB1 negatively regulates apoptotic cell death programs [19,21,53] while sensitization to apoptosis occurs when the level of this protein is artificially decreased [54–57]. This suggests physiological anti-apoptotic roles of HspB1, particularly in cancer cells where its constitutive expression promotes tumor aggressivity [58,59] and metastasis formation [56,60]. In this respect, HspB1 is the major sHsp expressed in human carcinoma and estrogen-dependent cancer cells [18,61]. HspB1 counteracts apoptosis by acting both upstream and downstream of the release of cytochrome c from mitochondria. Depending on the apoptotic inducer, the upstream effect occurs at the level of different signaling pathways, one of them being related to F-actin architecture integrity [54]. The F-actin pathway probably requires the small phosphorylated oligomers of HspB1 since this is the structural form that protects F-actin network integrity. Interference with the upstream pathways delays the accumulation of cytochrome c in the cytosol and subsequently caspase activation [54,62]. Upstream pathways targeting the pro-apoptotic protein Bax are also modulated by HspB1 [63]. Indeed, through its interaction with Akt, HspB1 indirectly inhibits Bax conformational activation, oligomerization, and translocation to mitochondria [40,41,63]. However, the structural organization of HspB1 responsible of the effect is unknown. Downstream of mitochondria, HspB1 interferes with pro-caspase-9 activation [64] through a rather weak interaction with cytosolic cytochrome c [36,54]. Further downstream, caspase-3 is client protein of HspB1; a phenomenon which impairs its activation by the apoptosome-associated pro-caspase-9 [39]. At least, one of the downstream effects described above could be linked to the large oligomeric structures of HspB1. Indeed, in colon tumors, this structural organization of HspB1 is required for anti-apoptotic and tumorigenic activities. In addition, large oligomers of recombinant HspB1 added to cytosolic extracts decrease cytochrome c mediated caspase activation [65]. HspB1 was also shown to modulate additional apoptotic pathways. For example, small oligomers of HspB1 interact with DAXX and interfere with the apoptotic pathway dependent of this protein [37]. Hence, only very few data are available today concerning the dynamic structural organization of HspB1 in cells exposed to stimuli inducing apoptosis. In addition, the relative protective efficiency of HspB1 against different apoptosis inducers is also not well defined. The only information available to date relates to the modulation of the apoptotic processes in cells over- or under-expressing HspB1 and the interaction of this protein with some key apoptotic regulators [39]. However, the stoichiometry of the interactions and the active structures of HspB1 are not known. In addition, in cells that express high levels of different sHsps, i.e. muscle cells, HspB1 can further form complex mosaic hetero-oligomeric structures with other sHsps [66]. Such interactions are not observed in most human carcinoma cells, such as HeLa, since, in these cells, HspB1 is the major constitutively expressed sHsp. Due to its tumorigenic and metastatic roles, HspB1 has therefore been referred as being a potential anti-cancer therapeutic target [18,61]. These facts prompted us to analyze and compare different properties of the constitutively expressed HspB1 polypeptide of HeLa cells in response to inducers that trigger apoptosis through different pathways: etoposide, Fas, staurosporine and cytochalasin D. Complex and inducer-specific localization, oligomerization and phosphorylation patterns of HspB1 were detected which suggest that the constitutively expressed HspB1 polypeptide of HeLa cells has multiple facets to counteract differentially induced apoptotic programs.

Materials and methods

Cells and reagents

Parental, control (HeLa-neo15) as well as HspB1 under-expressing (HeLa-ASHsp27-1; anti-sense strategy) HeLa cells were previously characterized [54]. They were grown at 37 °C in Dulbecco's modified Eagle medium containing 10% fetal calf serum (Invitrogen, Abingdon,

UK) in the presence of 5% CO_2. The growth medium of HeLa-neo15 and HeLa-ASHsp27-1 cells was further supplemented with 500 μg/ml of G418 (Sigma, St Louis, MO). Transient transfection assays, using lipofectamine reagent (Invitrogen, Abingdon, UK), were performed using previously described pKS27wt (wild type HspB1), pKS2711-3A (non-phosphorylatable mutant: the three phosphoserines 15, 78 and 82 replaced by alanine) or pKS2711-3D (phospho-mimicry mutant: the three phosphoserines 15, 78 and 82 replaced by aspartic acid) DNA vectors [6]. Empty pKS vector (Stratagene, Amsterdam, The Netherlands) was used as transfection control. Monoclonal anti-human Hsp70 and HspB1 antibodies as well as those that specifically recognize HspB1 phosphorylated at either serine 15, 78 or 82 were from Stressgen (Victoria, BC, Canada). Anti-actin antibody and FITC-conjugated goat anti-mouse secondary antibody were from Santa Cruz Biotechnology-Tebu (Le Perray en Yvelines, France). Anti-cytochrome c antibody (clone 7H8.2C12) was from Pharmingen (San Diego, CA), anti-Fas antibody (clone CH-11) was from Upstate Biotechnology (Lake Placid, NY) and Alexa Fluor™ 488 Phalloidin was from Molecular Probes/Interchim (Montluçon, France). Staurosporine, cytochalasin D, etoposide, actinomycin D, and Hoechst 33258 were from Sigma (St Louis, MO).

Measurement of caspase activity

For the determination of DEVD-dependent caspase-3 like activation, 10^6 HeLa cells were harvested and subsequently washed in ice-cold PBS, pH 7.4. Determination of DEVD-AFC activity was performed using a caspase-3 fluorometric Assay kit (MBL, Nagoya, Japan). Excitation was at 400 nm and emission at 505 nm in a Victor Wallach Cytofluorometer (EG&G Instruments, Evry, France). Analysis of transiently transfected cells was performed as follows: 24 h after transfection, cells were trypsinized and allowed to grow for 24 h in white-walled 96-well plates (10^4 cells/well) before being treated and analyzed using caspase-glo® 3/7 assay kit (Promega, Charbonnières, France).

Immunoblotting

One and two-dimensional immunoblot analyses were performed as already described [5]. After SDS-polyacrylamide gel electrophoresis (SDS-PAGE), proteins were transferred to a nitrocellulose membrane (Protan BA 85, Whatman Schleicher & Schuell, Versailles, France). Immunoblots, first probed with an antibody specific to the targeted protein, were incubated with either goat anti-mouse or goat anti-rabbit immunoglobulins conjugated to horseradish peroxidize (Santa Cruz Biotechnology-Tebu, Le Perray en Yvelines, France) and revealed with the ECL kit (Amersham Corp., Buckinghamshire, UK). Autoradiographs were recorded onto X-Omat LS films (Eastman Kodak Co, Rochester, USA). Films were scanned (4990 Epson film scanner) and analyzed with ImageJ software™ (NIH, Bethesda). The duration of the exposure was calculated as to be in the linear response of the film.

Cytochrome c release from mitochondria

The method used for monitoring mitochondrial cytochrome c release into the cytosol was described in one of our previous publication [54]. In brief, HeLa cells (2.10^6) were lysed and cytosolic cytochrome c, released from mitochondria, was analyzed in immunoblots probed with anti-cytochrome c antibody.

Immunofluorescence analysis

HeLa cells ($10^4/cm^2$) growing on glass cover slips, treated or not with apoptotic inducers, were fixed for 10 min with freshly prepared 3.7% formaldehyde, pH 7.0 in PBS before being permeabilized for 5 min in cold acetone. F-actin was stained for 20 min with Alexa Fluor™ 488 Phalloidin (5 U per ml of PBS). HspB1 localization was detected by incubating the coverslips for 1 h with monoclonal anti-HspB1 antibody (diluted 1/100 in PBS containing 0.1% BSA). After washing, HspB1 staining was revealed by incubating cells for 1 h with FITC-conjugated goat anti-mouse immunoglobulins (1/200 in PBS containing 0.1% BSA). Control experiments performed with non-immune sera or only the second antiserum confirmed that all detectable HspB1 fluorescence was specific. Hoechst 33258 staining was used to analyze the morphology of nuclei. The stained cells were then examined and photographed using appropriate filters with a Zeiss Axioskop microscope equipped with a 63× objective lens with a 1–25 numerical aperture and a digital camera device. Individual as well as merge analysis were performed.

Cell fractionation and gel filtration analysis

HeLa cells were washed in ice-cold PBS, pH 7.4 and then lysed in a Dounce homogenizer in TEM lysis buffer (Tris HCl pH 7.4, 20 mM; NaCl 20 mM; MgCl2 5 mM; EDTA 0.1 mM) in the absence or presence of 0.1% Triton X100. The lysates were centrifuged at 10,000 ×*g* for 10 min. SDS sample buffer (1× or 5×) was then added to the resulting pellets and supernatants to obtain samples that had similar volumes. Samples were then prepared for SDS-PAGE and immunoblot analysis using appropriate antibodies. Gel filtration analysis was performed as already described [6]. In brief, 2.10^7 HeLa cells, treated or not, were lysed as above in TEM supplemented with 0.1% Triton X100. The 10,000 ×*g* supernatant was applied onto a sepharose 6B gel filtration column (1 × 100 cm) (Pharmacia, Ullis, France) equilibrated and developed in TEM lysis buffer devoid of Triton X100 and calibrated with a molecular weight markers kit (Kit for Molecular Weights 29,000–700,000 for Gel Filtration Chromatography, Sigma, St Louis, MO). The fractions eluting from the column were analyzed by immunoblotting.

Results

Variability in HspB1 protective activity against unrelated apoptotic inducers

HeLa cells were either kept untreated (NT) or treated for different time periods with either 500 μM etoposide (topoisomerase II inhibitor), 20 ng/ml CH-11 anti-Fas agonist antibody (death receptor activation) + 5 ng/ml actinomycin D (to enhance the killing efficiency of agonist Fas antibody) (Fas Ab) or 0.125 μM staurosporine (kinase inhibitor). The concentration of the apoptotic inducers was chosen as to induce rather similar kinetics of cytosolic cytochrome c accumulation and caspase activation (see Figs. 1A,B). Cells were also treated with cytochalasin D (0.5 μM). This drug rapidly inhibits F-actin polymerization and induces an apoptotic process [54] counteracted, at least in part, by the ability of HspB1 small oligomers to stabilize F-actin integrity [33,54,67].

We first compared the kinetics of cytochrome c released from mitochondria in response to the different apoptotic inducers (see

Materials and methods). Fig. 1A shows that, in staurosporine treated cells, cytochrome c was quantitatively released after 1 h of treatment. In response to Fas Ab and etoposide the phenomenon occurred 2 h later and was further delayed in response to cytochalasin D. In response to etoposide, pro-caspase-3-like (DEVDase) activation was detectable after 1 h of treatment (Fig. 1B). 2 h later, the stimulation was of 1.3-fold and reached 5.5-fold after 12 h. Roughly similar kinetics were observed in response to Fas Ab and staurosporine. After 12 h of treatment with these inducers, the stimulation was of 6.9- and 6.4-fold, respectively. In contrast, in cells exposed 12 h to cytochalasin D, the stimulation was of only 2-fold in spite of the release of cytochrome c from mitochondria (Fig. 1A) and the rapid disruption of F-actin architecture (see below Fig. 2). Hence, the different concentrations of etoposide, Fas Ab and staurosporine that were used showed rather similar kinetics of apoptosis induction while the process was less intense or delayed in cytochalasin D treated cells, probably because of the weak apoptotic efficiency of this inducer.

We next compared HspB1 protective efficiency against the different inducers. We used a genetically modified HeLa cell line (HeLa-ASHsp27-1) expressing reduced levels of HspB1 (2.4 instead of 4 ng per μg of total proteins) (Fig. 1C) that were already described to be more sensitive to staurosporine treatment than the corresponding control (HeLa-neo15) and parental HeLa cells [54]. For every apoptotic inducer tested, the decrease in HspB1 expression correlated with enhanced cytochrome c accumulation and DEVDase activity (Figs. 1D,E). The stimulation of DEVDase activity (1.5 to 2.5 fold) was dependent on the inducer (maximal effect in response to Fas Ab) and to a lesser extent on the duration of the treatment (3 or 6 h). Hence, the inducer-specific variability in HspB1 protective activity supports the hypothesis that, in addition to its role at the level of the common execution phase of apoptosis (cytochrome c/caspase activation) [36,39,54], this protein may differentially modulate inducer-specific upstream transduction pathways.

Apoptotic inducer-specific changes in HspB1 intracellular localization

Dynamic and transient changes in intracellular localization, oligomerization and phosphorylation have been shown to correlate with HspB1 ability to counteract the deleterious effects induced by heat shock or oxidative stress [5,48,68]. In contrast, less is known about HspB1 localization and structural organization in cells exposed to apoptosis inducers. HspB1 intracellular localization was first analyzed using an immunofluorescence approach in cells treated with the different inducers (same concentrations as indicated in Fig. 1). Treatments of 3 h were chosen to analyze the early phase of the apoptotic programs and thus avoid too drastic effects on cell morphology. F-actin structural organization and nuclear morphology were determined to estimate these effects. In growing non-treated HeLa cells (NT), HspB1 showed a diffuse cytoplasmic localization, particularly in the perinuclear region. This protein was also present in membrane ruffles (Figs. 2A,B). In these cells, F-actin displayed characteristic transcytoplasmic fiber appearance and co-localized with HspB1 in membranes ruffles (arrow). Analysis of cells exposed to the different inducers revealed profound and specific effects induced by these compounds. In etoposide and Fas Ab treated cells, in spite of still showing a diffuse cytoplasmic distribution, HspB1 localized in particular cell surface membrane blebs (up to 15 blebs per cell, size 1–3 μm in diameter). In these cells, the transcytoplasmic fiber appearance of F-actin was lost. However, in agreement with a previous report [69], F-actin fibers were still present and accumulated at the cell periphery where they formed a dense spherical network known to generate membrane blebbing activities [70]. Of interest, in etoposide treated cells, HspB1 containing membrane blebs co-stained with phalloidin, hence revealing the presence of F-actin in these structures (see the arrow in merge analysis, Fig. 2B). In Fas Ab treated cells, the co-localization was restricted to the base (cytoplasmic side) of the blebs (Fig. 2B). In cells exposed to staurosporine, HspB1 was mainly concentrated in cytoplasmic domains devoid of phalloidin staining. In contrast, but in agreement with previous reports [71–73], the transcytoplasmic and/or cell periphery fibers were lost and F-actin staining was recovered at the level of HspB1-devoid areas dispersed throughout the cytoplasm. In response to cytochalasin D, and as previously described, the transcytoplasmic and/or cell periphery fibers were lost and most F-actin staining was dispersed within the cytoplasm and at the level of particular HspB1 positive cell surface rounded structures (one to two per cell, 5–8 μm in diameter). Analysis of these structures revealed that they were decorated by HspB1 positive small bleb-like sub-structures; only some of them, localized inside the large rounded structures, co-stained with phalloidin (see arrows in enlarged images of Fig. 2B). HspB1 not present in the cell surface rounded structures had a diffuse cytoplasmic distribution. No fragmentation of nuclei was observed confirming that the analysis was performed during the early phase of the different apoptotic processes. Moreover, in etoposide and Fas Ab treated cells, the cell surface HspB1-containing blebs were Hoechst staining negative suggesting that they were not DNA-containing apoptotic bodies but more probably an already described early, F-actin integrity dependent, apoptotic manifestation that usually occurs in cells exposed to stressful stimuli [70].

We next analyzed the intracellular distribution of HspB1. Fig. 3A shows that, following lysis in the absence of detergent, only 39% of HspB1 present in exponentially growing HeLa cells was recovered in the 10,000×*g* supernatant fraction indicating that a large fraction of this protein co-sedimented with cellular structures. Analysis of the effects mediated by 3 h of treatment with staurosporine, Fas Ab or etoposide revealed a moderate increase of HspB1 level in the soluble fraction (44, 45 and 47%, respectively). Similar distributions of HspB1 were observed when cells were exposed for longer time periods to the inducers (not shown). In regards to the localization analysis presented in Fig. 2, it can be concluded that the presence of HspB1 in membrane blebs does not significantly alter its overall distribution following cell lysis. Moreover, when cells were lysed in the presence of 0.1% of Triton X-100, 80% or more of the cellular content of HspB1 was recovered in the supernatant fraction. In the absence of detergent, etoposide, Fas Ab or staurosporine did not significantly alter the distribution of actin. Indeed, its distribution was close or identical to that observed in non-treated cells (about 32% in the soluble fraction). In the presence of detergent, the level of actin in the soluble fraction drastically increased but the phenomenon was less intense in cells treated with etoposide, Fas Ab or staurosporine (58, 62, 55%, respectively) than in non-treated cells (69%). Concerning Hsp70, it is worth taking note that in non-treated cells this protein had a distribution similar to actin independently of the presence or not of detergent. Treatments with etoposide, Fas Ab or staurosporine increased the percentage of Hsp70 in the soluble fraction in the absence of detergent and, as observed in the case of actin, had the

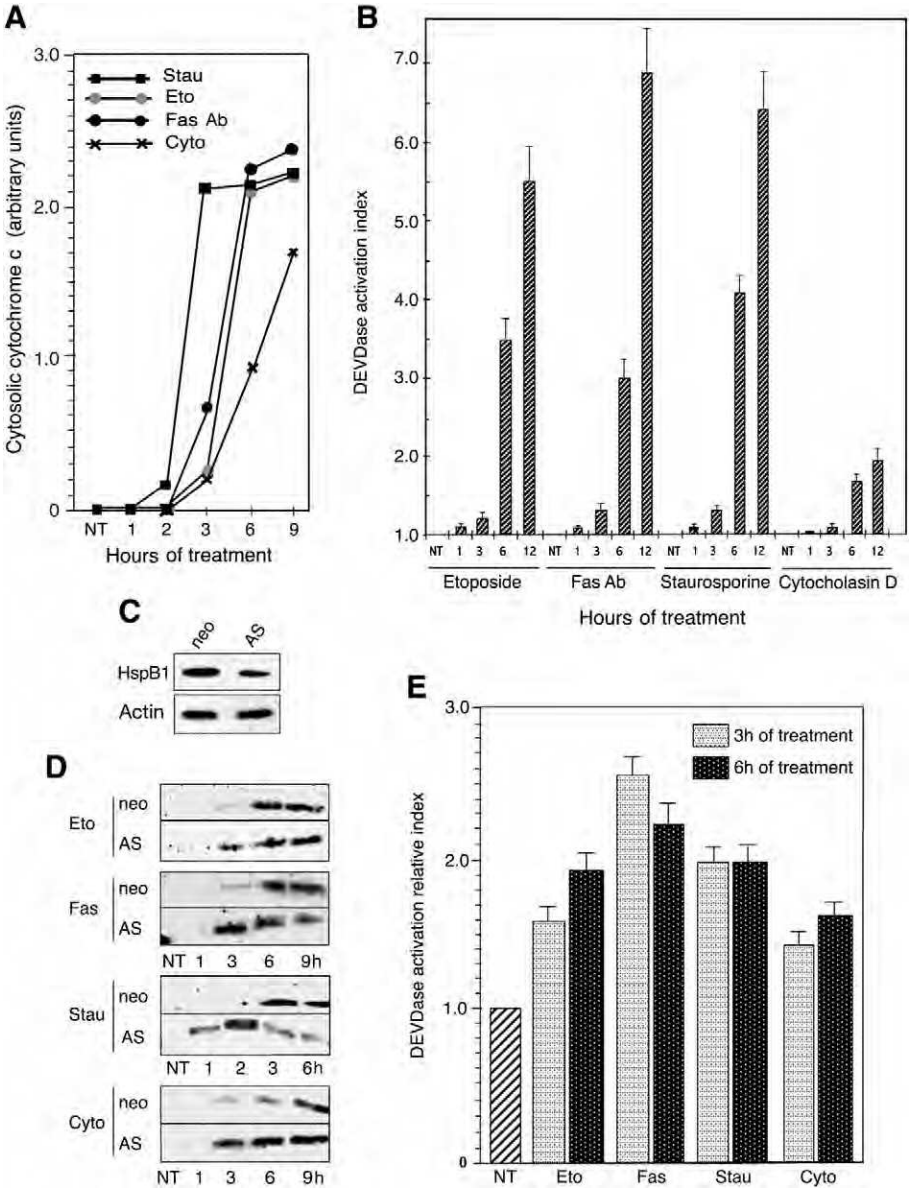

Fig. 1 – Apoptotic treatments and protection mediated by HspB1. A) Analysis of cytosolic cytochrome c level. HeLa cells were either kept untreated (NT) or exposed for various times (1 to 9 h) to either 0.125 μM staurosporine (Stau), 0.5 μM cytochalasin D (Cyto), 500 μM etoposide (Eto), or 20 ng/ml anti-Fas antibody + 5 ng/ml actinomycin D (Fas Ab). Quantitative analysis of cytosolic cytochrome c level (see Materials and methods) is presented. B) Kinetics of DEVDase (pro-caspase-3-like) activity. Activation index was determined as the ratio between the activities measured in treated cells to that determined in non-treated cells. The histograms shown are representative of three identical experiments, standard deviations are presented ($n = 3$). C–E) Underexpression of HspB1 stimulates cytosolic cytochrome c accumulation and DEVDase activation. (C) Immunoblot analysis of HspB1 and actin present in growing HeLa-neo15 (neo) and HeLa-ASHsp27-1 (AS) cells. (D) Effect of HspB1 underexpression towards cytosolic cytochrome c accumulation. HeLa-neo15 control (neo) and HeLa-AS27-1 (AS) cells were either kept untreated (NT) or treated for various time periods with the different apoptotic inducers (as above). Cytosolic cytochrome c was analyzed in immunoblots probed with anti-cytochrome c antibody. Autoradiographs of ECL-revealed immunoblots are presented. Note that cytochrome c is present in the cytosol of HeLa-AS27-1 cells earlier than in control HeLa-neo15 cells which contain a normal level of HspB1. (E) DEVDase activity in HeLa-neo15 and HeLa-ASHsp27-1 cells. Cells were analyzed after 3 and 6 h of treatment and the DEVDase activation relative index was determined for each treatment as the ratio between the activities in extracts of HeLa-AS27-1 cells to that measured in extracts of control HeLa-neo15 cells. 1.0 corresponds to the value observed in control HeLa-neo cells. The histogram shown is representative of three identical experiments, standard deviations are presented ($n = 3$).

tendency to retain Hsp70 in pellet fraction in the presence of detergent.

Cytochalasin D had the most pronounced effect on the distribution of HspB1 and actin. Indeed, a large fraction (69%) of HspB1 was recovered in the 10,000 ×*g* supernatant fraction in the absence of detergent (85% in the presence of detergent). In contrast, actin showed an equal distribution between the supernatant and pellet fractions that was not significantly altered by the presence of

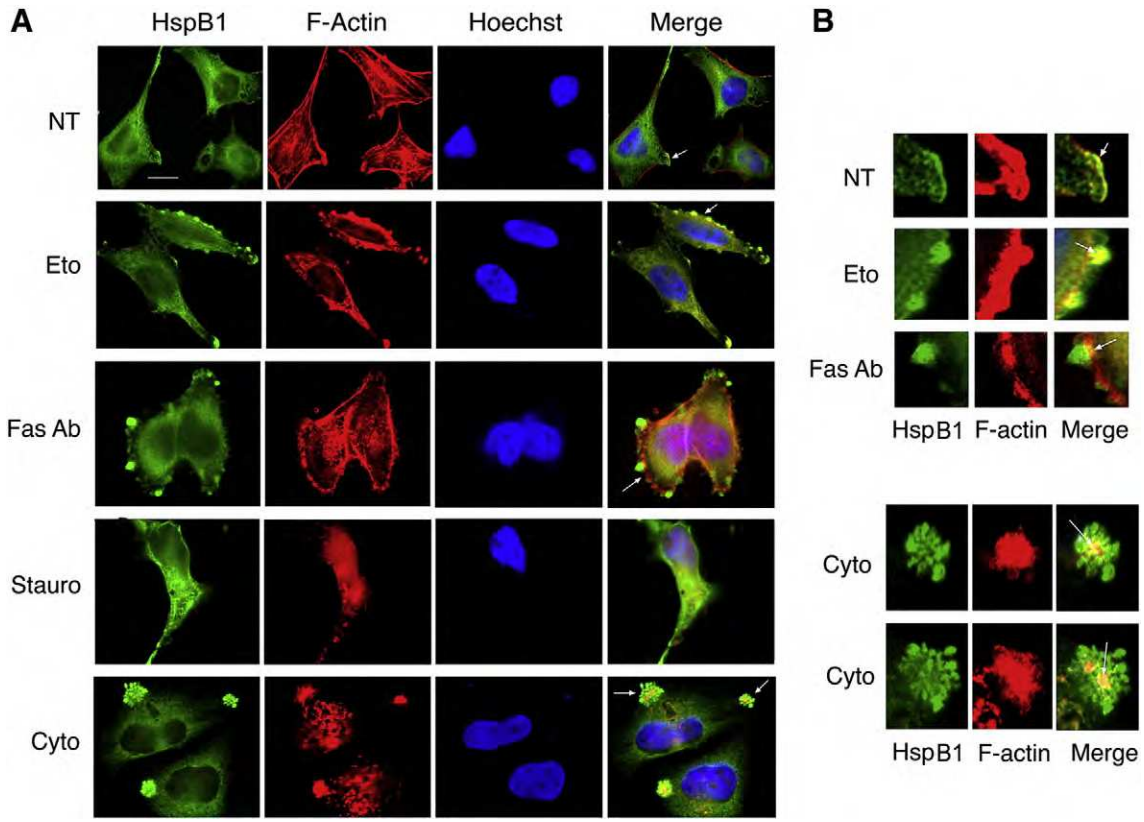

Fig. 2 – Intracellular localization of HspB1 in HeLa cells exposed to different apoptotic inducers. A) Fluorescence photomicrograph analysis. Cells were then either kept non-treated (NT) or treated for 3 h with apoptotic inducers as described in Fig. 1. Thereafter, cells were prepared for detection of HspB1, F-actin and nuclei as described in Materials and methods. Bar: 10 μm. B) Enlargements of cells presenting a co-localization of HspB1 and F-actin (indicated by arrows in the merge analysis presented in A). Note the co-localization of HspB1 and F-actin in membrane ruffles of untreated cells (arrow). Note also the presence of HspB1 in membrane blebs (1–3 μm) formed in response to etoposide and Fas Ab and the presence of F-actin in the basal part of the blebs (arrows). Analysis of the cell surface structures (5–8 μm) formed in response to cytochalasin D revealed that HspB1 and actin co-localized only in the central part of the structure (arrows).

detergent. In the absence of detergent, similarly to actin, an equal distribution of Hsp70 between the supernatant and pellet fractions was observed. In the presence of detergent, 41% of Hsp70 still remained associated with the pellet fraction.

Taken together, these observations confirm that the distribution of HspB1 is specific and that a substantial amount of this protein has the tendency to associate, in an F-actin integrity dependent way, with detergent sensitive structures, such as the plasma membrane cytoskeleton compartment where actin nucleation occurs [74,75]. Hence, in cytochalasin D treated cells, the association of HspB1 with large cell surface rounded structures (Figs. 2A,B) is easily destroyed upon cell lysis, probably as a consequence of F-actin integrity disruption. Control experiments revealed, that throughout the experiments, the different inducers did not alter the total cellular level of HspB1 and actin (see Fig. 4B).

Apoptotic inducer-specific redistribution of HspB1 dynamic oligomeric size

Since HspB1 is an oligomeric protein [76], we have investigated whether apoptotic stimulations could modify its native molecular mass. The 10,000 ×*g* supernatant (S fraction) of Triton X-100 lysed HeLa cells (at least 80% of the cellular content of HspB1) was therefore analyzed onto Sepharose 6B gel filtration columns. As previously described [5,77], in exponentially growing HeLa cells, HspB1 was recovered almost equally in two major oligomeric structures with heterogeneous native molecular masses broadly comprised between 50 and 200 kDa (small oligomers, population I) and 200 and 700 kDa (large oligomers, population II) (Fig. 3B). It can also be noted that a low population of Hsp27 molecules is present in the intermediate 150 to 400 kDa range. Similar size distributions of HspB1 have been observed *in vitro* [78]. As observed in Fig. 3B, HspB1 was not detected in the void volume of the column, hence suggesting that it was not associated with Triton X-100 resistant structures larger than 10^6 Da. Up to 6 h of treatment with etoposide, HspB1 had the gradual tendency to concentrate in large structures (population II) (Fig. 3B). After 12 h, the size distribution of HspB1 was back to normal (see Fig. 5A for a more complete analysis of the phenomenon). A rather similar redistribution of HspB1 was observed in cells exposed to Fas Ab. However, in this case, the two oligomeric populations were more clearly defined and the maximal accumulation of HspB1 in population II occurred later (9 h) than in cells exposed to etoposide (see data presented in Fig. 5A). As in the case of etoposide, after

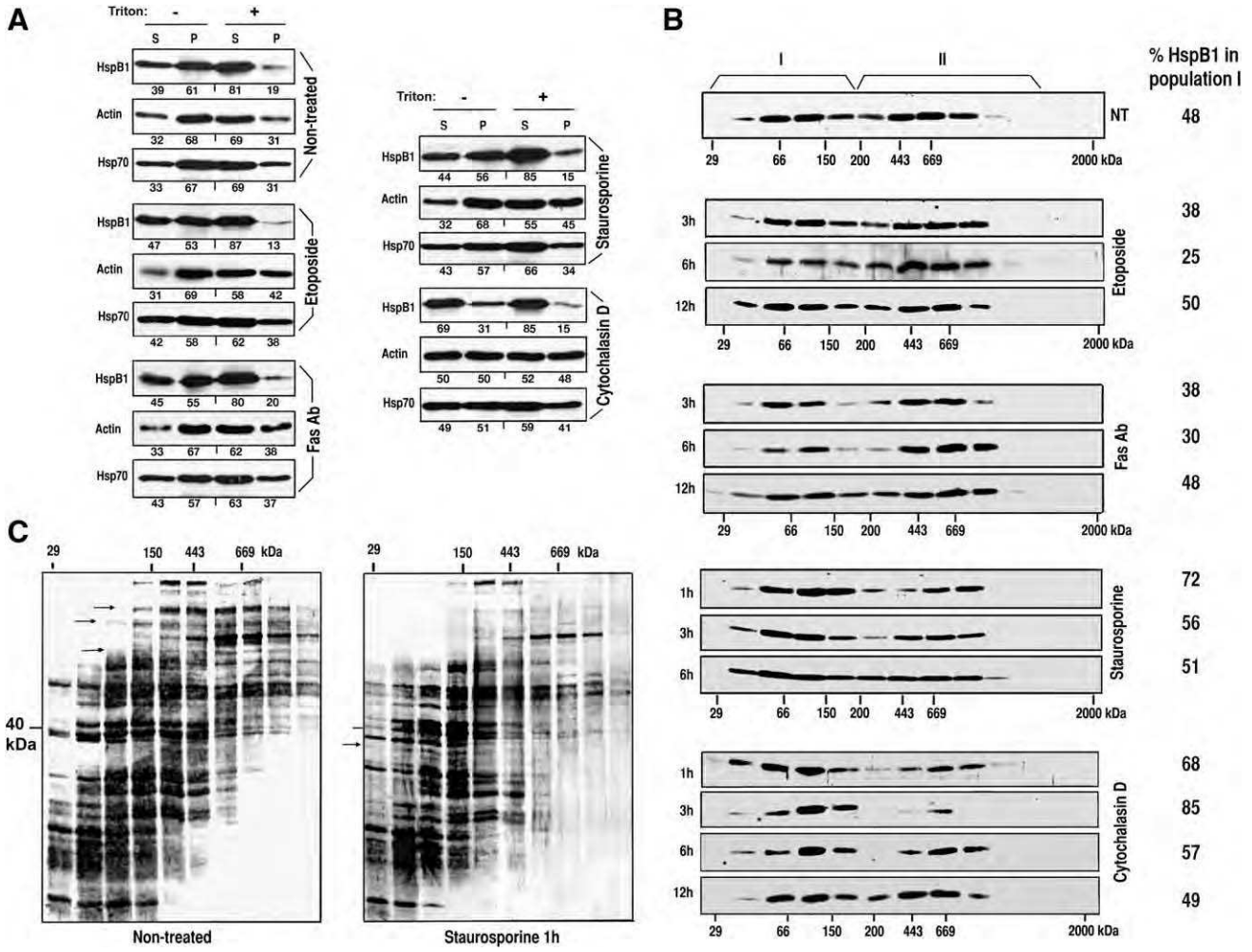

Fig. 3 – HspB1 cellular distribution and native size in response to different apoptotic treatments. A) Cellular distribution upon cell lysis. HeLa cells were either kept untreated (NT) or treated for 3 h with the different apoptotic inducers (same concentrations as in Fig. 1). Cells were then lysed in the absence (−) or presence (+) of 0.1% Triton X-100 and spun at 10,000 ×*g* as described in Materials and methods. The levels of HspB1, actin and Hsp70 present in the supernatant and pellet fractions were detected in immunoblots probed with the corresponding antibody (see Materials and methods). Autoradiographs of ECL-revealed immunoblots are presented. B) Analysis of HspB1 native size. HeLa cells were either kept untreated (NT) or treated with the apoptotic inducers as described above. 10,000 ×*g* soluble cytosolic fractions were applied to Sepharose 6B gel filtration columns (see Materials and methods). The presence of HspB1 in pooled fractions eluted from the columns was detected in immunoblots probed with anti-HspB1 antibody. Autoradiographs of ECL-revealed immunoblots are presented. 29, 66, 150, 200, 443 and 669 kDa are gel filtration markers. The exclusion size of the column is indicated (2000 kDa). Population I corresponds to native sizes < 200 kDa and population II to native sizes > 200 kDa. The percentage of HspB1 in population I is presented (% of ratio population I to population II) (see Fig. 5A and Materials and methods). C) Control experiment. HeLa cells, either kept untreated (NT) or treated for 1 h with 0.125 μM staurosporine, were lysed as above and the cytosolic fractions were applied to Sepharose 6B gel filtration columns as above. The proteins present in the eluted fractions were analyzed and gels were silver stained. Note that in response to staurosporine treatment the native size of the majority of the proteins was not altered. Small arrows point to minor changes between the two column profiles.

12 h of treatment, HspB1 oligomerization profile was back to normal. Hence, in response to these two inducers, HspB1 had the gradual, but transient, tendency to concentrate in structural forms that display large native sizes. Analysis performed in cells exposed to either staurosporine or cytochalasin D gave intriguing results since these inducers rapidly (during 1 to 3 h of treatment) concentrated HspB1 in the form of small oligomers (population I). The phenomenon was more intense in response to cytochalasin D (85% of HspB1 in small oligomers <200 kDa) than in cells exposed to staurosporine (72%). The phenomena were reversible and the oligomerization profile of HspB1 was back to normal after 12 h of treatment. This later time period was characterized by the ability of HspB1 to reform large structures (population II). Control experiments were performed to verify that the particular changes in HspB1 oligomerization were specific and not shared by most cytosolic proteins. An example, shown in Fig. 3C, allows to conclude that the redistribution of HspB1 towards small oligomers in response to 1 h of staurosporine was not shared by the bulk of

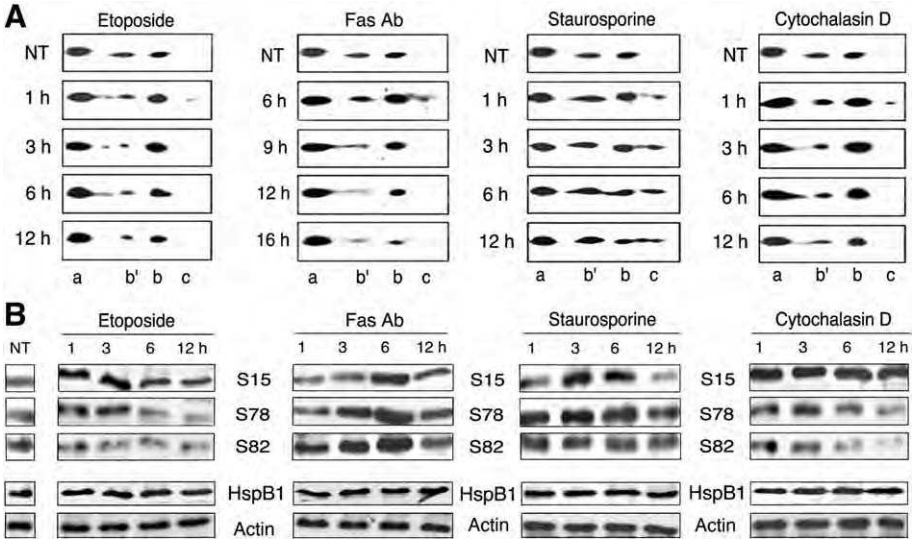

Fig. 4 – Analysis of HspB1 phosphorylation. A) HspB1 isoforms revealed by two-dimensional gel analysis. HeLa cells were either kept untreated (NT) or treated for different time periods with the different apoptotic inducers as above. Total cellular proteins were collected and processed for two-dimensional immunoblot analysis. HspB1 isoforms were detected by probing 2-D blots with anti-HspB1 antibody. Autoradiographs of the ECL-revealed immunoblots are presented. The acidic end is to the right. The «a» isoform represents the unphosphorylated form of the protein. The «b» and «c» isoforms are representative of HspB1 phosphorylated at one or two sites, respectively. The nature of the b′ isoform is still not known. B) Immunoblot analysis of HspB1 phosphorylation at the three serine sites. HeLa cells were either kept untreated (NT) or treated with the different apoptotic inducers. At the time indicated, total cellular protein contents were analyzed in immunoblots probed with antibodies that are specific for HspB1 phosphorylation at either serine 15 (ser 15), serine 78 (ser 78) or serine 82 (ser 82) (see Materials and methods). The corresponding levels of total HspB1 and actin are shown as controls. Autoradiographs of ECL-revealed immunoblots are presented.

cytosolic proteins showing a native size larger than 200 kDa. Two types of inducers can therefore be defined: etoposide and Fas Ab which shift HspB1 towards large oligomeric structures and staurosporine and cytochalasin D which rapidly concentrate HspB1 in the form of small oligomers.

Control experiments revealed that the different apoptotic inducers did not stimulate the expression of HspB1 (see Fig. 4B) or other sHsps, such as those that are heat inducible, i.e. HspB5 (αB-crystallin) and HspB8 (not shown). This excludes that HspB1 could form hetero-oligomeric structures in HeLa cells committed to apoptosis. Moreover, it should also be noted that the presence of actinomycin D in Fas Ab treated cells excludes interference by Fas-induced gene expression.

Apoptotic inducer-specific changes in HspB1 isoform composition and phosphorylation

In two-dimensional gels HspB1 is resolved in several major isoforms, denoted a, b and c, which correspond to the non- (a), mono- (b) and bi- (c) phosphorylated forms of HspB1 [77]. The minor b′ isoform originates from a still unknown modification. Cells were exposed or not (NT) for different time periods to the different apoptosis inducers described above. In non-treated cells, the non-phosphorylated (a) isoform as well as the b′ and b isoforms were detected (Fig. 4A). Isoform b results of the phosphorylation of HspB1 induced by mitogens in the culture medium [77]. In cells exposed to etoposide, the level of the b phospho-isoform gradually increased (up to 3 h) while the c phospho-isoform was detectable only after one hour of treatment. Their levels corresponded to about half of the cellular content of HspB1. After 12 h, the isoform composition of HspB1 was back to normal confirming the transient nature of the phosphorylation induced by etoposide. A similar phenomenon was observed in Fas Ab treated cells. In these cells, the maximal accumulation of HspB1 phospho-isoforms was observed after 6 h of treatment and after 12 h the isoform composition was close to that observed in untreated cells. A further treatment up to 16 h revealed a sharp decrease in the level of the b and c isoforms suggestive of HspB1 dephosphorylation. Staurosporine also stimulated the level of the b and c isoforms. The maximal effect was observed between 3 to 6 h of treatment. After 12 h, the b isoform was back to normal but the c isoform was still present. Cytochalasin D also increased the level of the b isoform, particularly during the 1 to 6 h period of the treatment. The c isoform was detectable only after 1 h of treatment. Concerning the non-phosphorylated b′ isoform its levels gradually decreased during etoposide, Fas Ab and cytochalasin D treatments. In contrast, its level increased in staurosporine treated cells.

We then tested whether the gradual increase in b and c phospho-isoforms described above reflected uniform or differentially increased phosphorylation of the different phosphoserine sites of HspB1. Immunoblot analysis of total cellular proteins was then performed using antibodies that specifically recognized HspB1 phosphorylated at either serine 15 (S15), serine 78 (S78) or serine 82 (S82) (Fig. 4B). Until 3 h of treatment, etoposide drastically increased the phosphorylation of serine 15. A less pronounced effect was observed at the level of serine 78. After 12 h

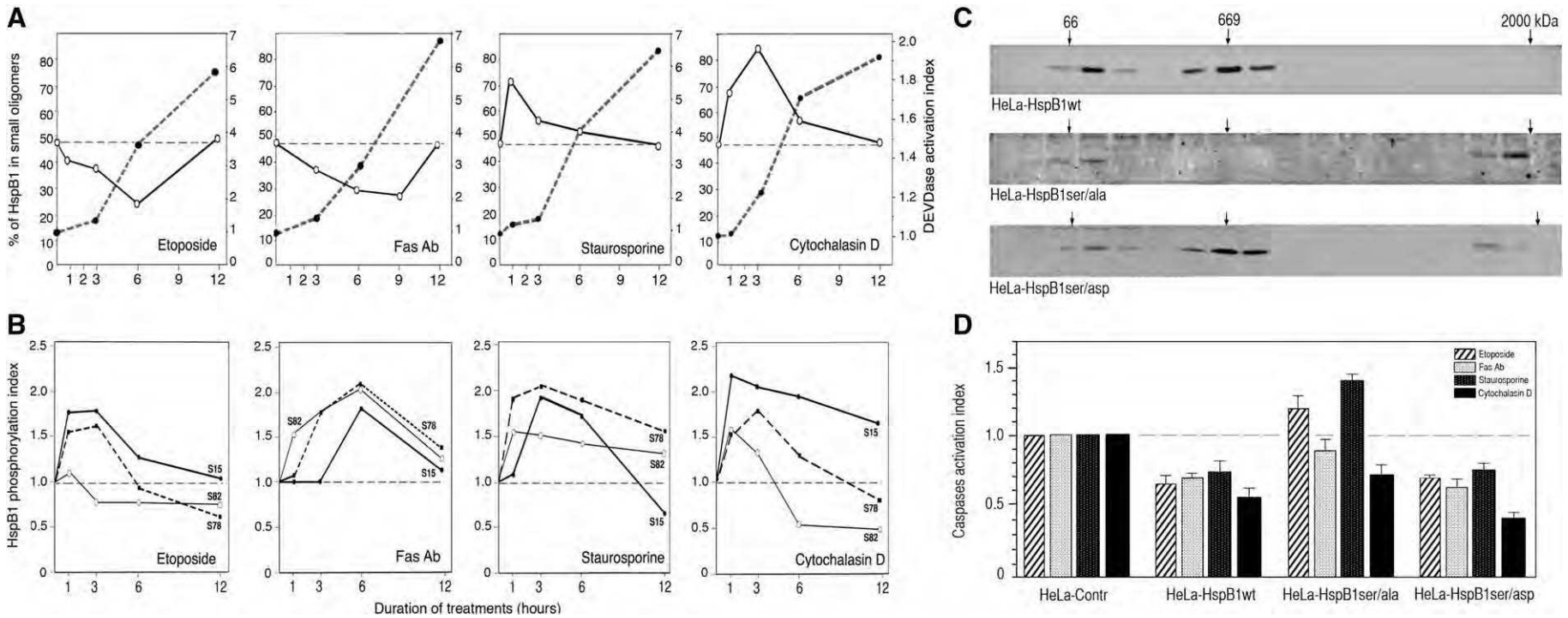

Fig. 5 – Quantitative analysis of HspB1 oligomerization and phosphorylation in relation to DEVDase activation. A) Changes in HspB1 native size and DEVDase activation. The oligomerization data presented in Fig. 3B were quantified (see Materials and methods) to compare, in function of the duration of the different apoptotic treatments, the fraction of HspB1 in the form of population I (<200 kDa) to that in population II (>200 kDa). The percentage of the calculated ratio is presented (open circles). On the same graphs, and for each treatment, DEVDase activation index (see Fig. 1A) is reported (closed circles, dotted thick lane). B) HspB1 phosphorylation. The immunoblots presented in Fig. 4B were quantified to determine the HspB1 phosphorylation index at either serine 15 (S15, thick line), serine 78 (S78, dotted line) or serine 82 (S82, thin line). The index was calculated as the ratio between the values determined in cells exposed to an apoptotic inducer to that observed in non-treated cells. The index value of 1 (horizontal thin dotted line) represents the phosphorylation observed in non-treated cells. Report to (A) for the corresponding percentage of HspB1 in population I (<200 kDa) and DEVDase activation index. C–D) Effects of phosphorylation mutants on HspB1 oligomerization and caspase activation. HeLa cells were transiently transfected with pKS27wt (wild type HspB1), pKS2711-3A (3 phosphoserine sites replaced by alanine) or pKS2711-3D DNA vector (3 phosphoserine sites replaced by aspartic acid) (see Materials and methods). Control experiment was performed using an empty pKS vector. Transiently transfected cells were treated or not for 6 h with the apoptosis inducers (as above) before being analyzed. C) HspB1 native size. Experiment was as described in Fig. 3B except that more fractions of the column were analyzed to include native sizes up to 2000 kDa. D) DEVDase activation. Experiments were performed as described in Fig. 1B using caspase-glo® 3/7 assay kit (Promega, Charbonnières, France). DEVDase activation index was determined, for each apoptotic treatment, as the ratio between the activity measured in extracts of cells transfected with a specific vector (HeLa Hsp27wt, HeLa Hsp27ser/ala or HeLa Hsp27ser/asp) to that measured in extracts of cells transfected with the empty vector (control HeLa). The histograms shown are representative of three identical experiments, standard deviations are presented ($n = 3$). 1.0 corresponds to the DEVDase activity induced by the different inducers in control HeLa cells.

of treatment, phosphorylation of serines 78 and 82 was less intense than in non-treated cells. Hence, the high level of b isoform (see Fig. 4A) probably corresponds to serine 15 and 78 phosphorylation. In response to Fas Ab, phosphorylation of serine 15 began to increase after 3 h of treatment and was maximal 3 h later. After 12 h, its level was almost back to normal. Serine 78 showed a rather similar kinetic of phosphorylation except that the stimulation was already intense after 3 h and decreased less rapidly than

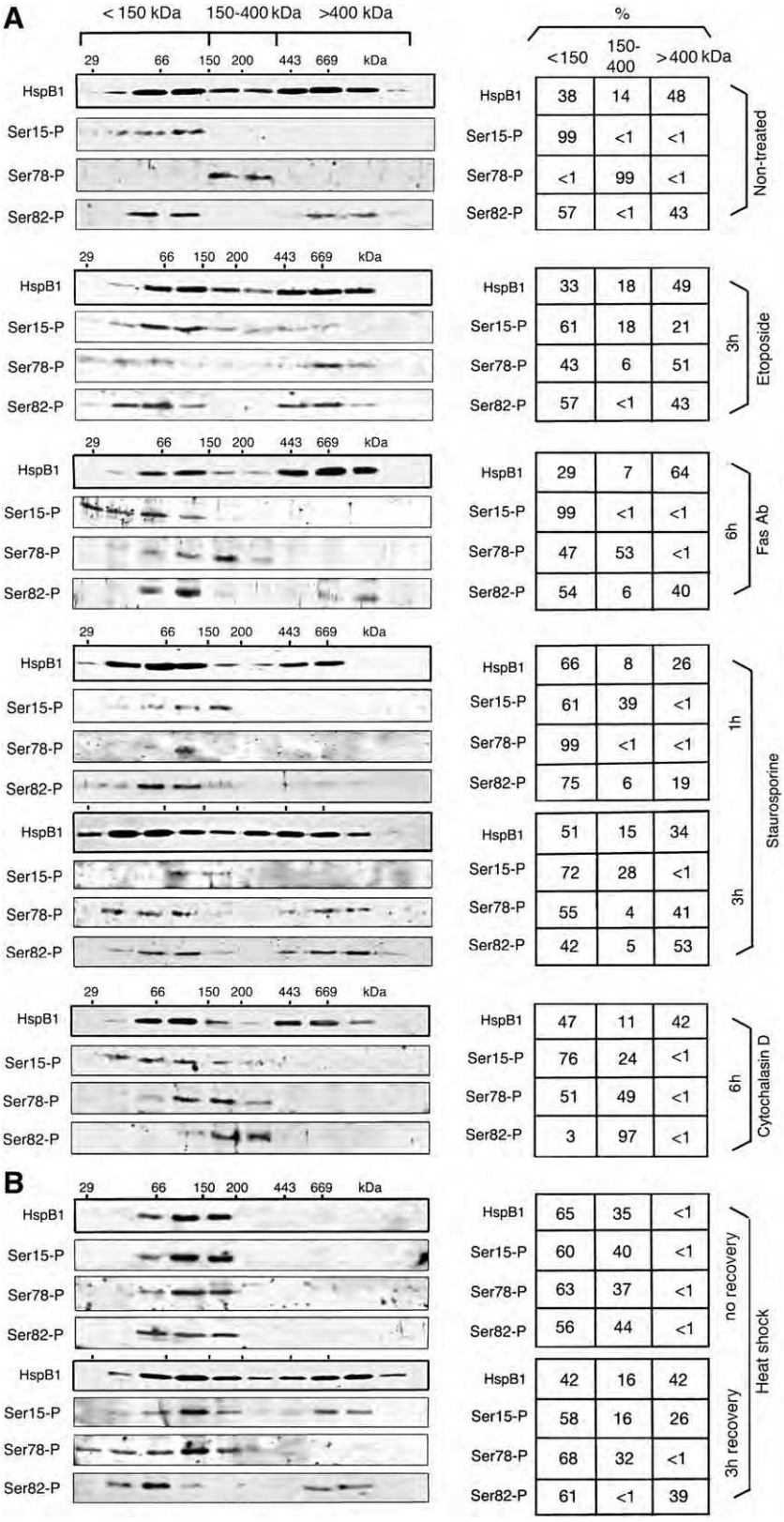

in the case of serine 15. Concerning serine 82, the stimulation was already intense after 1 h of treatment and was still elevated 5 h later. As indicated above in the case of etoposide, a good correlation was observed between the maximal phosphorylation of the serine sites and the highest level of accumulation of the b and c isoforms (see Fig. 4A). In response to staurosporine, the maximal level of phosphorylation of serines 15 and 78 occurred between 3 to 6 h of treatment, in agreement with the highest level of the b and c isoforms (Fig. 4A). However, as in the case of Fas Ab, serine 78, in contrast to serine 15, showed an increased phosphorylation early after the beginning of the treatment (3 h) that still remained elevated 9 h later. Phosphorylation of serine 82 showed a completely different kinetic of phosphorylation. The maximal effect was observed after 1 h. Then, it decreased very slowly and was still intense after 12 h of treatment. The presence of the b and c phospho-isoforms at this time period (see Fig. 4A) may therefore result in serine 78 and 82 intense phosphorylation. Analysis of the effects induced by cytochalasin D revealed kinetics of HspB1 phosphorylation that had no common features with those induced by etoposide, Fas Ab or staurosporine. Indeed, only serine 15 showed an intense phosphorylation that remained about constant all over the time period of the analysis. In contrast, serines 78 and 82, after a short period of stimulation, were gradually dephosphorylated. After 12 h of treatment, the main phosphorylated site of HspB1 was serine 15 which corresponded to the b isoform (see Fig. 4A). In these cells, the gradual overall decrease in the level of b isoform observed after 1 h of treatment may therefore be a consequence of the dephosphorylation of serines 78 and 82.

Quantitative analysis of the dynamic and inducer-specific changes in HspB1 oligomerization and phosphorylation in respect to caspase activation

To estimate the significance of the changes in oligomerization and phosphorylation of HspB1 with respect to its anti-apoptotic activities, we first compared, in each condition, the percentage of HspB1 in small oligomers to that of DEVDase activation. A compilation of the data presented in Figs. 1B and 3B is presented in Fig. 5A. In this figure the percentage of HspB1 in small oligomers (<200 kDa, population I) as well as the DEVDase activation index is presented in relation to the duration of the treatments with the different inducers. Based on the results presented in Fig. 4B, the phosphorylation stimulation index of each serine site was also determined for each inducer (Fig. 5B). The index of one particular phosphoserine site was calculated as the ratio between the values determined in inducer treated cells to those observed in non-treated cells. To compare for each time point, the percentage of HspB1 which is phosphorylated, in the form of small oligomers (<200 kDa, population I) and DEVDase activation, the phosphorylation data are presented below those describing oligomerization-DEVDase activation.

It can be concluded from Fig. 5A that the shift of HspB1 oligomers towards large molecular masses (population II) observed in response to the first class of inducers (etoposide and Fas Ab) occurred when DEVDase activation was still weak. Then, in both cases, the maximal changes in HspB1 oligomerization corresponded to a time period characterized by the logarithmic activation phase of DEVDase. Thereafter, DEVDase activity continued to increase while HspB1 oligomerization was back to normal. Hence, one hypothesis could be that HspB1 redistributes towards large oligomers (population II) to counteract DEVDase activation since, in cells containing 40% less of this protein, DEVDase activation occurred more rapidly and was 1.5- to 2-fold more intense (see Fig. 1E). Analysis of the second class of inducers (staurosporine and cytochalasin D) revealed that the transient accumulation of HspB1 in the form of small oligomers (<200 kDa, population I) was a rapid phenomenon. In staurosporine treated cells, it even preceded DEVDase activation. Thereafter, HspB1 reformed large oligomers and their appearance was concomitant with the time period where DEVDase activation was drastically enhanced. As described above for the first class of inducers, at later time period DEVDase activity continued to increase while HspB1 native size profile was back to that observed in untreated cells. These particular and rather similar behaviors induced by the second class of inducers are intriguing and suggests that HspB1 small oligomers may interfere with early events triggered by these inducers. The reformation of large oligomers at later time period may be related to DEVDase activity as described above in the case of etoposide and Fas Ab treatments. In this respect, only staurosporine and cytochalasin D induced the rapid destruction of F-actin fibers (see Fig. 2A); the phenomenon being more intense in cytochalasin D treated cells. Indeed, between 1 and 3 h of treatment these fibers were destroyed; a time period which corresponded to the maximal accumulation of HspB1 in the form of small oligomers. Since small phosphorylated oligomers of HspB1 are known to act as F-actin stabilizers that interfere with cytochalasin D disrupting activity [31], one possibility hence exists that the early change observed in HspB1 structural organization in response to staurosporine and cytochalasin D may be related to F-actin stabilization.

Fig. 6 – Native size of phosphorylated HspB1 in HeLa cells exposed to apoptotic inducers or heat shock. A) Apoptotic inducers. HeLa cells were either kept untreated (NT) or treated as before with the different apoptotic inducers. At the time indicated, 10,000×*g* cytosolic fractions were analyzed by gel filtration column as described in Fig. 3B and Materials and methods. Immunoblot analysis of the proteins present in the pooled fractions was performed using antibodies that are specific to either total or phosphorylated (Ser15-P, Ser78-P or Ser82-P) HspB1. In each condition, the oligomerization profile of total HspB1 is shown to better visualize the oligomers that show modified level of phosphorylation (indicated as HspB1 and marked by a dark line surrounding immunoblots). B) Effect of heat shock. HeLa cells, treated for 1 h at 42 °C followed or not by a 3 h recovery period at 37 °C, were analyzed as described in (A). Quantification was performed as described in Materials and methods and presented as percentage of the total and/or phosphorylated HspB1 present in the three size fractions of the column. In spite of the fact that the profile of phosphorylated oligomers is specific to each condition it is mainly recovered in three major structural organizations: oligomers whose size is smaller than 150 kDa, oligomers that display a native size comprised between 150 and 400 kDa and those that have a larger size.

Analysis of Fig. 5B allows to conclude that the stimulation of phosphorylation in response to the different inducers is an early event that corresponds to the time period when HspB1 changes its oligomerization pattern and when DEVDase is only weakly activated. However, each inducer activates HspB1 phosphorylation differently. Serine 15 was the major phosphorylated site in response to cytochalasin D while serine 78 was highly stimulated by staurosporine. Serine 82 was only efficiently stimulated in response to Fas Ab and was rapidly dephosphorylated after a short period of stimulation in etoposide and cytochalasin D treated cells.

To approach the question of how critical phosphorylation is in relation to HspB1 oligomerization profile and ability to counteract caspase activation, we transiently transfected HeLa cells with DNA vectors encoding either HspB1 wild type, non-phosphorylatable or phospho-mimicry mutant [6]. The experiment was performed with the aim that the transfected exogenous HspB1 polypeptide would interact with the endogenous and constitutively expressed HspB1 and, if mutated, would act as a dominant mutant spreading its effect at the level of the resulting mosaic oligomeric structures. Following transfection with wild type HspB1 DNA vector, the

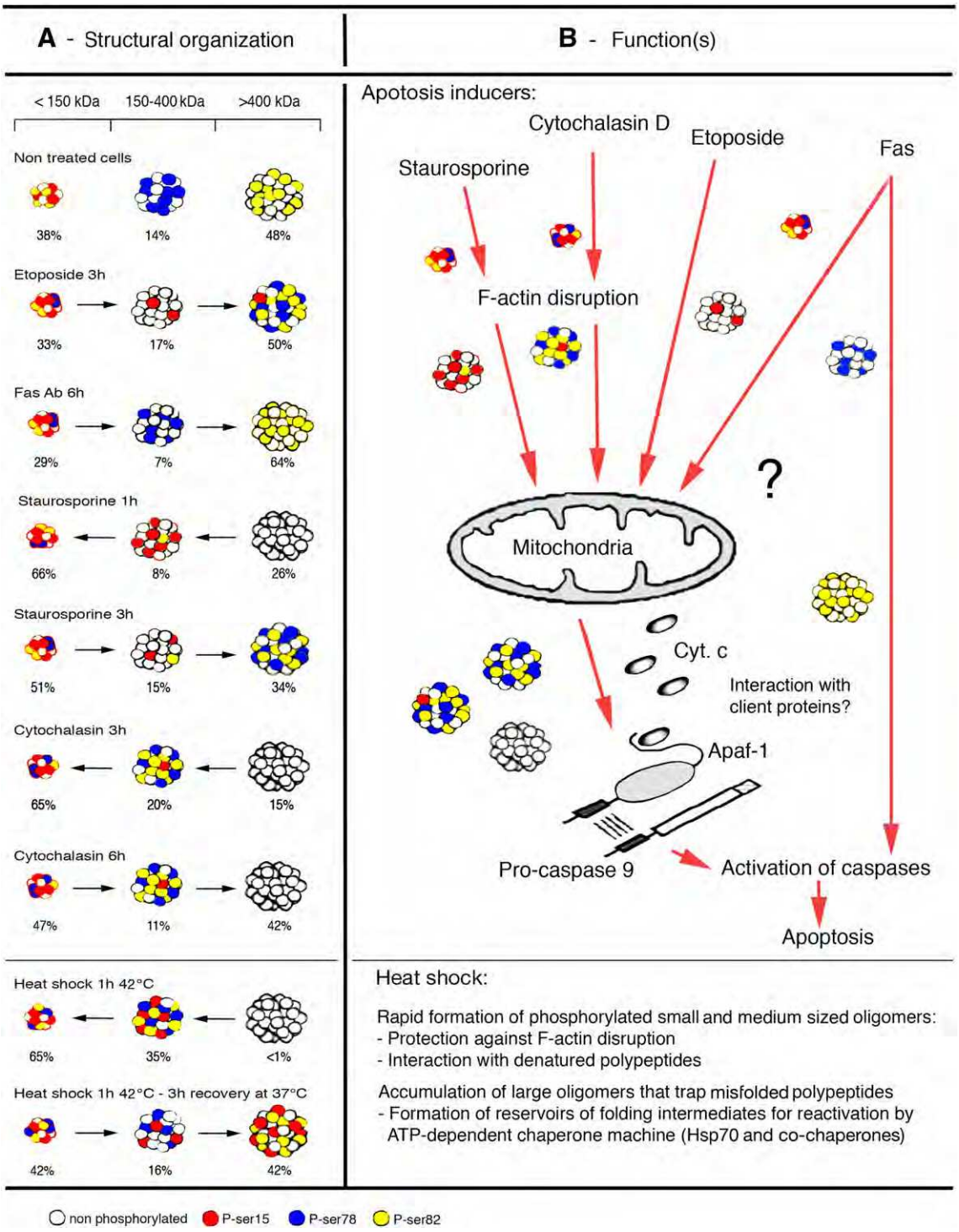

overall oligomerization profile of HspB1 (exogenous plus endogenous) was not changed (Fig. 5C). This correlated with an increased cellular resistance to DEVDase activation (30 to 40% depending on the inducer) (Fig. 5D). Transient expression of the non-phosphorylatable (the 3 phosphoserines 15, 78 and 82 replaced by alanines — Ser to Ala) mutant drastically altered the oligomerization of HspB1 which was now recovered in small and very large (up to 2000 kDa) structures. Hence, exogenous mutated HspB1 can modify the structural organization of endogenously expressed HspB1, probably through mutual interactions. Transient expression of the non-phosphorylatable mutant reduced the gain in protective activity generated by wild type HspB1 against Fas and cytochalasin D and was toxic in cells exposed to etoposide and staurosporine. Indeed, in these cells a dominant negative effect toward endogenous HspB1 was observed that resulted in the stimulation of DEVDase activity. HspB1 oligomerization profile observed in cells transfected with the phospho-mimicry (the 3 phosphoserines 15, 78 and 82 replaced by aspartic acid — Ser to Asp) mutant resembled that observed in non transfected or empty vector transfected cells, except for the presence of HspB1 in very large (up to 2000 kDa) structures and a more intense signal in the 400 to 700 kDa range. In these cells, an increased cellular resistance to DEVDase activation was observed that resembled that induced by wild type HspB1 and appeared even more intense in the case of cytochalasin D. Hence, in contrast to the non-phosphorylatable mutant, addition of a phospho-mimicry negatively charged HspB1 appears rather iniquitous to wild type HspB1. These observations, in spite of giving no information on the precise role of each phosphoserine site, nevertheless show that phosphorylation modulates HspB1 protective activity against caspase activation.

Inducer-specific phosphorylation of three different HspB1 oligomeric sub-structures

We next analyzed the phosphorylation of the different oligomeric structures of HspB1. To do so, immunoblots from the analysis of HspB1 native molecular masses were probed with antibodies that recognize phosphorylated serine 15 (Ser15-P), 78 (Ser78-P) and 82 (Ser82-P). It is seen in Fig. 6A that, in non-treated HeLa cells, three HspB1 populations could be defined, based on their native sizes (<150 kDa, 150-400 kDa and >400 kDa), which concentrated the different phosphorylated serines. Oligomers of less than 150 kDa contained all phosphoserine 15 present in HspB1 and 57% of phosphoserine 82; the remaining being at the level of the large oligomeric structures. The medium sized oligomers (150 to about 400 kDa) were only phosphorylated at the level of serine 78, a phosphoserine recovered only in these structures. HspB1 with native masses larger than 400 kDa was phosphorylated solely at the level of serine 82 (43% of total HspB1 content of this modification). We next analyzed the effect of 3 h of etoposide treatment when HspB1 showed maximal phosphorylation (Fig. 4B) and began to redistribute towards large oligomeric structures (Fig. 3B). Phosphoserine 15 had a distribution close to that observed in untreated cells, except for a fraction that shifted towards larger native sizes. Only minor changes were observed in the level (see Fig. 4B) and oligomeric distribution of phosphoserine 82. The major drastic change was observed at the level of phosphoserine 78 which, instead of being in the 150–200 kDa range, was now recovered in small oligomers (up to about 66 kDa) (43%) and in structures larger than 400 kDa (51%). A similar distribution was already observed after only 1 h of treatment or at later time periods (not shown). In the case of Fas Ab treated cells, the effects were analyzed after 6 h of treatment when HspB1 showed its highest level of phosphorylation (at the level of the three serine sites) and drastically redistributed in two populations, the major one being the large oligomeric structures (>400 kDa). In response to Fas Ab, only minor changes were observed such as the slight shift of phosphoserine 15 and 78 towards smaller oligomeric sizes and the more intense presence of phosphoserine 82 in the small oligomers. Hence, in contrast to the effect mediated by etoposide, in Fas Ab treated cells the formation of large oligomers was not concomitant with the redistribution of phosphoserine 78 towards large oligomeric structures. Consequently, the large

Fig. 7 – Scheme of putative HspB1 structural organization and functions. A) Representation of HspB1 phosphorylation in the three size fractions defined in Fig. 6. It is hypothesized that non-phosphorylated and phosphorylated HspB1 polypeptides have the same ability to oligomerize and form mosaic structures. Color chart was used to distinguish between dephosphorylated (40 to 60% of total HspB1, see 2-D blot analysis in Fig. 4A) and phosphorylated (serines 15, 78 and 82) HspB1 polypeptides (Figs. 4B, 5B and 6). The percentage of total HspB1 present in each oligomeric size fraction is indicated. Arrows point to the redistribution of the oligomers towards small or large native sizes, a phenomenon that depends on the inducer and on the duration of the treatment. Note that the large (serine 82 phosphorylation) and medium sized (serine 78 phosphorylation) oligomeric structures induced by Fas Ab resemble those observed in normal unstressed cells. The medium (weakly phosphorylated) and large (serine 78 and 82 phosphorylation) oligomeric structures observed in etoposide treated cells resemble those that reform after several hours of staurosporine treatment. In contrast, the large structures that reform after several hours of treatment with cytochalasin D are dephosphorylated while those that form during heat shock recovery show a unique phosphorylation pattern at the level of serines 15 and 82. B) Putative functions of HspB1 oligomeric structures. Staurosporine and cytochalasin D induce the rapid accumulation of small phosphorylated (serines 15, 78 and 82) oligomers of HspB1. One hypothesis is that they attenuate F-actin disruption induced by these inducers. In contrast, the phosphorylated pattern of the middle-sized and large oligomers is complex and inducer-specific. Intriguingly, the large structures that accumulate in etoposide and Fas treated cells (as well as those which reform in response to staurosporine and cytochalasin D) display inducer-specific patterns of phosphorylation. Whether these structures play roles in apoptotic events by interacting with specific regulators will remain to be determined. Since, the heat induced HspB1 oligomeric structures that entrap misfolded polypeptides have a different phosphorylated pattern, this raises the question as to whether the oligomeric structures that form in response to apoptotic stimulations behave as "heat-shock like" ATP-independent chaperones or not.

oligomers formed in response to Fas Ab contained only phosphoserine 82 (40%), as observed in untreated cells. Analysis of staurosporine treated cells was performed after 1 h of treatment when HspB1 phosphorylation was intense and when this protein had the tendency to concentrate in small structures (see Figs. 3B and 5A). The remaining large structures showed a decrease in phophoserine 82 which concentrated in small oligomers. In contrast, the medium sized oligomers gained a fraction of total phosphoserine 15 (up to 39%) but had lost their phosphoserine 78 content which shifted towards smaller oligomers. After 3 h of treatment, concomitantly with the reformation of large oligomeric structures, phosphoserine 82 was back in the >400 kDa range and phosphoserine 78 displayed a surprising dual redistribution between the small and large oligomers, as observed in etoposide treated cells. No major changes were observed at the level of phosphoserine 15. Concerning cytochalasin D, the analysis was performed after 3 h of treatment when most of HspB1 was in the form of small or medium sized highly phosphorylated oligomers (see Figs. 3B and 4B). The small oligomers contained mostly phosphoserines 15 and 78. Compared to non-treated cells, the distribution of phosphoserine 82 was highly modified and recovered essentially in the medium sized oligomers. After 6 h of treatment, the large structures (>400 kDa) reformed without being phosphorylated. No other major changes were observed between 3 and 6 h of treatment. Concerning serine 15, which displayed the major phosphorylated stimulation in response to cytochalasin D, its distribution among the oligomers was rather similar to that observed in non-treated cells. Hence, in contrast to what was observed in response to staurosporine, the reformation of large oligomers in cytochalasin D treated cells occurred in the absence of their phosphorylation.

We then tested whether the complex and inducer-specific distribution of the three phosphoserines among oligomeric structures showed some resemblances with the well known phosphorylation of HspB1 that occurs in cells exposed to heat shock. Indeed, an early effect of heat shock is the redistribution of HspB1 in the form of small oligomers consequently of its intense phosphorylation [48]. Subsequently, large oligomeric structures reform [5] and act as reservoirs for misfolded polypeptides. Of interest, in thermotolerant cells, no changes in the structural organization and phosphorylation of HspB1 are observed, hence suggesting that they are directly correlated to the severity of the heat shock treatment [5]. Analysis was performed in HeLa cells exposed 1 h at 42 °C and allowed to recover or not for 3 h at 37 °C. It is seen in Fig. 6B that, immediately after heat shock, HspB1 was quantitatively recovered in highly phosphorylated small (60–150 kDa) (65%) and medium (150–200 kDa) sized oligomers (35%). Heat shock shifted phosphoserines 78 and 82 from the medium sized oligomers to smaller ones. After allowing cells to recover for 3 h at normal temperature, HspB1 reformed large oligomeric structures (42%). In contrast to the effects mediated by the apoptotic inducers, the reformation of large oligomers after heat shock occurred concomitantly with the phosphorylation of both phosphoserines 15 (26%) and 82 (39%). Analysis made 3 h later gave similar results (not shown). Hence, HspB1 oligomerization and phosphorylation are complex and inducer-specific processes. The data presented here are summarized in Fig. 7. In this schematic representation, it is postulated that the non-phosphorylated (about 40 to 50% of the protein) and phosphorylated HspB1 polypeptides share the same ability to interact and form mosaic hetero-oligomeric structures. However, it cannot be excluded that the phosphorylated polypeptides may preferentially interact with each other and form different types of phosphorylated oligomeric structures.

Discussion

HeLa cells are characterized by a high level of constitutive expression of HspB1. Numerous studies, including ours, have shown that HspB1 is an anti-apoptotic polypeptide. Here, analysis of inducers that have similar apoptotic efficiency (etoposide, Fas Ab and staurosporine), but activate different pathways, revealed some inducer-dependent variability in HspB1 ability to counteract caspase activation. The protective activity against cytochalasin D was more difficult to interpret since this inducer was less efficient. These results nevertheless suggest that HspB1 has different strategies to negatively modulate transduction pathways upstream of the execution phase of apoptosis. Analysis of the effects mediated by the different inducers at the morphological level revealed that both etoposide and Fas Ab induced the appearance of HspB1 positive, but Hoechst negative, cell surface membrane blebs. Membrane blebbing, which is a fairly general response of cells to stress, is also considered as a hallmark of apoptosis commitment which requires the presence of cell periphery F-actin fibers, as observed in etoposide and Fas treated cells [70,79,80]. The phenomenon was not observed in response to staurosporine and cytochalasin D, probably because these drugs rapidly disrupt F-actin network [71–73].

Gel filtration analysis revealed major and inducer-specific changes in the heterogeneous native size distribution of HspB1. Of interest, these changes were transient and could have resulted in HspB1 rapid involvement to interfere and delay cytochrome c release from mitochondria and DEVDase activation. Indeed, after about 12 h of treatment with the different inducers, the native size distribution of HspB1 was back to that observed in non-treated cells, that is about equal distribution between two major oligomeric populations. Population I (50–200 kDa) contained the small and medium sized oligomers of HspB1 while population II (200–700 kDa) was made of medium sized and large oligomers [76] and probably also of complexes formed by HspB1 bound to polypeptides involved in apoptosis regulation. Two classes of inducers could be defined: etoposide and Fas Ab which had the gradual tendency to increase HspB1 native sizes (population II) and staurosporine and cytochalasin D which first concentrated HspB1 in small oligomers (population I) before they later induced the reformation of large structures (population II). Concerning the second class of inducers, the effect was more intense in response to cytochalasin D than in cells exposed to staurosporine; a phenomenon which correlated with the rapid F-actin network disrupting activity triggered by these inducers. Hence, it could be hypothesized that HspB1 rapidly concentrates in the form of small oligomers to interfere with an F-actin disruption dependent upstream apoptotic pathway. This assumption is supported by the following observations: i) HspB1 small phosphorylated oligomers are known to protect against F-actin disruption [31], and ii) the lack of accumulation of HspB1 in small oligomers in response to etoposide and Fas Ab, two inducers that do not rapidly disrupt F-actin. The formation of cell periphery F-actin fibers and membrane blebs generated by these inducers is probably not sensed by HspB1 as being toxic enough to generate its accumulation in small oligomers. By comparing the dynamic changes in

HspB1 native size to DEVDase activation, it was concluded that they were early phenomena, particularly the increase in population I, which occurred before the onset of the exponential phase of DEVDase activation. In contrast, the accumulation of HspB1 in the form of large structures, which was observed later in response to all inducers, was concomitant with DEVDase activation. Thereafter, HspB1 native size regained its normal pattern despite the still increasing DEVDase activity. The formation of HspB1 large oligomeric structures may therefore be an attempt to interfere and delay DEVDase activation. This hypothesis is supported by the fact that the large oligomers of recombinant HspB1 inhibit DEVDase activation in cell free post-mitochondrial caspase activation assay [36].

Transfection with DNA vectors expressing phospho-mimicry and non-phosphorylatable mutants confirmed the essential role of phosphorylation in the structure dependent anti-apoptotic activity of HspB1. However, future work will have to determine the precise role played by each phosphoserine site. This could be achieved by using specific mutants expressed in human cells that are devoid of sHsp constitutive expression to eliminate the problem caused by the formation of mosaic oligomeric structures that modulate the effects of the mutations. In response to the different inducers, HspB1 phosphorylation transiently increased until about half of the cellular content of the polypeptide was phosphorylated. However, subtle and inducer-specific changes were detected at the level of HspB1 three phosphoserine sites. For example, serine 15 was the more proeminent phosphorylated site in response to etoposide and cytochalasin D while serine 78 was the preferred serine site in response to staurosporine and to a less extent to Fas Ab. In contrast, Fas Ab was the only inducer to stimulate the phosphorylation of serine 82, a residue that was rapidly dephosphorylated in etoposide and cytochalasin D treated cells. Nevertheless, quantification of the phenomena and analysis of the kinetics revealed that the major changes occurred early during the treatments, concomitantly with changes in HspB1 native size and before the intense stimulation of DEVDase activity. To perform more in-depth analysis we determined the level of phosphorylated serines in HspB1 oligomeric populations. Surprisingly, the phosphorylated serines decorated three distinct HspB1 populations, characterized by native sizes of less than 150 kDa, 150 kDa to about 400 kDa and larger than 400 kDa. This particular pattern of HspB1 phosphorylation showed marked changes that were inducers and duration of the treatment specific. In non-treated cells, small oligomers contained the majority of phosphoserine 15 and a fraction of total phosphoserine 82. The medium sized oligomers were specifically phosphorylated at the level of serine 78 while the population characterized by large native sizes contained only serine 82. Drastic and specific changes were mediated by the inducers: for example, the main effect of etoposide was to shift serine 78 phosphorylation from the medium sized oligomers to the small and large ones. The resulting population of large oligomers was then phosphorylated at the level of both serines 78 and 82. A similar effect on phosphoserine 78 was observed after several hours of staurosporine treatment when HspB1 large structures reformed. In contrast to etoposide, the large oligomeric structures that accumulated in response to Fas Ab showed a pattern of phosphorylation similar to that observed in normal unstressed cells while the large structures that reformed after several hours of treatment with cytochalasin D were completely dephosphorylated. Hence, only etoposide and staurosporine shared a similar size redistribution of phosphoserine 78 when large oligomers were forming. Of interest, these two inducers are also those that exacerbate DEVDase activity in cells transiently expressing the Ser to Ala non-phosphorylatable HspB1 mutant (probably complexed to endogenous wild type HspB1). This suggests a crucial role for phosphoserine 78 in response to these two inducers. Concerning phosphoserine 82, only cytochalasin D altered its distribution and induced its accumulation in medium sized oligomers. In this regard, in cells exposed to cytochalasin D, HspB1 phospho-mimicry mutant complexed to endogenous HspB1 stimulated the protection against DEVDase activation. It is intriguing to note that the large HspB1 oligomeric structures that form during heat shock recovery are specifically phosphorylated at the level of serines 15 and 82. This suggests that a special form of HspB1 oligomers is active in heat stressed cells which may be related to the "holdase molecular sponges" activity described *in vitro* to entrap denatured client polypeptides [24–26,81,82]. Consequently, in cells committed to apoptosis, the significance of the complex and inducer-specific changes in HspB1 oligomerization and phosphorylation is not yet clear (see Fig. 7). One possibility could be that these changes are required to target and hold a large number of crucial and inducer-specific client polypeptides that regulate apoptosis. Indeed, *in vitro*, phosphorylation in the N-terminal domain of sHsp has been suggested to be important for the process of recognition and binding to particular substrates [83] and for changing their conformation, as for example to render them aggregation-incompetent [78]. However, *in vitro* sHsp data should be interpreted with caution since they are generated without the dynamic and complex signaling-related/damage-dependent responses that are clearly reported here to occur in living cells.

Conclusions

In response to apoptotic stimulation induced by either etoposide, Fas agonist antibody, staurosporine or cytochalasin D, HspB1 shows inducer-specific changes in its localization, oligomeric size and phosphorylation that differed from those observed after heat shock. These complex changes could be related to the ability of HspB1 to interfere with inducer-specific events, as for example the rapid disruption of F-actin architecture induced by cytochalasin D and staurosporine. Hence, HspB1 appears to have multiple and complex strategies to negatively modulate apoptotic programs. This raises the question as to whether HspB1 acts as a "heat-shock like" ATP-independent chaperone in cells exposed to apoptotic inducers. Moreover, the complex changes in HspB1 structural organization described here could be key parameters that will have to be taken into account to design strategies aimed at negatively modulating HspB1 anti-apoptotic functions in human cancer cells expressing high levels of this protein.

Acknowledgments

We wish to thank Dominique Guillet for the excellent technical assistance. S.S. was supported by an AFM post-doctoral fellowship and BG by a doctoral Cible 06 fellowship from the Region Rhône-Alpes. This work was supported by the Association Française pour les Myopathies (AFM) and the Région Rhône-Alpes (to A.-P.A.).

REFERENCES

[1] S. Lindquist, The heat-shock response, Annu. Rev. Biochem. 55 (1986) 1151–1191.
[2] T.D. Ingolia, E.A. Craig, Four small heat shock proteins are related to each other and to mammalian a-crystallin, Proc. Natl Acad. Sci. U. S. A. 79 (1982) 2360–2364.
[3] A.-P. Arrigo, J. Landry, Expression and function of the low-molecular-weight heat shock proteins, in: R.I. Morimoto, A. Tissieres, C. Georgopoulos (Eds.), The Biology of Heat Shock Proteins and Molecular Chaperones, Cold Spring Harbor Laboratory Press, Cold Spring Harbor, NY, 1994, pp. 335–373.
[4] W.W. de Jong, G.J. Caspers, J.A. Leunissen, Genealogy of the alpha-crystallin—small heat-shock protein superfamily, Int. J. Biol. Macromol. 22 (1998) 151–162.
[5] A.-P. Arrigo, J.P. Suhan, W.J. Welch, Dynamic changes in the structure and intracellular locale of the mammalian low-molecular-weight heat shock protein, Mol. Cell. Biol. 8 (1988) 5059–5071.
[6] P. Mehlen, E. Hickey, L. Weber, A.-P. Arrigo, Large unphosphorylated aggregates as the active form of hsp27 which controls intracellular reactive oxygen species and glutathione levels and generates a protection against TNFa in NIH-3T3-ras cells, Biochem. Biophys. Res. Commun. 241 (1997) 187–192.
[7] C. Garrido, Size matters: of the small HSP27 and its large oligomers, Cell Death Differ. 9 (2002) 483–485.
[8] M. Ehrnsperger, H. Lilie, M. Gaestel, J. Buchner, The dynamics of hsp25 quaternary structure. Structure and function of different oligomeric species, J. Biol. Chem. 274 (1999) 14867–14874.
[9] H. Lambert, S.J. Charette, A.F. Bernier, A. Guimond, J. Landry, HSP27 multimerization mediated by phosphorylation-sensitive intermolecular interactions at the amino terminus, J. Biol. Chem. 274 (1999) 9378–9385.
[10] G. Kappe, E. Franck, P. Verschuure, W.C. Boelens, J.A. Leunissen, W.W. de Jong, The human genome encodes 10 alpha-crystallin-related small heat shock proteins: HspB1-10, Cell Stress Chaperones 8 (2003) 53–61.
[11] J. Landry, P. Chretien, H. Lambert, E. Hickey, L.A. Weber, Heat shock resistance conferred by expression of the human HSP 27 gene in rodent cells, J. Cell Biol. 109 (1989) 7–15.
[12] P. Mehlen, J. Briolay, L. Smith, C. Diaz-Latoud, D. Pauli, A.-P. Arrigo, Analysis of the resistance to heat and hydrogen peroxide stresses in COS cells transiently expressing wild type or deletion mutants of the *Drosophila* 27-kDa heat-shock protein, Eur. J. Biochem. 215 (1993) 277–284.
[13] P. Mehlen, X. Préville, P. Chareyron, J. Briolay, R. Klemenz, A.-P. Arrigo, Constitutive expression of human hsp27, Drosophila hsp27, or human alpha B-crystallin confers resistance to TNF- and oxidative stress-induced cytotoxicity in stably transfected murine L929 fibroblasts, J. Immunol. 154 (1995) 363–374.
[14] E.H. Richards, E. Hickey, L.A. Weber, J.R. Master, Effect of overexpression of the small heat shock protein HSP27 on the heat and drug sensitivities of human testis tumor cells, Cancer Res. 56 (1996) 2446–2451.
[15] S.A.W. Fuqua, S. Oesterreich, S.G. Hilsenbeck, D.D. Von Hoff, J. Eckardt, C.K. Osborne, Heat shock proteins and drug resistance, Breast Cancer Res. Treat. 32 (1994) 67–71.
[16] S. Oesterreich, C.-N. Weng, M. Qiu, S.G. Hilsenbeck, C.K. Osborne, S.W. Fuqua, The small heat shock protein hsp27 is correlated with growth and drug resistance in human breast cancer cell lines, Cancer Res. 53 (1993) 4443–4448.
[17] C. Garrido, P. Mehlen, A. Fromentin, et al., Inconstant association between 27-kDa heat-shock protein (Hsp27) content and doxorubicin resistance in human colon cancer cells. The doxorubicin-protecting effect of Hsp27, Eur. J. Biochem. 237 (1996) 653–659.
[18] D.R. Ciocca, S.K. Calderwood, Heat shock proteins in cancer: diagnostic, prognostic, predictive, and treatment implications, Cell Stress Chaperones 10 (2005) 86–103.
[19] P. Mehlen, K. Schulze-Osthoff, A.P. Arrigo, Small stress proteins as novel regulators of apoptosis. Heat shock protein 27 blocks Fas/APO-1- and staurosporine-induced cell death, J. Biol. Chem. 271 (1996) 16510–16514.
[20] A.P. Arrigo, sHsp as novel regulators of programmed cell death and tumorigenicity, Pathol. Biol. (Paris) 48 (2000) 280–288.
[21] C. Garrido, S. Gurbuxani, L. Ravagnan, G. Kroemer, Heat shock proteins: endogenous modulators of apoptotic cell death, Biochem. Biophys. Res. Commun. 286 (2001) 433–442.
[22] B. Lelj-Garolla, A.G. Mauk, Self-association of a small heat shock protein, J. Mol. Biol. 345 (2005) 631–642.
[23] U. Jakob, M. Gaestel, K. Engels, J. Buchner, Small heat shock proteins are molecular chaperones, J. Biol. Chem. 268 (1993) 1517–1520.
[24] M. Ehrnsperger, M. Gaestel, J. Buchner, Analysis of chaperone properties of small Hsp's, Methods Mol. Biol. 99 (2000) 421–429.
[25] M. Ehrnsperger, S. Graber, M. Gaestel, J. Buchner, Binding of non-native protein to Hsp25 during heat shock creates a reservoir of folding intermediates for reactivation, EMBO J. 16 (1997) 221–229.
[26] G.J. Lee, A.M. Roseman, H.R. Saibil, E. Vierling, A small heat shock protein stably binds heat-denatured model substrates and can maintain a substrate in a folding-competent state, EMBO J. 16 (1997) 659–671.
[27] T. Rogalla, M. Ehrnsperger, X. Preville, et al., Regulation of Hsp27 oligomerization, chaperone function, and protective activity against oxidative stress/tumor necrosis factor alpha by phosphorylation, J. Biol. Chem. 274 (1999) 18947–18956.
[28] A.L. Bryantsev, S.Y. Kurchashova, S.A. Golyshev, et al., Regulation of stress-induced intracellular sorting and chaperone function of Hsp27 (HspB1) in mammalian cells, Biochem. J. 407 (2007) 407–417.
[29] H. McDonough, C. Patterson, CHIP: a link between the chaperone and proteasome systems, Cell Stress Chaperones 8 (2003) 303–308.
[30] M. Nivon, E. Richet, P. Codogno, A.P. Arrigo, C. Kretz-Remy, Autophagy activation by NFkappaB is essential for cell survival after heat shock, Autophagy 6 (2009) 766–783.
[31] J.N. Lavoie, H. Lambert, E. Hickey, L.A. Weber, J. Landry, Modulation of cellular thermoresistance and actin filament stability accompanies phosphorylation-induced changes in the oligomeric structure of heat shock protein 27, Mol. Cell. Biol. 15 (1995) 505–516.
[32] J. Huot, F. Houle, D.R. Spitz, J. Landry, HSP27 phosphorylation-mediated resistance against actin fragmentation and cell death induced by oxidative stress, Cancer Res. 56 (1996) 273–279.
[33] N. Mounier, A.P. Arrigo, Actin cytoskeleton and small heat shock proteins: how do they interact? Cell Stress Chaperones 7 (2002) 167–176.
[34] O. Goldbaum, M. Riedel, T. Stahnke, C. Richter-Landsberg, The small heat shock protein HSP25 protects astrocytes against stress induced by proteasomal inhibition, Glia 57 (2009) 1566–1577.
[35] X. Preville, F. Salvemini, S. Giraud, et al., Mammalian small stress proteins protect against oxidative stress through their ability to increase glucose-6-phosphate dehydrogenase activity and by maintaining optimal cellular detoxifying machinery, Exp. Cell Res. 247 (1999) 61–78.
[36] J.M. Bruey, C. Ducasse, P. Bonniaud, et al., Hsp27 negatively regulates cell death by interacting with cytochrome c, Nat. Cell Biol. 2 (2000) 645–652.
[37] S.J. Charette, J.N. Lavoie, H. Lambert, J. Landry, Inhibition of daxx-mediated apoptosis by heat shock protein 27, Mol. Cell. Biol. 20 (2000) 7602–7612.
[38] R. Cuesta, G. Laroia, R.J. Schneider, Chaperone Hsp27 inhibits translation during heat shock by binding eIF4G and facilitating dissociation of cap-initiation complexes, Genes Dev. 14 (2000) 1460–1470.

[39] P. Pandey, R. Farber, A. Nakazawa, et al., Hsp27 functions as a negative regulator of cytochrome c-dependent activation of procaspase-3, Oncogene 19 (2000) 1975–1981.
[40] M.J. Rane, Y. Pan, S. Singh, et al., Heat shock protein 27 controls apoptosis by regulating akt activation, J. Biol. Chem. 278 (2003) 27828–27835.
[41] R. Wu, H. Kausar, P. Johnson, D.E. Montoya-Durango, M. Merchant, M.J. Rane, Hsp27 regulates Akt activation and polymorphonuclear leukocyte apoptosis by scaffolding MK2 to Akt signal complex, J. Biol. Chem. 282 (2007) 21598–21608.
[42] C. Andrieu, D. Taieb, V. Baylot, et al., Heat shock protein 27 confers resistance to androgen ablation and chemotherapy in prostate cancer cells through eIF4E, Oncogene (Jan. 18 2010) (Electronic publication ahead of print).
[43] D. Stokoe, K. Engel, D. Campbell, P. Cohen, M. Gaestel, Identification of MAPKAP kinase 2 as a major enzyme responsible for the phosphorylation of the small mammalian heat shock proteins, FEBS Lett. 313 (1992) 307–313.
[44] J. Rouse, P. Cohen, S. Trigon, et al., A novel kinase cascade triggered by stress and heat shock that stimulates MAPKAP kinase-2 and phosphorylation of the small heat shock proteins, Cell 78 (1994) 1027–1037.
[45] D. Chevalier, B.G. Allen, Two distinct forms of MAPKAP kinase-2 in adult cardiac ventricular myocytes, Biochemistry 39 (2000) 6145–6156.
[46] M. Gaestel, R. Benndorf, K. Hayess, E. Priemer, K. Engel, Dephosphorylation of the small heat shock protein hsp25 by calcium/calmodulin-dependent (type 2B) protein phosphatase, J. Biol. Chem. 267 (1992) 21607–21611.
[47] G. Guy, J. Cairns, S. Ng, Y. Tan, Inactivation of a redox-sensitive protein phosphatase during the early events of tumor necrosis factor/interleukin-1 signal transduction, J. Biol. Chem. 268 (1993) 2141–2148.
[48] K. Kato, K. Hasegawa, S. Goto, Y. Inaguma, Dissociation as a result of phosphorylation of an aggregated form of the small stress protein, hsp27, J. Biol. Chem. 269 (1994) 11274–11278.
[49] A.V. Pivovarova, N.A. Chebotareva, I.S. Chernik, N.B. Gusev, D.I. Levitsky, Small heat shock protein Hsp27 prevents heat-induced aggregation of F-actin by forming soluble complexes with denatured actin, Febs J. 274 (2007) 5937–5948.
[50] P. Mehlen, C. Kretzremy, J. Briolay, P. Fostan, M.E. Mirault, A.P. Arrigo, Intracellular reactive oxygen species as apparent modulators of heat-shock protein 27 (hsp27) structural organization and phosphorylation in basal and tumour necrosis factor alpha-treated T47D human carcinoma cells, Biochem. J. 312 (1995) 367–375.
[51] J. Becker, V. Mezger, A. Courgeon, M. Best-Belpomme, On the mechanism of action of H2O2 in the cellular stress, Free Radic. Res. Commun. 12–13 (1991) 455–460.
[52] I. Dalle-Donne, R. Rossi, A. Milzani, P. Di Simplicio, R. Colombo, The actin cytoskeleton response to oxidants: from small heat shock protein phosphorylation to changes in the redox state of actin itself, Free Radic. Biol. Med. 31 (2001) 1624–1632.
[53] A. Samali, T.G. Cotter, Heat shock proteins increase resistance to apoptosis, Exp. Cell Res. 223 (1996) 163–170.
[54] C. Paul, F. Manero, S. Gonin, C. Kretz-Remy, S. Virot, A.P. Arrigo, Hsp27 as a negative regulator of cytochrome C release, Mol. Cell. Biol. 22 (2002) 816–834.
[55] M. Kamada, A. So, M. Muramaki, P. Rocchi, E. Beraldi, M. Gleave, Hsp27 knockdown using nucleotide-based therapies inhibit tumor growth and enhance chemotherapy in human bladder cancer cells, Mol. Cancer Ther. 6 (2007) 299–308.
[56] M.A. Bausero, A. Bharti, D.T. Page, et al., Silencing the hsp25 gene eliminates migration capability of the highly metastatic murine 4T1 breast adenocarcinoma cell, Tumour Biol. 27 (2006) 17–26.
[57] M.T. Aloy, E. Hadchity, C. Bionda, et al., Protective role of Hsp27 protein against gamma radiation-induced apoptosis and radiosensitization effects of Hsp27 gene silencing in different human tumor cells, Int. J. Radiat. Oncol. Biol. Phys. 70 (2007) 543–553.
[58] C. Garrido, A. Fromentin, B. Bonnotte, et al., Heat shock protein 27 enhances the tumorigenicity of immunogenic rat colon carcinoma cell clones, Cancer Res. 58 (1998) 5495–5499.
[59] C. Garrido, M. Brunet, C. Didelot, Y. Zermati, E. Schmitt, G. Kroemer, Heat shock proteins 27 and 70: anti-apoptotic proteins with tumorigenic properties, Cell Cycle 5 (2006) 22.
[60] H.Y. Song, Y.K. Liu, J.T. Feng, et al., Proteomic analysis on metastasis-associated proteins of human hepatocellular carcinoma tissues, J. Cancer Res. Clin. Oncol. 132 (2006) 92–98.
[61] D.R. Ciocca, S. Oesterreich, G.C. Chamnes, W.L. McGuire, S.A.W. Fuqua, Biological and clinical implications of heat shock proteins 27000 (Hsp27): a review, J. Natl. Cancer Inst. 85 (1993) 1558–1570.
[62] A. Samali, J.D. Robertson, E. Peterson, et al., Hsp27 protects mitochondria of thermotolerant cells against apoptotic stimuli, Cell Stress Chaperones 6 (2001) 49–58.
[63] A. Havasi, Z. Li, Z. Wang, et al., Hsp27 inhibits Bax activation and apoptosis via a phosphatidylinositol 3-kinase-dependent mechanism, J. Biol. Chem. 283 (2008) 12305–12313.
[64] C. Garrido, J.M. Bruey, A. Fromentin, A. Hammann, A.P. Arrigo, E. Solary, HSP27 inhibits cytochrome c-dependent activation of procaspase-9, Faseb J. 13 (1999) 2061–2070.
[65] J.M. Bruey, C. Paul, A. Fromentin, et al., Differential regulation of HSP27 oligomerization in tumor cells grown in vitro and in vivo, Oncogene 19 (2000) 4855–4863.
[66] A. Zantema, M.V.-D. Vries, D. Maasdam, S. Bol, Eb. Avd, Heat shock protein 27 and aB-crystallin can form a complex, which dissociates by heat shock, J. Biol. Chem. 267 (1992) 12936–12941.
[67] J.N. Lavoie, G. Gingras-Breton, R.M. Tanguay, J. Landry, Induction of Chinese hamster HSP27 gene expression in mouse cells confers resistance to heat shock, J. Biol. Chem. 268 (1993) 3420–3429.
[68] P. Mehlen, A. Mehlen, D. Guillet, X. Préville, A.-P. Arrigo, Tumor necrosis factor-a induces changes in the phosphorylation, cellular localization, and oligomerization of human hsp27, a stress protein that confers cellular resistance to this cytokine, J. Cell. Biochem. 58 (1995) 248–259.
[69] Q. Song, T. Wei, S. Lees-Miller, E. Alnemri, D. Watters, M.F. Lavin, Resistance of actin to cleavage during apoptosis, Proc. Natl. Acad. Sci. U. S. A. 94 (1997) 157–162.
[70] J. Huot, F. Houle, S. Rousseau, R.G. Deschesnes, G.M. Shah, J. Landry, SAPK2/p38-dependent F-actin reorganization regulates early membrane blebbing during stress-induced apoptosis, J. Cell Biol. 143 (1998) 1361–1373.
[71] K.K. Hedberg, G.B. Birrell, D.L. Habliston, O.H. Griffith, Staurosporine induces dissolution of microfilament bundles by a protein kinase C-independent pathway, Exp. Cell Res. 188 (1990) 199–208.
[72] J.C. Yu, A.I. Gotlieb, Disruption of endothelial actin microfilaments by protein kinase C inhibitors, Microvasc. Res. 43 (1992) 100–111.
[73] A. Nakazono-Kusaba, F. Takahashi-Yanaga, S. Morimoto, M. Furue, T. Sasaguri, Staurosporine-induced cleavage of alpha-smooth muscle actin during myofibroblast apoptosis, J. Invest. Dermatol. 119 (2002) 1008–1013.
[74] N.M. Tsvetkova, I. Horvath, Z. Torok, et al., Small heat-shock proteins regulate membrane lipid polymorphism, Proc. Natl. Acad. Sci. U. S. A. 99 (2002) 13504–13509.
[75] S. Pichon, M. Bryckaert, E. Berrou, Control of actin dynamics by p38 MAP kinase — Hsp27 distribution in the lamellipodium of smooth muscle cells, J. Cell Sci. 117 (2004) 2569–2577.
[76] A.-P. Arrigo, W. Welch, Characterization and purification of the small 28,000-dalton mammalian heat shock protein, J. Biol. Chem. 262 (1987) 15359–15369.
[77] P. Mehlen, A.-P. Arrigo, The serum-induced phosphorylation of mammalian hsp27 correlates with changes in its intracellular localization and levels of oligomerization, Eur. J. Biochem. 221 (1994) 327–334.
[78] D. Hayes, V. Napoli, A. Mazurkie, W.F. Stafford, P. Graceffa, Phosphorylation dependence of hsp27 multimeric size and

molecular chaperone function, J. Biol. Chem. 284 (2009) 18801–18807.
[79] K. Schulze-Osthoff, P.H. Krammer, W. Droge, Divergent signalling via APO-1/Fas and the TNF receptor, two homologous molecules involved in physiological cell death, EMBO J. 13 (1994) 4587–4596.
[80] E. Rudolf, M. Cervinka, Membrane blebbing in cancer cells treated with various apoptotic inducers, Acta Medica (Hradec Kralove) 48 (2005) 29–34.
[81] F. Stengel, F. Stengel, A.J. Baldwin, A.J. Painter, N. Jaya, E. Basha, L.E. Kay, E. Vierling, C.V. Robinson, J.L.P. Benesch, Quaternary dynamics and plasticity underlie small heat shock protein chaperone function, Proc. Natl Acad. Sci. U. S. A. 107 (2010) 2007–2012.
[82] J.E. Eyles, L.M. Gierasch, Nature's molecular sponges: small heat shock proteins grow into their chaperone roles, Proc. Natl Acad. Sci. U. S. A. 107 (2010) 2727–2728.
[83] H.A. Koteiche, H.S. McHaourab, Mechanism of chaperone function in small heat-shock proteins. Phosphorylation-induced activation of two-mode binding in alphaB-crystallin, J. Biol. Chem. 278 (2003) 10361–10367.

PUBLICATION - 3

PUBLICATION 3 - Characterization of specific peptide aptamers targeting Hsp27 tumorigenic activities.

En révision Cancer Research

Les protéines de choc thermique ont été décrites comme une classe de protéines subissant une modification de leur niveau d'expression en réponse à différents changements néfastes de l'environnement générant un stress cellulaire. Lorsqu'elles sont surexprimées, la grande majorité des Hsp procurent une forte protection contre la mort cellulaire et plus particulièrement contre l'apoptose. Ainsi, les Hsp appartiennent à la catégorie émergente des protéines de survie dont la principale fonction est d'inhiber la mort apoptotique comme Bcl-2 ou la Survivine.

Notre étude est centrée sur la petite protéine de Hsp27 qui est une cible thérapeutique majeure en cancérologie. Dans ce contexte nous avons cherché une approche permettant d'inhiber ses activités anti-apoptotiques et tumorigènes. Nous avons choisi l'approche des aptamères peptidiques en collaboration avec la société Aptanomics. Nous avons ainsi recherché des molécules capables de se lier spécifiquement à Hsp27 et d'inhiber son activité.

Les aptamères sont des petites molécules artificielles formées, dans notre étude, de peptides de 8 à 13 acides aminés de séquences aléatoires, intégrés dans une plate-forme rigide formée par la thioredoxine A d'*E.coli* et qui possèdent une structure tridimensionnelle conduisant à une interaction spécifique du peptide avec des partenaires protéiques (Braines et Colas, 2006). La thioredoxine bactérienne est inactivée par la présence du peptide et, dans ce contexte, la séquence peptidique est stable et non dégradée. On peut définir les aptamères peptidiques comme des anticorps artificiels capables de fournir une inhibition allostérique, par compétition ou par perte d'activité enzymatique de leur cible protéique (Colas *et al.*, 1996).

Les aptamères peptidiques ciblant Hsp27 ont été sélectionnés à partir d'une banque par crible double hybride en levures. Cette technique permet de visualiser des interactions entre une protéine et sa cible par activation de différents gènes dont le rapporteur codant la β-galactosidase. Le mélange de deux banques d'aptamères possèdant des régions variables respectivement de 8 et 13 acides aminés, a été criblé par la technique du double hybride de levure. La complexité de séquences de la région variable de chaque banque d'aptamères est estimée à 1 milliard. 180 clones présentant une interaction aptamère/Hsp27, symbolisée par la synthèse de β-galactosidase, ont été isolés. Les vecteurs codant les aptamères ont ensuite été individuellement extraits des 180 clones de levures.

Les séquences codant les peptides de la région variable des aptamères, insérées dans la plateforme thioredoxine ont été déterminées après confirmation des interactions entre Hsp27 et les aptamères. Une séquence consensus apparaît être commune à 50% des aptamères isolés.

Afin de cartographier les régions d'interactions entre Hsp27 et les aptamères, nous avons établi une matrice d'interaction. Cette dernière permet d'étudier en double hybride de levure, les interactions entre la protéine Hsp27 et ses différents mutants avec tous les aptamères isolés. Nous avons pu mettre en évidence une absence d'interaction entre les aptamères sélectionnés et de nombreux mutants de Hsp27. La délétion des acides aminés 141-175 du domaine α-cristallin semble être primordiale pour les interactions entre monomères de Hsp27. Par ailleurs, la spécificité d'interaction entre Hsp27 et les aptamères a été déterminée par des tests d'interaction entre les aptamères et l'αB-cristallin et son mutant R120G, dont les séquences présentent une grande homologie avec celle de Hsp27. De nombreux aptamères (45%) interagissent également avec l'αB-cristallin et la forme mutante R120G. Ces aptamères ne présentent donc pas une grande spécificité pour Hsp27 et n'ont pas été conservés pour la suite de l'étude. En effet, il semble possible que la présence des aptamères puisse perturber les phénomènes dynamiques d'oligomérisation qui régissent les fonctions biochimiques de Hsp27.

Les aptamères ont été reclonés dans des vecteurs d'expression mammifères. Nous avons sélectionné deux aptamères PA11 et PA50 isolés lors d'un premier crible de mort cellulaire. Il apparaît que la présence de ces aptamères induit un effet délétère pour la survie de cellules cancéreuses traitées avec différents agents chimiothérapeuthiques, tels que le cisplatine et la doxorubicine. De plus, nous avons montré que la présence des aptamères favorisait la mort par apoptose liée à une importante activation de la caspase 3.

Il apparaît que PA50 perturbe la dimérisation de la protéine de manière identiqueà celle du mutant Hsp27-C137A (Diaz-Latoud *et al.*, 2005). La dimérisation est un évènement clef dans la formation de formes oligomériques fonctionnelles. PA11 perturbe la dynamique de formation des structures de haut poids moléculaire ce qui peut semble conduire à leur inactivation fonctionnelle.

Nous avons réalisé des tests *in vivo* de l'activité des aptamères sur un modèle murin. L'effet pro-apoptotique des aptamères a été analysé dans des cellules SQ20B de carcinome squameux du cancer tête-cou (head and neck cancer) surexprimant fortement Hsp27. Des lignées exprimant de manière stable les aptamères 11 et 50 ainsi que des aptamères ne ciblant pas Hsp27 ont été construites. En parallèle, cette étude a été réalisée avec une lignée exprimant le shRNA ciblant Hsp27. Il a été montré que les aptamères confèrent un effet radio sensibilisant comme il

avait été montré au cours d'une précédente étude en utilisant un shARN ciblant Hsp27 (Aloy *et al.*, 2008). Les cellules de ces lignées ont été réinjectées dans des souris Nude. Après obtention de xénogreffes, un suivi de croissance tumorale a été réalisé. Il apparaît ainsi que les tumeurs exprimant les aptamères et le shRNA se développent 70% moins rapidement que celles contenant les aptamères contrôles ou l'ARN interférant contrôle. De plus, les analyses cytologiques montrent une réduction de la prolifération cellulaire et une mort cellulaire accrue dans les tumeurs issues de cellules contenant les aptamères. Le ciblage de Hsp27 par les aptamères inhibe donc la tumorigenèse de la même manière qu'une stratégie de ciblage *via* l'interférence ARN. Nous avons pu montrer que le cycle cellulaire était bloqué en phase G2, en corrélation avec l'accumulation du marqueur de sénescence p21 waf1.

Nous avons donc pu caractériser deux aptamères qui semblent avoir des activités différentes. Les aptamères peptidiques semblent être un outil prometteur pour le ciblage des protéines anti-apoptotiques comme Hsp27. Ils sont capables de perturber les fonctions cytoprotectrices de cette protéine sans moduler son taux de synthèse. Ils permettent d'envisager des solutions de ciblage spécifique pour des protéines dont les fonctions dans la cellule sont multiples et dont les structures supramoléculaires ne sont pas totalement déterminées. Par ailleurs, la modélisation de la structure tridimensionnelle des peptides contenus dans le site actif, peut conduire à établir une recherche de molécules chimiques agonistes de l'effet des aptamères (Guida *et al.*, 2008).

Inhibition of heat shock protein 27 (HspB1) tumorigenic functions by peptide aptamers

Benjamin Gibert [1], Elie Hadchity [2], Anna Czekalla [1], Marie-Thérèse Aloy [2], Pierre Colas [3], Claire Rodriguez-Lafrasse [2], André-Patrick Arrigo [1], and Chantal Diaz-Latoud [1]*

[1] Centre de Génétique Moléculaire et Cellulaire, CNRS UMR5534, Université Lyon 1, Lyon, France

[2] Laboratoire de Radiobiologie Cellulaire et Moléculaire, EA-3738, Faculté de Médecine Lyon-Sud, Université de Lyon 1, Oullins, France.

[3] CNRS USR 3151, Station Biologique, Place Georges Teissier, 29680 Roscoff, France.

Running title: Peptide aptamers inhibitors of Hsp27: new therapeutic agents.

Key words: Hsp27, HspB1, peptide aptamers**,** cell death, proliferation, apoptosis, therapeutic target.

Contact: diazc@recherche.univ-lyon1.fr

Abstract

Human heat shock protein 27 (Hsp27, HspB1) is an anti-apoptotic protein characterized for its tumorigenic and metastatic properties and now referenced as a major therapeutic target in many types of cancer. Hsp27 biochemical properties rely on a structural oligomeric and dynamic organization. Down regulation by siRNA or inhibition with dominant-negative mutant have proven their efficiency to counteract the anti-apoptotic and protective properties of Hsp27. In the present study we report the isolation and characterization of Hsp27 targeted molecules interfering with its structural organization. Using the Peptide Aptamer (PA) strategy, we isolated PAs that specifically interact with Hsp27 and not with the other members of the small heat shock proteins family (sHsp). In mammalian cell cultures, PAs expression perturbed the dimerization and oligomerization of Hsp27 and acted as negative regulators of the anti-apoptotic and cytoprotective activities of this protein. Further studies in SQ20B cell xenographts in immunocompromised mice showed that PAs strongly reduced tumor development through cell cycle arrest. Our data suggest that PAs could provide a potential tool to develope strategies for the discovery of Hsp27 chemical inhibitors.

Introduction

Hsp27 belongs to the family of "survival proteins", which also includes other members of Hsps family, anti-apoptotic BH3, survivin and IAPs family. This stress protein can interfere with a pleiotropic number of cell death pathways induced by heat shock, oxidative stress or death receptor agonist (1, 2). Hsp27 directly interferes with upstream events or key components of the apoptotic cascade like cytochrome-*c* release from mitochondria, procaspase-3, or DAXX, a mediator protein on Fas/Apo1 induced apoptosis (3-5). Hsp27 can modulate cell proliferation by interacting with the Akt pathway, which plays an important role for the survival of many types of cancer cells (6). Expression of Hsp27 is up regulated in numerous types of tumors (particularly breast, colon, ovarian and head and neck tumors) and promotes unfavorable outcome (7). Overexpression of this protein is frequently associated with increased resistance to radiotherapy and to anti-cancer drugs like cisplatin, doxorubicin, etoposide (8-10). Others and we have shown that targeting Hsp27 by antisense strategy increases cancer cell death *in vitro* and *in vivo* (11, 12).

Hsp27 pleiotropic functions are dependent on its three-dimensional structure. Hsp27, like the other members of the small Hsps family, presents an α-crystallin domain and can form different oligomeric structures of variable size, from 27 to 800 kDa. This phenomenon depends on the phosphorylation status of three serine residues, mostly controlled by the MAPKAPK2, 3 (13). Every oligomeric form may display a different role, present various biochemical functions and interact with multiple partners. Disturbing these oligomeric structures allows to interfere with Hsp27 biochemical properties and may inhibit tumor growth.

Since anti-sense technologies are not easy to handle *in vivo*, the use of specific peptides that inhibit the anti-apoptotic activity of Hsp27 by interfering with its biochemical properties without altering its level of expression could lead to a new approach for anti-cancer therapies. We have previously shown that dominant negative mutants of the protein disrupt several functions of Hsp27 (14). Here, we used a new approach to specifically target and inhibit Hsp27. Peptide aptamers (PAs) are made of short peptides of random sequence inserted into a scaffold protein, (here, the thioredoxin A (=TrxA) of *E.*

Coli). The role of the scaffold is to display a conformationally constrained sequence of amino acids and to stabilize them in the cellular environment. PAs can specifically bind to and modulate the activities of a wide range of intracellular proteins including oncogenes, transcription factors, cell-cycle regulators, etc (15-17).

In this study, we characterized two aptamers that functionally inhibit Hsp27 and sensitize cancer cells to apoptosis *in vitro* and *in vivo* by disrupting the biochemical functions of the protein. This study confirms that Hsp27 is a therapeutic target in cancer and provides promising guides for the discovery of chemical inhibitors of Hsp27.

Materials and Methods

Reagents.

Nonidet P-40, Triton X-100, desoxycholic acid, dithioerythritol, staurosporine, doxorubicin, cisplatin and G418 were from Sigma. Cell culture media and complements were from Invitrogen (Cergy Pontoise). Anti-caspase-3 was from Alexis Biochemical Qbiogen (Illkirsch). The primary antibodies were detected with either anti-rabbit or anti-mouse immunoglobulin conjugated to horseradish peroxidase (Amersham Corp). Protease inhibitors complete cocktail was from Roche Diagnostics.

Yeast plasmids.

LexA-fused bait and B42-fused prey hsp27 or αB-crystalline coding sequences were cloned into EcoRI/XhoI sites in pEG202 or pJG4-5 plasmids, respectively. Wild type hsp27 and D100G, C137A, R140G, Δ51-88 and Δ141-175 hsp27 mutant cDNA were PCR-amplified from the pCINeo vectors already described (1, 18) using 5' primer: CGGAATTCATGACCGAGCGCCGCGTCCCC and 3' primer CCCTCGAGCTTTACTTGGCGGCAGTCTCATC. pJK103 *lexAop-lacZ* reporter plasmid has been already described (19).

Yeast strains.

Saccharomyces cerevisiae strains MB210 (MATa *leu2*::*6LexAop-LEU2 ade2*::*8LexAop-ADE2 his3 trp1 ura3*) and MB226 (MATα *leu2 ade2 his3 trp1 ura3*) were used for the screening. Strains TB50 (MATα) and EGY42 (MATa) were used to confirm interactions (20).

Eukaryotic expression vectors.

Aptamer cDNA sequences from screen isolated prey plasmids were PCR-amplified with specific primers (5'-CCGGAATTCGGATGAGCGACAAGATCA and 3'-CGGGGTACCTTAGGCCAGGTTGGC) and cloned into EcoRI/KpnI sites of the pCMV-myc vector (Clontech). The cDNA sequences were further EcoRI-NotI digested from pCMV-myc and subcloned in pCIneo vector (Sigma). psuperNeo vector encoding a shRNA27 or a mismatch control RNA will be described elsewhere.

Peptide aptamer selection.

Peptide aptamer selection was performed using an improved version of the yeast two-hybrid interaction trap, essentially as previously described (26). Yeast strain MB226α was transformed with pJK103 and pEG202-Hsp27. Yeast strain MB210a was transformed with a mix of randomized 8-mer and 13-mer peptide aptamer libraries in pWP2 vector (21). Plasmids containing the selected PAs were recovered from the yeast using phenol/chloroform procedure and transformed into MH3 *E.coli* strain onto M9 minimal medium. Interactions were confirmed by an interaction mating assay after retransformation of bait and aptamer plasmids in EGY48a and TB50α strains, respectively (21, 22).

Cell culture and transfections.

All cells were grown at 37°C in a humidified atmosphere containing 5% CO_2. HeLa and SQ20B cells were grown in Dubelcco's modified Eagle's medium (DMEM) supplemented with 10% heat inactivated fetal calf serum. For transient expression, exponentially growing HeLa cells were seeded at a density of 1.5 x 10^6 cells/78cm^2 one night before transfection with 7µg of DNA according to the Lipofectamine™ reagent procedure (Invitrogen). Forty-eight hours after transfection, cells

were submitted to the different treatments. Stably transfected SQ20B cells were grown under G418 (600µg/ml) selection.

Cell death and/or cell survival determination.

Twenty-four hours after transfection, cells were seeded in 96-wells plates (7.5 x 10^3/well). Twelve hours later, cells were treated for 18 hours with drugs. Viable cells were rinsed twice with PBS and stained for 15min with 0.5% cresyl-violet in 50% methanol. Afterward, plates were rinsed and dried before a medium containing 0.1M sodium citrate (pH 5.4) and 20% methanol was added to solubilize the stained cells. Absorbance was read at 570nm with a Wallac1420 Multilabel-Counter (PerkinElmer). The percentage of cell survival was based on the ratio of the relative absorbance of the different samples to that of untreated cells (23).

Cell proliferation was measured using the WST-1 assay, which required pre-incubation of cells in media for 4h with the tetrazolium salt (4-[3-(4-Iodophenyl)-2-(4-nitrophenyl)-2H-5-tetrazolio]-1,3-benzene disulfonate) followed by absorbance measurement at 450nm. The percentage of cell proliferation was calculated based on control absorbance (100%).

Gel electrophoresis and immunobloting.

After treatment, cells were immediately rinsed twice in ice-cold PBS and scraped off the dish. At this point, aliquots were withdrawn for determination of protein concentration. Thereafter, cells were lysed in boiling SDS buffer (62.5mM Tris-HCl, pH6.8; 1% SDS; 0.1M dithioerythritol; 10% glycerol and 0.001% bromophenol blue). Alternatively, for detection of Hsp27 dimers, cells were lysed in Non Reducing SDS buffer without dithioerythritol. Cell lysates were then subjected to SDS-PAGE (24) and immunoblots, were performed as previously described (2). The detection of immunoblots was performed with the ECL^{TM} system (Amersham Life Science). Autoradiographs were recorded onto X-Omat LS films (Eastman Kodak Co).

Clonogenic assay.

Cell survival curves following irradiation were generated by means of a standard colony-formation assay (25). The survival α and β variables were fitted according to the linear quadratic equation

(SF=exp [$\alpha \times D - \beta \times D^2$]) (Eq1), where SF is survival fraction and D represents radiation doses (25). The SF at 2Gy (SF2) was determined as an index of radiosensitivity.

Sizing Chromatography.

Transfected HeLa cells were washed in PBS, harvested and lysed in 20mM Tris, pH7.4 ; 5mM $MgCl_2$; 20mM NaCl ; 0.1% Triton X-100 ; and 0.1mM EDTA. Cell lysates were spin at 10,000x*g* for 10min and supernatant was loaded on a sepharose CL-6B column (Sigma). Fractions were analyzed by SDS-PAGE and immunoblotted as described previously (3).

Tumor growth.

A suspension of 2.5 x 10^6 SQ20B transfected cells in 200µl of PBS was subcutaneously inoculated in the inner thigh of 5-week-old female athymic nude mice (Charles River Laboratories) via a 23-gauge needle under ketamine/xylazine anesthesia. All animal procedures were performed according to local guidelines on animal care. Tumor volume was measured weekly and calculated according to the formula: 0.5236 (LxW^2), where (L) and (W) are respectively the length and width diameters. For each mice group, histological and biochemical analyses were performed on tumors taken after animal sacrifice at the end of week 9.

Histological analyses.

The morphology of tumors was assessed on formalin-fixed, paraffin-embedded tissue sections, after Giemsa staining (25).

Results

Selection of peptide aptamers interacting with Hsp27.

In order to validate the use of Hsp27 in the yeast two-hybrid method and to map crucial domains of this chaperone, interactions between Hsp27 and mutant forms of the protein were tested by a yeast two-hybrid approach (Fig. 1A and B). Strong Hsp27 homodimerisation was observed as well as interaction of WT Hsp27 with several mutant forms. In contrast, point mutant □B-crystallin-R120G, responsible for human myopathies and cataracts, and deletion mutant Hsp27Δ141-175 did not give a detectable interaction phenotype with LexA-Hsp27 (Fig. 1B) (26). However, the weak interaction phenotypes observed with LexA-Hsp27Δ141-175 was not due to a lack of expression of this construct as shown by the interaction of this mutant with PA54 (Fig. 1D). Altogether, these results establish that the LexA-Hsp27 fusion protein is a well-behaved bait (i.e. well expressed, properly folded, localized in the nucleus, and without a detectable transcriptional activity) that can thus be used for a yeast two-hybrid peptide aptamer selection. They also show that the R120 residue and the region comprised between amino acids (AAs) 141 and 175 are essential to Hsp27.

To identify Hsp27 interacting aptamers, a yeast two-hybrid screening was performed using wild type Hsp27 as bait and a mix of randomized 8 and 13-mer peptide aptamer libraries as preys. 160 peptide aptamers that showed a yeast two-hybrid interaction phenotype with the LexA-Hsp27 construct were initially isolated from a screen of 11 x 10^9 yeast colonies. The aptamer plasmids were recovered from yeast and the interaction phenotypes were verified after retransformation and mating assays. Sequences of 50 aptamers showing strong interaction phenotypes with LexA-Hsp27 were determined, out of which 25 unique variable regions were identified (Fig. 1C). A consensus sequence I/LLRRL can be identified in 50% of the sequenced peptides. Although the screening was performed on an equal mix of an 8 and 13-mer peptides aptamers libraries, only 7 aptamers contain a 13-mer variable region and only one of them presents the consensus sequence. These 25 peptide aptamers were tested for their interaction with Hsp27 and various mutants, as shown in panel 1D. The aptamers presented different profiles of interaction, indicating that they bind to different

molecular surfaces of Hsp27. Aptamers presenting an interaction phenotype with □B-crystalline and/or □B-crystalline-R120G were removed from further studies due to their lack of specificity toward Hsp27 (Fig. 1D).

Inhibition of Hsp27 antiapoptotic activity by peptide aptamers in HeLa cells.

To identify aptamers able to counteract Hsp27 protective activity against apoptotic treatments in human cells, we tested the activity of the selected aptamers in HeLa cells. Twenty two aptamer coding sequences were subcloned into the pCINeo vector bearing a neomycin resistance gene. HeLa cells were transfected with the pCINeo vectors encoding specific Hsp27 aptamers or with 3 different non-specific control aptamers or with a pCINeo vector encoding an shRNA directed against Hsp27 messenger RNA. Transfected HeLa cells were treated for 12 hours with 0.2µmol/L staurosporine, caspases activation was determined and 10 PAs able to apoptosis were identified (data not shown). Among them PA11 and PA50, displaying 13 and 8-AAs in their variable region respectively, were selected upon their high specificity of interaction with wild type Hsp27 in yeast.

Then, control experiments were performed to test whether PAs expression in HeLa cells could induce a stress response. This was performed by analyzing the level of expression of Hsp60, 70 and 90 in cells transiently expressing PAs 11 and 50. As shown in Fig.2A no significative increase in either major Hsp was observed.

A WST-1 test was performed in order to determine cell proliferation. In this transient expression experiment PAs 11 and 50 induced a decrease of HeLa cell proliferation while control aptamer and shRNA27 did not (Fig. 2B).

Hsp27 has been reported to induce high resistance to some of the drugs used in chemotherapy (8-10). To assess effects of PA on drug response, HeLa cells transfected with PA11 or PA50 were treated for 18 hours with cisplatin or doxorubicin. As shown in Fig. 2C, a 20% increase in cell death was observed after cisplatin treatment. The increase was up to 50% after doxorubicin treatment of PA50 or shRNA transfected cells. In contrast, control aptamer (PAc) or MsRNA27 did not induce a cell death increase as compared to mock-transfected cells. These results indicate that PAs interfere

with Hsp27 cytoprotective properties as much as does an shRNA that reduced the expression level of Hsp27 below the detection threshold (Fig. 2A).

Studies were also performed with the kinase inhibitor staurosporine. As observed with doxorubicin, Hsp27 shRNA or PAs strongly increased staurosporine induced cell death (Fig. 2D). The processing of executioner caspase 3 is a hallmark of apoptosis. To assess caspase 3 activation in cells expressing or not PAs, protein extracts were analyzed by immunoblot after a 4-hour staurosporine treatment (Fig. 2D). The high level of processed fragments p17 and, to a lesser extend, of p12 fragments, indicated that PAs are also able to counteract Hsp27 antiapoptotic activity.

Aptamers modify the biochemical properties of Hsp27.

The protection induced by Hsp27 is highly correlated with its biochemical state (27). To determine whether peptide aptamers could modify the properties of Hsp27, we first analyzed the oxidative stress induced dimerization of the protein in nonreducing PAGE (Fig. 3A). As a positive control we expressed Hsp27-C137A, a dominant negative mutant able to disrupt Hsp27 dimerization (14). The negative control PAc and PA11 did not induce any modification of the dimeric state of the protein. In contrast, PA50 expression, strongly inhibited Hsp27 dimerization, to a much higher extend than that of Hsp27-C37A mutant.

To further characterize perturbations of Hsp27 biochemical properties, we tested the oligomerization pattern of Hsp27 in HeLa cells expressing PAs. For this experiment we used myc-tagged PAs, in order to enhance the detection of PAs in elution fractions. As already shown in exponentially growing mock HeLa cells, Hsp27 was recovered in two major structures with heterogeneous native molecular masses, small oligomers (<400kDa) and large oligomers (>400kDa), (Fig. 3B) (28). The non-interacting control aptamer, PAc did not induce any modification of Hsp27 oligomerization profile. In PA11 transfected cells we observed strong modifications in Hsp27 oligomerization pattern. Quantification of western blot pointed out that Hsp27 was redistributed in two distincts populations with a singular elution profile when compared

to the other profiles (Fig. 3B, upper right panel). Furthermore, and only 31.4% of Hsp27 was detectable in the small oligomers (<400 kDa) (Fig. 3B). In contrast PA50 transfection did not affect Hsp27 oligomerization pattern as shown by the western blot quantification profiles. These data indicate that although both PAs are able to induce apoptosis, different biochemical mechanisms may underlie this target protein inhibition.

To confirm the interaction observed in yeast we performed co-immunoprecipitation assays directly using fractions of sizing chromatography columns. Hsp27 was immunoprecipitated from the 200kDa column fraction containing both Hsp27 and PAs. The presence of the aptamers was detected by immunoblot with an anti-myc antibody (Fig. 3C). This experiment confirms the interaction between Hsp27 and PA11 and 50.

Inhibition of tumor growth by Hsp27 Peptide Aptamers.

To assess the ability of PAs to inhibit tumor growth, we produced constitutively expressing PA clones in the head and neck squamous cell carcinoma (HNSCC) SQ20B cell line (Fig. 4A). WST-1 experiment was realized in order to determine the proliferation rate of SQ20B clones. As shown in figure S1A, PAs did not statically modulated cell proliferation. We further tested the sensitivity to staurosporine of the PAs expressing cells. As observed for HeLa cells, PAs induced a sensitizing effect to apoptotic stimulus as depicted by an increase in caspase activation (Fig. S1B an S1C). We had previously shown that targeting Hsp27 by antisense approach sensitizes the radioresistant SQ20B cells to γ-irradiation (11). To test the radiosensitizing effect of PAs, cell survival curves were established after irradiation of SQ20B-PAs and SQ20B-PAc control cells at doses varying between 1 and 8Gy. PA 11 and 50 increased the clonogenic cell death after irradiation as revealed by an exponential decrease in the percentage of surviving cells (Fig. 4B*)*. The survival fraction at 2Gy (SF2), used as an index of radiosensitivity, shifted from 0.75 in SQ20B-PAc cells to 0.40 and 0.51, respectively, in SQ20B-PA11 and SQ20B-PA50 cell lines (Fig. 4B).

To better characterize PAs induced inhibition, we performed tumor xenograft studies by injecting PAs expressing cells (and RNAi27 expressing cells) in female NUDE mice and measuring tumor volume by external calipers weekly after injection (Fig. 4C). Each animal was also injected with the appropriate control (Ms27 for RNAi27, and PAc for PA11 and PA50), to circumvent inter-animal variability. PA11 and 50 cells showed a strongly reduced tumor growth of 80 and 50% respectively, as compared to PAc cells (Fig 4D). shRNA cells, used here as a positive control, displayed a reduced tumor growth but to a lesser extend than PA expressing cells. These data indicate that targeting Hsp27 with PAs is more efficient in inhibiting Hsp27 tumorigenic activity than downregulating its expression with a shRNA.

Aptamers inhibit the proliferation of tumor xenografts.

To define the mechanism of action of PA in inducing a reduced tumor growth inhibition, we performed immunohistochemical staining of Ki67 proliferation marker, Giemsa coloration and Tunel apoptosis assay (Fig 5A). Photomicrographs of tumor sections and quantification of Ki67 marker revealed that the lack of tumor development with PA11 and 50 was due an alteration of proliferation process (Fig.5A and B). We have previously reported that a Hsp27 RNAi induces a small delay in tumor progression, without modulation of the Ki67 marker (25). Moreover, Tunel assay on tumor section showed that PA11 and PA50 did not increase apoptosis, probably as a result of a lack of pro-apoptotic stimulation (Fig. 5A). Although PAs statistically modulated proliferation in cancer cell line, our data suggest that tumor environment of xenograft may play a crucial role in inhibition of tumor development in mice with SQ20B-PA11 and 50 cells.

The above findings show that PA expression induces a reduced proliferation of SQ20B cells. We therefore investigated whether PAs could modulate cell cycle components. For this, we analyzed by western blot the expression level of cell cycle markers in the recessed tumors. As shown in Fig.5C levels of p21-waf1, a CDK inhibitor was increased in PA11 and 50 expressing tumors. In contrast, the level of p27 another CDK inhibiting protein, was not affected.

Discussion

Hsp27 is an anti-apoptotic protein over-expressed in a variety of tumors (7). Because of its cytoprotective and oncogenic properties, Hsp27 has emerged as a major therapeutic target in cancer therapy (29). We have developed a peptide aptamer approach to functionally target Hsp27 without modulating its expression.

In the present work, we have identified PAs able to interact with Hsp27. Two of them promoted apoptosis induced by different radio or chemotherapeutic treatments in HeLa or SQ20B cells. In addition, PA11 and 50 counteracted Hsp27 pro-survival functions *in vivo* and strongly inhibited tumor growth. Interestingly, PAs were significantly more efficient than the shRNA27 to reduce tumor growth. Restricted tumor analyzes suggested that cell cycle was blocked due to the up regulation of the tumor suppressor protein p21-waf1, a p53 target gene implicate in cell cycle modulation (30). In contrast, p27 expression level was not affected in our study, although Hsp27 has been shown to promote the ubiquitination and degradation of this CDK inhibitor (31).

One of the major challenges of targeting Hsps in cancer therapy is the induction of expression of other Hsps genes, which show functional redundancy and can trigger compensatory mechanisms. The Hsp90 inhibitor 17-AAG is currently used in clinical trials for its antitumor activity. However, 17-AAG triggers the transcription and elevation of antiapoptotic Hsp27, 70 and 90, which lead to chemoresistance of cancer cells (32). Interestingly, targeting Hsp27 by PAs did not modulate other Hsps levels, either in cells or *in vivo* (data not shown), thus validating Hsp27 as a highly promising target in oncology.

Two aptamers, PA11 and PA50 (13-mer and 8-mer variable regions, respectively) were further characterized because of their specific features. PA11 was the only selected aptamer displaying no interaction with Hsp27-D100G. PA50 presents the consensus hydrophobic sequence found in 50% of Hsp27 interacting aptamers isolated in this study. PA11 and PA50 interacted specifically with Hsp27 and did not present any interaction with □B-crystalline an other member of sHsps family sharing a strong conformational homology with Hsp27. Interestingly, those aptamers that did not interact with Hsp27-R140G mutant did not present any interaction with □B-crystalline

(expect for Apt166). This mutant was designed by homology with □B-crystalline-R120G responsible for human myopathies and cataracts (26). □B-crystalline-R120G did not present an interaction with any of the sHsps tested in our two-hybrid assays. Arginine 120 residue might be of importance for all sHsps based interactions strongly suggesting its implication in PAs binding specificity.

To determine the mechanism of action of PAs, we studied the structural organization of Hsp27 in PA expressing cells, since anticancerous properties of this sHsp rely on its oligomeric status. Although biochemical mechanisms underlying Hsp27 structural dynamic changes are not clearly understood yet, it has been shown that dimerization of protein monomers is a crucial event to form larger oligomers. PA50 was able to inhibit dimerization without disrupting Hsp27 large oligomers, thus mimicking the dominant negative Hsp27-C137A mutant endowed with the ability to disrupt dimer formation and functional properties of wild type Hsp27 without abolishing large oligomers formation (14). Other PAs with the conserved amino acid motif I/LLRRL tested in same conditions did not disrupt dimer formation of Hsp27 (data not shown). These data suggest that the cystein residues in the variable region of PA50 are able to interfere with the formation of Hsp27 disulfide bridges. PA11 did not interfere with Hsp27 dimerization but inhibited the turn over of oligomeric Hsp27 forms since the oligomeric profile of Hsp27 was greatly modified in PA11 expressing cells. Interestingly, PAs were only detected in fractions containing small oligomeric forms of Hsp27, suggesting an interference with the structural organization dynamic process of Hsp27 to form high oligomeric forms. In addition PAs were able to inhibit Hsp27 anti-apoptotic activity at different levels of conformational state. Hence, these data confirm that sHsp functions are dependent on its structural organization since exogenous molecules targeting Hsp27 monomers inhibit Hsp27 induced cellular protection by interfering with its conformational state.

In conclusion, our work demonstrates that PAs are able to interact with Hsp27 and to interfere with its biochemical properties, thus inducing apoptosis in cancerous cell line and inhibiting tumors proliferation *in vivo*. PAs may be exploited to specifically target Hsp27 and discover new insights into Hsp27 structure-function relationship. The *in silico* search for molecules

interfering with sHsps is a challenge since the tri-dimentional structure of Hsp27 is unknown, due to the high difficulty to obtain stable crystals of the oligomeric form of this protein. Therefore PA may represent potential tools to initiate a screening, by modelisation of interaction docking site, and guide to the discovery of Hsp27 chemical inhibitors (33).

Disclosure of Potential Conflicts of Interest

No potential conflicts of interest were disclosed.

Acknowledgments

We wish to thank D.Guillet for excellent technical assistance and Marc Bickle for helpful discussions. This work was supported by a research grant from the Comité du Rhône of la Ligue Contre le Cancer and La Région Rhône-Alpes. G. B. was supported by a PhD training grant from La Région Rhône-Alpes.

References:

1. Arrigo AP, Virot S, Chaufour S, Firdaus W, Kretz-Remy C, Diaz-Latoud C. Hsp27 consolidates intracellular redox homeostasis by upholding glutathione in its reduced form and by decreasing iron intracellular levels. Antioxid Redox Signal 2005;7:414-22.
2. Mehlen P, Briolay J, Smith L, et al. Analysis of the resistance to heat and hydrogen peroxide stresses in COS cells transiently expressing wild type or deletion mutants of the Drosophila 27-kDa heat-shock protein. Eur J Biochem 1993;215:277-84.
3. Bruey JM, Ducasse C, Bonniaud P, et al. Hsp27 negatively regulates cell death by interacting with cytochrome c. Nat Cell Biol 2000;2:645-52.
4. Charette SJ, Landry J. The interaction of HSP27 with Daxx identifies a potential regulatory role of HSP27 in Fas-induced apoptosis. Ann N Y Acad Sci 2000;926:126-31.
5. Pandey P, Saleh A, Nakazawa A, et al. Negative regulation of cytochrome c-mediated oligomerization of Apaf-1 and activation of procaspase-9 by heat shock protein 90. EMBO J 2000;19:4310-22.
6. Rane MJ, Pan Y, Singh S, et al. Heat shock protein 27 controls apoptosis by regulating Akt activation. J Biol Chem 2003;278:27828-35.
7. Ciocca DR, Calderwood SK. Heat shock proteins in cancer: diagnostic, prognostic, predictive, and treatment implications. Cell Stress Chaperones 2005;10:86-103.

8. Hansen RK, Parra I, Lemieux P, Oesterreich S, Hilsenbeck SG, Fuqua SA. Hsp27 overexpression inhibits doxorubicin-induced apoptosis in human breast cancer cells. Breast Cancer Res Treat 1999;56:187-96.
9. Zhang Y, Shen X. Heat shock protein 27 protects L929 cells from cisplatin-induced apoptosis by enhancing Akt activation and abating suppression of thioredoxin reductase activity. Clin Cancer Res 2007;13:2855-64.
10. Kim EH, Lee HJ, Lee DH, et al. Inhibition of heat shock protein 27-mediated resistance to DNA damaging agents by a novel PKC delta-V5 heptapeptide. Cancer Res 2007;67:6333-41.
11. Aloy MT, Hadchity E, Bionda C, et al. Protective role of Hsp27 protein against gamma radiation-induced apoptosis and radiosensitization effects of Hsp27 gene silencing in different human tumor cells. Int J Radiat Oncol Biol Phys 2008;70:543-53.
12. Matsui Y, Hadaschik BA, Fazli L, Andersen RJ, Gleave ME, So AI. Intravesical combination treatment with antisense oligonucleotides targeting heat shock protein-27 and HTI-286 as a novel strategy for high-grade bladder cancer. Mol Cancer Ther 2009;8:2402-11.
13. Landry J, Lambert H, Zhou M, et al. Human HSP27 is phosphorylated at serines 78 and 82 by heat shock and mitogen-activated kinases that recognize the same amino acid motif as S6 kinase II. J Biol Chem 1992;267:794-803.
14. Diaz-Latoud C, Buache E, Javouhey E, Arrigo AP. Substitution of the unique cysteine residue of murine Hsp25 interferes with the protective activity of this stress protein through inhibition of dimer formation. Antioxid Redox Signal 2005;7:436-45.
15. Nouvion AL, Thibaut J, Lohez OD, et al. Modulation of Nr-13 antideath activity by peptide aptamers. Oncogene 2007;26:701-10.
16. Buerger C, Nagel-Wolfrum K, Kunz C, et al. Sequence-specific peptide aptamers, interacting with the intracellular domain of the epidermal growth factor receptor, interfere with Stat3 activation and inhibit the growth of tumor cells. J Biol Chem 2003;278:37610-21.
17. Chattopadhyay A, Tate SA, Beswick RW, Wagner SD, Ko Ferrigno P. A peptide aptamer to antagonize BCL-6 function. Oncogene 2006;25:2223-33.
18. Gonin S, Diaz-Latoud C, Richard MJ, et al. p53/T-antigen complex disruption in T-antigen transformed NIH3T3 fibroblasts exposed to oxidative stress: correlation with the appearance of a Fas/APO-1/CD95 dependent, caspase independent, necrotic pathway. Oncogene 1999;18:8011-23.
19. Estojak J, Brent R, Golemis EA. Correlation of two-hybrid affinity data with in vitro measurements. Mol Cell Biol 1995;15:5820-9.
20. Gyuris J, Golemis E, Chertkov H, Brent R. Cdi1, a human G1 and S phase protein phosphatase that associates with Cdk2. Cell 1993;75:791-803.
21. Bickle MB, Dusserre E, Moncorge O, Bottin H, Colas P. Selection and characterization of large collections of peptide aptamers through optimized yeast two-hybrid procedures. Nat Protoc 2006;1:1066-91.
22. Finley RL, Jr., Brent R. Interaction mating reveals binary and ternary connections between Drosophila cell cycle regulators. Proc Natl Acad Sci U S A 1994;91:12980-4.
23. Javouhey E, Gibert B, Arrigo AP, Diaz JJ, Diaz-Latoud C. Protection against heat and staurosporine mediated apoptosis by the HSV-1 US11 protein. Virology 2008;376:31-41.
24. Laemmli UK. Cleavage of structural proteins during the assembly of the head of bacteriophage T4. Nature 1970;227:680-5.
25. Hadchity E, Aloy MT, Paulin C, et al. Heat Shock Protein 27 as a New Therapeutic Target for Radiation Sensitization of Head and Neck Squamous Cell Carcinoma. Mol Ther 2009.
26. Vicart P, Caron A, Guicheney P, et al. A missense mutation in the alphaB-crystallin chaperone gene causes a desmin-related myopathy. Nat Genet 1998;20:92-5.
27. Bruey JM, Paul C, Fromentin A, et al. Differential regulation of HSP27 oligomerization in tumor cells grown in vitro and in vivo. Oncogene 2000;19:4855-63.
28. Mehlen P, Hickey E, Weber LA, Arrigo AP. Large unphosphorylated aggregates as the active form of hsp27 which controls intracellular reactive oxygen species and glutathione levels and generates a protection against TNFalpha in NIH-3T3-ras cells. Biochem Biophys Res Commun 1997;241:187-92.

29. Arrigo AP, Simon S, Gibert B, et al. Hsp27 (HspB1) and alphaB-crystallin (HspB5) as therapeutic targets. FEBS Lett 2007;581:3665-74.
30. Deng C, Zhang P, Harper JW, Elledge SJ, Leder P. Mice lacking p21CIP1/WAF1 undergo normal development, but are defective in G1 checkpoint control. Cell 1995;82:675-84.
31. Parcellier A, Brunet M, Schmitt E, et al. HSP27 favors ubiquitination and proteasomal degradation of p27Kip1 and helps S-phase re-entry in stressed cells. FASEB J 2006;20:1179-81.
32. Cervantes-Gomez F, Nimmanapalli R, Gandhi V. Transcription inhibition of heat shock proteins: a strategy for combination of 17-allylamino-17-demethoxygeldanamycin and actinomycin d. Cancer Res 2009;69:3947-54.
33. Baines IC, Colas P. Peptide aptamers as guides for small-molecule drug discovery. Drug Discov Today 2006;11:334-41.

Figure legends

Figure 1. Identification of Hsp27 interacting PAs. *A*, Hsp27 and mutants cloned into the two hybrid interaction system. □B-crystalline and □B-crystalline-R120G were used as a control of aptamers specificity. *B*, Interaction mating assay with the different baits and preys. PAc was used as a negative control of interaction with Hsp27. *C*, table of Hsp27 interacting aptamers, two consensus sequence where identified into several aptamers (in red and blue). *D*, Interactions of Hsp27 and mutants with identified PAs were tested in an interaction matting assay. All PAs presented a positive interaction with wild type Hsp27.

Figure 2: Peptide aptamers inhibit Hsp27 anti-apoptotic functions and decrease cancerous cell survival in response to chemotherapy. PAs 11 and 50 were cloned into pCI-Neo mammalian expression vectors and transiently expressed in HeLa cells that constitutively express a high level of human Hsp27. PAc was used as a negative control and did not present any interaction with Hsp27. ShRNA27 and control MsRNA27 were used as a positive control of Hsp27 targeted induced apoptosis. *A*, samples were collected 48h after transfection and levels of Hsp27, 60, 70 and 90 were analyzed by western blot. Expression of aptamers was revealed by PA scaffold protein detection with an anti-thioredoxin A antibody (=TrxA). *B*, WST-1 test was performed each 12 hours during three days following transfection. Proliferation index was determined and reported for each cell line ($p< 0.01$). *C*, Sensitivity to cell death was determined by crystal violet as described in materials and

methods. Chemotherapeutics agents (cisplatin and doxorubicin) were used to induce cell death ($p<$ 0.01). *D*, cell viability after 12h staurosporine treatment was determined by crystal violet method ($p<$ 0.01). Samples of HeLa treated with 0.15µmol/L staurosporine for 4h, were analyzed by western blot for caspase3.

Figure 3: Functional and biochemical inhibition of Hsp27 by PAs. These experiments were performed in HeLa cells transiently expressing myc-tagged PAs. *A*, cells were treated or untreated with 1mmol/L H_2O_2 to induce Hsp27 dimerization. Hsp27-C137A mutant was used as a positive control of dimerization inhibition. Western blot was performed with PAGE nonreducing conditions. *B*, PAs were cloned in pCMV-myc mammals expression vector. Transfected HeLa cells were lysed in the presence of 0.1% Triton X-100 and the 10,000×g soluble cytosol was applied to Sepharose CL-6B gel filtration columns as described in materials and methods. The presence of Hsp27 in pooled fractions eluted from the columns was detected by immunoblots. 29, 66, 150, 200, 443, 669 and 2000 indicate the apparent native size of gel filtration markers (kDa). Column elution profiles were realized by quantification of immunoblots. Quantification of Hsp27 oligomers of apparent native size <400 kDa was also determined. Total Hsp27 and Myc-PAs in samples were determined with an immunoblot on 1/100 of the loaded fraction. *C*, intracellular interactions between Hsp27 and aptamers were analyzed by Co-IP upon expression of aptamers in HeLa cells. After immunoprecipitation from column fractions with anti-Hsp27 antibody, immunoprecipited proteins and input cell lysates were analyzed by Western Blot.

Figure 4: Targeting Hsp27 by peptide aptamers inhibits tumor growth. *A*, SQ20B squamous oral carcinoma were transfected to constitutively express PAs. Expression of aptamers was detected by immunoblots revealed by an anti-TrxA antibody. *B*, Cell survival after exposure of the stably transfected cell lines and their respective controls to radiation at doses varying between 1 and 6Gy. Colonies with more than 64 cells after six cell divisions were scored. Survival curves were fitted with the linear quadratic equation (Eq 1). Table: SF2 = survival fraction at 2Gy. *C*, Photographs of

tumor xenografts in immunocompromised BALBc/Nude mice 9 weeks after implantation. Controls and Aptamers or shRNA expressing tumor cells were injected two by two in the inner thigh of mice (n=13 for each group of mice). *D*, Tumor volume was determined by external caliper measurement once weekly after injection. Tumor volume was determined by external caliper measurements and results were expressed as mean ± standard deviation. Statistical significance was determined by unpaired t test, revealing $p < 0.05$ for comparison of control with RNAi27, PA11 or PA50 at all times.

Figure 5: PAs inhibit tumor cell proliferation by blocking cell cycle. *A*, Detection of tumor cell proliferation using Ki67 immunostaining on tumors excised at the end of week 9 (100x magnification). Tissue morphology of tumors assessed on paraffin-embedded tissue sections after Giemsa staining (100x). Detection of apoptosis using TUNEL staining on paraffin-embedded tumor sections (100x magnification). *B*, The proliferative index was calculated as the percentage of Ki-67 positive cells counted in 50 random fields at 100x magnification for each tumor. ($p< 0.05$). *C*, Immunoblot analysis of p21 waf1, p27 and actin in SQ20B-PAc and SQ20B-PAs xenograft tumors at the end of week 9.

Supplementary Figure Legends

Figure S1. Effect of PAs on proliferation and apoptosis of SQ20B cells. *A*, WST-1 test was performed every 12 hours during three days to determined proliferation index. *B*, cell viability was determined by cresyl-violet method after 12h staurosporine treatment. *C*, caspase activation was determined using a Caspase-Glo3-7 essay.

A

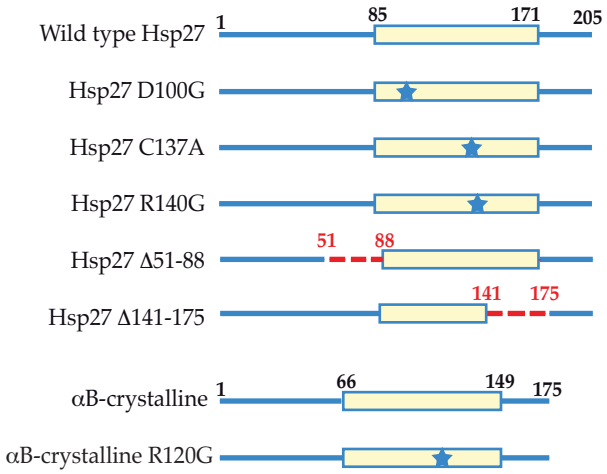

B

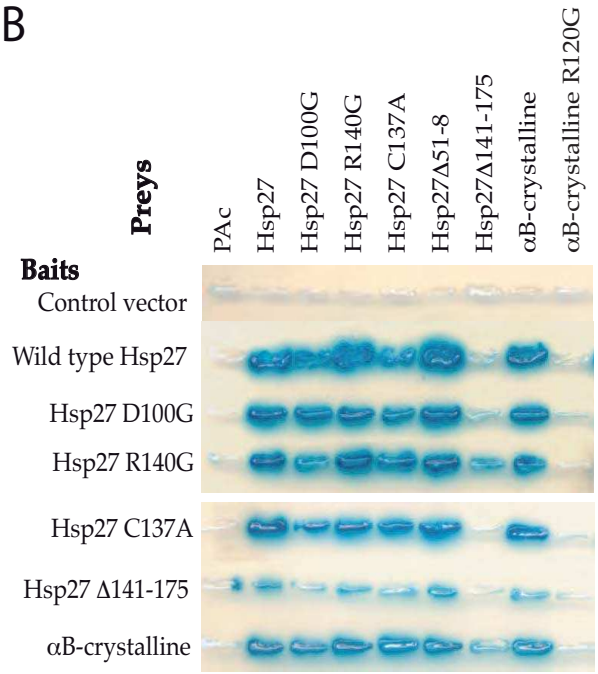

C

Aptamer	PEPTIDE SEQUENCE													Occurence
11		Q	L	S	G	W	V	G	R	C	L	N	I	N	
16	I	I	F	Q	L	P	M	Y							
17	E	I	L	R	R	W	V	D							6
21	H	L	L	R	R	V	L	A							
23	Y	I	L	R	R	A	S	R							3
33	E	I	L	R	R	L	V	C							2
36	E	I	L	R	R	A	L	H							
37	S	I	L	R	R	M	A	A							
39	V	T	G	E	L	W	F	I							2
42	H	L	L	R	R	V	L	A							
43	A	L	L	R	R	L	L	S							2
47	A	L	L	R	R	L	A	N							
50	Y	L	L	R	R	L	C	C							
53	L	H	N	E	V	W	V	V							3
54	A	E	C	L	M	W	V	G							5
57	Y	I	L	R	R	L	L	D							
58	Y	L	L	R	K	L	V	S							
82	S	L	L	R	R	L	L	T							
84	A	L	L	R	R	V	L	N							
87	H	I	L	R	R	M	L	R							
89	R	I	Y	L	L	N	D	T							
91	G	L	L	R	R	L	L	N	Q	E	Q	K	H		
140	Q	I	F	Q	L	T	D	S							
166	R	F	Y	I	T	R	V	L	W	A	A	I	F		
172	Y	L	M	R	R	L	I	A							

D

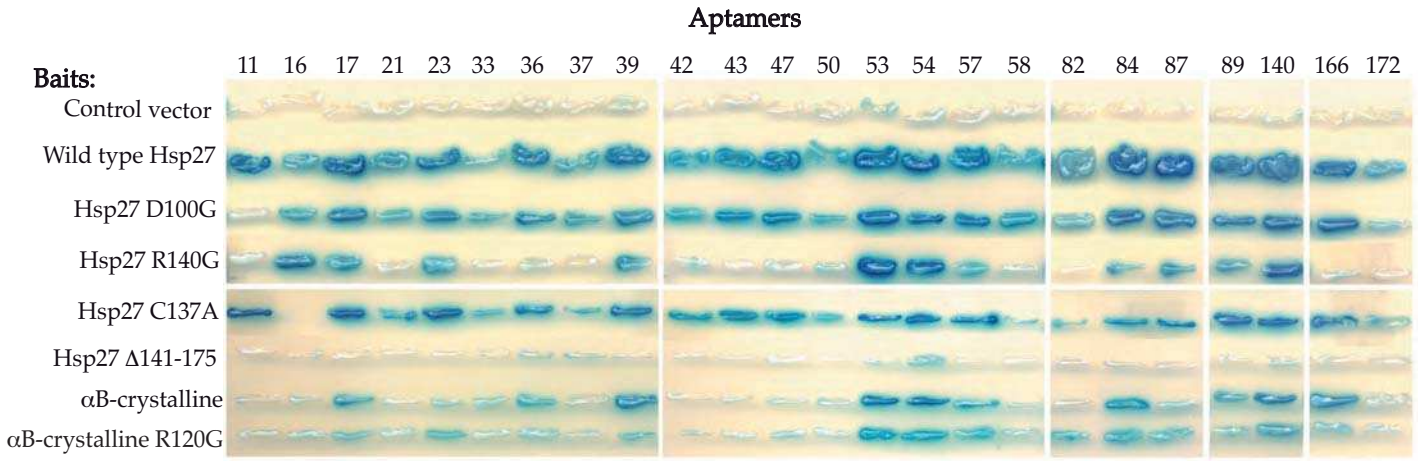

Gibert et al. FIGURE 1

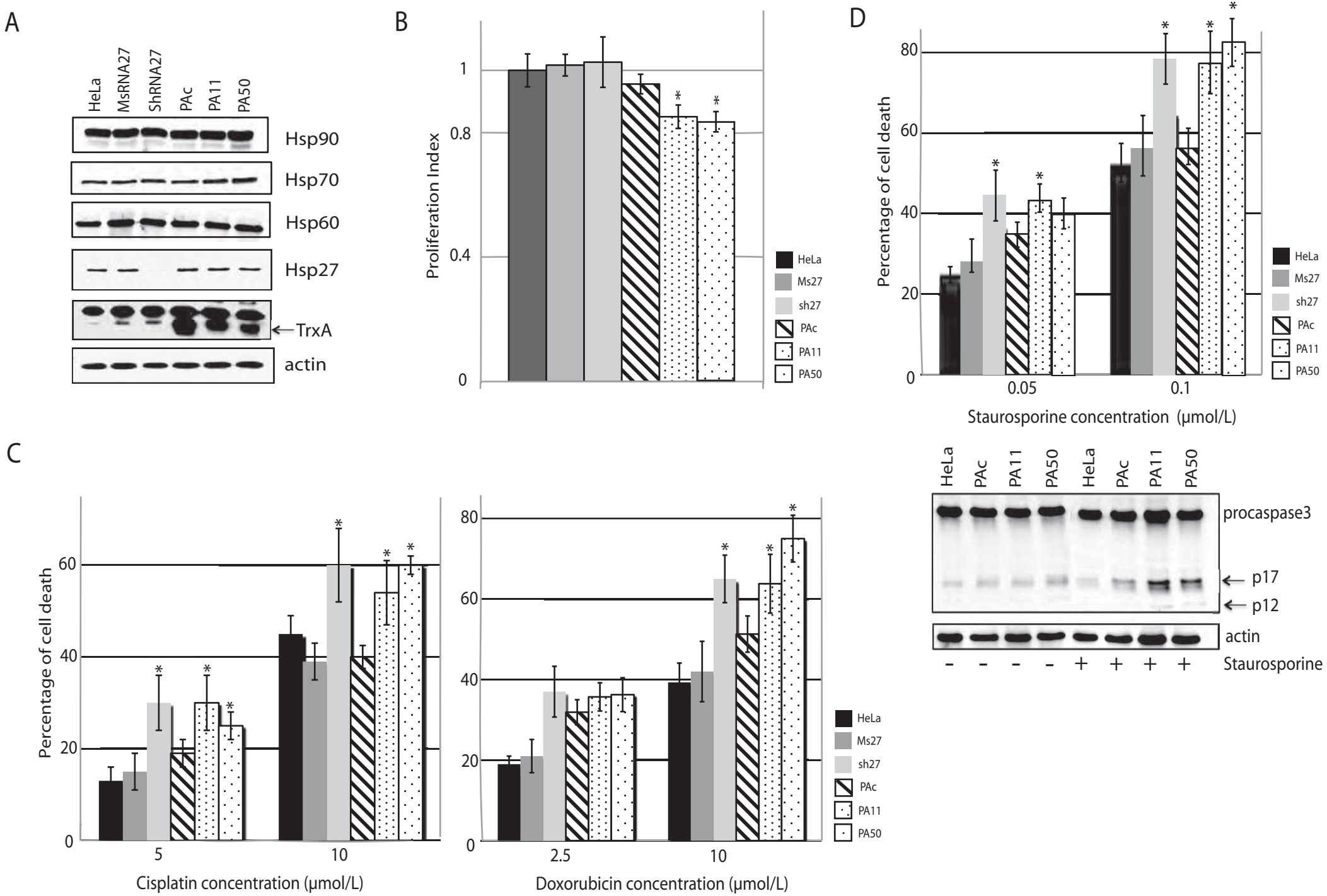

Gibert et al. FIGURE 2

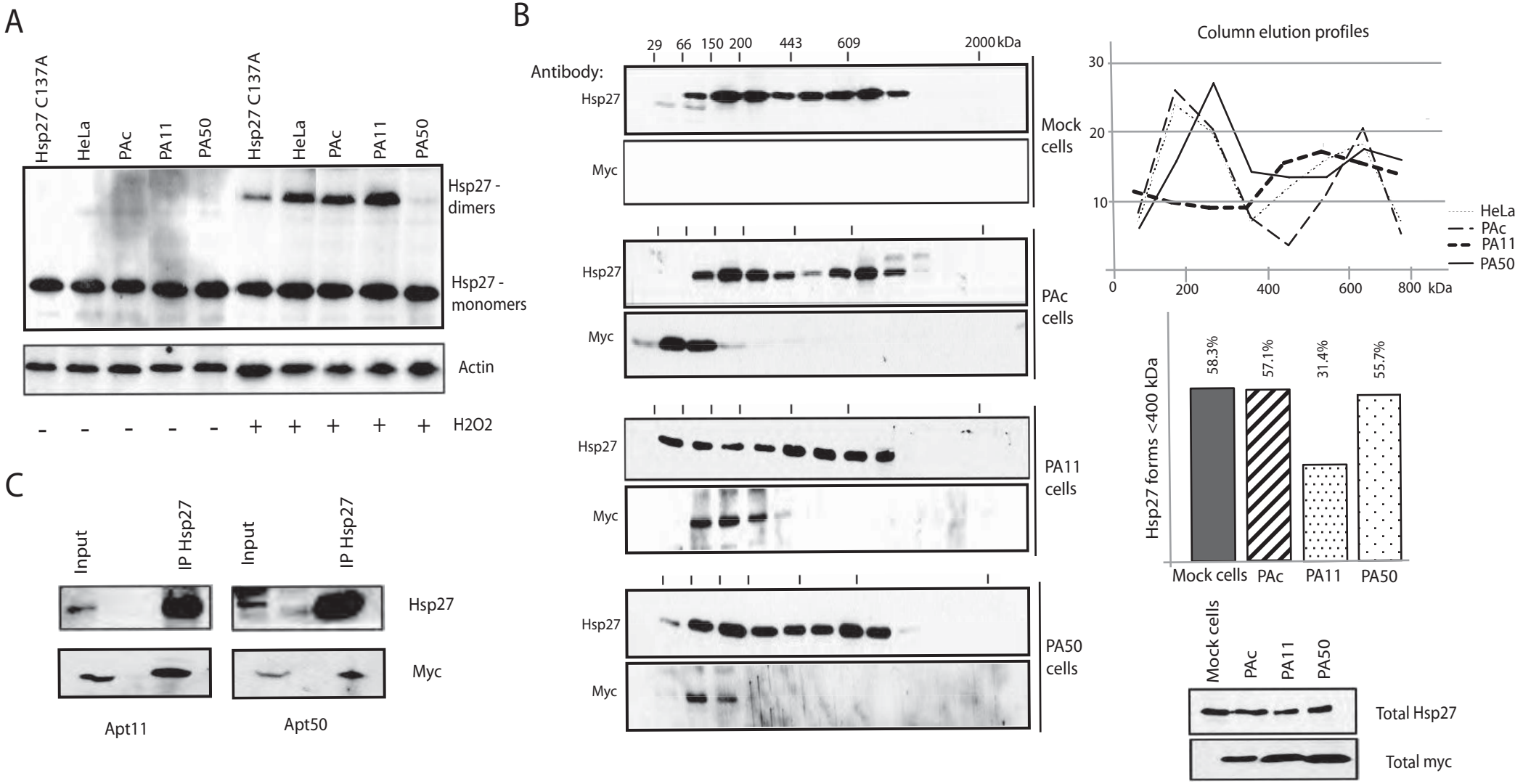

Gibert et al. FIGURE 3

A

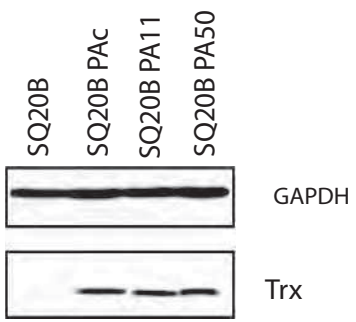

B

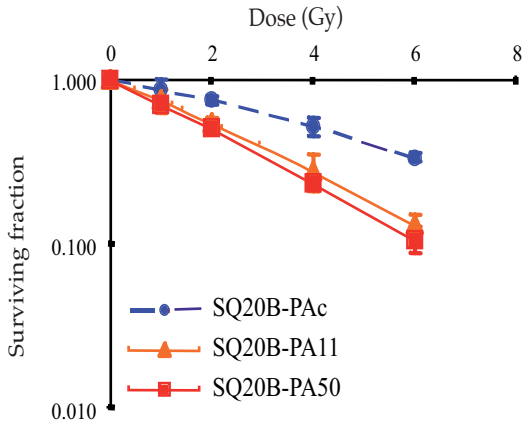

	SF2
SQ20-PAc	0.75
SQ20-PA11	0.40
SQ20-PA50	0.51

C

1

2

3

D

1

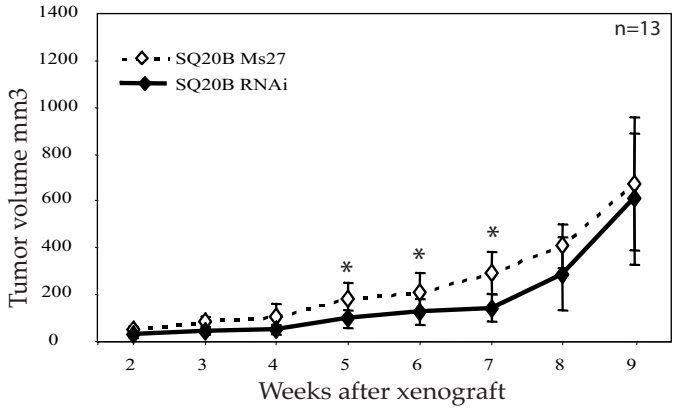

2

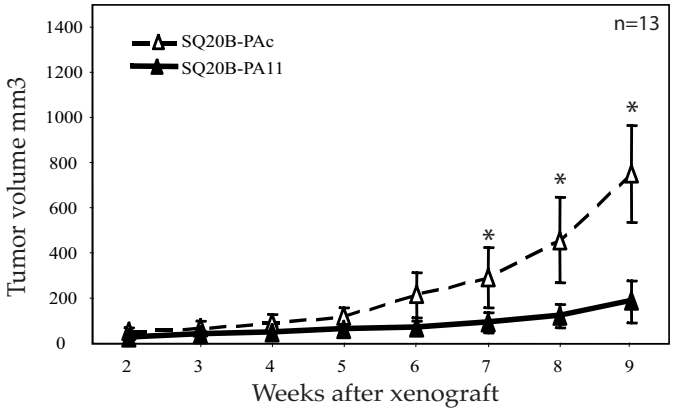

3

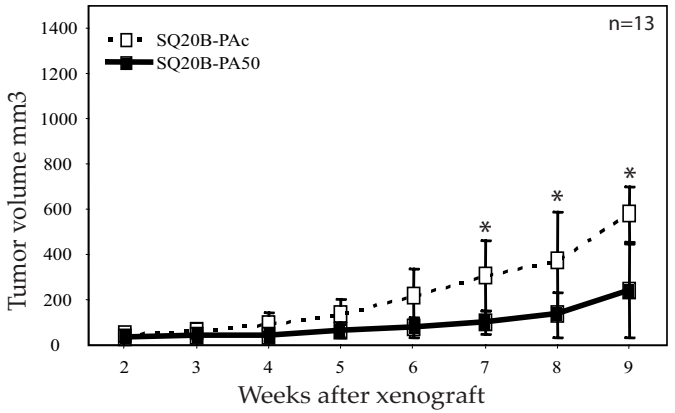

Gibert et al. FIGURE 4

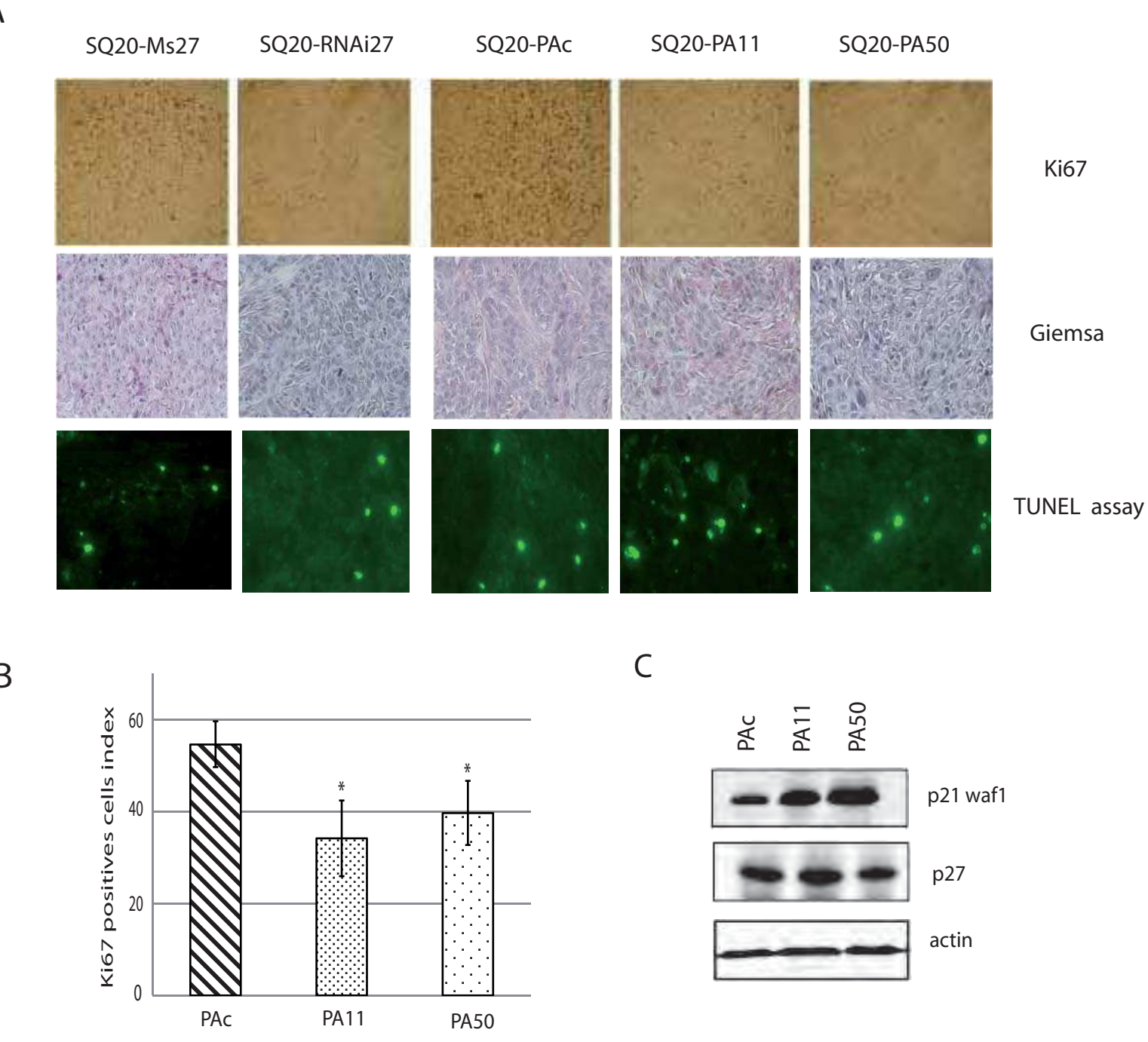

Gibert et al. FIGURE 5

PUBLICATION - 4

PUBLICATION 4 - Knock down of heat shock protein 27 induces degradation of several client proteins.

En cours d'écriture et de travaux complémentaires

Hsp27 comme toutes les petites protéines de stress possède des propriétés de chaperon moléculaire. Elle n'est pas un chaperon moléculaire au sens strict puisqu'elle ne peut pas ou peu reconformer des polypeptides altérés au cours d'un stress. Cependant, elle possède la faculté d'interagir avec des polypeptides altérés et de les stocker avant leur adressage vers le système chaperon classique pour reconformation ou vers une dégradation vers le protéasome après ubiquitination.

Nous avons construit des lignées exprimant de manière stable un ShARN ciblant l'expression de Hsp27 dans les lignées HeLa et MCF-7. Cette baisse du niveau de Hsp27 endogène induit le blocage du cycle cellulaire en G2/M sur les deux lignées construites. Nous avons pu montrer que cet arrêt du cycle était corrélé à des problèmes de structuration du cytosquelette dans la lignée HeLa avec des cellules ayant une cytokinèse défaillante et présentant jusqu'à 40 noyaux. Nous avons pu mettre en évidence que ces défauts avaient pour origine une hyper acétylation des tubulines. Cette dérégulation est concomitante à la chute du niveau de la deacétylase de classe II responsable de la deacétylation des tubulines : HDAC6 (Histone DeACétylase 6). Nous avons pu démontrer par des expériences de PCR quantitative que cette dérégulation n'avait pas lieu au niveau transcriptionel mais protéique. En effet, le niveau de HDAC6 est augmenté dans des clones traités avec l'inhibiteur au MG132, un inhibiteur de la dégradation protéique par le proteasome.

De même, les niveaux protéiques de procaspase 3 et du facteur de transcription STAT2 sont diminués de manière constitutive dans les clones déplétés en Hsp27. Comme pour HDAC6, cette dérégulation n'a pas lieu au niveau des transcrits mais au niveau protéique. Ainsi, empêcher la dégradation protéique dépendante du protéasome permet d'augmenter le taux de procaspase3 et de STAT2.

Par ailleurs, nous avons pu montrer ou re-confirmer par des expériences de co-immunoprécipitation que ces trois protéines HDAC6, STAT2 et la procaspase3 interagissaient toutes directement avec Hsp27. L'ensemble de ces résultats suggère que Hsp27 possède à la

manière de Hsp90 des protéines dites clientes (Whitesell et Lindquist, 2005). Ainsi, Hsp27 *via* son activité chaperon permettrait la stabilisation de protéines cellulaires et l'augmentation de leur demi-vie. L'analyse des interactions entre Hsp27 et ses protéines clientes en présence des deux aptamères peptidiques précédemment caractérisés (c*f.* publication II) est actuellement en cours. Nous espérons mettre en évidence que la présence des aptamères induit le décrochage ou la dégradation de la cliente de Hsp27 à la manière des inhibiteurs peptidiques de Hsp90 sur le modèle de la Shepherdine (*cf.* introduction C-2.1.3.).

Knock-down of heat shock protein 27 (HspB1) induces the degradation of several client proteins

Benjamin Gibert [1], Bénédicte Eckel [6], Lydie Fasquelle [2], Maryline Moulin [3], Frantz Bouhallier [4], Vincent Gonin [6], Gregory Mellier [5], Stéphanie Simon [1], Carole Kretz-Remy [1], , André-Patrick Arrigo [1] and Chantal Diaz-Latoud [6]*.

[1] Centre de Génétique Moléculaire et Cellulaire, CNRS UMR5534, Université Lyon 1, Université de Lyon, 43 Bd 11 Novembre 1918, 69622 Villeurbanne Cedex.

[2] Inserm U 583, Institut des Neurosciences, Hôpital Saint Eloi, 34091 Montpellier, France; Université Montpellier 1, 34091 Montpellier, France.

[3] Department of Biochemistry, La Trobe University, Kingsbury Drive, Victoria 3086, Australia.

[4] igfl, umr5242, cnrs, inra, uclb, ens, ensl, 46 allée d'Italie, f-69364 Lyon cedex07, France

[6] INSERM U664, Université Lyon 1, Université de Lyon, Villeurbanne, France.

Running title: STAT2, procaspase-3 and HDAC6 are Hsp27 client proteins.

Key words: Hsp27, HspB1, STAT2, STAT3, proliferation, caspase-3, client proteins, HDAC6, cell cycle, apoptosis, therapeutic target.

Contact: chantal.diaz@recherche.univ-lyon1.fr

Abstract

Hsp27 belongs to the heat shock family of proteins and acts as a chaperone that binds and can store stress-induced misfolded and damaged polypeptides. Apart from its well-described function of counteracting apoptosis, and in spite of being a well-referenced therapeutic target, the role of the abundant level of constitutively expressed Hsp27 in some cancer cells is still not well-defined. In the present study, we show that the histone deacetylase HDAC6 and the transcription factor STAT2 are degraded in HeLa cells depleted in Hsp27. In addition, co-immunoprecipitation studies revealed that these polypeptides interact with Hsp27. Hence, HDAC6 and STAT-2, similarly to previously described procaspase-3, appear to be client proteins of Hsp27. Altogether these findings highly suggest that, in cancer cells, Hsp27 has a pleiotropic role in the folding and regulation of several crucial polypeptides.

Introduction

The small heat shock Hsp27, also called HspB1, is an important stress protein with anti-apoptotic properties. It is a member of the family of small heat shock proteins characterized by a highly conserved α -cristallin domain (1). Hsp27 interacts and/or modulates several components of the apoptotic machinery. For example, it interferes with apoptotic receptor like CD95- Fas/Apo1 by sequestering the Daxx protein, crucial for the death signal transduction (2) (3). Hsp27 binds directly to cytochrome *c* released from mitochondria and therefore prevents apoptosome formation (4). It also binds to procaspase-3 and prevents its cleavage into active caspase-3 (5). Hsp27 also interferes with upstream signals, such as those mediated by F-actin disruption and aggregation. Interference with upstream signals increases the delay in cytochrome *c* accumulation in the cytosol and subsequently reduces caspases activation (6). Hsp27 also promotes the activation of the pro-survival serine/threonine kinase Akt (7).

Hsp27 is well referenced as a major therapeutic target in some cancers (8). Indeed, a high level of expression of this protein is observed in a lot of tumor types which correlates with a bad prognostic for patients and a lack of response to many cancer therapies (9), such as those based on chemotherapeutic drugs like cisplatin or bortezomib (10, 11). Moreover, a high levels of Hsp27 expression generates a protection against radiotherapeutic radiations while targeting Hsp27 level by antisense strategies sensitized cells (12).

Hsp27, like other members of the Hsp family of proteins, is a molecular chaperone. This molecular distinctiveness implicates that Hsp27 could interfere with polypeptides involved in many different cellular process. In that regards, one member of the heat shock protein family, Hsp90 is well characterized to interact with an important number of client proteins implicated in cell cycle regulation, signal transduction or gene transcription (13, 14).

By doing so, Hsp90 promotes the stability and functionally regulates these polypeptides. Studies performed with inhibitors of Hsp90 chaperone activity (benzoquinone ansamycin geldanamycin or 17-allylamino-17-demethoxygeldanamycin (17-AAG) which bind the ATPase box) have revealed that these agents can disrupt the interaction between the Hsp90 and its client proteins, leading to their degradation through the ubiquitin-dependent proteasomal pathway (15). This kind of mechanism is well referenced for Hsp90 but no yet for other ATP-dependent chaperones, due to the absence of specific inhibitors. Similarly, no inhibitors of Hsp27 chaperone activity are known, hence the only way to test for a putative client-protein interaction is to analyze chaperone depleted cells.

In this study we show that Hsp27 interacts with histone deactetylase 6 (HDAC6), the signal transducer and activator of transcription 2 (STAT2). Moreover, a stable depletion of Hsp27 induced their degradation. Degradation of procaspase-3 was also observed, confirming earlier observations made by Pandey *et al*. (5). To our knowledge this is the first evidence and characterization of client proteins of Hsp27. These modulation of polypeptides implicated in many cellular processes, like cytoskeleton deacetylation, signal transduction and apoptosis, confirm the pleotropic role played by Hsp27.

Materials and Methods

Gel electrophoresis and immunoblotting

After treatment, cells were immediately rinsed twice in ice-cold PBS and scraped off the dish. At this point, aliquots were withdrawn for determination of protein concentration. Thereafter, cells were lysed in boiling SDS buffer (62.5 mM Tris-HCl, pH 6.8; 1% SDS; 0.1 M dithioerythritol; 0.001% bromophenol blue and 10% glycerol). Cell lysates were subjected to SDS-Polyacrylamide Gel Electrophoresis (SDS-PAGE) performed as previously described (16). Immunoblots probed with different antibodies were revealed with

the ECL™ system (Amersham Life Science). Autoradiographs were recorded on X-Omat LS films (Eastman Kodak Co, Rochester, NY).

Cell culture and transfections

All cells were grown at 37°C in a humidified atmosphere containing 5% CO_2. HeLa or MCF-7 cells were grown in Dubelcco's modified Eagle's medium (DMEM) supplemented with 10% heat inactivated fetal calf serum. For transient expression, one day before transfection, exponentially growing cells were seeded at a density of 1.5 x 10^6 cells/78 cm^2. According to the Lipofectamine™ reagent procedure (Invitrogen, Cergy Pontoise, France), DNA vector was left on cells for 3 h, thereafter cells were washed once with PBS before being further incubated in fresh medium. Forty-eight hours after transfection, cells were submitted to the different treatments and analyzed.

Sizing Chromatography.

HeLa or MCF-7 cells, used to prepare sample lysates for sizing chromatography experiments, were grown as described above. Cells from five 100-mm culture plates were harvested on ice by scraping and spun by centrifugation (1000 xg, 5 min, 4°C). Thereafter, they were washed and lysed in the column equilibration buffer (20mM Tris, pH7.4 ; 5mM $MgCl_2$; 20mM NaCl and 0.1mM EDTA) supplemented with 0.1% Triton X-100. Cell lysates were spun (10,000 x*g*, 10 min) and the supernatant was loaded on a sepharose CL-6B column (Sigma) equilibrated and developed in the column equilibration buffer. Columns fractions were analyzed by immunoblotting as previously described (4). Molecular-mass markers used to calibrate the gel-filtration column included carbonic anhydrase (29kDa), albumin (66kDa), alcohol dehydrogenase (150kDa), β-amylase (200kDa), apoferritin (440kDa), thyroglobulin (669kDa) and Dextran Blue (> 2000kDa).

Co-Immunoprecipitation experiments (Co-IP).

All Co-IP experiments were realized in column equilibration buffer as described above. 2ml samples of the indicating column fractions were incubated (1 h, 4°C) with Hsp27 antibody (goat polyclonal anti-Hsp27 antibody, Santa Cruz Biotechnologies) followed by incubation (1 h, 4°C) with protein G sepharose (50 μl of a 50% bead slurry per sample, GE Healthcare). Samples were briefly centrifuged (5,000x*g*, 30 s), supernatants were discarded (bien dommage, le reviewer va sauter là-dessus) and bound proteins were eluted from beads. Co-immunoprecipitated proteins were detected by immunobloting with the corresponding antibodies.

ShRNA construction

The pSuperNeo plasmid (Oligoengine) was used for DNA vector-based shRNA construction. Based on the cDNA of Hsp27 (HUGO gene nomenclature committee accession No. HGNC:5246) and the shRNA designing tool provided freely by Ambion at its website (http://www.ambion.com), we synthesized DNA templates encoding one Hsp27-specific shRNA (Sh27) and two missense controls (Sc27 and Ms27). The Hsp27 targeting sequence of the designed oligonucleotides was: 5′-GCTGCAAAATCCGATGAG-3′. After annealing, ligation and transformation of the resulting DNA vector into competent DH5α bacteria (Invitrogen, France), antibiotic resistance was used to select the positive bacterial colonies. The correct sequences of the final DNA preparations were confirmed by sequencing (GenomExpress, Meylan, France). pSuperNeo-ScRNA27, pSuperNeo-MsRNA27 DNA vectors were designed as respectively random (Sc27) and degenerated (Ms27) controls from the above sequence of Sh27. pCI-Neo vector was used as a positive control of cell transfection. ShRNA-HDAC6 and its random controls will be described elsewhere (?).

Generation of stable HeLa and MCF-7 cells containing reduced levels of Hsp27

Five dishes of cells culture were seeded at 1×10^5 cells/78cm^2. HeLa and MCF-7 cells transfections were performed as described above. One day later, transfected HeLa and MCF-7 cells were incubated in the presence of neomycin at a concentration of 0.5 or 1 mg/ml, respectively. Neomycin resistant clones were tested for their level of Hsp27 by immunobloting. Five independent clones for each cell line expressing minimal endogenous Hsp27 (named: HSh27 for HeLa and MSh27 for MCF-7) and four independent control clones expressing normal levels of Hsp27 (named: HMs27 and MMs27) were selected, propagated and used for further experiments.

Cell death and/or cell survival determination

Twenty-four hours after transfection cells were seeded in 96-wells plates (7.5 x 10^3/well). Twelve hours later, cells were treated for 18 hours with staurosporine. After treatment culture medium was discarded and the remaining viable cells were rinsed twice with PBS buffer and stained for 15 min with 0.5% crystal violet in 50% methanol. Afterward, plates were rinsed and dried before 0.1 M sodium citrate (pH 5.4) in 20% methanol was added to solubilize the stained cells. The absorbance of each well was read at 570 nm with a Wallac 1420 Multilabel Counter (PerkinElmer, Courtabœuf, France). The percentage of cell survival was based on the ratio of the relative absorbance of the different samples to that of untreated cells (17).

Cell proliferation was determined using the WST-1 assay, which requires a 4 h pre-incubation of cells in media (which one, ref Method) with the tetrazolium WST-1 salt (4-[3-(4-Iodophenyl)-2-(4- Bonitrophenyl)-2H-5-tetrazolio]-1,3-benzene disulfonate) (10 µl/well) followed by absorbance measurement at 450 nm. The percentage of cellular proliferation was calculated based on a control absorbance.

Cell cycle analysis was realized as previously described (18). Briefly, cells were fixed in 70% ethanol, treated with RNAse A and stained with propidium iodide before being analyzed by flow cytometry.

Immunofluorescence analysis

Cells growing on glass cover slips were fixed for 5 min with freshly prepared 4% para-formaldehyde, pH7.0. Thereafter, cells were permeabilized by treatment with 0.1% Triton X100 in PBS for 5 min. The cover slips were incubated for one hour with monoclonal anti-Hsp27 antibody. After washing, cover slips were further incubated for one hour with FITC-conjugated goat anti mouse immunoglobulin. Actin detection was performed using Alexa Fluor™ 488 Phalloidin. Hoechst staining was used to count and analyze morphology of nuclei. Photographs were realized using appropriate filters with Zeis Axioskop microscope equipped with a 63X lens and a digital camera device.

Results

shRNA–mediated targeting of Hsp27 promotes apoptosis of HeLa cells.

HeLa cells were transitently transfected with pCI-Neo vector (pCI-Neo), pSuperNeo-ScRNA27 (Sc27), pSuperNeo-MsRNA27 (Ms27) and pSuper-ShRNA27 (Sh27). 48 h after transfection, cells were recovered and Hsp27 analysis was performed by western blot. As shown in figure 1.A. Sh27 was able to strongly reduce Hsp27 expression whereas the controls did not. Hsp27 is characterized by its strong antiapoptotic activity, we therefore analyzed whether a decreased level of Hsp27 could sensitize cells to apoptosis. For this, depleted cells were treated with the kinase inhibitor staurosporine and cell death was determined after 18 h of treatment. The depletion of Hsp27 promoted a 40% increase of cell death after a 0.075μmol/L treatment (Figure 1.B). We also analyzed the activation of caspase-3, characterized by the processing in p12 and p17 fragments from an inactive

precursor the procaspase-3. Protein extracts were analyzed by immunoblot after a 3 hours staurosporine treatment at different concentrations. The different levels of p17 processed fragment after a 0.3 μmol/L staurosporine treatment in Sh27 compared to Ms27 cells, confirmed that depletion of Hsp27 increased caspase-3 activation and apoptosis of transfected HeLa cells (Figure 1.C).

Depletion in Hsp27 levels induces a G2M cell cycle arrest and modulate pro- and anti-apoptotic expression profiles.

To analyze the cellular consequences of reduced Hsp27 levels, we next produced Sh27 stable transfectants of HeLa and MCF-7 cells. Independent clones of HeLa and MCF-7 cell lines were isolated and level of Hsp27 was compared to the level detected in parental cell lines (Figure 2.A). HeLa clones HSh27-1.10 and HSh27-2.2 displayed a 70% and 95% depletion of their Hsp27 levels, respectively, whereas the level of Hsp27 in MCF-7 clones MSh27-1.3 and MSh27-2.1 was decreased up to 60%. This weaker efficiency could result of the fact that Hsp27 level is ten fold higher in MCF-7 than in HeLa cells (figure 2.A) (19). As it is well referenced that targeting one member of the family could modify the expression of other Hsps, their levels were also investigated (15). The constitutive depletion of almost all the cellular content of Hsp27 observed in HSh27-2.2 cells did not induce any modification of Hsp70 and Hsp90 levels (Figure 2.A). Similarly, the partial depletion of Hsp27 in HSh27-1.10 (HeLa) and MSh27-1.13 and -2.1 (MCF-7) cells had no effects towards Hsp90 and Hsp70 levels.

Hsp27, as well as Hsp90 and Hsp70 are part of the survival protein family (ref), thus levels of other survival or pro-apoptotic proteins was analyzed. As shown in figure 1.B, decreased levels of Hsp27 correlated with important changes in pro- and antiapoptotic BH3 protein profils. In contrast to Bcl-2, survivin, an antiapoptotic BH3 mimetic protein, was

overexpressed in HeLa clones deficient in Hsp27. However, the level of this protein was not altered in the partially depleted MCF-7 clones. Surprizingly, the level of Bcl-2 drastically increased in the MCF-7 clones. In all the cells analyzed, BclXS/L level was not modified. Of interest, in both cell lines, levels of pro-apoptotic Bax and Bid proteins were up regulated as a consequence of reduced Hsp27 levels (Figure 2.B).

To further characterize the cellular effects mediated by decreased levels of Hsp27 ~~depletion~~, a WST-1 test (see Materials and Methods) was performed to determine cell proliferation. As seen in Fig. 2C, the proliferation index was decreased in HeLa and MCF-7 cells lines under-expressing Hsp27. In order to determine whether the reduced proliferation was linked to cell cycle modifications, exponentially growing cells were analyzed by flow cytometry. A 10% and 20% decrease in cell proliferation was observed for HeLa HSh27-1.10 and HSh2.2 clones, respectively. The two clones of MCF-7 cells showed a 10% decrease (Figure 2.D). In both cell lines, cell cycle appeared blocked in G2/M. In HSh27-2.2 cells, 26.8% of cells were in G2/M phase while this phase represented only 16.9% of the control cell line. A similar 5.3% increase in G2/M phase was observed in depleted MSh27-1.3 MCF-7 cells. The same increase in G2/M phase was observed in the other Hsp27 deficient cells (data non shown) suggesting that a partial depletion of Hsp27 was enough to induce the phenomenon. Furthermore, in Hsp27 depleted cells, we were able to detect strong increase in the level of sub-G2 cells. 7.4% instead of 1.9% in control cells. A similar phenomenon was observed in MCF-7 cells with an increase from 1.7% to 3.5%.

Hsp27 is essential to maintain cytoskeleton integrity through an HDAC6 dependant mechanism.

To better characterize the reduced proliferation of Hsp27 depleted cells, morphological assessments of the different cells lines were investigated. Hoechst staining revealed that the nucleus of Hsp27 depleted HeLa cells had lost their round shape appearance

and showed an altered morphology (figure 3.A). Moreover, in the highly depleted clone HSh27-2.2, giant cells containing up to 20 nuclei were abundant (Figure 3.B). This polyploïdic morphology could result of the increase in G2 phase blocked cells (figure 2.D). Interestingly, an increase in plurinucleated cells was also detected by flow cytometry analysis of MCF-7 clones but this increase was not associated to any aberrant morphology of the nuclei probably because of the important remaining level of Hsp27 (Data not shown).

Hsp27 is well referenced to support cytoskeletal integrity, particularly by protecting F-actin disruption in stress condition (20). Consequently, we tested if the above-described morphological alterations of nuclei could be linked to an alteration of the cytoskeleton consequently of Hsp27 decreased levels. As seen in Fig. 3C, immunofluorescence analysis of F-actin did not demonstrate any modifications of microfilament integrity. The organization of microtubules and intermediates filaments, detected by tubulin and vimentin antibodies, respectively were similarly not altered in HeLa depleted clones (data not shown).

Biochemical post-translational modifications of cytoskeleton components were also analyzed. The acetylated form of α -tubulin, which is present in various microtubule structures, plays a role in stabilizing these structures and is implicated in many pathways like cell growth, cell migration and morphogenesis (21). As revealed by immunobloting analysis, α-tubulin was hyperacetylated in Hsp27 depleted HeLa cells (Figure 3.D). Histone deacetylase 6 (HDAC6) is the enzyme responsible of the deacetylation of α -tubulin in mammalian cells (21). Of interest, the level of HDAC6 was drastically decreased in Hsp27 depleted HeLa cells; a phenomenon which was negatively correlated with α-tubulin hyperacetylation (Figure 3.D). Similar increase in α -tubulin hyperacetylation was observed when HDAC-6 protein level was artificially decreased in HeLa cells (transiently??) transfected with a specific shRNA-HDAC6 encoding vector (Figure 3.D). We next tested whether a similar phenomenon occurred in MCF-7 cells containing reduced Hsp27 levels. As

seen in Fig. 3D, the level of HDAC-6 was only slightly decreased in MSh27-1.3 cells and α-tubulin was not hyperacetylated (Fig. 3D). This rather modest decrease is probably due to the only partial depletion of Hsp27; a phenomenon correlated with the lack of nucleus aberration phenotype. We then further decrease Hsp27 level using an approach based on a transient transfection of MSh27-1.3 cells with Si27 RNAi (see Materials and Methods). In these conditions, a drastic decrease in the level of Hsp27 correlated with an almost complete depletion of HDA6, hence confirming the results obtained in HeLa cells.

To better characterize the mechanism of HDAC6 protein depletion in absence of Hsp27, we performed a quantification of *hdac6* gene product by quantitative PCR (qPCR). As shown in figure 3.E, HDAC6 mRNA was not significantly decreased in HSh27-2.2 cells, as compare to HMs27 cells. This strongly suggests that HDAC6 depletion results of a post-translational phenomenon (Figure 3.E).

In order to determine if the level of HDAC6 resulted of a post-translational event, such as a reduced half-life, the effect of proteolytic inhibitors, such as MG132 proteasome inhibitor or the calpain inhibitor ALLN was tested. Control experiment revealed that, in our conditions, proteasome inhibition by MG132 correlated with poly-ubiquitin accumulation (Figure 3.F). As the result of ALLN and MG132 treatments of HSh27cells, HDAC6 level was increased. This suggests that an intense degradation of HDAC6 occurs in the absence of Hsp27.

Endogenous level of procaspase-3 was decreased in Hsp27 depleted cells.

Hsp27 has been well referenced to interact with the prodomain of procaspase-3, a key protease implicated in the executive pathway of apoptosis (22). Physical interaction between Hsp27 and procaspase-3 inhibits processing leading to the activation of the apoptotic caspase and participates to the mechanism of cellular survival occurred by Hsp27 (5). Moreover, decreased levels of Hsp27 correlated with a reduced level of pro-caspase-3 (5). Similarly, in

our conditions, the level of endogenous procaspase-3 was down regulated in Hsp27 depleted HeLa clones (figure 4 panel A). Quantitative analysis revealed a 79.6% decrease in procaspase-3 level in the most Hsp27 depleted clone HSh27-2.2. Moreover, after a 4 h treatment with 0.2 μmol/L staurosporine, processing of procaspase-3 in p17 (Figure 4B) and p12 (not shown) fragments was increased in the two Hsp27 depleted HeLa clones. In contrast, the cleaved fragments were not observed in absence of apoptotic stimulation allowing us to conclude that the decrease in procaspase-3 level was not due to an increased caspase-3 processing (data not shown).

To investigate if the reduced amount of procaspase-3 protein resulted of a transcriptional event, *procaspase-3* mRNA was quantified by quantitative RT-PCR (Figure 4.C). A 50% up-regulation of procaspase-3 mRNA was detected in HSh27-2.2 clone, indicating an increased transcriptional activity when compared to control cells. As a consequence, these data strongly suggested that the phenomenon was due to an increased rate of degradation of the protein. Thus, we tested procaspase-3 protein level when proteasomal and calpain proteolytic activities were inhibited by MG132 and ALLN, respectively (Figure 4.D). It is seen in Figure 4.D that the level of procaspase-3 was drastically increased and even higher than in control cells as a consequence of MG132 treatment. In contrast, it was not restored by ALLN treatment, suggesting an ubiquitin/proteasomal degradation in absence of Hsp27.

Hsp27 constitutive depletion induces STAT2 degradation and modulates STAT3 phosphorylation.

Hsp27 has been shown to interact with STAT3, a crucial transcription factor implicated in the maintenance of cancerous state by activating the expression of genes like Bcl-XL and survivin (23, 24). Consequently, we explored whether Hsp27 could interact with other member of the STAT family of proteins. As revealed by western blot analysis, STAT2

protein level was dramatically decreased in Hsp27 depleted HeLa clones (Figure 5.A). In contrast, the level of the other members of the STAT transcription factor family, including the Hsp27 interacting STAT3 polypeptide, was not altered (Figure 5.A). Analysis of MCF-7 clones also revealed a decreased level of STAT2 in cells partially depleted in Hsp27. However, the effect was not as drastic as that observed in HeLa cells. Quantitation analysis revealed a decreased of 18.2% and 9,8% in MSh27-1.3 and MSh27-2.1 clones, respectively (Figure 5.B). Of interest, STAT2 transcription factor is implicated in process like viral or interferon responses and was not previously described to interact with Hsp27 (25).

A preceding study has demonstrated the role of the depletion of STAT3 in prostate cells when Hsp27 was transiently decreased by an antisense strategy (26). In contrast, in our conditions of constitutive depletion of Hsp27, endogenous level of STAT3 remained constant. Moreover, STAT3 mRNA level was not modified in Hsp27 depleted clones (Supplementary data 1.A). A confirmation of Rocchi *et al*. (26) results was nevertheless obtained when our cells were transient transfected with the Sh27 vector. This suggests an adaptation mechanism that restores a normal level of STAT3 in cells constitutively (and not transiently) depleted in Hsp27 (Supplementary data 1.B).

Investigation of the level of STAT3 phosphorylation by interleukin-6 (IL-6) or by heat-shock revealed that this modification was drastically decreased in Hsp27 depleted cells. qPCR experiments revealed that STAT2 mRNA level was slightly increased in Hsp27 depleted clones (Figure 5.D). Furthermore, degradation of STAT2 was inhibited when proteasomal degradation was inhibited by MG132 but not with ALLN treatments.

Taken together, these results implicate the crucial role of Hsp27 in the stability of STAT2 (Figure 5.E).

STAT2, HDAC6 and procaspase3 directly interact with Hsp27.

In accordance with the “foldase” and “molecular sponges” theories, we hypothesized that Hsp27 can stabilize and modulate half-life of client proteins (27, 28). Chaperone activity is highly correlated with Hsp27 dynamic structures ranging from monomers to oligomeric structures of about 800kDa (29) (30). Hsp27 oligomerization profiles were therefore analyzed by the use of size exclusion columns (Figure 6.A). In non-stressed cells, Hsp27 was recovered in two distinct size populations, the small oligomers (≤ 200kDa) and the large oligomeric structures larger than 200kDa. Immunoblots analysis revealed that Procaspase-3 was in the 150-200 kDa range whereas STAT2 and HDAC6 proteins showed higher, but distinct, native molecular weights (Figure 6.A). Of interest, these three polypeptides were recovered in column fractions containing Hsp27 oligomers, thus an interaction with this stress protein is therefore possible. Physical interactions between Hsp27 and procaspase3, HDAC6 and STAT2 were tested by Co-IP experiments using the different pooled fractions containing the putative client polypeptide proteins. Goat polyclonal antibody raised against Hsp27 was therefore added to the fractions of apparent native sizes of 100kDa (procaspase-3), 600kDa (STAT2) and 800kDa (HDAC6), respectively. Immunoblots analysis of the immunoprecipated complexes were revealed with antibodies specific to the putative client polypeptides (Figure 6.B). It is seen in Fig. 6B, that procaspase-3, STAT2 and HDAC6 co-immunoprecipitated with Hsp27 suggesting that these polypeptides interact with different structural organization of Hsp27. Indeed, interactions were restrained for small amount of total proteins, and should be highly correlated with structural organizations of the different partners.

Discussion

In the present study, we characterized HeLa cells lines depleted to different extent in Hsp27. This was achieved by constitutively expressing a specific ShRNA targeting Hsp27

mRNA. This constitutive knock down of Hsp27 induces the proteasome-dependent degradation of HDAC6, STAT2 and procaspase-3 proteins without any down regulation of their transcripts levels. Furthermore, co-immunoprecipitation studies were in favor of a biochemical interaction of Hsp27 with procaspase-3, HDAC6 and STAT2. In spite of the fact that we cannot exclude that Hsp27 could interact with complexes containing these proteins, rather than directly interacting with them, our results are highly suggestive of a new function of Hsp27 aimed at molecular chaperoning non-denatured polypeptide in non-stressed cells.

Analysis of the different clones revealed that the constitutive knock down of Hsp27 did not modulate other major Hsp levels. In contrast, pro-apoptotic proteins like Bax and Bid were over-expressed; a phenomenon which can participate to the apoptotic susceptibility of cancer cells lacking Hsp27 (30) (26) (12). Depending of the targeted cell, the over-expression of survival proteins like survivin or Bcl-2 could be explain by an adaptative mechanism allowing cells to survive without Hsp27.

Additionally, HeLa clones able to adapt to Hsp27 knock down, displayed nucleus abnormalities and polyploidy. The observed lack of cytokinesis was probably the origin of the blockade in the G2/M phase of cell cycle; a phenomenon that maybe connected to the activation of senescence observed by others (19). Nuclear phenotype, associated to Hsp27 depletion, might be a consequence of α-tubulin hyper-acetylation, linked to HDAC6 level down degradation. HDAC6 has many functions that can therefore be modulated by Hsp27. For, example, HDAC6 is a major component of stress response and could address denatured proteins to degradation (31). Moreover, it can participate to the misfolding response with other heat shock proteins (32). Large oligomers of Hsp27 have been described to store unfolded proteins when the molecular chaperone pathway is saturated (33). Hence, a link probably exists between Hsp27 and HDAC6 in the altered protein response. On the other hand, HDAC6 can promote *hsp27* transcription linked to stress response (34). Furthermore,

HDAC6 is a powerful modifier of carcinogenesis and its stabilization by Hsp27 may contribute to oncogenic pathways (35).

Procaspase-3 is a major cysteine protease implicated in apoptosis and differentiation pathways (36, 37). An interaction has already been described between the prodomain of procaspase-3 and Hsp27, which modulates procaspase-3 cleavage and activation (22). Our results are in accordance with a previous study that described procaspase-3 down-regulation when Hsp27 was immunodepleted (5). Here, we bring the new information that, in the absence of stress and Hsp27, procapase-3 can be degraded by the ubiquitin/proteasome pathway. This point could not tested in MCF-7 clones because, in these cells, caspase-3 is inactivated due to a deletion mutation in exon 3 of the gene (38).

STAT2 is an important transcription factor involved in interferon and anti-viral responses (25) which is degraded in Hsp27 depleted cell lines. The phenomenon is transcriptionally independent. This protein co-immunoprecipitate with Hsp27 large oligomers, suggesting that it interacts with these structures. An other target is the proto-oncogene STAT3 which has been already been demonstrated to interact with Hsp27 (23, 26). In our cell models, we found that STAT3 phosphorylation was modulated by Hsp27 level but its level remain stable. However, transient transfection approaches allowed us to confirm that that STAT3 was degraded when Hsp27 was transiently depressed. The phenomenon also correlated with a modulation of its phosphorylation state, indicating a highly tight regulation between STAT3 stabilization and activation (26).

Recently, a powerful mass-spectrometry study had identified an important number of proteins able to binds sHsp under thermal conditions (41). Nevertheless this study did not demonstrate any interaction between sHsp and proteins under non-stressed conditions. Based on the Hsp90 chaperoning model, our findings suggest that Hsp27 could have its own client proteins (15). Although, we only tested interaction between Hsp27 with endogenous wild-

type proteins, it is nevertheless possible that Hsp27 could also stabilize mutant forms of these proteins. In cancer cell, Hsp27 is an abundant protein, and its over-expression may contribute to the stabilization of several oncogenic proteins, as for example, HDAC6 in bortezomib treated cancer or STAT3 in tumors where this proto-oncogene is constitutively activated (11, 26, 39). Rational design of stable peptides based on those are described in the Shepherdin model (40) will be probably a good approach to target Hsp27 interaction with oncogenic client proteins.

Hsp90 regulates an/or stabilizes a high number of polypeptides, evaluated at approximately 10% of yeast proteome (13). As referred to the "foldase" or "molecular sponges", Hsp27, like other sHsp, could be a key regulator of a pleiotropic numbers of proteins but identification of Hsp27 client proteins is still difficult at this point, due to the lack of drugs that inactivate its chaperone activity (27, 28).

Disclosure of Potential Conflicts of Interest

No potential conflicts of interest were disclosed.

Acknowledgments

We wish to thank Dominique Guillet for excellent technical assistance. This work was supported by a research grant from the Comité du Rhône of la Ligue Contre le Cancer.

References

1. Taylor RP, Benjamin IJ. Small heat shock proteins: a new classification scheme in mammals. J Mol Cell Cardiol 2005;38:433-44.
2. Mehlen P, Schulze-Osthoff K, Arrigo AP. Small stress proteins as novel regulators of apoptosis. Heat shock protein 27 blocks Fas/APO-1- and staurosporine-induced cell death. J Biol Chem 1996;271:16510-4.
3. Charette SJ, Landry J. The interaction of HSP27 with Daxx identifies a potential regulatory role of HSP27 in Fas-induced apoptosis. Ann N Y Acad Sci 2000;926:126-31.

4. Bruey JM, Ducasse C, Bonniaud P, et al. Hsp27 negatively regulates cell death by interacting with cytochrome c. Nat Cell Biol 2000;2:645-52.
5. Pandey P, Saleh A, Nakazawa A, et al. Negative regulation of cytochrome c-mediated oligomerization of Apaf-1 and activation of procaspase-9 by heat shock protein 90. EMBO J 2000;19:4310-22.
6. Paul C, Manero F, Gonin S, Kretz-Remy C, Virot S, Arrigo AP. Hsp27 as a negative regulator of cytochrome C release. Mol Cell Biol 2002;22:816-34.
7. Rane MJ, Pan Y, Singh S, et al. Heat shock protein 27 controls apoptosis by regulating Akt activation. J Biol Chem 2003;278:27828-35.
8. Arrigo AP, Simon S, Gibert B, et al. Hsp27 (HspB1) and alphaB-crystallin (HspB5) as therapeutic targets. FEBS Lett 2007;581:3665-74.
9. Ciocca DR, Calderwood SK. Heat shock proteins in cancer: diagnostic, prognostic, predictive, and treatment implications. Cell Stress Chaperones 2005;10:86-103.
10. Zhang Y, Shen X. Heat shock protein 27 protects L929 cells from cisplatin-induced apoptosis by enhancing Akt activation and abating suppression of thioredoxin reductase activity. Clin Cancer Res 2007;13:2855-64.
11. Chauhan D, Li G, Shringarpure R, et al. Blockade of Hsp27 overcomes Bortezomib/proteasome inhibitor PS-341 resistance in lymphoma cells. Cancer Res 2003;63:6174-7.
12. Aloy MT, Hadchity E, Bionda C, et al. Protective role of Hsp27 protein against gamma radiation-induced apoptosis and radiosensitization effects of Hsp27 gene silencing in different human tumor cells. Int J Radiat Oncol Biol Phys 2008;70:543-53.
13. Zhao R, Davey M, Hsu YC, et al. Navigating the chaperone network: an integrative map of physical and genetic interactions mediated by the hsp90 chaperone. Cell 2005;120:715-27.
14. Whitesell L, Lindquist SL. HSP90 and the chaperoning of cancer. Nat Rev Cancer 2005;5:761-72.
15. Blagosklonny MV. Hsp-90-associated oncoproteins: multiple targets of geldanamycin and its analogs. Leukemia 2002;16:455-62.
16. Diaz-Latoud C, Buache E, Javouhey E, Arrigo AP. Substitution of the unique cysteine residue of murine Hsp25 interferes with the protective activity of this stress protein through inhibition of dimer formation. Antioxid Redox Signal 2005;7:436-45.
17. Javouhey E, Gibert B, Arrigo AP, Diaz JJ, Diaz-Latoud C. Protection against heat and staurosporine mediated apoptosis by the HSV-1 US11 protein. Virology 2008;376:31-41.
18. Moulin M, Arrigo AP. Long lasting heat shock stimulation of TRAIL-induced apoptosis in transformed T lymphocytes. Exp Cell Res 2006;312:1765-84.
19. O'Callaghan-Sunol C, Gabai VL, Sherman MY. Hsp27 modulates p53 signaling and suppresses cellular senescence. Cancer Res 2007;67:11779-88.
20. Doshi BM, Hightower LE, Lee J. The role of Hsp27 and actin in the regulation of movement in human cancer cells responding to heat shock. Cell Stress Chaperones 2009;14:445-57.
21. Hubbert C, Guardiola A, Shao R, et al. HDAC6 is a microtubule-associated deacetylase. Nature 2002;417:455-8.
22. Voss OH, Batra S, Kolattukudy SJ, Gonzalez-Mejia ME, Smith JB, Doseff AI. Binding of caspase-3 prodomain to heat shock protein 27 regulates monocyte apoptosis by inhibiting caspase-3 proteolytic activation. J Biol Chem 2007;282:25088-99.
23. Song H, Ethier SP, Dziubinski ML, Lin J. Stat3 modulates heat shock 27kDa protein expression in breast epithelial cells. Biochem Biophys Res Commun 2004;314:143-50.
24. Aoki Y, Feldman GM, Tosato G. Inhibition of STAT3 signaling induces apoptosis and decreases survivin expression in primary effusion lymphoma. Blood 2003;101:1535-42.
25. Brierley MM, Fish EN. Stats: multifaceted regulators of transcription. J Interferon Cytokine Res 2005;25:733-44.
26. Rocchi P, Beraldi E, Ettinger S, et al. Increased Hsp27 after androgen ablation facilitates androgen-independent progression in prostate cancer via signal transducers and activators of transcription 3-mediated suppression of apoptosis. Cancer Res 2005;65:11083-93.
27. Veinger L, Diamant S, Buchner J, Goloubinoff P. The small heat-shock protein IbpB from Escherichia coli stabilizes stress-denatured proteins for subsequent refolding by a multichaperone network. J Biol Chem 1998;273:11032-7.

28. Eyles SJ, Gierasch LM. Nature's molecular sponges: small heat shock proteins grow into their chaperone roles. Proc Natl Acad Sci U S A;107:2727-8.
29. Bruey JM, Paul C, Fromentin A, et al. Differential regulation of HSP27 oligomerization in tumor cells grown in vitro and in vivo. Oncogene 2000;19:4855-63.
30. Paul C, Simon S, Gibert B, Virot S, Manero F, Arrigo AP. Dynamic processes that reflect anti-apoptotic strategies set up by HspB1 (Hsp27). Exp Cell Res.
31. Kwon S, Zhang Y, Matthias P. The deacetylase HDAC6 is a novel critical component of stress granules involved in the stress response. Genes Dev 2007;21:3381-94.
32. Hageman J, Rujano MA, van Waarde MA, et al. A DNAJB chaperone subfamily with HDAC-dependent activities suppresses toxic protein aggregation. Mol Cell;37:355-69.
33. Lelj-Garolla B, Mauk AG. Self-association and chaperone activity of Hsp27 are thermally activated. J Biol Chem 2006;281:8169-74.
34. Boyault C, Zhang Y, Fritah S, et al. HDAC6 controls major cell response pathways to cytotoxic accumulation of protein aggregates. Genes Dev 2007;21:2172-81.
35. Lee YS, Lim KH, Guo X, et al. The cytoplasmic deacetylase HDAC6 is required for efficient oncogenic tumorigenesis. Cancer Res 2008;68:7561-9.
36. Porter AG, Janicke RU. Emerging roles of caspase-3 in apoptosis. Cell Death Differ 1999;6:99-104.
37. Ribeil JA, Zermati Y, Vandekerckhove J, et al. Hsp70 regulates erythropoiesis by preventing caspase-3-mediated cleavage of GATA-1. Nature 2007;445:102-5.
38. Janicke RU, Sprengart ML, Wati MR, Porter AG. Caspase-3 is required for DNA fragmentation and morphological changes associated with apoptosis. J Biol Chem 1998;273:9357-60.
39. Hideshima T, Bradner JE, Wong J, et al. Small-molecule inhibition of proteasome and aggresome function induces synergistic antitumor activity in multiple myeloma. Proc Natl Acad Sci U S A 2005;102:8567-72.
40. Plescia J, Salz W, Xia F, et al. Rational design of shepherdin, a novel anticancer agent. Cancer Cell 2005;7:457-68.
41. Stengel F, Baldwin AJ, Painter AJ, et al. Quaternary dynamics and plasticity underlie small heat shock protein chaperone function. Proc Natl Acad Sci U S A;107:2007-12.

Figures

Figure 1: Down regulation of Hsp27 protein by expression of a shRNA sensitizes HeLa cells to death and promotes apoptosis. In all experiments, HeLa cells were transiently transfected with the different vectors. *A*, pCI-Neo vector, pSuperNeo-ScRNA27 (Sc27), pSuperNeo-MsRNA27 (Ms27) and pSuper-ShRNA27 (Sh27) were transiently expressed in HeLa cells. Samples were collected 48h after transfection and levels of Hsp27 analyzed by western blot. *B*, Sensitivity to cell death was determined by crystal violet analysis as described in Materials and methods. Staurosporine, a pro-apoptotic kinase inhibitor, was used to induce apoptosis

($p< 0.01$). *C*, HeLa cells were treated for 4 h with staurosporine and samples were analyzed by western blot using an anti caspase3 antibody.

Figure 2: Cell cycle analysis of Hsp27 knock-down clones shows an enrichment in G2/M phase which reduces cell proliferation. Constitutive Hsp27 depleted clones of HeLa or MCF-7 were isolated as described in Materials and methods. *A*, HeLa or MCF-7 samples of independent Hsp27 depleted clones were collected and the levels of Hsp27, 70 and 90 were analyzed by western blot. *B*, Immunoblot analysis of Hsp27, survivin, Bcl-2, $Bcl_{Xs/l}$, Bax, Bid and actin. *C*, WST-1 test was performed each 12 hours during five days. Proliferation index was determined and reported for each cell line ($p< 0.01$). *D*, Cell cycle study was performed by flow cytometry analysis as previously described (18). Quantitative analysis were realized and reported on tables presented on the left side of flow cytometry analysis.

Figure 3: HDAC6 is degraded in Hsp27 deficient cell lines. *A*, photographs of Hoechst stained nuclei of Hsp27 depleted HeLa cells. *B*, phase contrast pictures of the most depleted HeLa clone showing giant cells containing more than twenty nuclei. *C*, Fluorescence photomicrographs analysis of HspB1 and F-actin. HeLa cells were plated on glass cover slips and allowed to enter exponential cell growth for one day. Thereafter, cells were fixed and exposed to Hsp27 mouse monoclonal antibody followed by a goat anti-mouse FITC-conjugated antibody. They were also treated with TRICT-labeled phalloidin to visualize F-actin and with Hoechst to stain nuclei. Cells were then examined under a fluorescent microscope and photomicrographs including overlay analysis were recorded. Note the drastic modification of cells morphology induced by Hsp27 withdrawal. *D*, ShRNA-HDAC6 and MsRNA-HDAC6 were transitory transfected as a control of tubulin induced hyperacetylation. Samples of cell lines, were collected an analyzed by immunobloting incubated with the

indicated antibody. Quantification of western blot was reported on a table. *E*, quantification of *hdac6* gene relative expression by quantitative PCR analysis. *F*, proteasome activity inhibition by MG132 (0.5μmol/l- 20 hours) correlated with poly-ubiquitin accumulation as revealed immunoblot analysis. Cells were submitted to 20 h treatments with either 10μmol/l ALLN- 20 hours or 0.5μmol/l- MG132 which are calpain and proteasome inhibitors, respectively. Level of HDAC6 was revealed by immunobloting.

Figure 4: Knock out of Hsp27 induces procaspase3 proteasomal degradation without modulating procaspase-3 gene expression. *A*, Protein extracts of HeLa clones were submitted to western blot experiments. Immunoblots were incubated and revealed with the indicated antibody. Quantification of western blot intensity was reported on table. *B*, Each cell lines were treated 4 h with 0.25 μmol/l of staurosporine. Samples were analyzed by western blot using an anti caspase3 antibody. *C*, quantification of *procaspase3* gene relative expression by qPCR experiments. *D*, samples were collected after 20 h treatments with either 0.5μmol/l-MG132 or 10μmol/l ALLN. Level of procaspase3 was revealed by western blot analysis.

Figure 5: Endogenous level of STAT2 was decreased in Hsp27 depleted cell line. *A*, Hsp27 depleted and control HeLa cells were collected, and samples were analyzed by western blotting using the corresponding antibody. Quantification of western blot was reported on Table. *B*, MCF-7 depleted cells were submitted to western blot analysis. C, characterized HeLa clones were treated with interleukin-6 (125ng/ml) or heat shock (60 min, TEMPERATURE). Samples were collected and analyzed by immunobloting using STAT3, P-STAT3, Hsp27 and actin antibodies. *D*, quantification of *stat2* gene relative expression by qPCR analysis. *E*, Cells were submitted to 20 h treatments with either 0.5μmol/l MG132 10μmol/l ALLN. Levels of STAT2 were revealed by immunobloting.

Figure 6: HeLa cells were lysed in the presence of 0.1% Triton X-100 and the 10,000×g soluble supernatants was applied to sepharose CL-6B gel filtration columns as described above. 29, 66, 150, 200, 443, 669 and 2000 (kDa) indicate the apparent native size of gel filtration markers. *A*, The presence of Hsp27, HDAC6, STAT2 and procaspase3 in pooled fractions eluted from the columns was detected by western blot analysis. *B*, intracellular interactions between Hsp27 and clients proteins was determined by Co-IP experiments. After immunoprecipitation from column fractions of apparent native sizes of 100kDa for procaspase3, 600kDa for STAT2 and 800kDa for HDAC6, with a goat polyclonal anti-Hsp27 antibody, immunoprecipited proteins and input cell lysates were analyzed in immunoblots probed with the indicated antibodies.

Supplementary data 1: *A*, quantification of *stat3* gene relative expression by qPCR analysis. *B*, HeLa cells were transitively transfected with Sh27 or Ms27. 48h after transfections samples were collected and analyzed by western blot with STAT3 antibody.

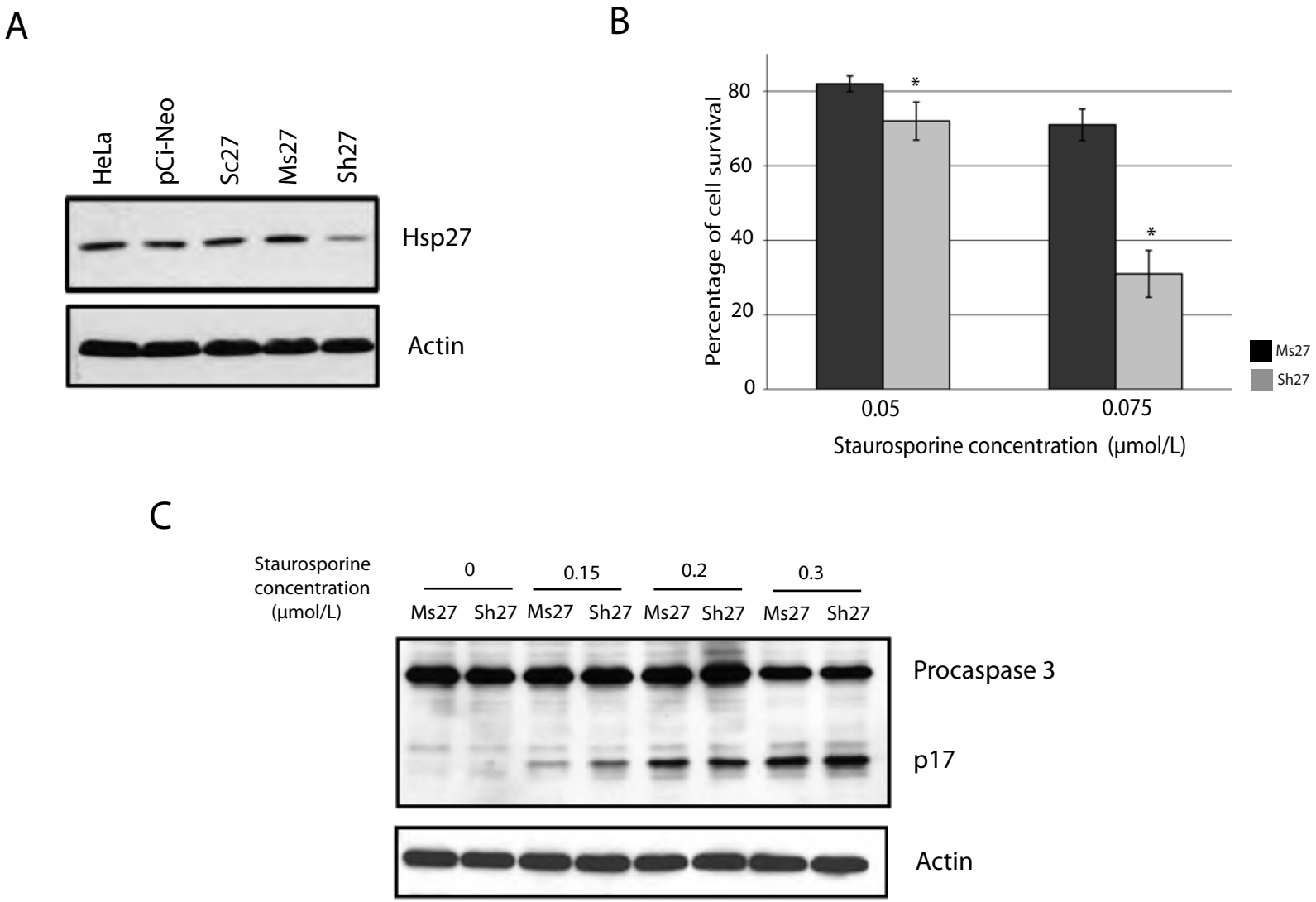
A
HeLa
pCi-Neo
Sc27
Ms27
Sh27
Hsp27
Actin
B
Percentage of cell survival
80
60
40
20
0
*
*
0.05
0.075
Staurosporine concentration (μmol/L)
Ms27
Sh27
C
Staurosporine concentration (μmol/L)
0
0.15
0.2
0.3
Ms27 Sh27 Ms27 Sh27 Ms27 Sh27 Ms27 Sh27
Procaspase 3
p17
Actin

FIGURE 1

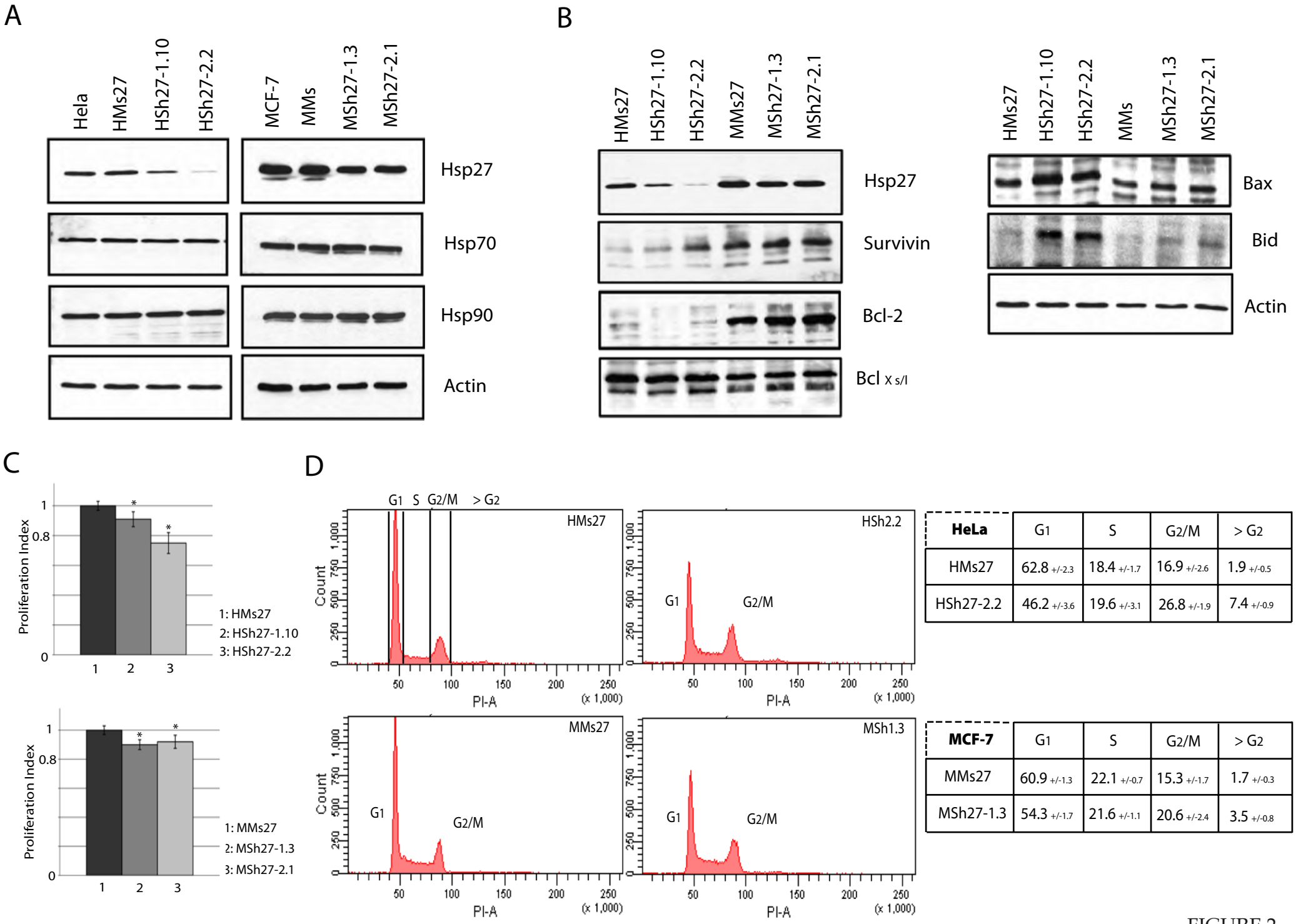

HeLa	G1	S	G2/M	> G2
HMs27	62.8 +/-2.3	18.4 +/-1.7	16.9 +/-2.6	1.9 +/-0.5
HSh27-2.2	46.2 +/-3.6	19.6 +/-3.1	26.8 +/-1.9	7.4 +/-0.9

MCF-7	G1	S	G2/M	> G2
MMs27	60.9 +/-1.3	22.1 +/-0.7	15.3 +/-1.7	1.7 +/-0.3
MSh27-1.3	54.3 +/-1.7	21.6 +/-1.1	20.6 +/-2.4	3.5 +/-0.8

FIGURE 2

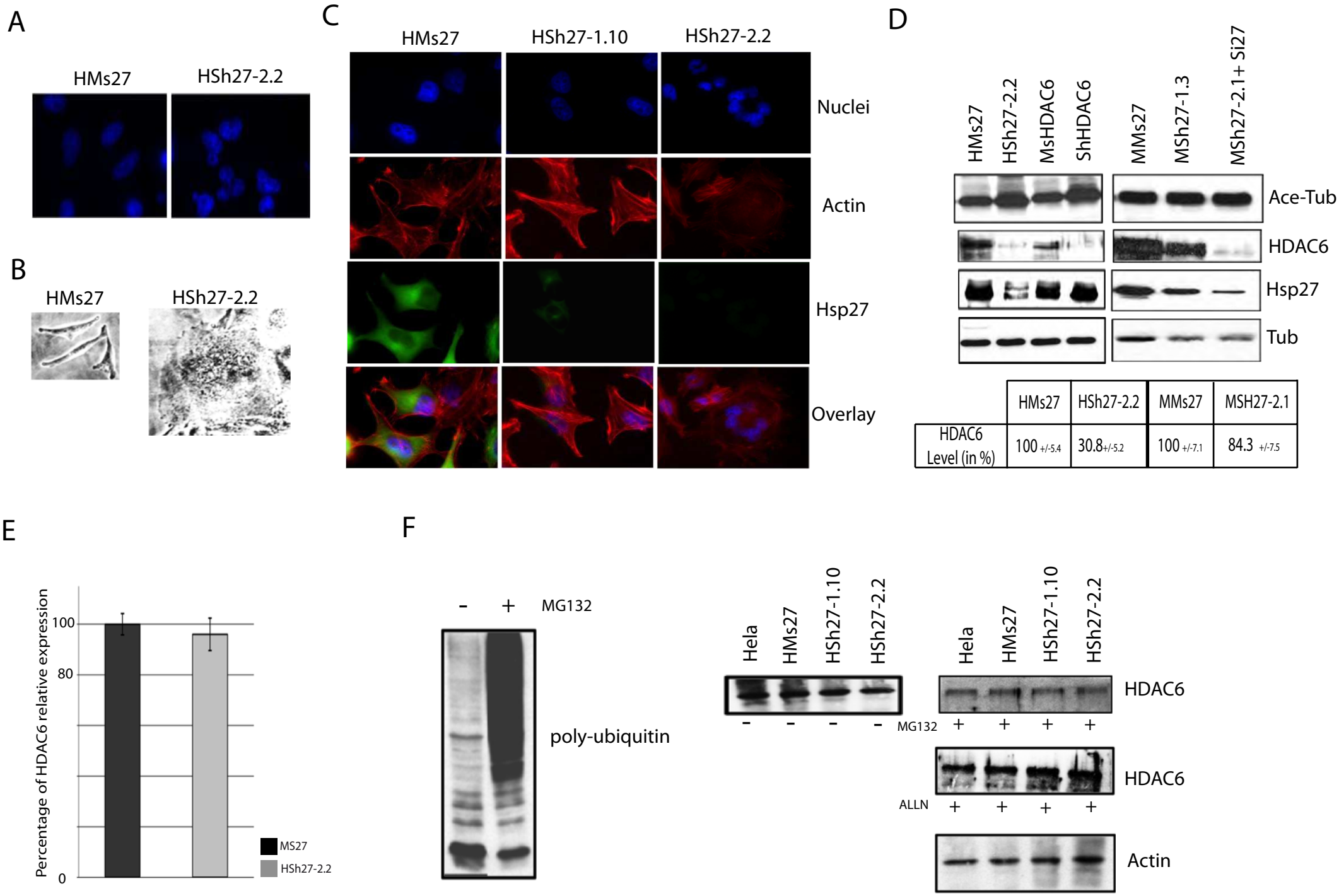
A
HMs27
HSh27-2.2
B
HMs27
HSh27-2.2
C
HMs27
HSh27-1.10
HSh27-2.2
Nuclei
Actin
Hsp27
Overlay
D
HMs27
HSh27-2.2
MsHDAC6
ShHDAC6
MMs27
MSh27-1.3
MSh27-2.1+ Si27
Ace-Tub
HDAC6
Hsp27
Tub
HMs27
HSh27-2.2
MMs27
MSH27-2.1
HDAC6 Level (in %)
100 +/-5.4
30.8+/-5.2
100 +/-7.1
84.3 +/-7.5
E
Percentage of HDAC6 relative expression
100
80
0
MS27
HSh27-2.2
F
- + MG132
poly-ubiquitin
Hela
HMs27
HSh27-1.10
HSh27-2.2
HDAC6
MG132
HDAC6
ALLN
Actin

FIGURE 3

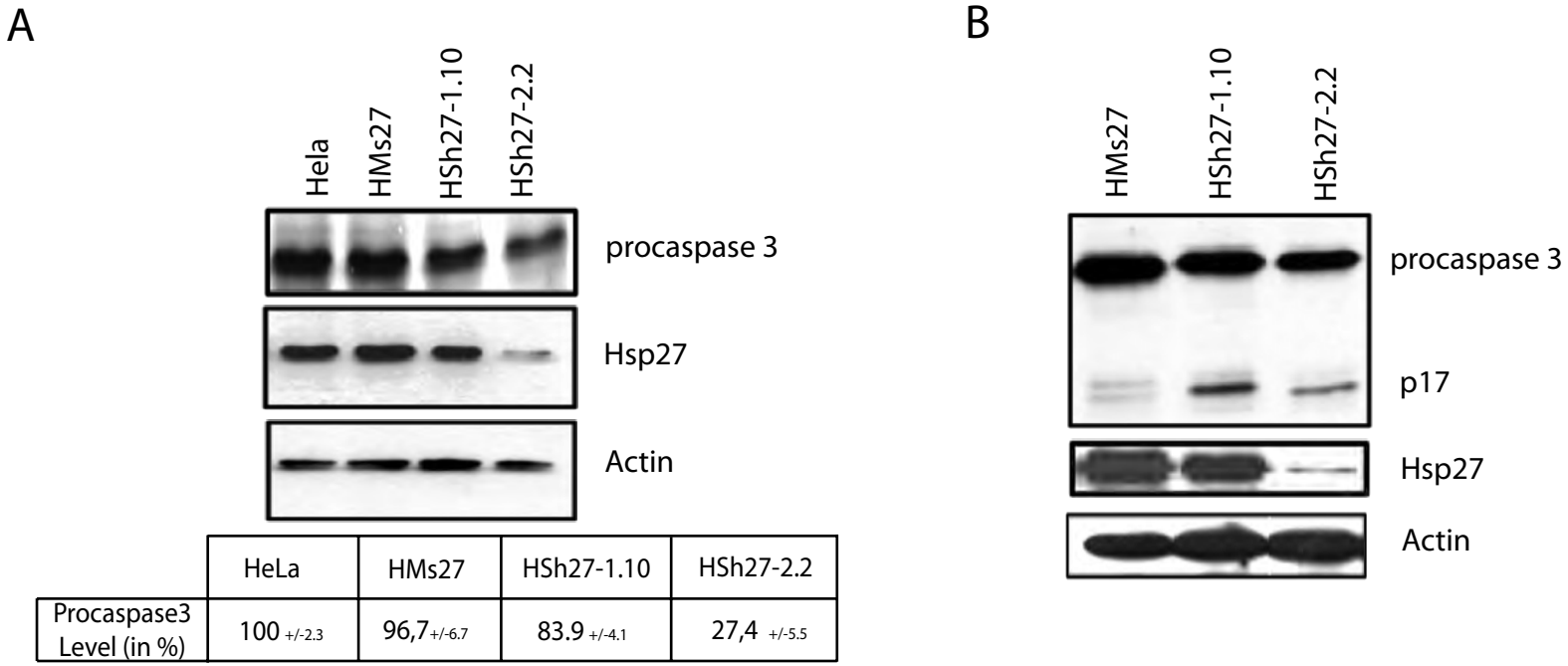

	HeLa	HMs27	HSh27-1.10	HSh27-2.2
Procaspase3 Level (in %)	100 +/-2.3	96,7 +/-6.7	83.9 +/-4.1	27,4 +/-5.5

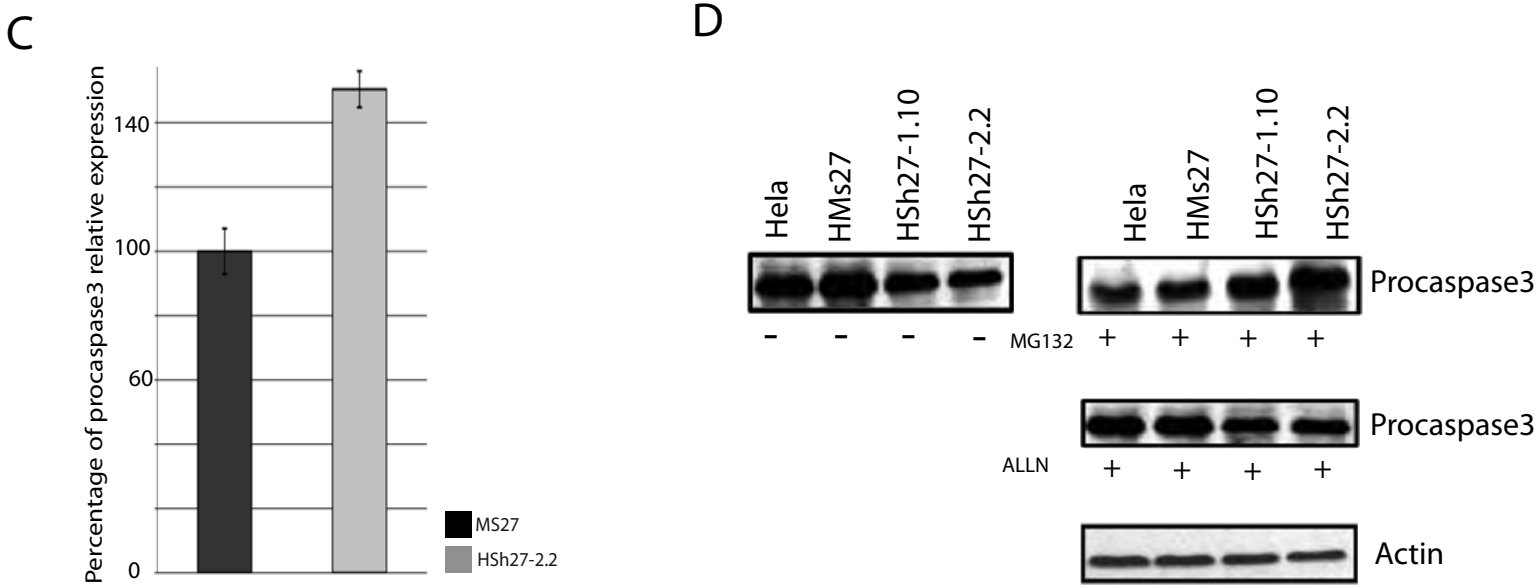

FIGURE 4

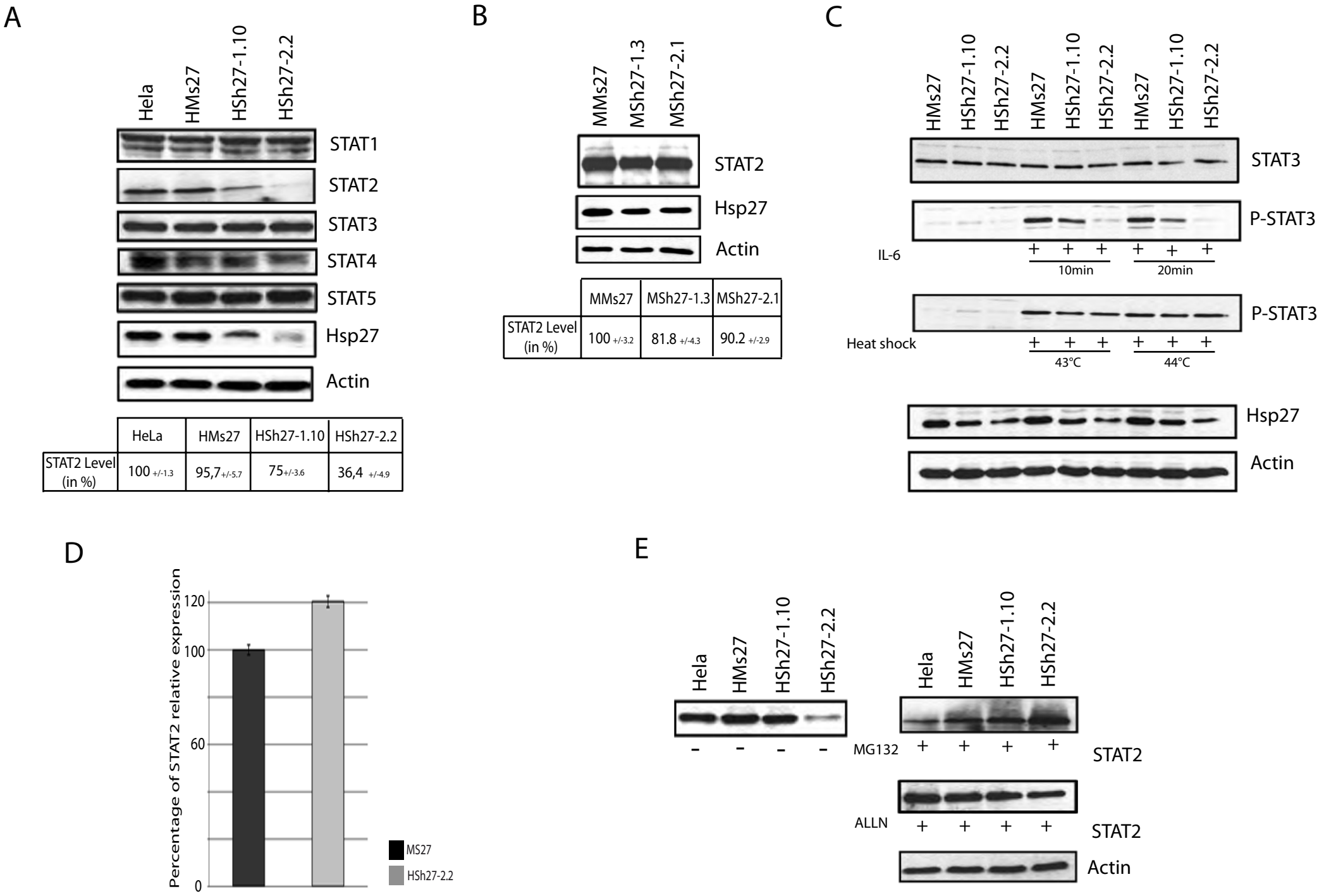
A
Hela
HMs27
HSh27-1.10
HSh27-2.2
STAT1
STAT2
STAT3
STAT4
STAT5
Hsp27
Actin
HeLa | HMs27 | HSh27-1.10 | HSh27-2.2
STAT2 Level (in %) | 100 +/-1.3 | 95,7+/-5.7 | 75+/-3.6 | 36,4 +/-4.9
B
MMs27
MSh27-1.3
MSh27-2.1
STAT2
Hsp27
Actin
MMs27 | MSh27-1.3 | MSh27-2.1
STAT2 Level (in %) | 100 +/-3.2 | 81.8 +/-4.3 | 90.2 +/-2.9
C
HMs27
HSh27-1.10
HSh27-2.2
STAT3
P-STAT3
IL-6
10min
20min
Heat shock
43°C
44°C
Hsp27
Actin
D
Percentage of STAT2 relative expression
120
100
60
0
MS27
HSh27-2.2
E
Hela
HMs27
HSh27-1.10
HSh27-2.2
MG132
STAT2
ALLN
STAT2
Actin

FIGURE 5

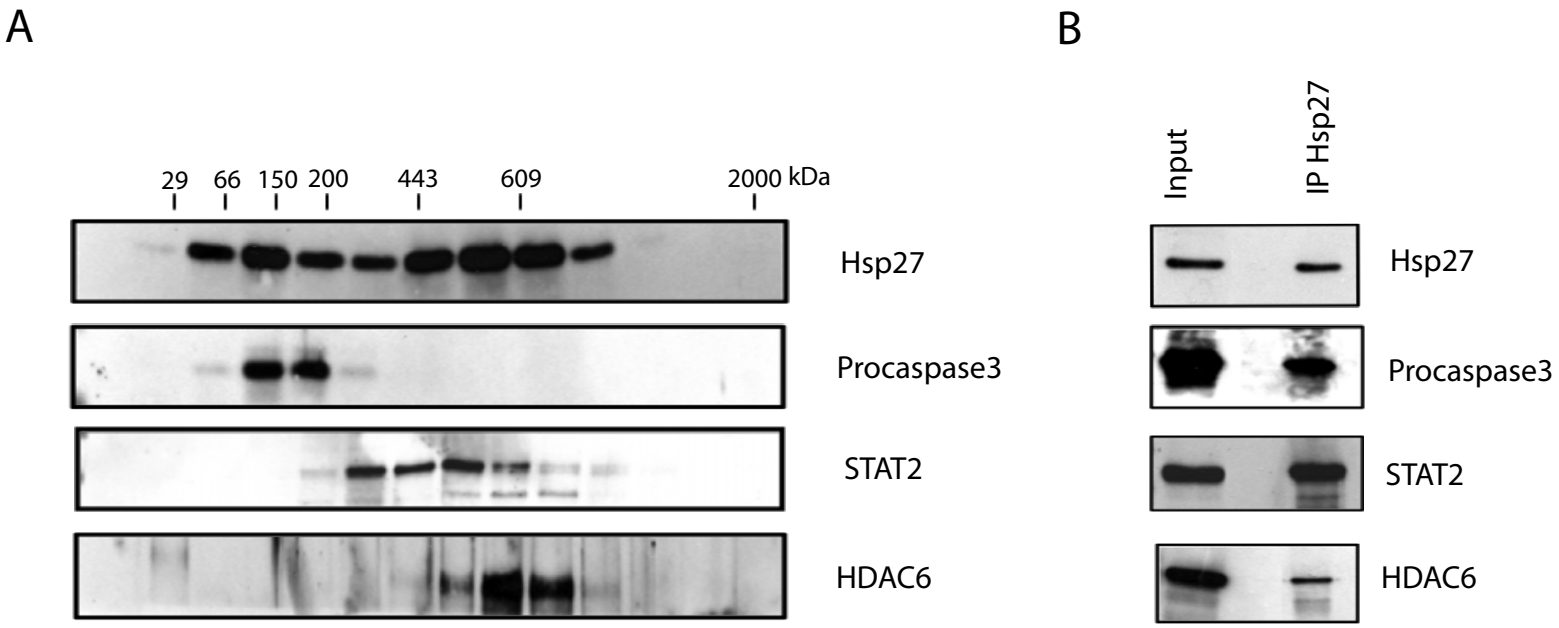
A
29
66
150
200
443
609
2000 kDa
Hsp27
Procaspase3
STAT2
HDAC6
B
Input
IP Hsp27
Hsp27
Procaspase3
STAT2
HDAC6

FIGURE 6

A

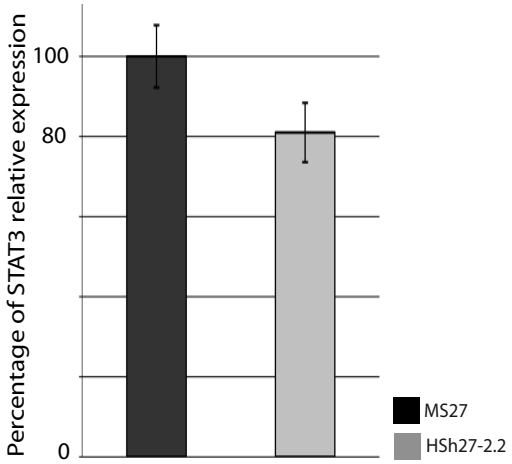

B

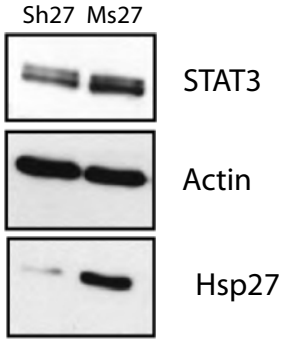

SUPPLEMENTARY DATA 1

PARTIE - 5

Partie 5 - Caractérisation de la déplétion de Hsp27 sur la formation de métastases et de tumeurs osseuses.

Travaux en cours

De nombreuses études protéomiques ont mis en évidence une corrélation entre la forte expression de Hsp27 et la présence de métastases chez les patients (Chen *et al.*, 2004 ; Li *et al.*, 2006 ; Yao *et al.*, 2009). Cependant aucune étude n'a été effectuée dans le but de déterminer le lien direct entre Hsp27 et la formation de métastases. Nous avons entrepris, en collaboration avec l'équipe du Docteur Philippe Clézardin (INSERM-U664, Lyon) de caractériser l'effet de la déplétion de Hsp27 sur la formation de métastases osseuses chez la souris.

Nous avons réalisé des clones stables dans la lignée B02 qui métastase spécifiquement dans la moelle osseuse de souris, une fois injection dans la circulation sanguine. Cette lignée a pour origine la lignée métastatique de cancer du sein humaine MDA-MB231. Elle a été obtenue par prélèvement spécifique des métastases osseuses et réinjection, après plusieurs passages chez l'animal (Peyruchaud *et al.*, 2001). Nous avons obtenu des clones indépendants fortement déplétés en Hsp27 (figure 1-A). Les clones déplétés en Hsp27 possèdent des difficultés de migration cellulaire (figure 1-B). Ces mêmes clones seront prchainement soumis à des tests d'invasion.

Par ailleurs ces mêmes cellules expriment constitutivement la luciférase. Un mélange de cellules issues de ces différents clones a été réinjecté dans les veines caudales de souris Nude. Le suivi d'envahissement métastatique a ensuite été réalisé chaque semaine avec détection de bioluminescence ainsi que quantification de la lyse osseuse après radiographie (figure 2-A et B). Les suivis de l'évolution métastatique révèlent que la formation des métastases et très fortement ralentie pour des cellules déplétées en Hsp27 (Figure 2-C).

En parallèle à cette étude de formation de métastases, nous avons réalisé une analyse de la formation de tumeurs primaires avec ces mêmes cellules déplétées en Hsp27. Des xénogreffes ont été réalisées directement par injection intra-tibiale afin de bénéficier des mêmes facteurs environnementaux de développement tumoral (Figure 3-A et B). En effet, la formation des métastases est extrêmement dépendante des conditions environnementales d'implantations. La greffe de tumeurs dans des conditions similaires de croissance dans la moelle osseuse, permet de corréler les données entre formation réelle des métastases et développement tumoral propre.

Comme observé avec d'autres lignées cellulaires lors d'autres tests réalisés *in vivo* la déplétion en Hsp27 ralentit la croissance tumorale (Figure 3-C).

En parallèle de ces analyses *in vivo*, nous réaliserons une étude de caractérisation moléculaire de ces clones. Nous avons déjà pu mettre en évidence que certaines protéines clientes comme STAT2 ont été dégradées dans les cellules où l'expression de Hsp27 est inhibée. Ainsi, nous analyserons la formation de structures importantes lors de l'envahissement métastatique comme la formation de l'invadopode. Cette structure a été montrée comme primordiale pour lors du franchissement de la lame basale des organes par les cellules métastatiques (Buccione *et al.*, 2009). Cette structure est fortement corrélée à l'action d'enzymes capables de lyser les composants de la matrice extracellulaire, ce qui favorise l'invasion et la migration des cellules métastatiques comme les MMP (Matrix Metallopeptidase) (Wolf et Friedl, 2009).

A

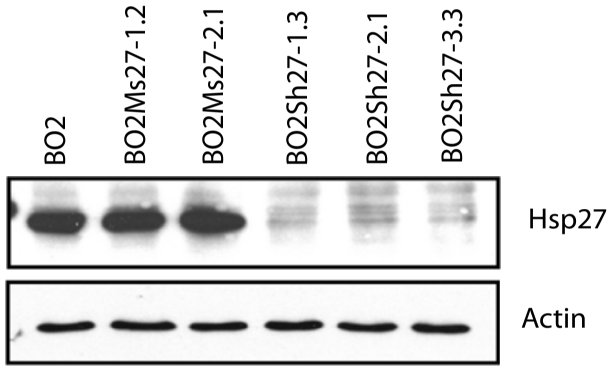
BO2
BO2Ms27-1.2
BO2Ms27-2.1
BO2Sh27-1.3
BO2Sh27-2.1
BO2Sh27-3.3
Hsp27
Actin

B

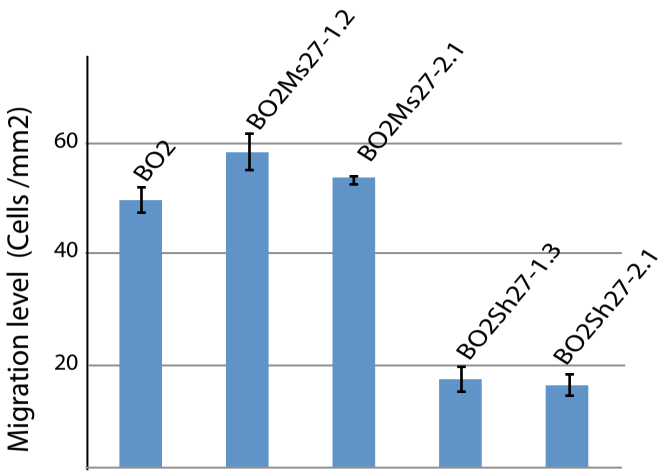
Migration level (Cells /mm2)
60
40
20
BO2
BO2Ms27-1.2
BO2Ms27-2.1
BO2Sh27-1.3
BO2Sh27-2.1

FIGURE -1

A

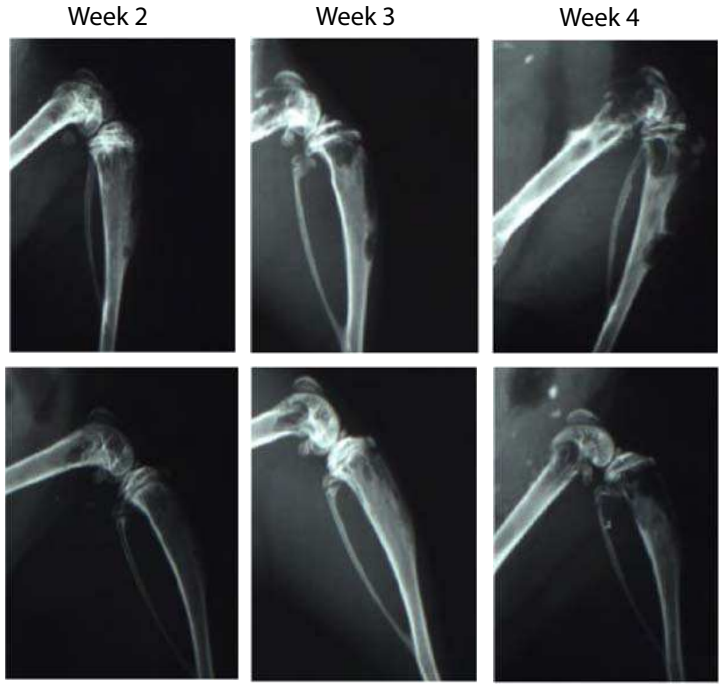
Week 2
Week 3
Week 4
BO2Ms27
BO2Sh27

B

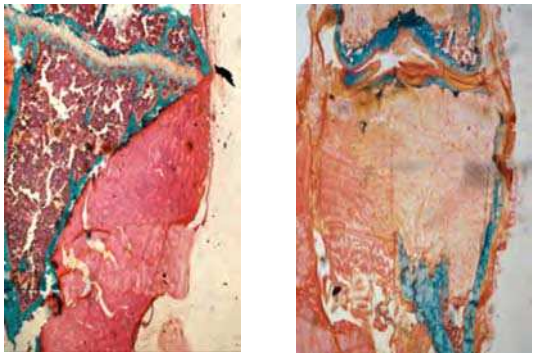
BO2Sh27
BO2Ms27

C

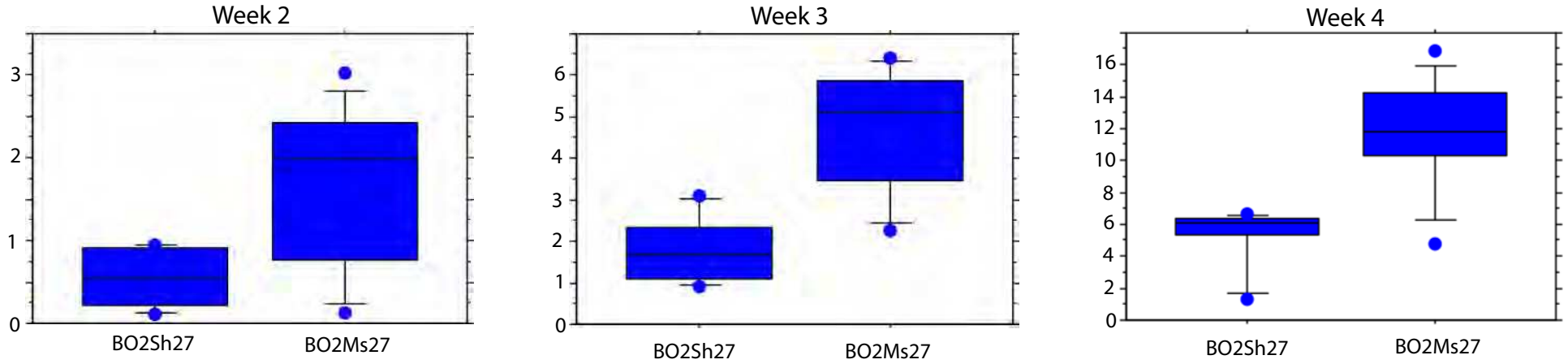
Week 2
3
2
1
0
BO2Sh27
BO2Ms27
Week 3
6
5
4
3
2
1
0
BO2Sh27
BO2Ms27
Week 4
16
14
12
10
8
6
4
2
0
BO2Sh27
BO2Ms27

FIGURE -2

A


Week 5
Week 6
BO2Sh27
BO2Ms27

B

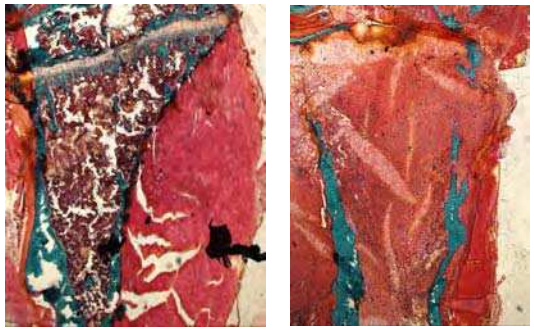
BO2Sh27
BO2Ms27

C

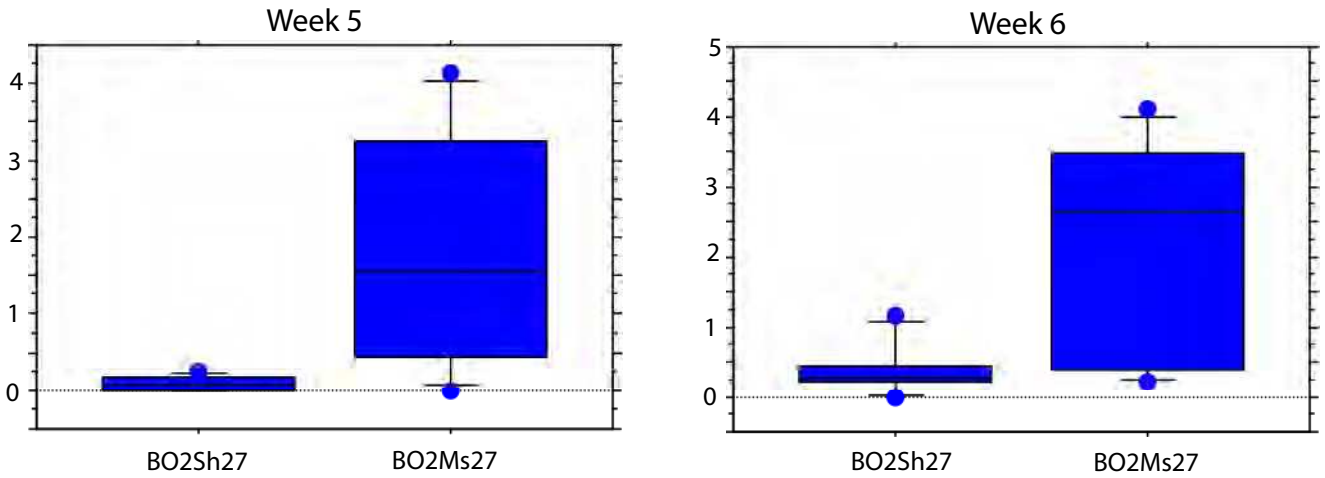
Week 5
Week 6
0
1
2
3
4
5
BO2Sh27
BO2Ms27

FIGURE -3

DISCUSSIONS PERSPECTIVES

DISCUSSIONS-PERSPECTIVES:

Après plusieurs décenies de travaux, des protéines sont apparues comme jouant un rôle crucial dans les processus de cancérisation. En effet, les protéines dites anti-apoptotiques favorisent l'apparition et la survie de cellules anormales pouvant mener à la formation de tumeurs. Par ailleurs, ces protéines peuvent conduire à des phénomènes de résistances de ces mêmes cellules aux traitements chimio et radio-thérapeutiques. Toutes ces protéines constituent des cibles thérapeutiques de choix car elles ne sont pas dérégulées dans des cellules non pathologiques. Ces protéines étant largement surexprimées dans les tumeurs, on peut imaginer qu'une thérapie les ciblant spécifiquement permette d'augmenter la spécificité tumorale.

Hsp27 appartient à cette classe de protéines dite de survie. Son expression est dérégulée dans de nombreux types de cancers où elle confère une résistance aux cellules face au système immunitaire ainsi que contre des traitements anti-cancéreux. Elle est donc une cible thérapeutique majeure en cancérologie. Nous avons recherché des molécules capables d'inhiber fonctionnellement Hsp27 sans moduler son taux de synthèse. Nous avons choisi l'approche des peptides aptamères qui ont été criblés pour être spécifiques de cette protéine. Nous avons isolé des aptamères capables d'inhiber les activités anti-mort cellulaire et tumorigène de Hsp27. Nous avons ainsi pu montrer que le ciblage de Hsp27 par ces peptides, inhibait la croissance tumorale chez l'animal en induisant le blocage du cycle cellulaire. Ces travaux peuvent permettre la modélisation des sites d'interactions par approche bioinformatique et la caractérisation de drogues agonistes de la structure des aptamères. Les composés chimiques présentant une structure tridimensionnelle proche de celles de la région variable des aptamères, pourront ainsi être testés afin d'étudier leurs effets sur les fonctions de Hsp27.

Les aptamères peuvent fournir un outil pour le développement de nouvelles molécules basées sur le principe des pertes d'interactions. La modélisation des structures agonistes d'interactions peptidiques semble être l'un des seules solutions pour envisager le ciblage direct de cibles thérapeutiques sans passer par l'étape très aléatoire du crible de molécules. Le « drug design » de molécules permettra potentiellement une toxicité plus faible liée à une réelle spécificité d'inactivation d'une cible donnée. Ce type d'approche a déjà été utilisé pour le ciblage du sillon d'interaction entre les protéines BH3 pro- et anti-apoptotiques de type Bax et Bcl-2 (Oltersdorf *et al.*, 2005). En outre, il semble fort probable que l'aptamère en lui-même ne puisse

pas être appliqué directement en thérapie humaine. Des vecteurs rétroviraux pourraient être utilisés mais il semble que les stratégies anti-sens s'avéreraient dans ce cas beaucoup plus puissantes. Par ailleurs, il apparaît que certains aptamères peuvent permettre la séquestration de leur cible, par exemple dans les agrésomes, ce qui peut engendrer une toxicité pour les cellules saines du reste de l'organisme (Tomai *et al.*, 2006).

Il est reste néammoins certain que la découverte de ces structures chimiques peut être un élément prépondérant pour cibler de nombreux types tumoraux surexprimant Hsp27. On peut cependant s'interroger sur la spécificité d'action de telles molécules. Hsp27 comme toutes les petites Hsp, ne possède pas d'activité dépendante de l'ATP. Nous avons pu montrer qu'un bon moyen d'inhiber les activités des sHsp est de déstabiliser leurs structures tridimentionelles. On peut donc s'interroger sur la spécificité d'action de composés sur l'ensemble de la famille des sHsp. En effet, même si le composé se liait spécifiquement à une seule cible de la famille, il est fort probable, compte tenu de la forte hétérogénéité des combinaisons structurales des sHsp entre elles, qu'une drogue engendre des modulations des fonctions de l'ensemble des autres sHsp. Par ailleurs, il semble légitime d'envisager que le ciblage de Hsp27 et des autres α-cristallines permettant la déstabilisation de leurs structures, puisse engendrer des formes d'agrégation de ces protéines. Ces agrégats toxiques dont les effets sont observables notament dans les muscles et le système nerveux lors de maladies génétiques résultant de mutations dans les gènes codant les sHsp, seront de toutes évidences des contraintes lors de thérapies anti-cancéreuses ciblant les sHsp (Vicart *et al.*, 1998 ; Evgrafov *et al.*, 2004).

L'autre alternative basée sur la création de drogues peptido-mimétiques est le décrochage des protéines interactices du chaperon, clientes ou non. Ainsi, l'interaction de Hsp27 avec différents acteurs de la cascade apoptotique comme le cytochrome *c*, HDAC6 ou la procaspase 3 pourrait être perturbée par la présence des aptamères ou des peptides de la région variable. Il a par ailleurs déjà été montré qu'un peptide pouvait fonctionnellement inhiber une interaction entre Hsp27 et l'un de ses partenaires protéiques. Ce peptide correspond à la zone d'interaction restreinte entre Hsp27 et la kinase PKC δ et possède une activité pro-apoptotique (Kim *et al.*, 2007).

D'un point de vue plus fondamental, les aptamères peuvent s'avérer être un outil très puissant pour comprendre les mécanismes moléculaires régis par Hsp27 et plus particulièrement envers ses protéines clientes. Il semble aussi important de comprendre les réseaux d'interaction

régis par Hsp27. Il a été montré que Hsp90 pouvait réguler par des interactions directes ou génétiques environ 10% du protéome de levure (Bukau *et al.*, 2006). Il semble envisageable que le nombre de partenaires protéiques soit aussi très élevé pour les autres chaperons comme Hsp27, ce qui pourrait expliquer la difficulté de démontrer une interaction physique entre Hsp27 et d'autres protéines. Cependant, nous ne sommes pas parvenus pour l'instant, à démontrer l'existence des protéines clientes de Hsp27 avec la technologie des aptamères peptidiques. L'hypothèse retenue est que nous n'avons pas pu réaliser des clones cellulaires exprimant de manière stable les aptamères, à des niveaux d'expression suffisamment élevés pour permettre le blocage complet des fonctions de Hsp27. Nous avons par exemple pu noter au cours de différentes expériences, que les aptamères possédaient une tendance à l'auto-agrégation et qu'une majeure partie était présente dans la fraction insoluble même en présence de détergent. Ces contraintes techniques mises à part, une autre incertitude réside dans l'activité de la protéine armature des aptamères (thioredoxine A de *E. Coli* dans notre étude). Outre son poids moléculaire relativement important compte tenu de la faible taille de la région variable, on peut imaginer qu'elle joue un rôle important dans l'inhibition des interactions. On peut imaginer que la région variable interagisse réellement avec sa cible mais que se soit la protéine squelette de l'aptamère qui par encombrement stérique, perturbe l'interaction entre Hsp27 et ses autres partenaires protéiques.

Nous n'avons pu démontrer l'existence de polypeptides dégradés en l'absence de Hsp27 que par l'utilisation de shARN exprimés de manière stable. Cette technique basée sur l'inhibition de la traduction d'une cible permet « d'éteindre » l'expression d'un gène dans des cellules données (Nilsen, 2007).

La première particularité inhérente à cette méthode réside dans les différences que nous avons pu constater entre des expériences d'expression réalisées de manière stable ou de manière transitoire. Nous n'avons pas pu démontrer de modifications de prolifération des lignées cancéreuses dans les expériences d'expression transitoire, corrélées à une faible diminution du taux de protéines clientes difficilement quantifiable. Il semble que pour observer des phénomènes d'inhibition de la prolifération comme la diminution du taux des protéines clientes, une expression constitutive du shARN doit être privilégiée. La sélection de clones stables sous-exprimant Hsp27 a été très différente suivant les lignées utilisées. Ainsi, il semble que Hsp27 joue un rôle plus ou moins important dans la cytoprotection selon un type cellulaire donné. Il est probable que la majeure partie des effets observés sur la prolifération a pour origine des difficultés de cytokinèse entrainant le retard de la division cellulaire. La dégradation des protéines clientes de Hsp27 est

semble-t-il aussi importante pour expliquer les modifications observées sur le cycle cellulaire et sans doute à l'origine de l'observation de sénescence lors d'une déplétion en Hsp27 (O'Callaghan-Sunol *et al.*, 2007). Comme pour Hsp90 il semble délicat de prédire quelles sont les protéines responsables de ce blocage, et il est même fort probable que se soient les multiples défections qui induisent cette accumulation des cellules en phase G2/M.

Il apparaît que l'existence de ces protéines clientes pour Hsp27, permette d'émettre sensiblement les mêmes hypothèses que celles émises pour Hsp90 (Queitsch *et al.*, 2002). Ainsi, il est possible que Hsp27 possède les mêmes capacités de masquage de mutations, ce qui donnerait aux chaperons un second niveau de régulation de l'évolution des génomes en permettant la conservation de mutations pourtant délétères. En outre, il semble probable que des mutations oncogéniques puissent elles aussi être conservées comme le stockage de mutants de p53 par Hsp90 (King *et al.*, 2001). Bien que difficilement quantifiable pour l'instant, le nombre d'interacteurs connus pour Hsp27 est en constante augmentation ce qui implique que le nombre des protéines clientes de Hsp27 puisse être relativement important.

Les fonctions de chaperon sur des polypeptides non mutés ou non altérés ne sont pas encore bien caractérisées. Il semble que le fait de « chaperonner » une protéine permette de l'isoler de la masse des protéines favorisant certaines interactions et certains types de réactions entre protéines. La conséquence directe de cette séquestration serait l'augmentation de la demi-vie de la cliente. La dégradation dépendante de l'ubiquitine et du proteasome, observée pour les clientes de Hsp27 comme pour celles de Hsp90, permet d'envisager que les clientes soient reconnues plus facilement par la machinerie de dégradation. Elles ne seraient donc pas laissées libres dans le cytosol puisqu'elles ne semblent pas être dégradées par des protéases non spécifiques de type calpain. Cependant, pour la protéine HDAC6 il est possible que les autres protéases puissent jouer un rôle, à moins que l'effet observé en présence d'inhibiteurs du protéasome soit lié aux facultés d'induction de HDAC6 en présence d'agrégats protéiques (Kwon *et al.*, 2007 ; Boyault *et al.*, 2007).

En outre, il semble aussi possible que la déplétion en Hsp27 puisse induire la dégradation des protéines clientes d'autres chaperons. Cet effet a déjà été observé en modifiant le taux de Hsp70 ou du cochaperon cdc37 qui provoque la déstabilisation et la dégradation des clientes de Hsp90 (Smith *et al.*, 2009).

Par ailleurs, ces fonctions chaperon et de protection contre une dégradation sont à mettre en relation avec les autres fonctions de Hsp27 précédemment caractérisées. Ainsi, il est possible

que Hsp27 participe au système de guidage des protéines vers une dégradation par le protéasome mais aussi en participant à leurs modifications post-traductionnelles comme la sumoylation ou l'acétylation (Brunet Simioni *et al.*, 2009). Il restera aussi à déterminer si les interactions entre Hsp27 et ses clientes potentielles sont des interactions fortuites partiellement aspécifiques de type chaperon/substrat à protéger ou si ces interactions interviennent dans des processus biochimiques complexes et régulés.

Dans des cellules normales, Hsp27 participe au maintien de l'homéostasie cellulaire. Ces fonctions de régulation de conformation protéique sont exacerbées en conditions de stress. Ces mêmes mécanismes semblent être dérégulés dans les cellules cancéreuses qui, pour survivre et s'échapper, « piratent » un nombre important de mécanismes cellulaires. La surexpression de Hsp27 fait partie de ces événements qui participent à l'échappement tumoral. La découverte d'inhibiteurs spécifiques à cette protéine, qu'ils soient peptidiques, à interférence ARN ou chimiques permettra la compréhension des mécanismes moléculaires sous-jacents. Hsp27 semble en outre, être une cible thérapeutique prometteuse et son ciblage permettra de compléter le panel des inhibiteurs dirigés contre les protéines de stress, afin d'inactiver spécifiquement tous les membres de la « réponse au choc thermique ».

ANNEXES

PUBLICATION - 6

PUBLICATION 6 - Protection against heat and staurosporine mediated apoptosis by the HSV-1 US11 protein

Virology. 2008 Jun 20;376(1):31-41.

Le choc thermique, provoque de profondes modifications de l'expression génique telles que l'inhibition de la réplication, de la transcription, de la maturation des messagers et enfin de la traduction. La régulation majeure se situe lors de l'étape cruciale d'initiation de la traduction (Holcik et Sonerberg, 2005). Pendant le choc thermique, la traduction de la majorité des messagers coiffés est donc inhibée. Toutefois la traduction des messagers codant les Hsp persiste. Les Hsp ainsi synthétisées favorisent la reprise de la synthèse protéique à l'issue du stress thermique. De même, l'infection de cellules humaines par de nombreux virus et en particulier par le virus herpès simplex de type 1 (HSV-1) induit, comme le choc thermique, une dérégulation de l'expression génique cellulaire. Au cours de l'infection, par le virus HSV-1, on observe une forte modification de l'expression génique résultant en une répression de la synthèse protéique des cellules infectées accompagnée de l'induction de l'expression des gènes codant pour les protéines de stress. Ces perturbations de la synthèse protéique induites par l'infection sont accompagnées d'une association aux fractions ribosomiques de nouvelles protéines phosphorylées, dont le produit du gène tardif *Us11*, apporté par le virion.

L'ensemble de ces données nous a conduits à analyser les fonctions de la protéine US11 dans des cellules soumises à un choc thermique ce qui constitue un modèle d'étude des interactions hôte-pathogène représenté par cette protéine virale présente lors de l'infection donc lors de la modification de l'expression génique cellulaire.

Nous avons mis en évidence que US11 exerce une protection contre la mort cellulaire induite par un stress hyperthermique. Nous avons ainsi montré que la protéine virale, après un choc thermique, inhibe de manière spécifique, l'activation de la caspase 3 et provoque un délai dans l'efflux de cytochrome *c* de la mitochondrie. Enfin, la protéine US11 protège également les cellules contre une apoptose induite par la staurosporine. La protéine virale agirait donc soit au niveau de la mitochondrie soit en amont au niveau des voies de signalisation régulant l'apoptose mitochondriale.

L'ensemble de nos observations suggère qu'il existe une relation entre la présence de la protéine US11 et la résistance au choc thermique et à l'apoptose qui pourrait jouer un rôle dans la réplication virale au cours de l'infection de la cellule hôte ou suite à une réactivation induite par la chaleur. La fièvre étant chez l'homme, l'un des facteurs les plus efficaces pour induire la réactivation du virus latent.

Virology 376 (2008) 31–41

Contents lists available at ScienceDirect

Virology

journal homepage: www.elsevier.com/locate/yviro

Protection against heat and staurosporine mediated apoptosis by the HSV-1 US11 protein

E. Javouhey [a], B. Gibert [a], A.-P. Arrigo [a], J.J. Diaz [b], C. Diaz-Latoud [a,*]

[a] *Laboratoire Stress, chaperons et mort cellulaire, Université de Lyon, Lyon, F-69003, France; Université Lyon 1, Lyon, F-69003, France; CNRS, UMR5534, Centre de génétique moléculaire et cellulaire, Villeurbanne, F-69622, France*

[b] *Laboratoire domaines nucléaires and Laboratoire pathologies, Université de Lyon, Lyon, F-69003, France; Université Lyon 1, Lyon, F-69003, France; CNRS, UMR5534, Centre de génétique moléculaire et cellulaire, Villeurbanne, F-69622, France*

ARTICLE INFO

Article history:
Received 13 November 2007
Returned to author for revision
11 December 2007
Accepted 28 February 2008
Available online 18 April 2008

Keywords:
Apoptosis
Heat shock
HSV-1
US11 protein
Caspase
Cytochrome *c*

ABSTRACT

US11 protein, one of herpes simplex virus type 1 (HSV-1) true late gene products, plays a role in the virally induced post-transcriptional control of gene expression. In addition, US11 expression also interferes with the cellular response to HSV-1 infection that can lead to apoptosis. We have previously shown that US11 expression enhanced the recovery of cellular protein synthesis and increased cell survival in response to thermal stress. Since heat shock can activate apoptosis, we tested for a possible anti-apoptotic behavior of US11. Here, we show that, in HeLa cells, US11 expression strongly reduced heat induced apoptosis, a phenomenon independent of Hsp expression and characterized by a delayed cytochrome *c* efflux from mitochondria and reduced caspase 3 activation. Moreover, US11 expression also protected against staurosporine induced apoptosis. Hence, our results favor an anti-apoptotic activity of US11 polypeptide that appears to be located at the level of mitochondria or upstream signaling pathways.

Introduction

Apoptosis or programmed cell death, a highly regulated process activated by various cell metabolism disturbing stimuli, is characterized by membrane blebbing, chromatin condensation, nuclear fragmentation and finally the formation of apoptotic bodies (Green, 1998). Apoptotic execution is associated with activation of a family of cysteine proteases known as caspases, which are broadly categorized as initiator (caspase-2, -8, -9, -10) or executioner caspases (caspase-1, -3, -4, -6, -7), that cleave specific proteins leading to the typical hallmarks of apoptosis (Earnshaw et al., 1999; Lavrik et al., 2005). Two main activation cascades for apoptosis induction have been identified. One is induced through death receptors such as Fas/CD95, TNFα (Baetu and Hiscott, 2002; Krammer, 2000) recruiting adapter proteins which in turn bind and directly activate caspases (Nagata, 1997). In the second pathway, through the action of pro-apoptotic Bcl-2 family of polypeptides, mitochondrial membrane permeability is enhanced and cytochrome *c* and other pro-apoptotic molecules are translocated from the mitochondria to the cytosol (Adams and Cory, 1998). After cytochrome *c* release, apoptosis is initiated by the formation of apoptosome, which triggers the caspase activation cascade (Li et al., 1997).

Transient exposure of cells to a mild heat shock activates cellular stress response and results in synthesis and accumulation of heat shock proteins (Hsps). These evolutionary conserved proteins render cells thermotolerant, resistant to subsequent lethal insults (Georgopoulos and Welch, 1993), and protect them from the cytotoxic effects induced by aggregated proteins (Hendrick and Hartl, 1993). They also function as key regulators in the control of apoptosis (Beere et al., 2000; Bruey et al., 2000; Mehlen et al., 1996; Park et al., 2001).

Severe heat shock can cause cell viability loss and the resulting cell death can occur through two morphologically and biochemical distinct pathways: either necrosis, followed, *in vivo*, by an inflammatory response (Harmon et al., 1990), or apoptosis with the involvement of either the extrinsic or the intrinsic canonical pathways (Tibbles and Woodgett, 1999; Zhao et al., 2006). The initial trigger for activation of apoptosis after heat shock is not clearly understood but as prolonged activation of the UPR can lead to apoptosis it might be linked to the unfolded protein response (UPR) (Schroder and Kaufman, 2005). Recent studies suggest that hyperthermia mediated cell death is

Abbreviations: DMEM, Dulbecco's modified Eagle's medium; DEVD-AFC, Asp-Glu-Val-Asp-7-amino-4-trifluoromethylcoumarin; ER, Endoplasmic Reticulum; FADD, FAS-associated death domain; GRP94, Glucose-Regulated protein 94; HSV-1, herpes simplex virus type 1; IETD-AFC, Ile-Glu-Thr-Asp-7-amino-4-trifluoromethylcoumarin; JNK, c-Jun NH_2 terminal kinase; LEHD-AFC, Leu-Glu-His-Asp-7-amino-4-trifluoromethylcoumarin; MOMP, mitochondrial outer membrane permeabilization; TNFα, tumor Necrosis Factor α.

* Corresponding author. Laboratoire stress, chaperons et mort cellulaire, CNRS UMR 5534, Centre de Génétique Moléculaire et Cellulaire, Université Claude Bernard, Lyon 1, 43, Bd du 11 Novembre, 69622 Villeurbanne Cedex, France. Fax: +33 472 43 26 85.
E-mail address: chantal.diaz@univ-lyon1.fr (C. Diaz-Latoud).

0042-6822/$ – see front matter © 2008 Elsevier Inc. All rights reserved.
doi:10.1016/j.virol.2008.02.031

independent of any of the known initiator caspase and therefore might be induced through a specific pathway involving a novel apical protease. This unidentified protease induces mitochondrial outer membrane permeabilization (MOMP), cytochrome *c* release from the mitochondria inter-membrane space to the cytoplasm and caspase 3 activation (Milleron and Bratton, 2006).

Apoptosis is also a mechanism of host cell defense against viral infections. Consequently, many viruses have developed mechanisms to block the premature death of the infected cells. Interestingly, HSV-1, a large DNA virus coding for at least 80 genes could be considered as a prototype of "anti-apoptotic" virus encoding several well defined proteins that are able to counteract the wide diversity of HSV infection-triggered cellular apoptosis albeit by mechanisms that remain still largely unknown for most of them (for a review see (Nguyen and Blaho, 2007)). US3, US5, ICP6 and LAT RNA are HSV gene products that are able to counteract apoptosis in the absence of other viral functions (Jerome et al., 1999; Langelier et al., 2002; Perng et al., 2000). Among these polypeptides, the one with the best characterized anti-apoptotic activity is the US3 protein kinase (Nishiyama and Murata, 2002). US3 kinase blocks apoptosis at a pre-mitochondrial stage by degradation or posttranslational modification of BAD, a pro-apoptotic member of the Bcl-2 family (Munger et al., 2001) or by suppression of JNK activation (Murata et al., 2002). US3 also exerts anti-apoptotic effect downstream mitochondria and this inhibition is dependent upon US3 catalytic activity (Ogg et al., 2004) and blocks the proteolytic cleavage of procaspase 3 (Benetti and Roizman, 2007).

US11 is an RNA-binding protein, post-transcriptional regulator of gene expression (Attrill et al., 2002; Bryant et al., 2005; Diaz et al., 1996). US11 interacts with several different cellular proteins such as human ubiquitous kinesin heavy chain (uKHC) (Diefenbach et al., 2002), homeodomain interacting protein kinase 2 (HIPK2) (Giraud et al., 2004), double-stranded RNA-dependent protein kinase (PKR) and a dsRNA-independent protein activator of PKR (PACT) (Cassady and Gross, 2002; Peters et al., 2002). US11 has been reported as a potent inhibitor of PKR activation through binding to dsRNA (Khoo et al., 2002) or through direct interaction with PKR in the context of viral infection (Cassady and Gross, 2002) and therefore could interfere with the PKR mediated host cell responses. PKR expression is stimulated by type 1 interferon during the cellular interferon-inducible antiviral response. This serine-threonine kinase appears to play a primary role in mediating the antiviral activities of infected cells through activation of the FADD/caspase 8 death-signaling pathway (Balachandran et al., 2000). PKR also plays an important role during ER stress-induced cell death and is essential for efficient induction of the stress protein GRP94 (Ito et al., 2007). Finally, US11 has been recently shown to also counteract the activity of the 2′–5′ oligoadenylate synthetase (OAS), a cellular protein critical for host cell defense (Sanchez and Mohr, 2007). All these observations suggest that US11 might be involved in the viral response against host cell defense and in particular in the inhibition of apoptosis induced by viral infection although none of these studies allow to clearly deciphering the molecular mechanisms by which this could occur. Furthermore, these studies did not address directly the question of whether HSV could counteract apoptosis induced by a non-viral stress – like heat shock – that is known to induce viral reactivation in humans.

We have previously shown that after heat shock, US11 exacerbates the recovery of cellular protein synthesis and provides an increased cell survival to thermal stress (Diaz-Latoud et al., 1997). Because severe thermal stress induces apoptosis and is also one of the most powerful inductor of HSV reactivation, we hypothesized that US11 mediated protection against the deleterious effects of heat stress could result from its ability to counteract heat induced-apoptosis. Here, we present evidence that in US11 expressing cells exposed to heat shock, caspase 3 activation is delayed and cytochrome *c* efflux from mitochondria strongly reduced. This suggests a yet undescribed anti-apoptotic role for this viral protein at the level of mitochondria or upstream signaling pathways that could be relevant for successful HSV replication following reactivation by the uncontrolled increase of cell temperature in infected humans.

Results

US11 protects cells against heat induced apoptosis

The resistance to heat induced apoptosis was analyzed in the previously characterized HeLa cells constitutively expressing US11, HL5e6 (Simonin et al., 1995). HL5e6 and control HLNeo7 cells were heat treated for 1 h at 44 °C and allowed to recover for 3 h. The extent of heat induced apoptosis was then determined by measuring the level of externalization of phosphatidylserines (PS), an event which is observed during maximal apoptosis and that can be visualized by the binding of (FITC)-conjugates Annexin V to non-permeabilized cells. Fig. 1A presents two-dimensional FACScan analysis of propidium iodide (PI) / Annexin V staining. Quantitative analysis (Fig. 1B) showed that, after heat shock treatment, the percentage of viable HLNeo7 cells (PI and Annexin V negative cells) dropped from 82% to 52% of the total cell population whereas the decrease was far less intense (77% to 73%) in US11 expressing cells. Statistical analysis demonstrated the significance of the differences in the percentages of viable cells observed between control and US11 expressing cells. These results strongly suggest that the expression of US11 protein protects HeLa cells against heat induced apoptosis.

US11 reduces caspase 3 activation after heat shock

The processing of the executioner caspase 3 is an essential event to complete the destructive phase of apoptosis (Slee et al., 1999). Therefore, to further characterize US11 protein function in HeLa cells during heat shock, we next analyzed whether this polypeptide could modulate the heat induced activation of caspase 3. To render the results more robust, these experiments were performed using two different clones of HeLa cells expressing constitutively different levels of US11, HL5e6 clone expressing 50% more viral protein than HL5a1 cells as already described (Diaz-Latoud et al., 1997). An immunoblot analysis of the 32 kDa procaspase 3 processing, in HeLa cells expressing or not US11, after a heat shock treatment (1 h at 44 °C) and during recovery at 37 °C is presented in Fig. 2A. The analysis of the pixel density of procaspase 3 band showed a strong decrease in the level of procaspase 3 in control cells after heat shock whereas no decrease was observed in US11 expressing cells. As expected the 17 kDa caspase 3 processed fragment was not detected in untreated cells. This fragment was clearly detected in HLNeo7 cells 2 h after the end of heat shock and its amount reached a maximum level after a 4 h recovery period. Conversely, this fragment was not detected in both US11 expressing cells after a 2 h recovery period and was barely detectable after 8 h of recovery in HL5a1 cells.

In order to monitor more finely this phenomenon, heat induced caspase 3 activity was then monitored by cleavage of fluorescent DEVD-AFC substrate analysis (Fig. 2B). As expected, heat shock induced an important increase of caspase activity in HLNeo7 control cells that reached up to a 10-fold activation after 4 h of recovery (Fig. 2B, black bars). Conversely, heat shock did not induced a significant caspase 3 activation in both US11 expressing cell lines whatever was the duration of recovery period (2, 4 and 6 h) (Fig. 2B, grey bars).

To determine if the delay in caspase 3 activation observed in US11 expressing cells was not a consequence of a cellular adaptation to the constitutive presence of US11, we performed the same type of experiments in HeLa cells transiently expressing US11. HeLa cells transfected with either an US11 expressing vector or a control vector were submitted to a one-hour heat shock at 44 °C 36 h after

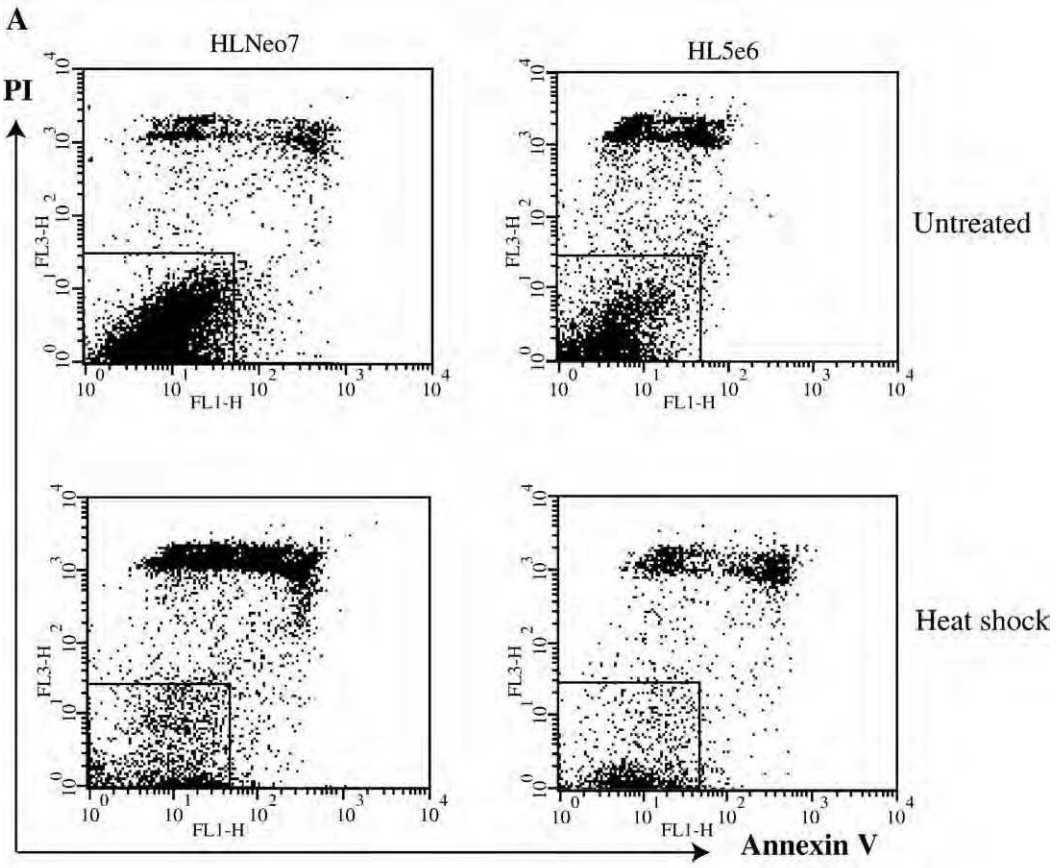

B

	HLNeo7	HL5e6
Untreated	80.47 % +/- 1.53	77.3 % +/-1.07
Heat shock	52.43 % +/- 2.63	72.99 % +/- 0.68

Percentage of viable cells

Fig. 1. US11 protein reduces heat induced apoptosis. HLNeo7 control and HL5e6 US11 expressing cells, treated for 1 h at 44 °C, were harvested 3 h after the heat shock treatment. (A) Cells were then stained with Annexin V and propidium iodide and analyzed as described in Materials and methods. Data are representative of one out of three experiments with comparable results. (B) Lower left square: Annexin V and PI negative cells quantification from panel A. Values represent mean ± S.D of three independent experiments. Student's *t* test analysis demonstrated significance $P=0.0035$ of the differences between staurosporine treated HLNeo7 and HL5e6 cell lines.

transfection and procaspase 3 processing was evaluated after 4 h of recovery at 37 °C. This experiment clearly showed that caspase 3 activation was 2-fold higher in cells transfected with the control vector than in cells transfected with the US11 expressing vector (data not shown). It was then concluded that the anti-apoptotic activity of US11 described here did not result from an adaptation of the cells to a prolonged expression of this viral protein.

US11 protein precludes heat shock induced cytochrome c release induced by heat shock

As most apoptotic inducers, heat shock induces the release of cytochrome *c* from the mitochondria inter-membrane space to the cytoplasm (Samali et al., 2001). We therefore determined the level of cytochrome *c* efflux from mitochondria in control HLNeo7 and US11 expressing HL5e6 cells either immediately after heat shock or after 3 h of recovery (Fig. 3A). Cells were heat shock treated for 1 h at 44 °C and the intensity of cytochrome *c* release was determined after cell fractionation as described in the Materials and methods section. As control of mitochondria integrity after cell fractionation, cytochrome *c* was undetectable in the supernatant fraction of untreated cells. A high level of cytochrome *c* was detected in the supernatant of control cells immediately after the heat treatment whereas the level found in HL5e6 cells was very low. Three hours after heat shock the level of cytochrome *c* detected in the cytosol of control cells was less important than immediately after heat shock suggesting a degradation of this polypeptide. At the same time period in HL5e6 cells, the level of cytosolic cytochrome *c* began to increase although it never reached that observed in control cells immediately after heat stress. These results lead to the conclusion that US11 protein dramatically delayed the cytochrome *c* efflux from mitochondria induced by heat shock.

The canonical mitochondria-dependent apoptotic pathway leads to the caspases cascade initiation resulting from the activation of

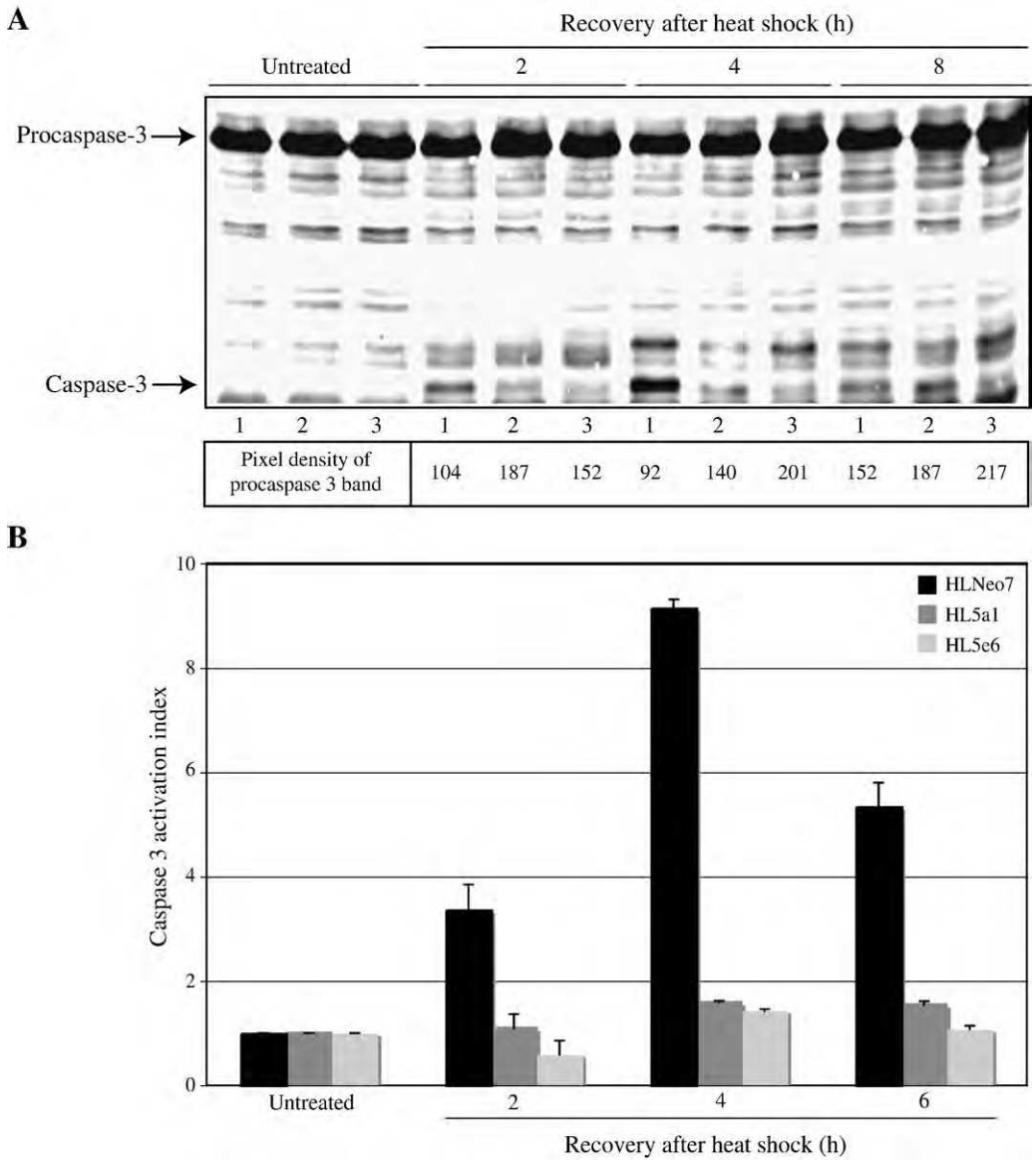

Fig. 2. US11 protein reduces caspase 3 activation after heat shock. (A) Procaspase 3 processing analysis. HLNeo7 control cells (lanes 1) or HL5a1 and HL5e6 US11 expressing cells (lanes 2 and 3 respectively) were heat shock treated for 1 h at 44 °C and allowed to recover for 2 to 8 h before analysis. Cell extracts were analyzed in immunoblots probed with anti-caspase 3 antibody. The procaspase 3 form was quantitated. (B) Caspase 3 activation analysis. Control HLNeo7 and US11 expressing HL5a1 and HL5e6 cells were treated as described above in (A) and allowed to recover for 2 to 6 h. Activity of DEVD-specific caspase was then measured using the fluorescent substrate DEVD-AFC as described in Materials and methods. Activation index was determined as the ratio between activities in extracts of treated cells to that measured in extracts of untreated cells. Columns represent the mean and error bars represent the standard deviation of three experiments. Note the protective activity of US11 protein observed 4 h after heat shock that correlates with the inhibition of procaspase 3 cleavage shown above in (A).

caspase 9 as a consequence of the formation of the apoptosome machinery which consists of procaspase 9, Apaf-1 and translocated cytochrome *c* (Li et al., 1997). Therefore, as we observed a reduced cytochrome *c* efflux from mitochondria in heat shock treated US11 cells, we next analyzed the level of procaspase 9 processing by western blot analysis (Fig. 3B) or by a fluorometric assay (Fig. 3C). This was done using HLNeo7 and US11 expressing cells, HL5e6 and HL5a1, exposed to heat shock. Cells were exposed or not to heat shock for 1 h at 44 °C and analyzed after 2 or 4 h of recovery at 37 °C. As shown in Fig. 3B, in control HLNeo7 cells exposed to heat shock, a slight decrease in the level of procaspase 9 was observed after 4 h of recovery following heat shock suggesting a cleavage. Conversely, no decrease in procaspase 9 level was observed in the US11 expressing HL5a1cells.

As shown in Fig. 3C, in control HLNeo7 cells, heat shock induced a moderate cleavage of the caspase 9 fluorogenic substrate LEHD-AFC in response to heat shock whereas the effect was attenuated in both US11 expressing cells, HL5e6 and HL5a1. It is also intriguing to note that in US11 cells allowed to recover for 6 h after heat shock, the activity of caspase 9 was even lower than the activity observed in untreated cells. These results show that US11 interferes with the weak caspase 9 activation in HeLa cells after heat shock.

US11 protein reduces caspase 8 activation after heat shock

The c-Jun NH_2-terminal kinase (JNK) activation in mammalian cells is an early event in stress induced apoptotic program (Adler et al., 1995). Furthermore JNK activation initiates a FADD-dependent caspase-8 signal transduction pathway leading to programmed cell death (Chen and Lai, 2001). These observations lead us to analyze procaspase 8 processing in HLNeo7 and HL5a1 after 2, 4 or 8 h of

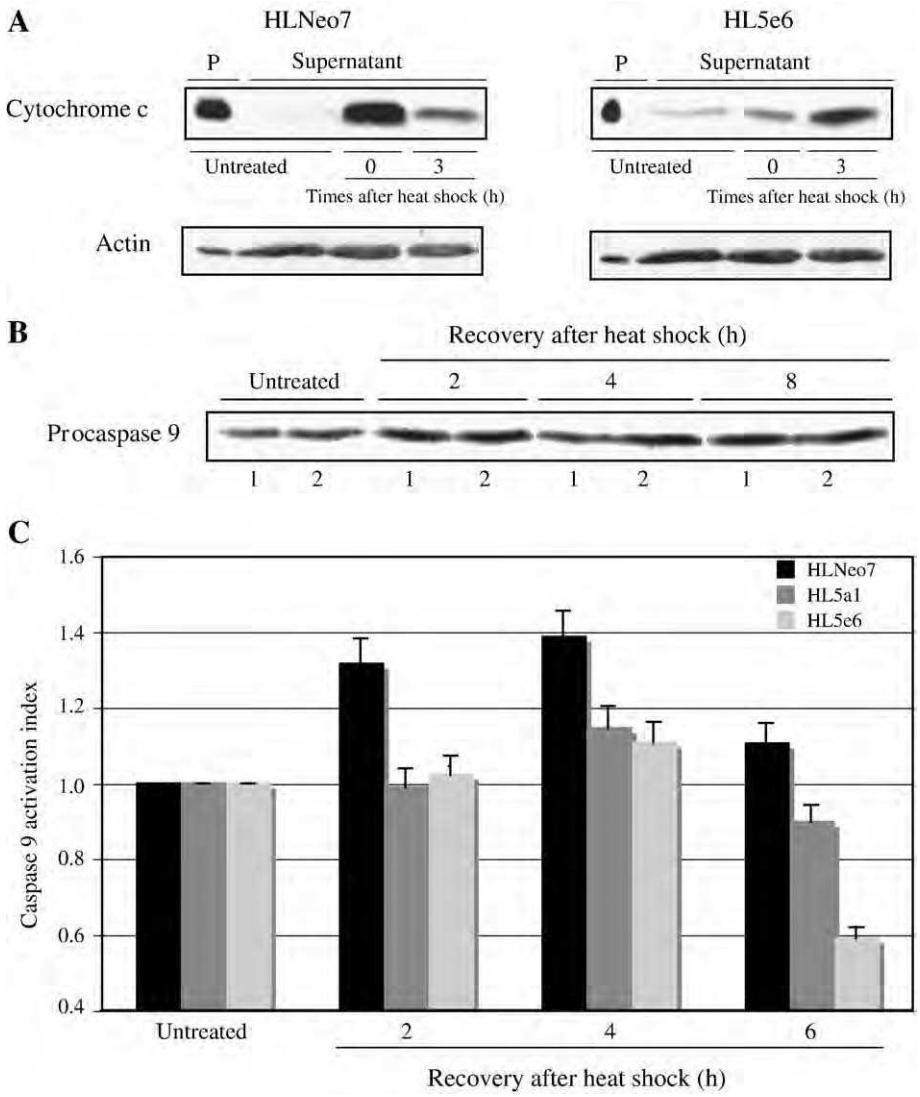

Fig. 3. US11 expression interferes with cytochrome *c* release and with the heat shock induced caspase 9 activation. (A) Cytochrome *c* release analysis. Control HLNeo7 and US11 expressing HL5e6 cells were either kept untreated or heat shock treated for 1 h at 44 °C and allowed or not to recover for 3 h. Cells were then processed and proteins were analyzed in immunoblots as described in Materials and methods. The presence of cytochrome *c* and actin in the different fractions is shown. P: pellet from untreated cells. Supernatant: soluble fraction of untreated cells or heat shock treated cells. Note that US11 protein strongly decreases the release of cytochrome *c* observed in control HLNeo7 cells immediately after heat shock. (B) Procaspase 9 processing analysis. Control HLNeo7 (lanes 1) and US11 expressing HL5a1 cells (lanes 2) were either kept untreated or heat shock treated for 1 h at 44 °C and allowed to recover for 2 to 8 h. Cells extracts were immunobloted with an anti-caspase 9 antibody. (C) Caspase 9 activation analysis. Control HLNeo7 and US11 expressing HL5a1 and HL5e6 cells were treated as described above in (B) and allowed to recover for 2 to 6 h. Caspase 9 activity was measured against fluorometric substrate LEHD-AFC as described in Materials and methods. Activation index was determined as the ratio between the activities in extracts of treated cells to that measured in extracts of non-treated cells. Columns represent the mean and error bars represent the standard deviation of three experiments. Note the protective activity of US11 protein that correlates with the inhibition of procaspase 9 cleavage shown above in (A).

recovery at 37 °C following a 1 h heat shock at 44 °C. As shown in the immunoblot (Fig. 4A), exposure of control HLNeo7 cells to heat shock resulted in a weak but reproducible decrease in the level of the p55 kDa procaspase 8 isoform and a stronger decrease of the p53 kDa isoform as shown by the pixel density analysis. In contrast, in HL5a1 cells the level of these proteins remained unchanged and this even 8 h after the heat shock treatment. Caspase 8 activation was also monitored using a fluorometric assay. US11 expressing, HL5a1 anHL5e6 and control HLNeo7 cells were heat shocked for 1 h at 44 °C and allowed to recover for 2, 4 or 6 h before caspase 8 activation was determined by the IETD-AFC cleavage assay. As shown in Fig. 4B, in control cells, heat shock induced a stimulation of the activity of caspase 8 that reached a maximum 2-fold intensity after 4 h of recovery. In contrast, heat shock did not stimulate caspase 8 activity in both US11 expressing cell lines but rather induced an inhibition of this activity.

US11 protects against apoptosis independently of the presence of the heat shock proteins

Since (i) after heat shock US11 protein enhances protein synthesis recovery and (ii) Hsps are known to protect against apoptosis, we next analyzed whether some of the effects described above could be attributed to an enhanced accumulation of Hsps after heat shock. For this, cells were treated with cycloheximide prior to heat shock treatment in order to inhibit translation during and after heat shock. Control HLNeo7 and US11 expressing HeLa cells were heat shock treated for 1 h at 44 °C in the presence or not of 20 μg/ml of cycloheximide and allowed to recover for 4 h before the immunoblot analysis of procaspase 3 processing was performed. As shown in Fig. 5A, cycloheximide treatment alone did not induce procaspase 3 cleavage in control or US11 expressing cell lines. In contrast, the processing of caspase 3 observed in control HLNeo7 cells exposed to

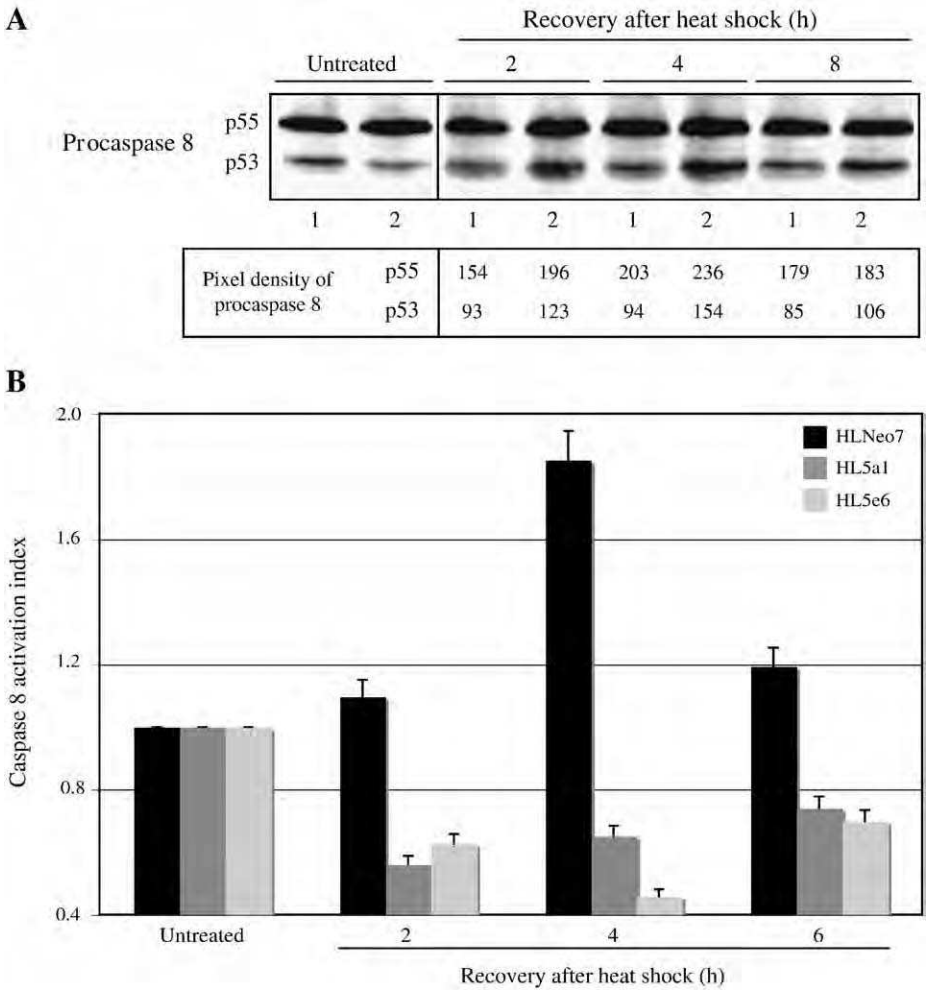

Fig. 4. US11 protein reduces caspase 8 activation after heat shock. (A) Procaspase 8 processing analysis. HLNeo7 control cells (lanes 1) and HL5a1 US11 expressing cells (lanes 2) were heat shock treated for 1 h at 44 °C and allowed recovering for 2 to 8 h before procaspase 8 analysis. Cell extracts were immunobloted with anti-caspase 8 antibody. The p53 and p55 procaspase peptides 8 were quantitated. Note the decreased level of procaspase 8 in control HLNeo7 cells allowed to recover 2 or 4 h after heat shock. (B) Caspase 8 activation analysis. Control HLNeo7 and US11 expressing HL5a1 and HL5e6 cells were treated as described above in (A) and allowed to recover for 2 to 6 h. Activity of caspase 8 was then measured using the fluorescent substrate IETD-AFC as described in Materials and methods. Activation index was determined as the ratio between the activities in extracts of treated cells to that measured in extracts of non-treated cells. Columns represent the mean and error bars represent the standard deviation of three experiments. Note the protective activity of US11 protein that correlates with the inhibition of procaspase 8 cleavage shown above in (A).

heat shock was highly increased in the presence of cycloheximide whereas no processing was observed in US11 expressing cells. Fluorometric analysis of caspase 3 activity was also performed. Results presented in Fig. 5B confirmed that cycloheximide, at the concentration used in this experiment, did not activate caspase 3 in the three cell lines. Interestingly, immediately after heat shock treatment, caspase 3 activity was increased 6.7-fold in control HLNeo7 cells whereas the increase was of only 2.7- and 1.2-fold in the case of HL5a1 and HL5e6 cell lines, respectively. After a 3 h recovery period the increase was up to 8.2-fold in HLNeo7 cells and only 4.4- and 2.7-fold in US11 expressing cells. These results indicate that the interference of US11 with caspase 3 activation process after heat shock was not dependant upon any *de novo* protein synthesis.

US11 also protects against staurosporine induced apoptosis

In order to further analyze the protective function mediated by US11 in HeLa cells, we have analyzed whether this protein could also interfere with the apoptotic process induced by the broad kinase inhibitor staurosporine (Fig. 6). To this aim, HLNeo7 and HL5e6 cells were exposed for 4 h to 0.3 μM of staurosporine. The intensity of the apoptotic process was subsequently estimated by staining the cells with Annexin V/PI (Fig. 6A). Quantitative analysis of the phenomenon revealed that after staurosporine treatment, the percentage of viable HLNeo7 cells (PI and Annexin V negative cells) dropped from 78% to 63% of the total cell population whereas the decrease was far less intense (77% to 72%) in US11 expressing cells. (Fig. 6B) shows a phase-contrast morphological analysis of cells realized after a 3 h treatment with 0.2 μM of staurosporine. HLNeo7 cells presented apoptotic features when compared with US11 expressing cells that had little to no features characteristic of apoptotic cells. Fig. 6C shows the caspases activities determined after staurosporine treatment. Caspases 3 and 8 activities were analyzed after a 4 h of treatment with 0.2 μM staurosporine. A significant 10-fold increase in caspase 3 activation was observed in HLNeo7 cells. In contrast, only a 4.5- and 5.5-fold increase was detected for the HL5a1 and HL5e6 cell lines, respectively. In the case of caspase 8, control HlNeo7 cells showed a 2.5-fold activation level, meanwhile US11 cells did not show any activation after staurosporine treatment. Caspase 9 activation level was determined after a 2.5 h treatment with either a 0.2 or 0.3 μM concentration of staurosporine. In control cells caspase 9 activation was 3.4-fold whereas in HL5a1 and HL5e6 cells it was 2.3 and 1.6 respectively. The

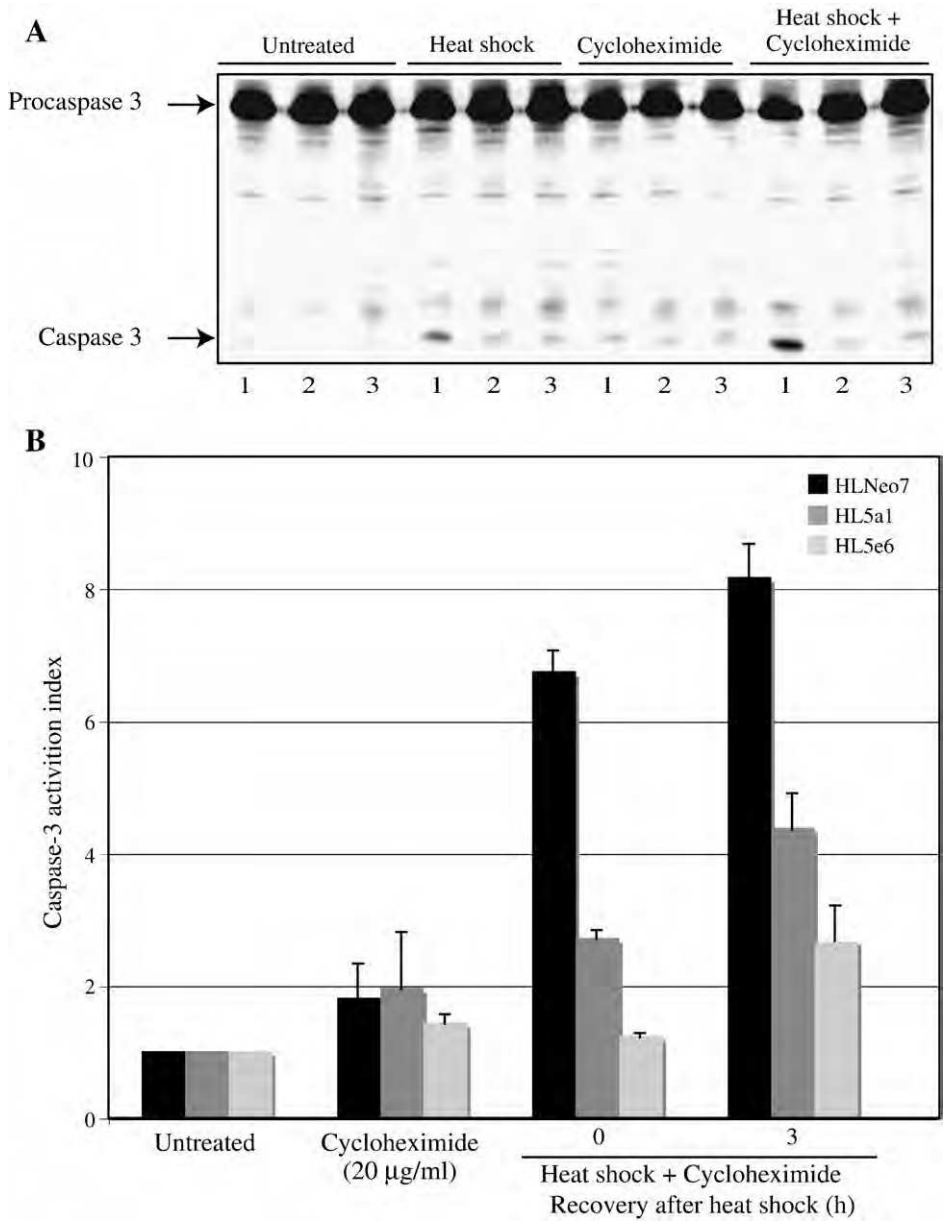

Fig. 5. US11 anti-apoptotic function is independent of Hsp neosynthesis. (A) HLNeo7 control cells (lanes 1) as well as HL5a1 and HL5e6 US11 expressing cells (lanes 2 and 3) were either kept untreated or exposed to a 1 h heat shock at 44 °C followed by a recovery period of 4 h at 37 °C. The experiment was performed in the presence or not of 20 µg/ml of cycloheximide. Cell extracts were immunobloted with anti-caspase 3 antibody. (B) Caspase 3 activation analysis. Control HLNeo7 and US11 expressing HL5a1 and HL5e6 cells were treated with cycloheximide and exposed to heat shock as described above in (A). Activity of DEVD-specific caspases was then measured using the fluorescent substrate DEVD-AFC (see Materials and methods) either immediately after heat shock or after a 3 h recovery period at 37 °C. Activation index was determined as the ratio between activities in extracts of treated cells to that measured in extracts of non-treated cells. Columns represent the mean and error bars represent the standard deviation of three experiments.

differences were obvious after a 0.3 µM treatment as control cells showed a 5.2-fold activation and the Us11 expressing cells a 3.7 and 2.5 activation level. The differences observed were significant as shown by the statistical analysis. These results clearly suggest that the anti-apoptotic activity of US11 is not restricted to heat shock and is also efficient towards staurosporine induced apoptosis.

Discussion

Previously, we have demonstrated that the expression of late viral protein US11 of HSV-1 enhanced protein synthesis recovery after heat shock and induced a cellular protection against this stress (Diaz-Latoud et al., 1997). The aim of this work was to determine if US11 was able to protect against heat shock through an anti-apoptotic activity. Consequently, in order to discriminate between the HSV-1 and heat induced apoptosis, we have analyzed the effects mediated by US11 expression alone and not in the context of viral infection. The results presented here show that in heat shock treated HeLa cells, US11 protein highly reduced the number of apoptotic cells, counteracted the dramatic cytochrome *c* efflux from mitochondria and powerfully inhibited the strong activation of the executioner caspase 3.

These results are of major interest in depicting the exact molecular mechanism underlying the heat induced apoptosis. We show a strong activation of caspase 3 and cytochrome *c* release in HeLa cells after heat shock along with minor caspase 8 and caspase 9 activations. This suggests that, in HeLa cells, the FADD pathway is not directly involved to trigger heat induced apoptosis but is probably activated by downstream executioner caspases amplifying the activity of upstream

caspases, such as caspase 8 (Wieder et al., 2001). Furthermore the weak caspase 9 activity in HeLa cells after heat shock suggests that caspase 9 activation is not induced by the apoptosome formation after cytochrome *c* release from mitochondria and might result from another activation pathway. These results are strengthened by Milleron and Bratton observations in Jurkat T cells showing that caspase 9 is not essential for activation of caspase 3 or the induction of apoptosis after heat shock (Milleron and Bratton, 2006).

Interestingly, in US11 expressing cells exposed to heat shock, caspase 3 activity is strongly inhibited. In the same conditions MOMP

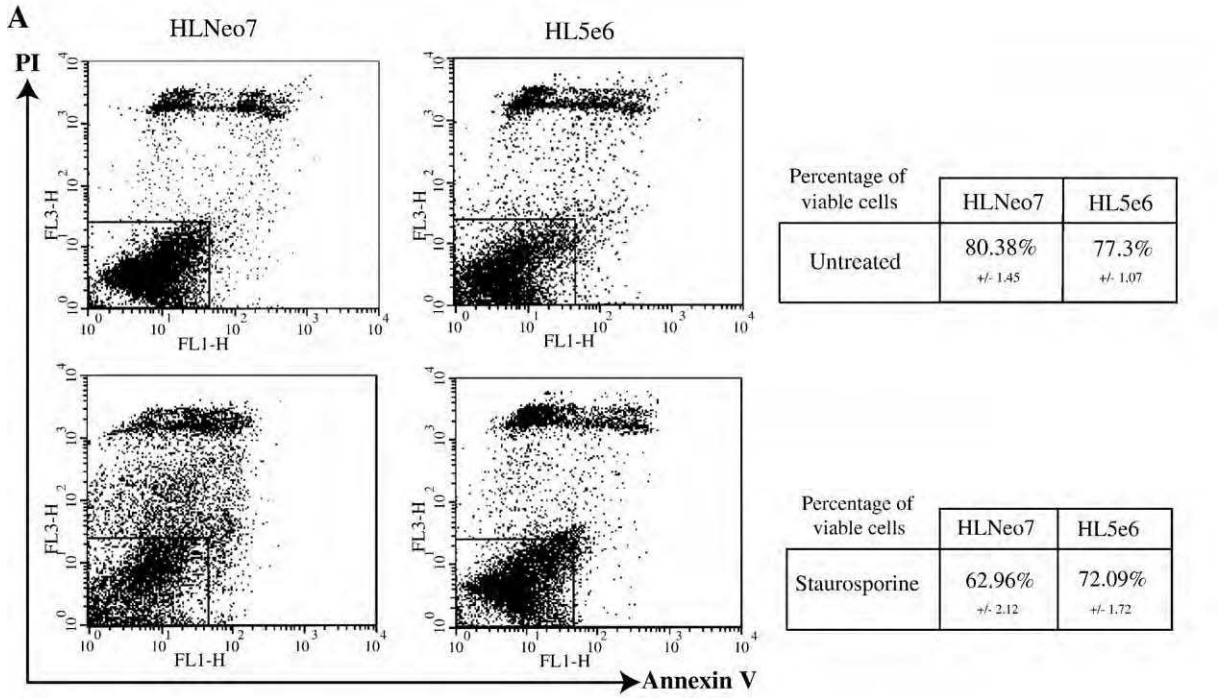

Percentage of viable cells	HLNeo7	HL5e6
Untreated	80.38% +/- 1.45	77.3% +/- 1.07

Percentage of viable cells	HLNeo7	HL5e6
Staurosporine	62.96% +/- 2.12	72.09% +/- 1.72

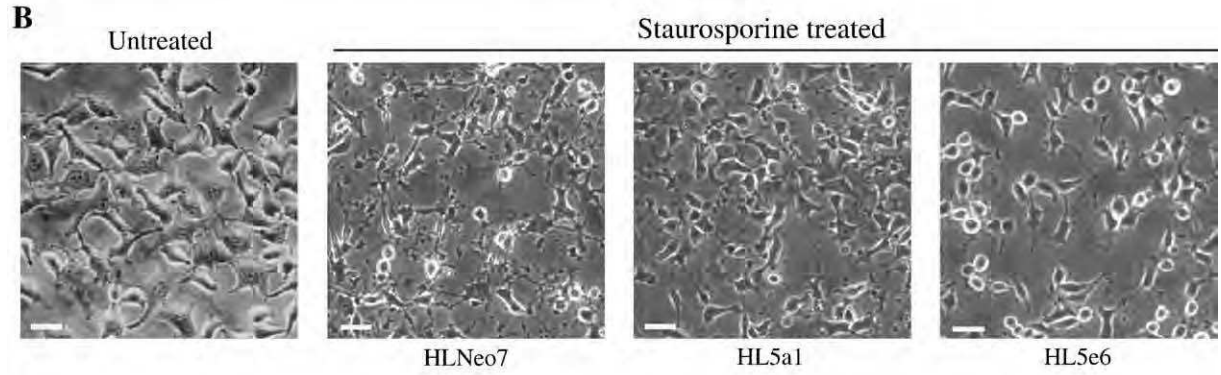

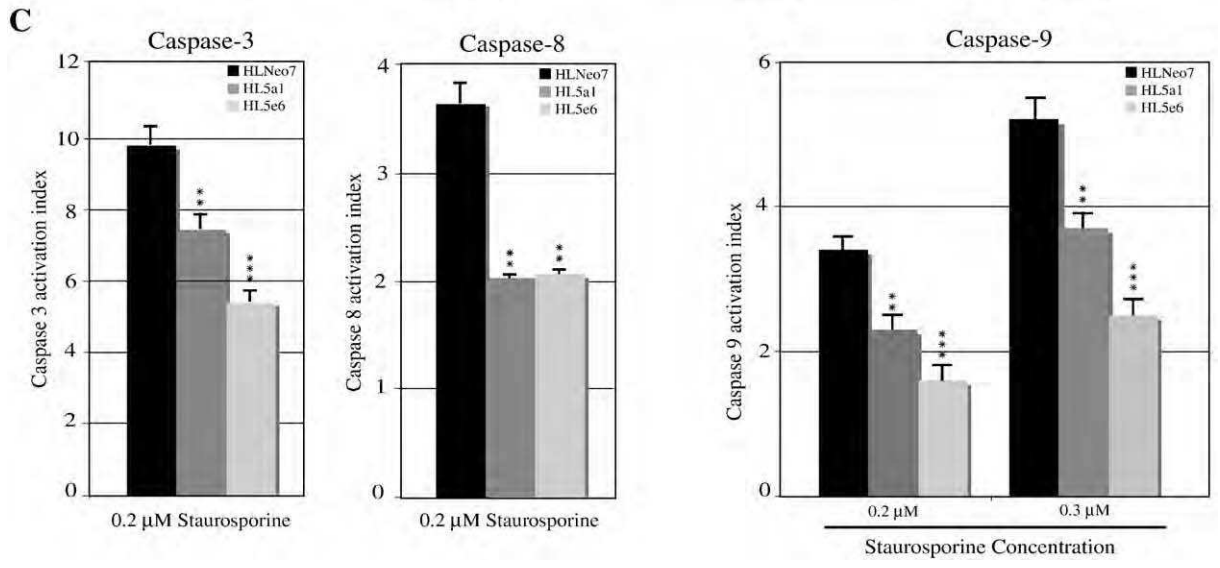

is probably highly reduced in the presence of US11 protein since cytochrome *c* efflux is not observed immediately after heat shock but slightly 3 h later and might result from a secondary response. We therefore concluded that this viral protein could interfere either with the heat shock induced mitochondria damage or with upstream signaling pathways activated by the heat shock treatment.

We have already shown that constitutive expression of US11 protein in HeLa cells does not induce any Hsp accumulation (Diaz-Latoud et al., 1997). As Hsp synthesis is an early cell response after heat shock we then tested whether US11 protective effect after heat shock was still observed in conditions where Hsps synthesis was inhibited during and after heat shock by the use of the protein synthesis inhibitor cycloheximide. This resulted in an increased activation of caspase 3 immediately after heat shock, hence confirming the apoptosis protection mediated by Hsps. Whatever in these conditions, the presence of US11 still induced a strong inhibition of caspase 3 activation, a result which indicates that this viral protein generates an anti-apoptotic property that is active in heat shock treated cells and whose function is independent of the presence of newly made Hsps interfering or up-regulating its activity.

Our results provide direct evidence for a causal relationship between the presence of US11 protein and an important delay and reduction in heat shock induced apoptosis in HeLa cells. This points out a mechanism by which HSV-1 could challenge apoptosis in cell submitted to heat stress. Indeed heat stress is one of the most efficient agent to induce reactivation of the latent virus *in vivo* (Roizman, 1990) and is currently used to reactivate the virus in mice latent model (Sawtell and Thompson, 1992).

In order to better characterize this anti-apoptotic activity of US11 protein, we also tested the activity of the viral protein in HeLa cells exposed to the broad apoptotic agent staurosporine. Our results clearly show that US11 expression also strongly decreased apoptosis of the cells and reduced caspase 3, -8 and -9 activations induced by staurosporine.

Altogether these observations demonstrate that US11 protein protects HeLa cells against apoptotic cell death induced by different means, thereby suggesting for this viral protein a novel undescribed function at the level of the apoptotic machinery. US11 could therefore be considered as an anti-apoptotic protein of HSV-1 like already characterized US3, US5, and ICP6 proteins. It has been shown that the accumulation of true late proteins is not required for apoptosis prevention (Aubert et al., 2001). However US11 is brought into the cell by the viral particle and its behavior differs from that of the protein synthesized at the late stage of viral infection (Tan and Katze, 2000). Interestingly it has been recently shown that HSV-1 blocks apoptosis by targeting Bax and precluding cytochrome *c* efflux from mitochondria (Aubert et al., 2007) one might speculate that US11 protein brought into the cell by the virion could be involved in this mechanism. Our results show that US11 preclude early cytochrome *c* efflux from mitochondria during heat shock and it would be of great interest to analyze whether US11 interacts with the pro-apoptotic Bax protein. It would be also of interest to determine if apoptosis is reduced or delayed in US11 expressing HeLa cells during HSV-1 infection.

Whether or not US11 protein could also protect from apoptosis the HSV-1 infected cells submitted to heat shock is an interesting hypothesis that could be tested by analyzing heat shock induced apoptosis in cells infected by virus containing mutations in US11 gene.

Materials and methods

Cells lines

All cells were grown at 37 °C in a humidified atmosphere containing 5% CO_2. HeLa cells were grown in Dulbecco's modified Eagle's medium (DMEM) supplemented with 10% heat inactivated fetal calf serum. Construction and selection of the two clones expressing US11 (HL5a1 and HL5e6) and control cell line (HLNeo7) have already been described (Simonin et al., 1995). For transient expression, exponentially growing HeLa cells were seeded at a density of 1.5×10^6 cells/78 cm^2 one night before transfection with 6.5 µg of pG9 vector according to the Lipofectamine™ reagent procedure (Invitrogen, Cergy Pontoise, France). In the pG9 construct US11 coding sequence is under the control of the cytomegalovirus promoter. The DNA was left on cells for 3 h; cells were then washed once with PBS buffer and further incubated in fresh medium. Twenty-four hours after transfection, cells were submitted to heat shock.

Heat shock was performed by immersing culture dishes into a water bath regulated at 44 °C±0.05 °C.

Reagents

Nonidet P-40, Triton X-100, desoxycholic acid, dithioerythritol, staurosporine, and G418 were from Sigma (St-Louis, MO). Cell culture media and complements were from Invitrogen (Cergy Pontoise, France). The specificity of anti US11-antibody has already been described (Diaz et al., 1993). Anti-caspase 9 antibody was from Stressgen (Victoria, BC, Canada). Anti-cytochrome *c* antibody clone 7H8.2C12, anti-caspase 3 and anti-caspase 8 antibodies were from Pharmingen (San Diego, CA). The primary antibodies were detected with either anti-rabbit or anti-goat immunoglobulins conjugated to horseradish peroxidase, Amersham Corp. (UK). Protease inhibitors, complete cocktail, were from Roche Diagnostics, (Meylan, France).

Measurement of apoptosis

Apoptosis was assessed by determination of the binding of FITC-conjugated Annexin V protein to the phosphatidylserine residues present on the outer leaflet of apoptotic cell membranes as already described (Gonin et al., 1999). Annexin V and propidium iodide (PI) staining were used to differentiate necrotic from apoptotic cells. Samples were analyzed by flow cytometry using a FACS Scan analyzer (Becton Dickinson, Le Pont de Claix, France). Annexin V–FITC and PI related fluorescence was recorded using FL1-H and FL-3H filters respectively.

Measurement of caspase activity

The caspase activity assays were performed with specific fluorometric substrates according to the protocols supplied by the manufacturers. Briefly, after treatment 10^6 cells (caspase 3 and caspase 8 assays) or 2×10^6 (caspase 9 assay) were harvested and subsequently

Fig. 6. US11 protein also reduces apoptosis induced by staurosporine. (A) HLNeo7 control cells or HL5e6 US11 expressing cells were treated for 4 h with 0.3 µM of staurosporine. After treatment, cells were stained with Annexin V and propidium iodide and analyzed as described in Materials and methods. Data are representative of one out of three experiments with comparable results. Lower left square Annexin V and PI negative cells quantification: values represent mean±S.D of three independent experiments. Student's *t* test analysis demonstrated significance $P=0.0005$ of the differences between staurosporine treated HLNeo7 and HL5e6 cell lines. (B) Phase-contrast morphological analysis of cells after staurosporine treatment. HLNeo7 control untreated cells or HLNeo7, HL5a1 and HL5e6 US11 expressing cells treated for 3 h with 0.3 µM of staurosporine. Scale bar=10 µM. (C) HLNeo7 control cells or HL5a1 and HL5e6 US11 expressing cells were treated with staurosporine. Caspase activation was determined as the ratio between the activities in extracts of treated cells to that measured in extracts of non-treated cells. Caspase 3 and caspase 8 activities were analyzed after 4 h of treatment with 0.2 or µM of staurosporine using the fluorescent substrate DEVD-AFC or the fluorescent substrate IETD-AFC respectively. Caspase 9 activity was measured against fluorometric substrate LEHD-AFC, as described in Materials and methods, after 2.5 h of treatment with either 0.2 or 0.3 µM of staurosporine. Columns represent the mean and error bars represent the standard deviation of three experiments. Student's *t* test analysis demonstrated significance ($^{**}P<0.005$ and $^{***}P<0.0001$) of the differences between HLNeo7 and HL5a1 or HLNeo7 and HL5e6 cell lines.

washed twice in ice-cold phosphate-buffered saline (PBS), pH 7.4. Thereafter, cells were spun at 200 ×*g* for 5 min and the dry cell pellets were stored at −80 °C. Caspase 3 and caspase 8 activities were determined by detection of the proteolytic cleavage of DEVD-AFC or IETD-AFC respectively using the ApoAlert fluorescent assay kits (Clontech, Montigny les Bretonneux, France). Determination of caspase 9 activity was performed using the caspase 9 Fluorometric Assay (R&D, Abingdon, UK) which is based on the caspase 9 fluorogenic substrate LEHD-AFC. Quantitation of fluorescence was determined in a Victor Wallach cytofluorometer (EG&G Instruments, Evry, France), excitation was at 400 nm and emission at 505 nm.

Gel electrophoresis and immunoblotting

After heat shock treatment, cells were either immediately scraped or allowed to recover for different time periods at 37 °C before being harvested. Cells were rinsed twice in ice-cold PBS and scraped off the dish. At this point, aliquots were withdrawn for determination of protein concentration. Thereafter, cells were lysed in boiling SDS buffer (62.5 mM Tris–HCl, pH 6.8; 1% SDS; 0.1 M dithioerythritol; 10% glycerol and 0.001% bromophenol blue). Cell lysates were subjected to SDS-PAGE (Laemmli, 1970) and immunoblots were performed as previously described (Diaz-Latoud et al., 2005). The detection of immunoblots was performed with the ECLTM system (Amersham Life Science). Autoradiographs were recorded onto X-Omat LS films (Eastman Kodak Co, Rochester, NY).

Cytochrome c release from mitochondria

The method described by Bossy-Wetzel et al. (1998) was used with some modifications. In brief, about 2×10^6 cells were harvested and subsequently washed twice in ice-cold PBS, pH 7.4. Cells were spun at 200 ×*g* for 5 min and then resuspended in 600 µl of extraction buffer containing protease inhibitors. Cells were incubated for 30 min on ice, then homogenized with a glass dounce and a B pestle (80 strokes). Lysates were spun for 15 min at 14, 000 ×*g*. Thereafter, pellets were directly dissolved in SDS sample buffer while supernatants were diluted 1:1 in 2× sample buffer and boiled for 5 min. Protein analysis was performed in 16.5% SDS-polyacrylamide gels. Gels were then processed for immunoblotting as described before.

Acknowledgments

We wish to thank Dominique Guillet for excellent technical assistance, Maryline Moulin for helpful discussions. This work was supported by grant #4602 from the Association pour la Recherche sur le Cancer and by the Région Rhône-Alpes. Benjamin Gibert is supported by a doctoral fellowship of the Région Rhône-Alpes (Cible 06).

References

Adams, J., Cory, S., 1998. The Bcl-2 protein family: arbiters of cell survival. Science 281 (5381), 1322–1326.
Adler, V., Schaffer, A., Kim, J., Dolan, L., Ronai, Z., 1995. UV irradiation and heat shock mediate JNK activation via alternate pathways. J. Biol. Chem. 270, 26071–26077.
Attrill, H., Cumming, S., Clements, J., Graham, S., 2002. The herpes simplex virus type 1 US11 protein binds the coterminal UL12, UL13, and UL14 RNAs and regulates UL13 expression in vivo. J. Virol. 76 (16), 8090–8100.
Aubert, M., Rice, S., Blaho, J., 2001. Accumulation of herpes simplex virus type 1 early and leaky-late proteins correlates with apoptosis prevention in infected human HEp-2 cells. J. Virol. 75 (2), 1013–1030.
Aubert, M., Pomeranz, L.E., Blaho, J.A., 2007. Herpes simplex virus blocks apoptosis by precluding mitochondrial cytochrome *c* release independent of caspase activation in infected human epithelial cells. Apoptosis 12 (1), 19–35.
Baetu, T.M., Hiscott, J., 2002. On the TRAIL to apoptosis. Cytokine Growth Factor Rev. 13 (3), 199–207.
Balachandran, S., Roberts, P., Kipperman, T., Bhalla, K., Compans, R., Archer, D., Barber, G., 2000. Alpha/beta interferons potentiate virus-induced apoptosis through activation of the FADD/Caspase-8 death signaling pathway. J. Virol. 74 (3), 1513–1523.
Beere, H., Wolf, B., Cain, K., Mosser, D., Mahboubi, A., Kuwana, T., Tailor, P., Morimoto, R., Cohen, G., Green, D., 2000. Heat-shock protein 70 inhibits apoptosis by preventing recruitment of procaspase-9 to the Apaf-1 apoptosome. Nat. Cell Biol. 2 (8), 469–475.
Benetti, L., Roizman, B., 2007. In transduced cells, the US3 protein kinase of herpes simplex virus 1 precludes activation and induction of apoptosis by transfected procaspase 3. J. Virol. 81 (19), 10242–10248.
Bossy-Wetzel, E., Newmeyer, D., Green, D., 1998. Mitochondrial cytochrome *c* release in apoptosis occurs upstream of DEVD-specific caspase activation and independently of mitochondrial transmembrane depolarization. EMBO J. 17 (1), 37–49.
Bruey, J., Ducasse, C., Bonniaud, P., Ravagnan, L., Susin, S., Diaz-Latoud, C., Gurbuxani, S., Arrigo, A., Kroemer, G., Solary, E., Garrido, C., 2000. Hsp27 negatively regulates cell death by interacting with cytochrome *c*. Nat. Cell Biol. 2 (9), 645–652.
Bryant, K.F., Cox, J.C., Wang, H., Hogle, J.M., Ellington, A.D., Coen, D.M., 2005. Binding of herpes simplex virus-1 US11 to specific RNA sequences. Nucleic Acids Res. 33 (19), 6090–6100.
Cassady, K., Gross, M., 2002. The herpes simplex virus type 1 U(S)11 protein interacts with protein kinase R in infected cells and requires a 30-amino-acid sequence adjacent to a kinase substrate domain. J. Virol. 76 (5), 2029–2035.
Chen, Y., Lai, M.Z., 2001. c-Jun NH2-terminal kinase activation leads to a FADD-dependent but Fas ligand-independent cell death in Jurkat T cells. J. Biol. Chem. 276 (11), 8350–8357.
Diaz, J.J., Simonin, D., Masse, T., Deviller, P., Kindbeiter, K., Denoroy, L., Madjar, J., 1993. The herpes simplex virus type 1 US11 gene product is a phosphorylated protein found to be non-specifically associated with both ribosomal subunits. J. Gen. Virol. 74 (3), 397–406.
Diaz, J.J., Dodon, M.D., Schaerer-Uthurralt, N., Simonin, D., Kindbeiter, K., Gazzolo, L., Madjar, J.J., 1996. Post-transcriptional transactivation of human retroviral envelope glycoprotein expression by herpes simplex virus Us11 protein. Nature 379 (6562), 273–277.
Diaz-Latoud, C., Diaz, J.J., Fabre-Jonca, N., Kindbeiter, K., Madjar, J.J., Arrigo, A.P., 1997. Herpes simplex virus Us11 protein enhances recovery of protein synthesis and survival in heat shock treated HeLa cells. Cell Stress Chaperones 2 (2), 119–131.
Diaz-Latoud, C., Buache, E., Javouhey, E., Arrigo, A.P., 2005. Substitution of the unique cysteine residue of murine Hsp25 interferes with the protective activity of this stress protein through inhibition of dimer formation. Antioxid. Redox Signal. 7 (3–4), 436–445.
Diefenbach, R., Miranda-Saksena, M., Diefenbach, E., Holland, D., Boadle, R., Armati, P., Cunningham, A., 2002. Herpes simplex virus tegument protein US11 interacts with conventional kinesin heavy chain. J. Virol. 76 (7), 3282–3291.
Earnshaw, W., Martins, L., Kaufmann, S., 1999. Mammalian caspases: structure, activation, substrates, and functions during apoptosis. Annu. Rev. Biochem. 68, 383–424.
Georgopoulos, C., Welch, W., 1993. Role of the major heat shock proteins as molecular chaperones. Annu. Rev. Cell Biol. 9, 601–634.
Giraud, S., Diaz-Latoud, C., Hacot, S., Textoris, J., Bourette, R.P., Diaz, J.J., 2004. US11 of herpes simplex virus type 1 interacts with HIPK2 and antagonizes HIPK2-induced cell growth arrest. J. Virol. 78 (6), 2984–2993.
Gonin, S., Diaz-Latoud, C., Richard, M., Ursini, M., Imbo, A., Manero, F., Arrigo, A., 1999. p53/T-antigen complex disruption in T-antigen transformed NIH3T3 fibroblasts exposed to oxidative stress: correlation with the appearance of a Fas/APO-1/CD95 dependent, caspase independent, necrotic pathway. Oncogene 18 (56), 8011–8023.
Green, D.R., 1998. Apoptotic pathways: the road to ruin. Cell 94 (6), 695–698.
Harmon, B., Corder, A., Collins, R., Gobe, G., Allen, J., Allan, D., Kerr, J., 1990. Cell death induced in a murine mastocytoma by 42–47 degrees C heating in vitro: evidence that the form of death changes from apoptosis to necrosis above a critical heat load. Int. J. Radiat. Biol. 58 (5), 845–858.
Hendrick, J., Hartl, F., 1993. Molecular chaperone functions of heat-shock proteins. Annu. Rev. Biochem. 62, 349–384.
Ito, M., Onuki, R., Bando, Y., Tohyama, M., Sugiyama, Y., 2007. Phosphorylated PKR contributes the induction of GRP94 under ER stress. Biochem. Biophys. Res. Commun. 360 (3), 615–620.
Jerome, K.R., Fox, R., Chen, Z., Sears, A.E., Lee, H., Corey, L., 1999. Herpes simplex virus inhibits apoptosis through the action of two genes, Us5 and Us3. J. Virol. 73 (11), 8950–8957.
Khoo, D., Perez, C., Mohr, I., 2002. Characterization of RNA determinants recognized by the arginine- and proline-rich region of Us11, a herpes simplex virus type 1-encoded double-stranded RNA binding protein that prevents PKR activation. J. Virol. 76 (23), 11971–11981.
Krammer, P., 2000. CD95's deadly mission in the immune system. Nature 407 (6805), 789–795.
Laemmli, U., 1970. Cleavage of structural proteins during the assembly of the head of bacteriophage T4. Nature 227 (259), 680–685.
Langelier, Y., Bergeron, S., Chabaud, S., Lippens, J., Guilbault, C., Sasseville, A.M., Denis, S., Mosser, D.D., Massie, B., 2002. The R1 subunit of herpes simplex virus ribonucleotide reductase protects cells against apoptosis at, or upstream of, caspase-8 activation. J. Gen. Virol. 83 (Pt 11), 2779–2789.
Lavrik, I.N., Golks, A., Krammer, P.H., 2005. Caspases: pharmacological manipulation of cell death. J. Clin. Invest. 115 (10), 2665–2672.
Li, P., Nijhawan, D., Budihardjo, I., Srinivasula, S., Ahmad, M., Alnemri, E., Wang, X., 1997. Cytochrome *c* and dATP-dependent formation of Apaf-1/caspase-9 complex initiates an apoptotic protease cascade. Cell 91 (4), 479–489.
Mehlen, P., Schulze-Osthoff, K., Arrigo, A.P., 1996. Small stress proteins as novel regulators of apoptosis. Heat shock protein 27 blocks Fas/APO-1- and staurosporine-induced cell death. J. Biol. Chem. 271 (28), 16510–16514.
Milleron, R.S., Bratton, S.B., 2006. Heat shock induces apoptosis independently of any known initiator caspase-activating complex. J. Biol. Chem. 281 (25), 16991–17000.

Munger, J., Chee, A.V., Roizman, B., 2001. The U(S)3 protein kinase blocks apoptosis induced by the d120 mutant of herpes simplex virus 1 at a premitochondrial stage. J. Virol. 75 (12), 5491–5497.
Murata, T., Goshima, F., Yamauchi, Y., Koshizuka, T., Takakuwa, H., Nishiyama, Y., 2002. Herpes simplex virus type 2 US3 blocks apoptosis induced by sorbitol treatment. Microbes Infect. 4 (7), 707–712.
Nagata, S., 1997. Apoptosis by death factor. PG — 355-65. Cell 88 (3), 355–365.
Nguyen, M.L., Blaho, J.A., 2007. Apoptosis during herpes simplex virus infection. Adv. Virus Res. 69, 67–97.
Nishiyama, Y., Murata, T., 2002. Anti-apoptotic protein kinase of herpes simplex virus. Trends Microbiol. 10 (3), 105–107.
Ogg, P.D., McDonell, P.J., Ryckman, B.J., Knudson, C.M., Roller, R.J., 2004. The HSV-1 Us3 protein kinase is sufficient to block apoptosis induced by overexpression of a variety of Bcl-2 family members. Virology 319 (2), 212–224.
Park, H.S., Lee, J.S., Huh, S.H., Seo, J.S., Choi, E.J., 2001. Hsp72 functions as a natural inhibitory protein of c-Jun N-terminal kinase. EMBO J. 20 (3), 446–456.
Perng, G.C., Jones, C., Ciacci-Zanella, J., Stone, M., Henderson, G., Yukht, A., Slanina, S.M., Hofman, F.M., Ghiasi, H., Nesburn, A.B., Wechsler, S.L., 2000. Virus-induced neuronal apoptosis blocked by the herpes simplex virus latency-associated transcript. Science 287 (5457), 1500–1503.
Peters, G., Khoo, D., Mohr, I., Sen, G., 2002. Inhibition of PACT-mediated activation of PKR by the herpes simplex virus type 1 Us11 protein. J. Virol. 76 (21), 11054–11064.
Roizman, B.a.A.E.S., 1990. Herpes simplex viruses and their replication, In: Fields, B.N., et al. (Eds.), Virology, 2nd. Raven Press, New York, pp. 1795–1841.
Samali, A., Robertson, J.D., Peterson, E., Manero, F., van Zeijl, L., Paul, C., Cotgreave, I.A., Arrigo, A.P., Orrenius, S., 2001. Hsp27 protects mitochondria of thermotolerant cells against apoptotic stimuli. Cell Stress Chaperones 6 (1), 49–58.
Sanchez, R., Mohr, I., 2007. Inhibition of cellular 2′–5′ oligoadenylate synthetase by the herpes simplex virus type 1 Us11 protein. J. Virol. 81 (7), 3455–3464.
Sawtell, N.M., Thompson, R.L., 1992. Rapid in vivo reactivation of herpes simplex virus in latently infected murine ganglionic neurons after transient hyperthermia. J. Virol. 66 (4), 2150–2156.
Schroder, M., Kaufman, R.J., 2005. The mammalian unfolded protein response. Annu. Rev. Biochem. 74, 739–789.
Simonin, D., Diaz, J., Kindbeiter, K., Pernas, P., Madjar, J., 1995. Phosphorylation of herpes simplex virus type 1 Us11 protein is independent of viral genome expression. Electrophoresis 16 (7), 1317–1322.
Slee, E., Adrain, C., Martin, S., 1999. Serial killers: ordering caspase activation events in apoptosis. Cell Death Differ. 6 (11), 1067–1074.
Tan, S.L., Katze, M.G., 2000. HSV.com: maneuvering the internetworks of viral neuropathogenesis and evasion of the host defense. Proc. Natl. Acad. Sci. U. S. A. 97 (11), 5684–5686.
Tibbles, L.A., Woodgett, J.R., 1999. The stress-activated protein kinase pathways. Cell. Mol. Life Sci. 55 (10), 1230–1254.
Wieder, T., Essmann, F., Prokop, A., Schmelz, K., Schulze-Osthoff, K., Beyaert, R., Dorken, B., Daniel, P., 2001. Activation of caspase-8 in drug-induced apoptosis of B-lymphoid cells is independent of CD95/Fas receptor–ligand interaction and occurs downstream of caspase-3. Blood 97 (5), 1378–1387.
Zhao, Q.L., Fujiwara, Y., Kondo, T., 2006. Mechanism of cell death induction by nitroxide and hyperthermia. Free Radic. Biol. Med. 40 (7), 1131–1143.

PUBLICATION - 7

PUBLICATION 7 - Nuclear protein and Cajal body-associated coilin modulates the mitochondrial apoptotic pathway after UV-C irradiation.

Soumis à J. Mol Biol.

La coiline est une protéine nucléaire localisée principalement dans les corps de Cajal. Elle subit une dérégulation de sa localisation au cours des différents stress comme les UV, les irradiations ou les infections virales. Il a été montré que la modulation d'expression de la coiline conduisait à des perturbations de la transcription (Morency *et al.*, 2007). Cependant la coiline n'est pas exclusivement localisée dans les corps de Cajal. En effet, la coiline est massivement retrouvée sur les centrosomes lors de stress, en compagnie d'autres protéines des corps de Cajal que sont la fibrilarine et SMN (Survival Motor Neuron). Ces trois protéines participeraient à un mécanisme de protection contre les aggressions que peuvent subir les centromères interphasiques (Morency *et al.*, 2007).

Au cours de cette étude, nous avons pu montrer que la coiline était une protéine importante lors de la réponse aux dommages de l'ADN liée aux UV-C. Ainsi, la déplétion de la coiline par siARN conduit à augmenter la survie de cellules ou la protéine suppresseur de tumeur p53 est mutée ou inactivée. Ces mêmes observations ont été réalisées dans des cellules HCT116 p53-/- ou p53 a été inactivée par recombinaison homologue (Bunz *et al.*, 1998). Cette augmentation de la survie est corrélée à une activation beaucoup plus faible des caspases exécutrices 3 et 7. De plus l'apoptose mitochondriale semble massivement inhibée en absence de coiline. Ainsi, la sortie du cytochrome *c* tout comme la formation des oligomères du BH3 pro-apototique Bax, semble largement inhibée dans des cellules privées de coiline. De plus, la modulation négative du taux de coiline semble spécifique d'une apoptose mitochondriale, puisque des stimulations par le liguant de mort TRAIL ne conduisent pas à une modulation de l'apoptose.

L'ensemble de ces résultats donne à penser que la coiline serait une protéine impliquée dans la détection des dommages à l'ADN et la transduction du signal pro-apoptotique ayant pour origine le noyau.

NUCLEAR PROTEIN AND CAJAL BODY-ASSOCIATED COILIN MODULATES THE MITOCHONDRIAL APOPTOTIC PATHWAY AFTER UV-C IRRADIATION

Pascale TEXIER[1], Mirna SABRA[1], Benjamin GIBERT[2], Nelly VEY[1], Jhony El MAALOUF[1]and Patrick LOMONTE[1*]

[1] *Viral Silencing and Centromeric Instability group,* [2] *Stress, Chaperones and Cell Death* group. Université de Lyon, Lyon, F-69003, France; CNRS-UMR5534, Centre de Génétique Moléculaire et Cellulaire, Villeurbanne, F-69622, France.

Running head: Coilin modulates induced mitochondrial apoptosis

Address correspondence to : Patrick Lomonte. Center for Molecular and Cellular Genetics, University of Lyon, CNRS-UMR5534, F-69622 Villeurbanne Cedex, France. Fax: ++33.472-432-685. E-mail: lomonte@cgmc.univ-lyon1.fr

Coilin, a major component of Cajal body nuclear domains, is a highly dynamic protein whose nuclear distribution changes dramatically following various stressful stimuli such as irradiation, drugs, and even viral infection. Since coilin was recently implicated in a cell response triggered by the uncontrolled disruption of interphase centromere chromatin, we assumed that any abrupt stress on chromatin, such as that induced by UV-C, might implicate coilin in a signalling pathway. Coilin was depleted with siRNAs in various cell lines before they were stressed with UV-C. The absence of coilin reduced susceptibility to apoptosis in a dose- and cell type-dependent manner and inhibited effector caspase activation and PARP-1 inactivation. The mitochondrial-controlled apoptotic pathway was suppressed in coilin-depleted HeLa cells correlated with a defect in mitochondrial cytochrome *c* release and the absence of Bax oligomere formation. This is the first report on the biological role of coilin as a modulator of the apoptotic intrinsic pathway following a stress affecting chromatin structure.

Since its discovery in the early 1990s (1), coilin has been described as a major structural component of the nuclear domains known as Cajal bodies (CBs), but its actual biological activity remains a mystery (2). Coilin is a conserved protein across species, and orthologs have been described in the mouse (3), *Arabidopsis thaliana* (4), *Xenopus laevi* (5), and recently, *Drosophila melanogaster* (6). Despite this evolutionary conservation suggesting an important role in cell physiology, coilin is not essential for development of mice (7), plants (4), or *Drosophila* (6). However, depending on their genetic background, coilin knockout mice can have significant viability, fertility and fecundity defects (7,8), which suggests that if coilin is not essential on a short timescale, it might be important over the entire life of an organism.

Coilin is a dynamic protein within CBs (9-11) that responds acutely to different cellular stresses mainly, but not solely, perturbing transcription (12-14). Therefore, coilin may have some hidden biological activities that might be important only in the context of acute, non-programmed, cellular changes that profoundly disturb cell homeostasis. Several studies and independent observations note that CB-associated coilin probably represents a small fraction (about 30%) of the total protein, leaving questions about putative non-CB-associated activities (15). We recently described the centromeric accumulation of coilin and two of its CB-associated partners, fibrillarin and the survival motor neuron (SMN) protein, following disruption of the chromatin structure of the interphase centromeres by a viral protein (14). Similarly, the depletion of the centromeric chromatin organizer CENP-B, and to a lesser extent the histone H3 centromeric variant CENP-A, also provokes the redistribution of coilin to centromeres. This change in the coilin pattern anticipates a role of non-CB-associated coilin in a process triggered by aberrant changes in the chromatin structure, even if this chromatin is centromeric.

UV-C (254 nm) irradiation at doses between 10 and 30 J/m^2 induces the rapid fragmentation of CBs, which is visualized by the distribution of coilin in microfoci throughout the nucleoplasm (13 ,16) and our

unpublished data). Contrary to a widespread idea, UV-C is poor at inducing oxygen species or generating DNA double-stranded breaks (DSBs), and direct UV-C DNA breakage has never been detected in mammalian cells (17). The vast majority of the damage induced by UV-C irradiation are helix-distorting DNA lesions, including cyclobutane pyrimidine dimers (CPDs) and pyrimidine (6-4) pyrimidone adducts (6,4-PP) (18). These lesions are known to profoundly modify chromatin structure and are repaired following an "access–repair–restore" (ARR) model, implicating the nucleotide excision repair (NER) mechanism (19,20). In the ARR model, disruption of the chromatin is required before the repair and restoration of the initial structure. However, this process is more or less efficient depending on the number of lesions. Indeed, at doses between 10 and 20 J/m^2, only about 0.1% of the induced photoproducts are estimated to be repaired at any one time (17). Therefore, if not processed in time, any step of the repair mechanism can activate a signalling pathway leading to apoptosis.

Apoptosis is an extremely complex process involving multiple signalling pathways, some of them probably as yet undiscovered. The two main pathways are driven by plasma membrane receptors (the extrinsic or receptor pathway) and by the mitochondria (the intrinsic or mitochondrial pathway) (21). The purpose of either pathway is to activate Cys-dependent Asp-specific proteases, called caspases, in a two-step process, some which are initiators, such as caspases 9 and 8, and others being executioners (effectors) such as caspases 3 and 7. All caspases are present in the cell in a latent form (a zymogen), and the process activates the latent caspases in a sequential cascade that usually ends in the activation of effector caspases and death of the cell. The intrinsic pathway is under the control of the BCL-2 family of proteins, some of them having anti- and others pro-apoptotic activities. Their activities are intimately linked to one another in a network of signalling cross talk to either prevent or promote the oligomerization of two mitochondrial proteins, Bax and Bak, depending on the anti- or pro-apoptotic signal, respectively (22). This oligomerization is the process that triggers the release of another mitochondrial protein, cytochrome *c*, in the cytosol, leading to the activation of caspase-9 and subsequently of effector caspases.

We thus decided to test if coilin could contribute to such a signalling pathway following UV-C irradiation. We found that the lack of coilin prevented the mitochondrial pathway of apoptosis in transient knockdown cells irradiated with UV-C. As a result, those cells showed a deficit in cytochrome *c* release from the mitochondria that matched the lack of pro-apoptotic protein Bax oligomerization in cells depleted of coilin. This effect was not cell-dependent, although the threshold of coilin contribution in the apoptotic pathway triggered by UV-C varies depending on cell type.

Experimental Procedures

Cell lines, UV-C irradiation, Immunofluorescence, and Western blotting- HeLa and U2OS, HCT116, Saos-2 cell lines were cultivated in BHK-21, DMEM, and McCoy's 5A medium, respectively, which were supplemented with 10% fetal bovine serum, L-glutamine (1% v/v), 10 U/mL penicillin, and 100 μg/mL streptomycin. Cells were irradiated with UV-C (254nm) using a BIO-LINK® (BLX) Crosslinker. Immunofluorescence was performed as described previously (14). All the samples were examined under a meta-confocal microscope (LSM 510; Carl Zeiss, Wetzlar, Germany) at a resolution of 512 × 512 pixels using optical slices of 0.8–1.0 μm thickness. The microscope used was a Zeiss Axiovert 200M at either 63× (NA 1.25) or 100× (NA 1.3) magnification under oil-immersion objectives. Data sets were processed with LSM 510 software and then exported in preparation for printing using Photoshop (Adobe Systems, San Jose, CA). For Western blotting (WB), 15-μg aliquots of total protein (5 μg for PARP-1 detection) were loaded per well in a SDS-polyacrylamide gel before electrophoresis, transfer, and detection.

siRNA transfections- Cells were seeded at very low confluency before siRNAs transfections. Two rounds of siRNAs transfections (Effectene Transfection Reagent; Qiagen, Hilden, Germany) were performed at 48-h intervals with the amount of siRNAs adjusted

to the number of cells following the manufacturer's protocol. Cells were then treated depending on the subsequent experiment to be performed. The siRNA sequences used were control siRNA 5'-UACAGCUCUCUCUCGACCC-3'; coilin siRNA-1 5'-CGACUGCCUCAGAGUUAAA-3'; coilin siRNA-2 5'-CCAACUGAGUUAUCAAAGG-3'; coilin siRNA-3 5'-CCAGAGGCAACAGCAAUUA-3'; fibrillarin siRNA-1 5'-UGAGGGUGUCUUCAUUUGU-3'; fibrillarin siRNA-2 5'-GGACCAACAUCAUUCCUGU-3'; fibrillarin siRNA-3 5'-GGAGCAGUUGACCCUUGAG-3'; SMN siRNA-1 5'-GCAUGCUCUAAAGAAUGGU-3'; SMN siRNA-2 5'-AGACGGUUGCAUUUACCCA-3'; p53 siRNA-1 5'-CAGUCUACCUCCCGCCAUA-3'; p53 siRNA-2 5'-GAAGAAACCACUGGAUGGA-3'.

Cell fractionation- The method used to fractionate cells for the measurements of cytochrome *c* release from mitochondria and Bax oligomerization was based on Bossy-Wetzel et al. (23) with some modifications. Two to five million cells were harvested and washed twice in ice-cold phosphate-buffered saline (PBS; pH 7.4). The cells were then spun at 200 × *g* for 5 min. The cell pellet was resuspended in 600 µL of extraction buffer containing 220 mM mannitol, 250 mM sucrose, 50 mM PIPES-KOH (pH 7.4), 50 mM KCl, 5 mM EGTA, 2 mM $MgCl_2$, 1 mM dithiothreitol, and protease inhibitors (complete cocktail from Boehringer Mannheim/Roche Diagnostics, Meylan, France). After 30-min incubation on ice, cells were homogenized with a glass Dounce homogenizer and a B pestle (80 strokes) and spun for 15 min at 14,000 × *g*. Pellets were directly resuspended in a sodium dodecyl sulfate (SDS) Laemmli sample buffer and the supernatants then diluted 1:1 in 2× SDS Laemmli sample buffer before being boiled for 5 min. Analysis was performed in SDS-16.5% polyacrylamide gels. Gels were then processed for immunoblotting as described above.

Sizing chromatography- SiRNAs transfected HeLa cells were washed in PBS, harvested, and lysed in 20 mM Tris (pH 7.4), 20 mM NaCl, 5 mM $MgCl_2$, 0.1% Triton X-100, and 0.1 mM EDTA. Cell lysates were spin at 10,000 × *g* for 10 min, and the supernatant was loaded on a Sepharose CL-6B column (Sigma, St. Louis, MO). Fractions were analyzed by SDS-PAGE and immunoblotted. Molecular-mass markers used to calibrate the gel-filtration column included carbonic anhydrase (29 kDa), albumin (66 kDa), β-amylase (200 kDa), apoferritin (440 kDa), thyroglobulin (669 kDa), and Dextran Blue (>2000 kDa).

Measurement of annexin V binding and caspase activity- SiRNA-transfected cells were split and harvested by treatment with accutase (PAA Laboratories, Linz, Austria) and then washed twice with PBS and counted. Labeling of phosphatidylserine on the outer leaflet of the cell membrane following apoptotic stimuli was performed using the annexin V–FITC kit (AbCys, Paris, France) according to the manufacturer's protocol. FITC labeling of cells was analyzed by flow cytometry. Counterstaining by propidium iodide allowed the discrimination of apoptotic cells.

Caspases 3, 7, and 9 activities were measured with Caspase-Glo 3/7 or 9 assays (Promega, Madison, WI) according to the manufacturer's protocol. Twenty thousand cells per sample were used to determine caspase activity by luminometry using a Victor Wallach luminometer (EG&G Instruments, Evry, France).

Antibodies- The following antibodies were used at the indicated dilutions for the IF or WB experiments: mouse monoclonal antibodies (mAbs) anti-Bad (C-7) (1:200 for WB; Santa Cruz Biotechnology, Santa Cruz, CA); anti-Bax (1 µg/mL for WB; Millipore, Billerica, MA); anti-Bcl-2 (C-2) (1:200 for WB; Santa Cruz Biotechnology); anti-Bcl-x_L (H-5) (1:200 for WB; Santa Cruz Biotechnology); anti-caspase-3 (31A1067) (1:500 for WB; Alexis, Farmingdale, NY); anti-caspase-7 (1:500 for WB; Stressgen, Victoria, BC, Canada); anti-coilin (1:500 for IF; 1 µg/mL for WB; Sigma); anti-cytochrome *c* [7H8.2C12] (denatured) (1 µg/mL for WB; Alexis), and [6H2.B4] (native) (1:500 for IF; Alexis); anti-cytochrome oxidase (COX) subunit II [12C4] (1 µg/mL for WB; Molecular Probes, Eugene, OR), anti-fibrillarin [38F3] (1:500 for WB; Abcam,

Cambridge, UK) and [72B9] (1:500 for IF); anti-Mcl-1 (22) (1:200 for WB; Santa Cruz Biotechnology); anti-SMN (1 μg/mL for WB; BD Biosciences, San Jose, CA): rabbit mAb: anti-Bak [Y164] (1 μg/ml for WB; Abcam): rabbit polyclonal antibodies: anti-actin (1 μg/mL for WB; Sigma); anti-Bim (H-191) (1:200 for WB; Santa Cruz Biotechnology); anti-caspase-8 (12F5) (1:500 for WB; Alexis); anti-caspase-9 (1:500 for WB; Alexis); anti-γ H2AX (phospho-S139 at 1:500 for IF; Abcam); anti-PARP-1 (H-250) (1:500 for WB; Santa Cruz Biotechnology): goat polyclonal antibody: anti-Bcl-w (C-20) (1:200 for WB; Santa Cruz Biotechnology); anti-BID (C-20) (1:200 for WB; Santa Cruz Biotechnology). For IFs, the secondary antibodies used were: goat anti-rabbit and anti-mouse, coupled to Alexa Fluor 488, 555 (1:200; Molecular Probes).

RESULTS

Depletion of coilin prevents chromatin condensation after UV-C- To test coilin's involvement in cell survival after UV-C stress, HeLa cells were depleted of coilin using specific siRNAs before irradiation by UV-C and subsequent immunofluorescence analysis. We tested a range of UV-C doses from 5 to 20 J/m^2 to ascertain the optimal UV-C dose giving the best ratio of condensed chromatin 4 h post- UV-C between controls (siCtl) and coilin (siCo)-transfected cells (Table 1). At the chosen dose of 10 J/m^2, UV-C cells started to show condensation of chromatin stained by diamidino-4',6-phenylindol-2 dichlorhydrate (DAPI), a sign of late apoptosis, about 3–4 h postirradiation. To control for irradiation, we stained the cells with an antibody detecting the phosphorylation of H2A.X (S139), which increases following UV-C irradiation (17). We noticed that the percentage of cells showing condensed chromatin was much higher in controls versus coilin-depleted cells as a function of time (Figure 1A). The small amount of coilin knockdown cells showing chromatin condensation suggested a defect in apoptosis in these cells. To confirm that cells were indeed undergoing apoptosis, we performed flow cytometry (FACS) to detect phosphatidylserine (PS, labeled by annexin V) on the outer leaflet of the cell membrane of coilin-depleted cells after UV-C irradiation (Figure 1B, Q4 areas in the FACS data, reported on the graph). In accordance with the previous results, coilin depletion resulted in a significant decrease in PS exposure compared to control cells. The ratios for annexin V values between coilin-depleted versus control cells in several independent experiments were significantly different ($p < 0.001$ at T4 and T6), reaching about 30% less annexin V labeling.

Depletion of coilin prevents activation of effector caspases after UV-C- Given the implication of fibrillarin and SMN working together with coilin in recognizing aberrant centromeric chromatin, we performed additional experiments with cells depleted of either fibrillarin or SMN. Unlike SMN, fibrillarin depletion resulted in even less annexin V labeling compared to coilin 4 h post-UV-C (Figure 2A, FACS data reported on the graph). Once again, the ratios of annexin V between coilin- or fibrillarin-depleted versus control cells in several independent experiments were significantly different ($p < 0.001$). These results suggest that the absence of coilin or fibrillarin, but not SMN, could affect the susceptibility of cells to apoptosis induced by UV-C irradiation.

To avoid any misinterpretation due to side effects of the siRNAs, we performed the same experiments with two or three different siRNAs that targeted different regions of the mRNAs (see Supplementary Figure S1). We obtained similar results as long as the siRNA significantly reduced the amount of the target protein. Then to establish a definite conclusion about an apoptotic process, UV-C-treated cells depleted in each of the three proteins were analyzed by Western blotting for caspase activation and PARP-1 inactivation (Figure 2B). As expected, after UV-C stress, coilin and fibrillarin, but not SMN-depleted cells, showed a clear reduction in the activation of procaspase-3 (visualized by the appearance of p17 and p12 active subunits) and procaspase-7 (visualized by the appearance of p32 and p19 active subunits) and in the inactivation of PARP-1 (visualized by the appearance of the p85 inactive product). Unlike caspases 3 and 7, procaspase-9 activation (visualized by the appearance of the p37/35 active products) seemed unaffected by the depletion of coilin or fibrillarin.

As expected, UV-C irradiation did not activate caspase-8 (visualized by the appearance of the p18 active subunit), which is

predominantly activated by the receptor apoptotic pathway. Caspase activity in the absence of coilin, fibrillarin, or SMN was then quantified by caspase activation assays, which confirmed the decrease of caspases 3 and 7, but not caspase-9 activities in the absence of coilin ($p < 0.001$) and fibrillarin ($p < 0.001$) (Figure 2C). In HeLa cells, p53 is inactivated as a result of its proteasomal degradation induced by human papilloma virus E6 proteins. We wanted to confirm our results by generating a p53-negative context in otherwise p53-positive cells. U2OS cells were then depleted of p53 by siRNAs in addition to coilin, fibrillarin, or SMN before irradiation with UV-C. In the presence of p53, caspases 3 and 7 were not differentially activated following depletion of coilin or fibrillarin at the time we harvested the cells. Additional p53 depletion mimicked the results obtained in HeLa cells (Figure 2D). Depletion of coilin in two isogenic HCT116 (HCT116 p53+/+ and p53 -/-) cell lines differing by the knockout of the p53 gene, and in the Saos-2 (a p53-mutated) cell line, gave similar results even if p53 is active (Figure S2). Altogether, these results suggest that coilin and fibrillarin are likely implicated in the control of apoptosis following UV-C irradiation. If for fibrillarin—an essential component of the nucleolus—one can assume that its depletion might affect some essential apoptosis-induced signals associated with this nuclear domain, the defect in apoptosis in cells depleted of coilin has no obvious explanation.

Depletion of coilin prevents the intrinsic (mitochondrial) pathway of apoptosis- We next investigated which apoptotic pathway, the intrinsic (mitochondrial) or extrinsic (receptor) pathway, was affected by the depletion of coilin and fibrillarin. We also verified that the effects previously described were not UV-C-dose-dependent, and finally we used another apoptotic inducer, etoposide, to analyze whether the participation of coilin and fibrillarin in the control of apoptosis was restricted to UV-C damage. Annexin V labeling combined with Western blotting data (Figure 3A and B) showed that whatever the dose of UV-C, depletion of coilin and fibrillarin significantly reduced the apoptotic process. This was also the case following etoposide treatment, although this way of inducing apoptosis seems to confer a role on SMN that it does not have following UV-C-induced apoptosis.

Activation of the extrinsic apoptotic pathway by the TRAIL ligand, which activates apoptosis in tumor cells by binding to the TNF death-signalling receptors, was not significantly affected by the depletion of either protein. This was visible in the annexin V and especially in the Western blotting experiments. Indeed, activation of procaspase-8 (visualized by the appearance of the p18 active subunit) was clearly not affected by the depletion of any of the three proteins. Once again, data on procaspase-9 confirmed that its activation was independent of the presence of coilin and fibrillarin. These data demonstrate that coilin (and to some extent, probably also fibrillarin) is implicated in the mitochondrial pathway of apoptosis, probably through the control of a signalling pathway not uniquely restricted to UV-C stress.

Cytochrome c release from the mitochondria is prevented following UV-C stress in the absence of coilin- The defect in apoptosis in cells depleted of coilin and fibrillarin is noticeable by the lack of activation of procaspases 3 and 7. In the intrinsic pathway, the optimal activation of procaspases 3 and 7 requires, in addition to the activation of the procaspase-9, the activation of a catalytic platform made of a multiprotein complex involving cytochrome *c*, the Apaf-1 protein, and ATP, which is known as the apoptosome (24). We thus hypothesized that the lack of activation of procaspases 3 and 7 could result from a defect in apoptosome activity due to the absence of one of its major components. Because cytochrome *c* needs to be released out of the mitochondria to activate the apoptosome, we checked by immunofluorescence the translocation of cytochrome *c* in the cytoplasm in cells depleted of coilin or fibrillarin before or after UV-C (Figure 4A). Clearly, the depletion of either protein prevented the mitochondrial release of cytochrome *c* in stressed cells, which is normally marked by the increase of the cytochrome *c* signal in the nuclei. To show that this was indeed the case, we performed the same treatments, but this time analyzed cytochrome *c* release by cell fractionation to specifically detect cytochrome *c* in the cytoplasm (i.e., supernatants) versus mitochondria (i.e., pellets) (Figure 4B). Following UV-C irradiation, control cells

rapidly showed an increase in cytoplasmic cytochrome *c* that reached a plateau around 3–4 h post-UV-C. The depletion of coilin almost completely abolished the release of cytochrome *c* in the cytoplasm, whereas depletion of fibrillarin showed from the start a higher amount of cytochrome *c* in the cytoplasm, but with no increase with time postirradiation. These data suggest that the absence of coilin, and to a lesser extent fibrillarin, prevents the release of cytochrome *c* out of the mitochondria after UV-C.

Coilin depletion prevents Bax oligomerization after UV-C stress- The release of cytochrome *c* out of the mitochondria is directly dependent on the interplay between a set of proteins from the B-cell lymphoma protein-2 (BCL-2) family that act as death agonists (pro-apoptotic) or antagonists (anti-apoptotic) (25). Therefore, we wanted to be sure that the depletion of coilin would not specifically affect the level of several proteins implicated in apoptotic signalling before or after UV-C. None of the proteins we tested showed significant modification in amount, including the Bax and Bak effector proteins (Figure 5A). Such data make unlikely any effect of the depletion of coilin on a modification of the balance between pro- and anti-apoptotic proteins that would affect the apoptotic process. Among the BCL2-family of proteins, Bax and Bak are both necessary and sufficient for the permeabilization of the outer mitochondrial membrane (MOMP) and the translocation of cytochrome *c* into the cytoplasm (26). Bax is a monomer under non-apoptotic conditions, which oligomerizes following apoptotic stimuli. We thus studied whether the depletion of coilin could affect the oligomerization of Bax after UV-C stress. Cells not transfected or transfected with a control siRNA displayed a clear increase in Bax oligomerization after treatment with UV-C or staurosporin (0.2 μM), another apoptotic inducer. In the absence of coilin, Bax oligomerization greatly decreased following UV-C. Overall, these results demonstrate that the absence of coilin has a major impact on the oligomerization of Bax following UV-C stress, which consequently results in a defect of cytochrome *c* release out of the mitochondria, thus preventing the apoptotic process.

DISCUSSION

Our recent discovery of the interphase centromere damage response (iCDR) triggered after centromeric chromatin destabilization and involving three proteins of the Cajal/gem bodies, strongly suggest the existence of biological activities of coilin, fibrillarin, and SMN out of the context of the nuclear domains in which they are concentrated (14). To that extent, a very recent study described the presence of coilin at the metaphase plate of *D. melanogaster* ovarian follicle and larval neuroblasts (6). We thus hypothesized that these proteins contribute to a signalling pathway that might be related to the repair of the centromeric structure. Considering the repair of a chromatinized nuclear structure, we must take into account the possibility of an inefficient repair mechanism either due to the absence of an essential component or to the accumulation of damage that could overwhelm the repair process. Both have different implications for the fate of the cell. The first process would lead to unrepaired problems whose accumulations are potentially genetically deleterious for the cells. This will at best induce cell death, and at worst it could be a pre-step toward genetic instability and tumorigenesis. The consequences of the second scenario are generally the triggering of programmed cell death. We then wanted to study the putative implication of the proteins of the iCDR in a signalling pathway that could lead to cell death, starting with coilin.

For reasons inherent to the activity of the viral protein ICP0 that we used to first describe the iCDR, we were unable to design an easy experimental procedure to analyze a putative signalling activity of the iCDR. Indeed, ICP0 has E3 ubiquitin ligase activity and contributes to the induced degradation of any cellular protein present in the neighborhood of the viral protein. To that extent, ICP0 induces the proteasomal degradation of all the centromeric proteins we have tested so far (27,28, 2007 #327); and our unpublished data). Should any signal coming from the interaction of the iCDR proteins with a damaged centromere, if this signal depends on proteins closely associated with centromere structure, it is likely that it might have been sent for degradation due to the previous presence of ICP0 at the centromeres. Hence,

the sole expression of ICP0 is not known to trigger massive apoptosis.

The iCDR has been found to target interphase centromeres, but the centromere is nothing more than a very complex chromatin structure. Therefore, we cannot exclude the possibility that this response might only represent one aspect of a broader cellular response that would signal any unexpected modification of the chromatin, whether this chromatin is heterochromatic (associated with centromeres/pericentromeres) or euchromatic. If so, we can anticipate the involvement of the three proteins in any signalling pathway associated with aberrant and sudden modifications of the chromatin structure. We then thought that one good way (among many others) to abruptly and profoundly challenge the chromatin was to irradiate the cells with UV-C light. Indeed, UV-C mainly provokes base modifications that induce helix-distorting DNA lesions. These lesions not only change the structure of the DNA backbone, but also greatly modify the shape of the chromatin associated with the affected region (18,29). We thus decided to use this type of irradiation to create conditions that might partly mimic the chromatin destabilization that we induced with ICP0 at the centromeres to analyze whether coilin plays a role in the apoptosis signalling pathway induced by UV-C stress. In addition, coilin has been shown to be very reactive to UV-C irradiation, leaving the CBs to adopt a nucleoplasmic multi-spot pattern (13 ,16) and our unpublished data).

Our data clearly show that the absence of coilin significantly affects the progression of cells toward apoptosis. Depletion of fibrillarin has the same effect, whereas SMN does not seem to play a major role. Fibrillarin is also a major component of the nucleoli, we thus cannot rule out an indirect effect of the absence of fibrillarin on a signalling apoptotic pathway that would require stable nucleoli. Indeed, given the presence of proteins implicated in the apoptotic process such as the tumor suppressor $p14^{ARF}$ within the nucleolus, one might anticipate that the disruption of the whole nucleolus will affect the behaviour of the cell toward stress-induced apoptosis (30,31). To that extent, we observed a similar defect of UV-C-induced apoptosis in HeLa cells depleted of nucleolin, another essential component of nucleoli (data not shown). Depletion of SMN never matched the effects observed in coilin or fibrillarin knockdown cells. This was not surprising because SMN is known to have anti-apoptotic properties (32,33), and depletion of SMN on its own seems, with time, renders cells more prone to apoptosis (34). Therefore, we would expect depletion of SMN to favour the apoptotic process after a stress even more than preventing it. However, the data obtained with etoposide induction of apoptosis showed that SMN might still have a positive role in that signalling pathway.

CBs are essentially factories concentrating many types of nuclear noncoding RNAs under the form of ribonucleoproteins, and which among other activities, are involved in pre-mRNA and pre-rRNA maturation (35). Therefore, one might think that because of its structural role in the maintenance of CBs, the depletion of coilin could prevent transcription of essential genes encoding pro-apoptotic proteins due to a defect in spliceosomal U small nuclear ribonucleoproteins (snRNPs), which would indirectly affect the pre-mRNA splicing process. This is unlikely for several reasons.

First, we did not observe any changes in the amount of tested pro- and anti-apoptotic proteins in the absence of coilin before or after the UV-C stress. Second, unlike coilin, SMN is essential for the cytoplasmic maturation of the snRNPs involved in pre-mRNA maturation (36). Therefore, the depletion of SMN should prevent apoptosis even better than the absence of coilin, and this is clearly not the case. Third, the depletion of coilin by RNAi does not affect the splicing of endogenous transcripts, although it can alter the splicing of an artificial reporter construct (37). Fourth, snRNPs are highly stable and abundant in cells. The RNAi depletion of proteins directly implicated in their metabolism, such as hTGS and SMN, as well as coilin, does not dramatically affect snRNPs biogenesis (34). Fifth, the function of small Cajal body specific RNAs (scaRNAs), implicated in the maturation of both rRNAs and snRNAs, is not affected in the absence of functional coilin at least in Drosophila (38). And finally, although mouse embryonic fibroblasts (MEFs) isolated from coilin knockout mice grow more slowly than their normal counterparts, they are still viable. Splicing and transcription processes, if affected, do not seem to perturb the homeostasis of unstressed cells (7).

Although coilin-depleted HeLa cells have been shown to grow slightly more slowly than control cells, they are still viable, and above all are not affected in their cell cycle as observed by FACS analysis (34) and our data not shown). Therefore, any indirect effect of the cell cycle on the apoptotic pathway in the absence of coilin is not plausible. All these data rule out an indirect effect of the absence of coilin on the apoptotic process by either a CB-associated signalling pathway or a mechanism that would depend on the cell cycle. They rather support the idea of a CB-independent role of coilin in a signalling pathway implicated in cell death.

Our results clearly showed that the depletion of coilin prevents the UV-C-induced intrinsic pathway of apoptosis. This was shown by the lack of cytochrome *c* release from the mitochondria when coilin was absent. As expected, this break in the apoptotic process was due to the absence of at least Bax (and probably Bak) oligomerization. This lack of apoptosis in the absence of coilin and following UV-C was visualized by different apoptosis markers such as caspases 3 and 7 activation, plasma membrane phosphatidylserine signals, and chromatin condensation. Nevertheless, our data showed that caspase-9 activation was not affected after UV-C stress even in the absence of coilin. This was unexpected because caspase-9 is normally activated within a cytosolic signalling platform called the apoptosome (24). The apoptosome is not functional without cytochrome *c*. Therefore, how do we explain the activation of caspase-9 in the coilin-depleted cells after UV-C stress in the absence of cytosolic cytochrome *c*? One possible explanation could lie in the fact that in certain situations, caspase-9 can be activated solely by its dimerization (39,40). To that extent, it is noteworthy that the level of procaspase-9 in coilin-depleted cells was consistently higher than in control siRNA-transfected cells, and also greater before than after the stress. Could that account for an apoptosome-independent caspase-9 activation? Additional and specific experimental procedures are required to answer these questions.

Many stimuli activate the intrinsic pathway of apoptosis. Most of them in one way or another affect the chromatin structure by inducing DNA damage that is under the tight control of DNA repair mechanisms. Probably central to the repair process is the ataxia telangiectasia-mutated/ataxia telangiectasia-related (ATM/ATR) signalling pathway at the crossroads between two main DNA repair mechanisms: base excision repair (BER) and nucleotide excision repair (NER) (41). The ATM/ATR pathway greatly influences the repair versus death process partly through the induced phosphorylation of p53.

Among other things, in mammalian cells, UV-C activates ataxia telangiectasia-related (ATR) kinase to induce the phosphorylation of proteins such as the S139 residue of H2A.X (γH2A.X) and p53 (42,43). However, one hallmark of UV-C-induced apoptosis is that it does not require a functional p53, as shown in a recent study on the p53-independent contribution of histone acetyltransferase Tip60 in the apoptotic process (44). That p53-negative cells are able to undergo apoptosis following all sorts of stresses such as drugs, ionizing radiation, or UV light is well-known. The $p14^{ARF}$ and Tip60 proteins are probably among those controlling the p53-independent apoptotic process (30,45). Our data suggest that coilin is also implicated to a certain extent in such a process, and support the idea that parallel, more or less important signalling pathways depending on stress and cell types, do exist in the cell. These extra pathways could supply the main apoptotic pathway with additional signals to fine-tune the apoptotic process, adding multiple quality-control steps, each of which, if not satisfied provides signals that at the end will push the cell toward its fatal destiny.

REFERENCES

1. Raska, I., Andrade, L. E., Ochs, R. L., Chan, E. K., Chang, C. M., Roos, G., and Tan, E. M. (1991) *Experimental cell research* **195**, 27-37
2. Gall, J. G. (2003) *Nat Rev Mol Cell Biol* **4**, 975-980

3. Tucker, K. E., Massello, L. K., Gao, L., Barber, T. J., Hebert, M. D., Chan, E. K., and Matera, A. G. (2000) *J Struct Biol* **129**, 269-277
4. Collier, S., Pendle, A., Boudonck, K., van Rij, T., Dolan, L., and Shaw, P. (2006) *Molecular biology of the cell* **17**, 2942-2951
5. Tuma, R. S., Stolk, J. A., and Roth, M. B. (1993) *The Journal of cell biology* **122**, 767-773
6. Liu, J. L., Wu, Z., Nizami, Z., Deryusheva, S., Rajendra, T. K., Beumer, K. J., Gao, H., Matera, A. G., Carroll, D., and Gall, J. G. (2009) *Molecular biology of the cell* **20**, 1661-1670
7. Tucker, K. E., Berciano, M. T., Jacobs, E. Y., LePage, D. F., Shpargel, K. B., Rossire, J. J., Chan, E. K., Lafarga, M., Conlon, R. A., and Matera, A. G. (2001) *The Journal of cell biology* **154**, 293-307
8. Walker, M. P., Tian, L., and Matera, A. G. (2009) *PloS one* **4**, e6171
9. Deryusheva, S., and Gall, J. G. (2004) *Proceedings of the National Academy of Sciences of the United States of America* **101**, 4810-4814
10. Dundr, M., Hebert, M. D., Karpova, T. S., Stanek, D., Xu, H., Shpargel, K. B., Meier, U. T., Neugebauer, K. M., Matera, A. G., and Misteli, T. (2004) *The Journal of cell biology* **164**, 831-842
11. Platani, M., Goldberg, I., Swedlow, J. R., and Lamond, A. I. (2000) *The Journal of cell biology* **151**, 1561-1574
12. Shav-Tal, Y., Blechman, J., Darzacq, X., Montagna, C., Dye, B. T., Patton, J. G., Singer, R. H., and Zipori, D. (2005) *Molecular biology of the cell* **16**, 2395-2413
13. Cioce, M., Boulon, S., Matera, A. G., and Lamond, A. I. (2006) *The Journal of cell biology* **175**, 401-413
14. Morency, E., Sabra, M., Catez, F., Texier, P., and Lomonte, P. (2007) *The Journal of cell biology* **177**, 757-768
15. Lam, Y. W., Lyon, C. E., and Lamond, A. I. (2002) *Molecular biology of the cell* **13**, 2461-2473
16. Bongiorno-Borbone, L., De Cola, A., Barcaroli, D., Knight, R. A., Di Ilio, C., Melino, G., and De Laurenzi, V. (2009) *Oncogene*
17. Marti, T. M., Hefner, E., Feeney, L., Natale, V., and Cleaver, J. E. (2006) *Proceedings of the National Academy of Sciences of the United States of America* **103**, 9891-9896
18. Gillet, L. C., and Scharer, O. D. (2006) *Chemical reviews* **106**, 253-276
19. Gontijo, A. M., Green, C. M., and Almouzni, G. (2003) *Biochimie* **85**, 1133-1147
20. Polo, S. E., Roche, D., and Almouzni, G. (2006) *Cell* **127**, 481-493
21. Danial, N. N., and Korsmeyer, S. J. (2004) *Cell* **116**, 205-219
22. Ow, Y. P., Green, D. R., Hao, Z., and Mak, T. W. (2008) *Nat Rev Mol Cell Biol* **9**, 532-542
23. Bossy-Wetzel, E., Newmeyer, D. D., and Green, D. R. (1998) *Embo J* **17**, 37-49
24. Riedl, S. J., and Salvesen, G. S. (2007) *Nat Rev Mol Cell Biol* **8**, 405-413
25. Youle, R. J., and Strasser, A. (2008) *Nat Rev Mol Cell Biol* **9**, 47-59
26. Wei, M. C., Zong, W. X., Cheng, E. H., Lindsten, T., Panoutsakopoulou, V., Ross, A. J., Roth, K. A., MacGregor, G. R., Thompson, C. B., and Korsmeyer, S. J. (2001) *Science (New York, N.Y* **292**, 727-730
27. Everett, R. D., Earnshaw, W. C., Findlay, J., and Lomonte, P. (1999) *Embo J* **18**, 1526-1538.
28. Lomonte, P., Sullivan, K. F., and Everett, R. D. (2001) *The Journal of biological chemistry* **276**, 5829-5835
29. Green, C. M., and Almouzni, G. (2002) *EMBO reports* **3**, 28-33
30. Sherr, C. J. (2006) *Nat Rev Cancer* **6**, 663-673
31. Krieghoff-Henning, E., and Hofmann, T. G. (2008) *Biochimica et biophysica acta* **1783**, 2185-2194
32. Iwahashi, H., Eguchi, Y., Yasuhara, N., Hanafusa, T., Matsuzawa, Y., and Tsujimoto, Y. (1997) *Nature* **390**, 413-417
33. Vyas, S., Bechade, C., Riveau, B., Downward, J., and Triller, A. (2002) *Hum Mol Genet* **11**, 2751-2764
34. Lemm, I., Girard, C., Kuhn, A. N., Watkins, N. J., Schneider, M., Bordonne, R., and Luhrmann, R. (2006) *Molecular biology of the cell* **17**, 3221-3231
35. Matera, A. G., and Shpargel, K. B. (2006) *Curr Opin Cell Biol* **18**, 317-324

36. Carvalho, T., Almeida, F., Calapez, A., Lafarga, M., Berciano, M. T., and Carmo-Fonseca, M. (1999) *The Journal of cell biology* **147**, 715-728
37. Whittom, A. A., Xu, H., and Hebert, M. D. (2008) *Cell Mol Life Sci* **65**, 1256-1271
38. Deryusheva, S., and Gall, J. G. (2009) *Molecular biology of the cell*
39. Renatus, M., Stennicke, H. R., Scott, F. L., Liddington, R. C., and Salvesen, G. S. (2001) *Proceedings of the National Academy of Sciences of the United States of America* **98**, 14250-14255
40. Pop, C., Timmer, J., Sperandio, S., and Salvesen, G. S. (2006) *Molecular cell* **22**, 269-275
41. Lavin, M. F., and Kozlov, S. (2007) *Cell cycle (Georgetown, Tex* **6**, 931-942
42. Latonen, L., and Laiho, M. (2005) *Biochimica et biophysica acta* **1755**, 71-89
43. Matsuoka, S., Ballif, B. A., Smogorzewska, A., McDonald, E. R., 3rd, Hurov, K. E., Luo, J., Bakalarski, C. E., Zhao, Z., Solimini, N., Lerenthal, Y., Shiloh, Y., Gygi, S. P., and Elledge, S. J. (2007) *Science (New York, N.Y* **316**, 1160-1166
44. Kranz, D., Dohmesen, C., and Dobbelstein, M. (2008) *The Journal of cell biology* **182**, 197-213
45. Tyteca, S., Vandromme, M., Legube, G., Chevillard-Briet, M., and Trouche, D. (2006) *Embo J* **25**, 1680-1689

FOOTNOTES

We thank Bert Vogelstein (Howard Hughes Medical Institute, Baltimore, MD) for the gift of the HCT116 p53+/+ and p53–/– cells and Pierre Hainaut (IARC, Lyon, France) for the gift of the Saos-2 cells. The present work was funded by the CNRS, the Ligue Nationale Contre le Cancer (LNCC), the Association pour la Recherche sur le Cancer (ARC), and the FINOVI Foundation.

The English in this document has been checked by at least two professional editors, both native speakers of English. For a certificate, see: http://www.textcheck.com/certificate/IW3ntx

FIGURE LEGENDS

Fig. 1. Coilin depletion reduces the susceptibility of HeLa cells to UV-C-induced apoptosis.
HeLa cells were double-transfected with control siRNA (siCtrl) or siRNA against coilin (siCo) for 96 h, then irradiated with UV-C at 10 J/m^2 and harvested from 0 to 4 h post-UV-C to perform either immunofluorescence (A) or FACS analysis (B). (A) The efficiency of irradiation was controlled via staining of the phosphorylation of H2A.X on S139 (γH2A.X, red). The efficiency of the siRNAs was checked by coilin staining (green). DNA condensation was visualized by DAPI staining of the chromatin. The percentage of nuclei with condensed chromatin was determined by counting nuclei from three independent experiments (about 200 nuclei per experiment). The values are the means of three experiments. (B) Live cells were harvested and stained with annexin V–FITC and propidium iodide (PI) before proceeding to the FACS analysis. The left panel shows a representation of the cell distribution for one experiment depending on their staining status. Q4 represents cells positive only for annexin V. The right panel shows the graphic representation of the Q4 mean ± SD values for at least three independent experiments. The individual and mean ratios of siCo vs. siCtrl annexin V-positive cells are presented in the table for the different experiments. The significance of the results was calculated with the paired Student's *t*-test with respect to siCtrl samples. * $p < 0.05$; ** $p < 0.01$; *** $p < 0.001$.

Fig. 2. Coilin and fibrillarin depletion prevents effector caspase activation following UV-C stress. HeLa cells were double-transfected with control siRNA (siCtrl) or siRNA against coilin (siCo), fibrillarin (siFib), or SMN (siSMN) for 96 h and then irradiated with UV-C at 10 J/m^2 and harvested 4

h post-UV-C to perform FACS analysis (A) and Western blotting (B). (A) Live cells were harvested and stained with annexin V–FITC and propidium iodide (PI) before proceeding to FACS analysis. The left panel shows a representation of the cell distribution for one experiment depending on their staining status. Q4 represents cells positive only for annexin V. The right panel shows the graph representation of the Q4 mean ± SD values for at least three independent experiments. The individual and mean ratios of siCo, siFib, or siSMN vs. siCtrl annexin V-positive cells are presented in the table for the different experiments. (B) Fifteen micrograms (5 μg for PARP-1) of total cell extract proteins were loaded for migration in gradient acrylamide pre-cast gels before transfer onto a nylon membrane and blotting for detection of PARP-1 and caspases 3, 7, 8, and 9. The efficiency of the siRNA treatments was first assessed for coilin, fibrillarin, and SMN depletion. Detection of actin was used as a loading control. The control lane represents untreated total cell extracts. (C) HeLa or (D) U2OS cells were double-transfected with the corresponding siRNAs for 96 h and then irradiated with UV-C at 5–10 J/m^2 and harvested 2 h post-UV-C to perform assays on the activities of caspases 3, 7, and 9. The significance of the results was calculated with the paired Student's *t*-test with respect to siCtrl samples. * $p < 0.05$; ** $p < 0.01$; *** $p < 0.001$.

Fig. 3. The intrinsic pathway of apoptosis is defective in the absence of coilin. HeLa cells were double-transfected with control siRNA (siCtrl) or siRNA against coilin (siCo), fibrillarin (siFib), or SMN (siSMN) for 96 h and then irradiated with various doses of UV-C (10, 25, 50 J/m^2), or treated with etoposide (250 μM) or the TRAIL ligand (0.5 ng/mL) and harvested 4 h post-UV-C, 6 h post-etoposide, or 3 h post-TRAIL ligand to perform FACS analysis (A) and Western blotting (B). (A) Data represent the percentage of cells positive for annexin V staining (±SD) following the different treatments based on three independent experiments. (B) Fifteen micrograms (5 μg for PARP-1) of total cell extract proteins were loaded for migration in gradient acrylamide pre-cast gels before transfer onto a nylon membrane and blotting for detection of PARP-1 and caspases 3, 7, 8, and 9. The efficiency of the siRNA treatments was assessed for coilin, fibrillarin, and SMN depletion. Detection of actin was used as a loading control. The control lane represents untreated total cell extracts. The significance of the results was calculated with the paired Student's *t*-test with respect to siCtrl samples. * $p < 0.05$; ** $p < 0.01$; *** $p < 0.001$.

Fig. 4. Coilin depletion prevents the release of cytochrome *c* out of the mitochondria following UV-C stress. HeLa cells were double-transfected with control siRNA (siCtrl) or siRNA against coilin (siCo) or fibrillarin (siFib) for 96 h and then irradiated with UV-C at 10 J/m^2 and harvested to perform immunofluorescence (A) and Western blotting (B) to detect cytochrome *c*. (A) Cells were harvested 4 h post-UV-C and the efficiency of the siRNAs against coilin and fibrillarin was determined for each sample to confirm the disappearance of each protein signal below the detection threshold in >99% of the nuclei. Then the staining of cytochrome *c* was performed on samples treated (UV) or not (No UV) by UV-C. (B) Cells were harvested between 0 and 4 h post-UV-C, and processed for soluble cytosolic (supernatant) and insoluble (pellets) fraction extractions (see Materials and methods). Then 15 μg of proteins were loaded for migration in gradient acrylamide pre-cast gels before transfer on a nylon membrane and blotting for detection of cytochrome *c* (Cytoch C) and cytochrome oxidase subunit II (COX). The efficiency of the siRNAs against coilin and fibrillarin was also verified using the pellet samples. Detection of actin was used as a loading control. Control represents whole-cell extracts.

Fig. 5. The lack of coilin affects the oligomerization of Bax following UV-C stress. HeLa cells were not transfected (Control), or double-transfected with control siRNA (siCtrl) or siRNA against coilin (siCo) for 96 h and then treated and harvested to perform Western blotting. (A) Cells were irradiated with UV-C at 10 J/m^2 (UV) or not (No UV) before the detection of pro- or anti-apoptotic proteins. Fifteen micrograms of total cell extract proteins were loaded for migration in gradient acrylamide pre-cast gels before transfer onto a nylon membrane and blotting. (B) Cells were not stressed, UV-C irradiated for 4 h (UV), or treated with staurosporine (STS) for 2 h (positive control) before being processed for gel chromatography filtration. Western blotting was then performed to detect Bax monomers and oligomers. The efficiency of the siRNAs against coilin was verified. Detection of actin was used as a loading control.

Fig. S1. Test of the efficiency of several siRNAs against coilin, fibrillarin, or SMN and their capacity to affect UV-C-induced apoptosis. HeLa cells were double-transfected with control siRNA (siCtrl) or several siRNAs against coilin (siCo #1, #2, #3), fibrillarin (siFib #1, #2, #3) or SMN (siSMN #1, #2) for 96 h before other treatments. (A) Cells were harvested to perform Western blotting to determine the efficiency of the different siRNAs on protein level. Fifteen micrograms of total cell extract proteins were loaded for migration in gradient acrylamide pre-cast gels before transfer onto a nylon membrane and blotting for detection of coilin, fibrillarin, or SMN. Detection of actin was used as a loading control. (B) SiRNA-treated cells were irradiated with UV-C at 10 J/m^2 and harvested 4 h post-UV-C. Live cells were stained with annexin V–FITC and propidium iodide (PI) before proceeding to FACS analysis. Data represent the percentage of cells positive for annexin V staining. The star indicates the siRNA chosen for the following experiments with respect to their efficiency for depleting the corresponding protein beyond 80%–90% of the normal amount (as determined by densitometry scanning), and to affect the entry into apoptosis following UV-C if relevant.

Fig. S2. Coilin depletion significantly reduces the activation of effector caspases 3 and 7 in p53+/+, p53–/–, and p53 mutated cell lines. Human HCT116 #8 (p53+/+), HCT116 #2 (genetically p53–/–), and Saos-2 (p53 mutated) were double-transfected with control siRNA (siCtrl) or siRNA against coilin (siCo) for 96 h and then not further treated (No UV) or irradiated (UV) with UV-C at 5 J/m^2 (HCT116) or 2.5 J/m^2 (Saos-2) and harvested 4 h post-UV-C to perform assays for caspases 3 and 7 activity. Data represent the percentage of cells (±SD) positive for annexin V staining based on three independent experiments. The significance of the results was calculated with the paired Student's *t*-test with respect to siCtrl samples. * $p < 0.05$; ** $p < 0.01$; *** $p < 0.001$. The efficiency of the siRNA against coilin in each cell line was assessed by Western blotting (data not shown).

Table 1

Table 1: Chromatin condensation after UV stress in coilin-depleted cells

Joule /m2	SiCtrl	SiCo
5	44 %	9 %
7.5	50 %	13 %
10(1)	> 80%	24 %
15	> 80 %	36 %
17.5	> 80 %	35 %
20	> 80 %	34 %

Percentage of nuclei with condensed chromatin (4 hours post-UV)

(1) UV-C dose chosen for the study on HeLa cells

A.

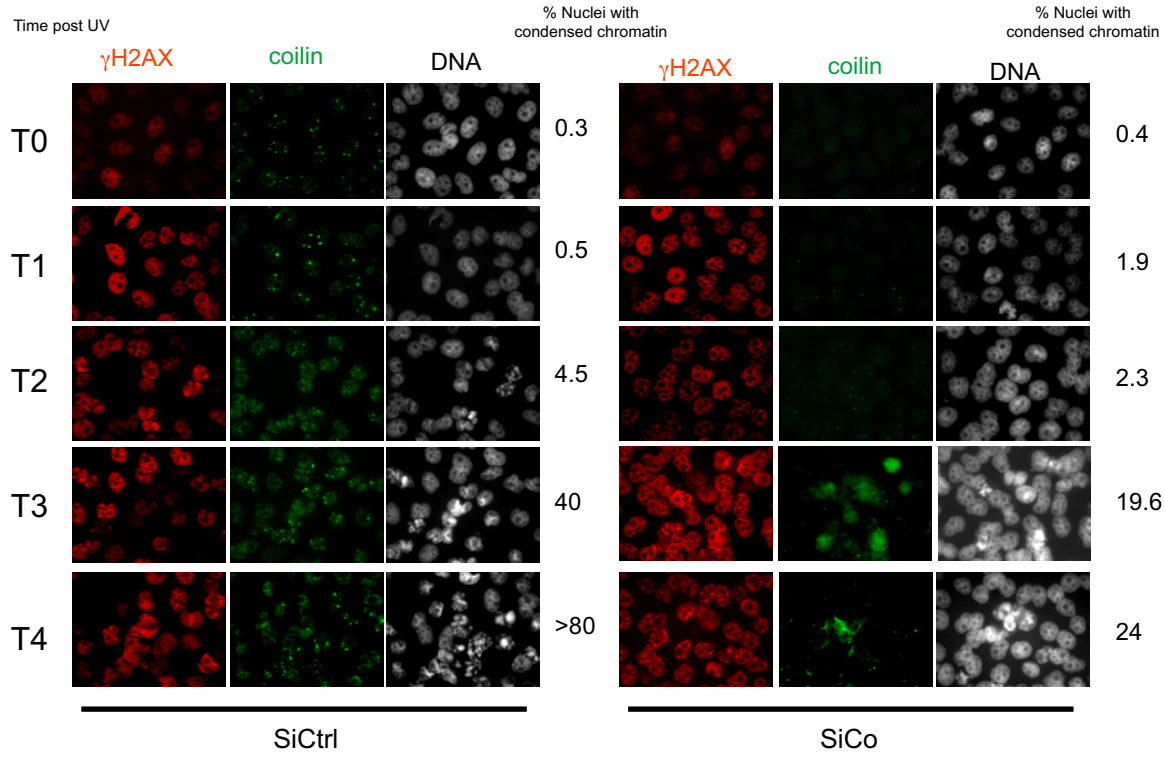

B.

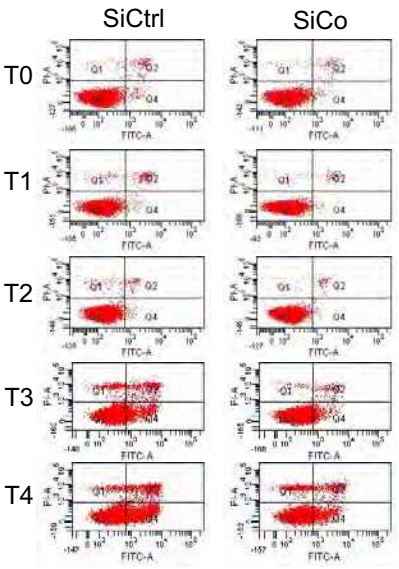

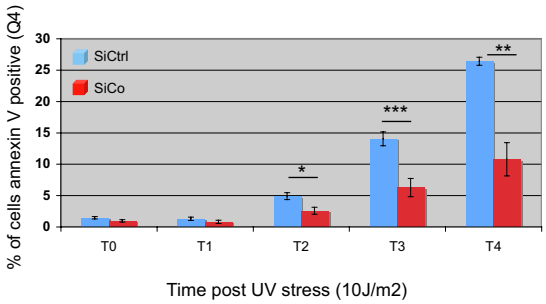

Ratios SiCo/SiCtrl for annexinV values in individual experiments

	Exp1	Exp2	Exp3	Exp4	Exp5	Mean (+/- SD)
T0	0.67	0.69	0.56	ND	ND	0.64 (+/-0.052)
T1H	0.5	0.69	0.6	ND	ND	0.6 (+/-0.066)
T2H	0.58	0.64	0.37	ND	ND	0.5 (+/-0.11)
T3H	0.44	0.51	0.37	ND	ND	0.44 (+/-0.046)
T4H	0.4	0.5	0.31	0.36	0.26	0.37 (+/-0.064)

Texier et al. FIGURE 1

A.

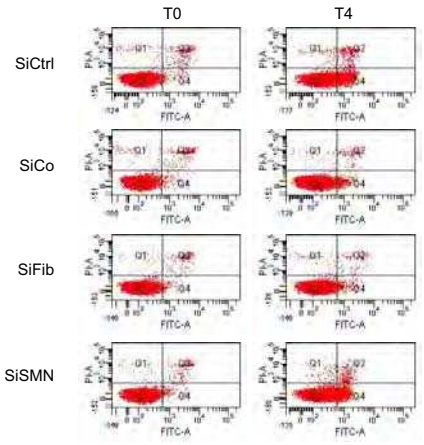

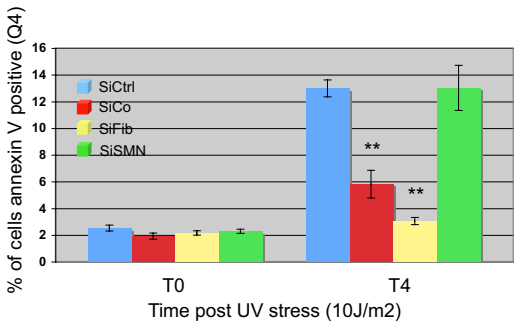

Ratios SiCo/SiCtrl, SiFib/SiCtrl, SiSMN/SiCtrl for annexinV values in individual experiments

	Experi ment 1			Experi ment 2			Experi ment 3					
	SiCo/ SiScr	SiFib/ SiScr	SiSMN/ SiScr	SiCo/ SiScr	SiFib/ SiScr	SiSMN/ SiScr	SiCo/ SiScr	SiFib/ SiScr	SiSMN/ SiScr	Mean SiCo/SiScr (+/- SD)	Mean SiFib/SiScr (+/- SD)	Mean SiSMN/Siscr (+/- SD)
T0	0.86	0.89	0,71	0.67	0.74	0.96	0.75	0.95	1.1	0.76 (+/-0.033)	0.86 (+/-0.04)	0.92 (+/-0.07)
T4	0.47	0.2	1,32	0.38	0.23	1,6	0.35	0.21	1.28	0.40 (+/-0.048)	0.21 (+/-0.01)	0.9 (+/-0.12)

B.

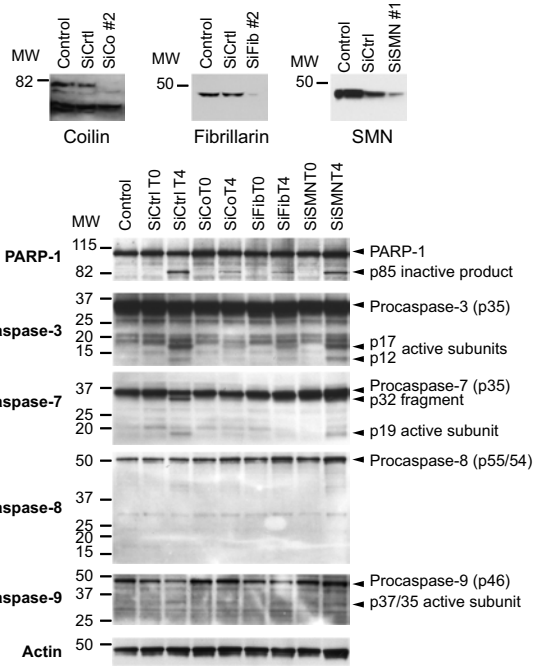

C.

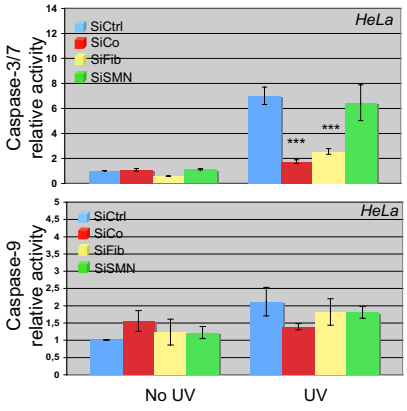

D.

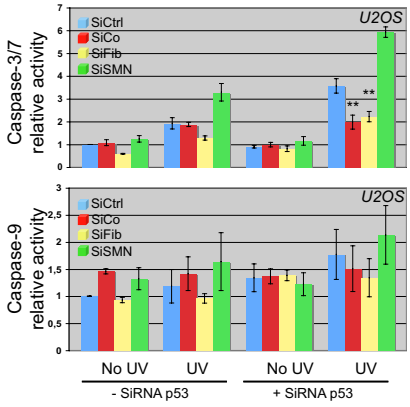

Texier et al. FIGURE 2

A.

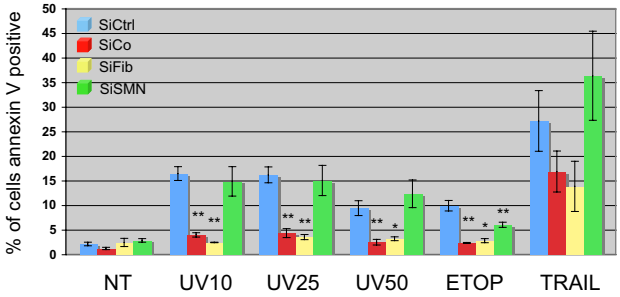

B.

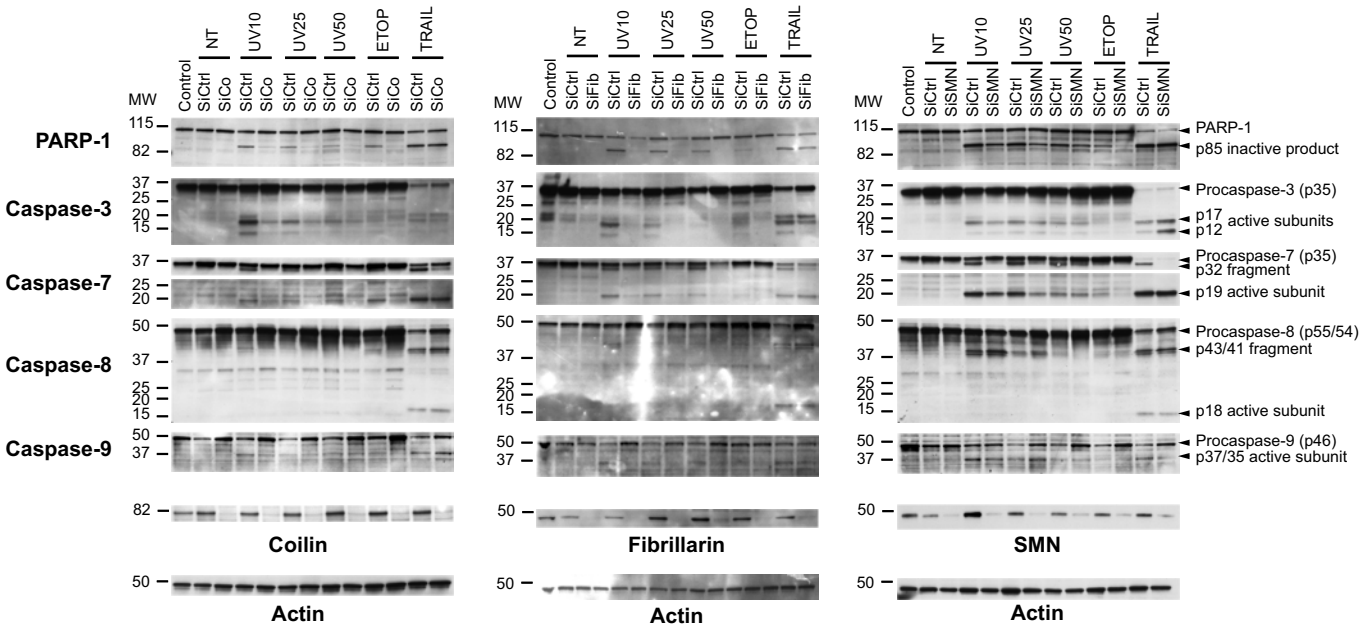

Texier et al. FIGURE 3

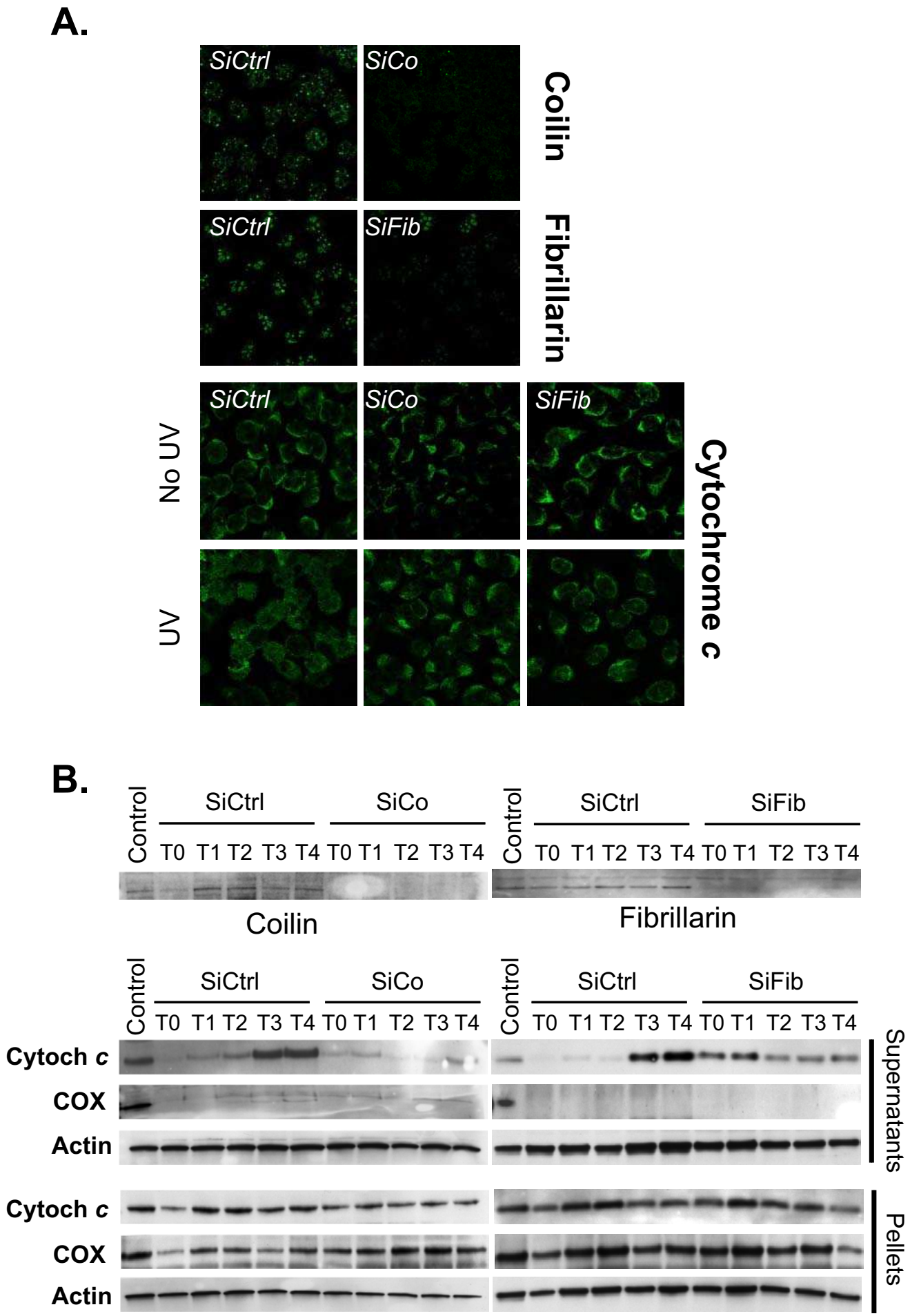

Texier et al. FIGURE 4

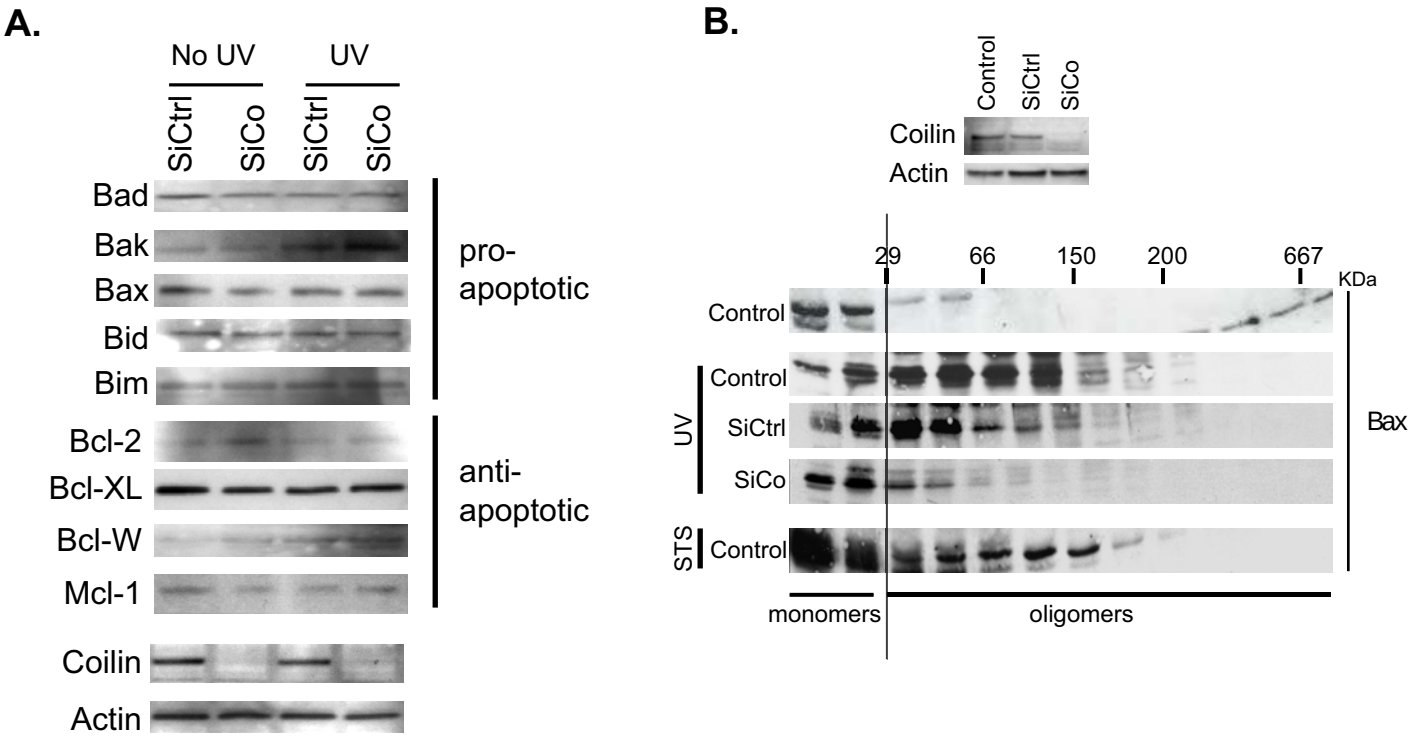

Texier et al. FIGURE 5

Supplementary figure S1

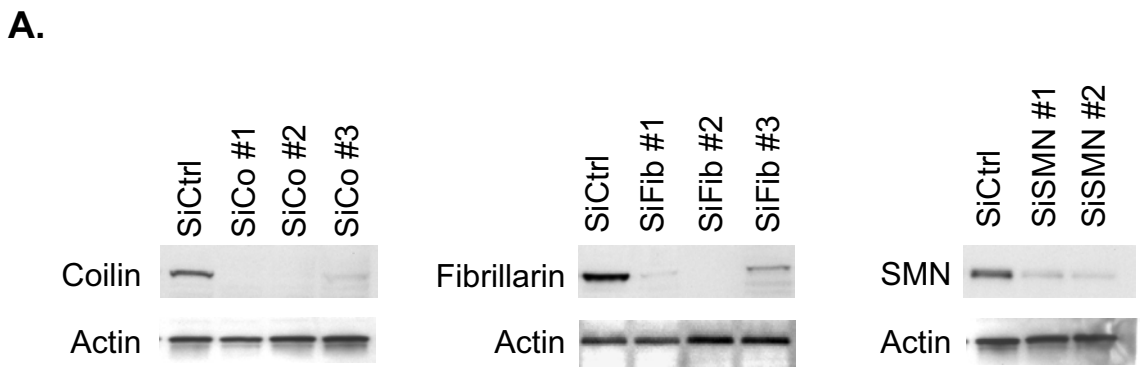

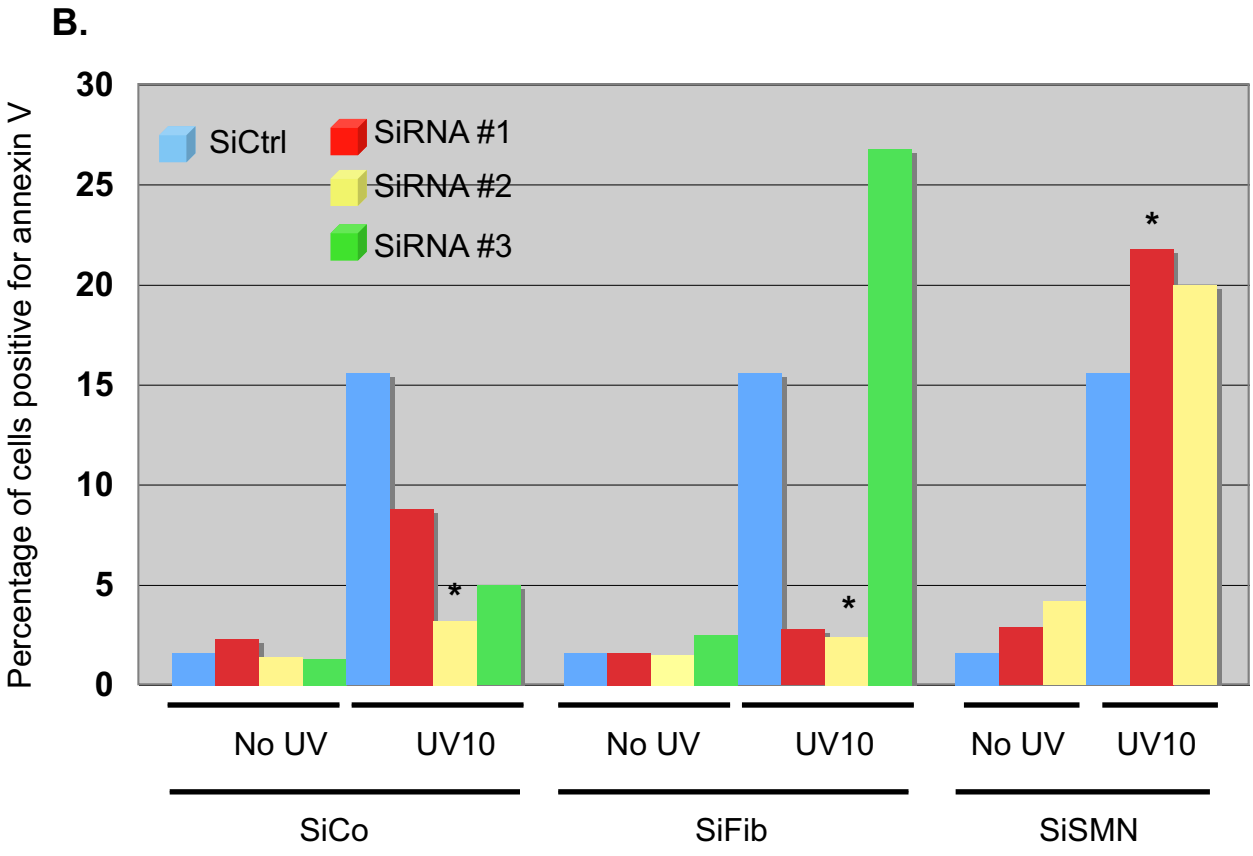

Texier et al. FIGURE S1

Supplementary figure S2

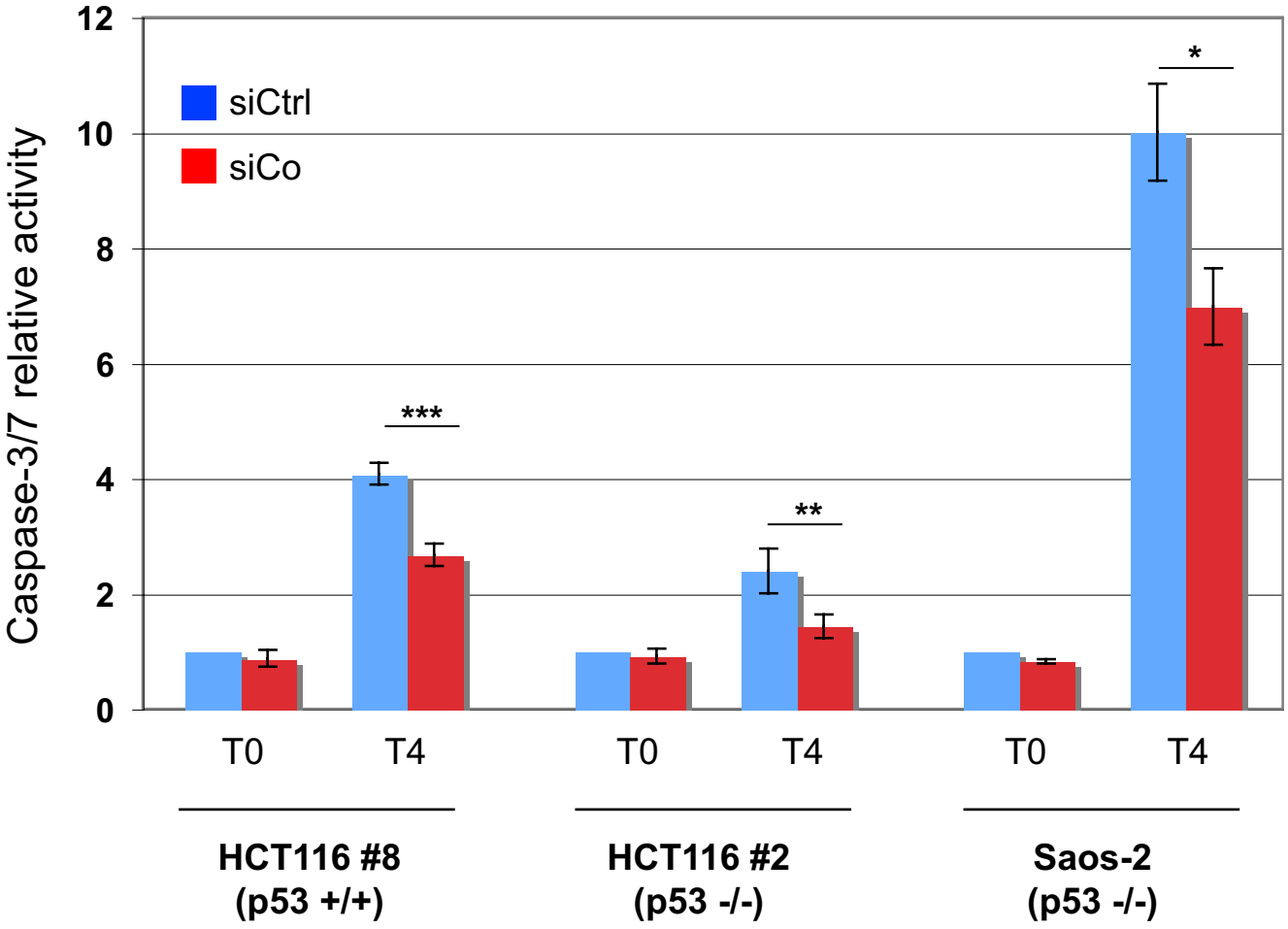

Texier et al. FIGURE S2

REFERENCES BIBLIOGRAPHIQUES

REFERENCES BIBLIOGRAPHIQUES :

Agarraberes FA, Terlecky SR, Dice JF. An intralysosomal hsp70 is required for a selective pathway of lysosomal protein degradation. J Cell Biol. 1997 May 19;137(4):825-34.

Agarraberes FA, Dice JF. A molecular chaperone complex at the lysosomal membrane is required for protein translocation. J Cell Sci. 2001 Jul;114(Pt 13):2491-9.

Aghdassi A, Phillips P, Dudeja V, Dhaulakhandi D, Sharif R, Dawra R, Lerch MM, Saluja A. Heat shock protein 70 increases tumorigenicity and inhibits apoptosis in pancreatic adenocarcinoma. Cancer Res. 2007 Jan 15;67(2):616-25.

Alford KA, Glennie S, Turrell BR, Rawlinson L, Saklatvala J, Dean JL. Heat shock protein 27 functions in inflammatory gene expression and transforming growth factor-beta-activated kinase-1 (TAK1)-mediated signaling. J Biol Chem. 2007 Mar 2;282(9):6232-41. Epub 2007 Jan 3.

Aloy MT, Hadchity E, Bionda C, Diaz-Latoud C, Claude L, Rousson R, Arrigo AP, Rodriguez-Lafrasse C. Protective role of Hsp27 protein against gamma radiation-induced apoptosis and radiosensitization effects of Hsp27 gene silencing in different human tumor cells. Int J Radiat Oncol Biol Phys. 2008 Feb 1;70(2):543-53. Epub 2007 Nov 5.

Ananthan P, Goldberg AL, Voellmy R. Abnormal proteins serve as eukaryotic stress signals and trigger the activation of heat shock genes. Science. 1986. 25;232(4749):522-4.

Arrigo AP. Heat shock proteins as molecular chaperones. Med Sci (Paris). 2005 Jun-Jul;21(6-7):619-25.

Arrigo AP, Gibert B, Simon S, Virot S, Manero F and Paul C. Dynamic processes that reflect anti-apoptotic strategies set up by HspB1. J Biol Chem. [Epub ahead of print]

Banerji U, O'Donnell A, Scurr M, Pacey S, Stapleton S, Asad Y, Simmons L, Maloney A, Raynaud F, Campbell M, Walton M, Lakhani S, Kaye S, Workman P, Judson I. Phase I pharmacokinetic and pharmacodynamic study of 17-allylamino, 17-demethoxygeldanamycin in patients with advanced malignancies. J Clin Oncol. 2005. 23(18):4152-61.

Basto R, Gergely F, Draviam VM, Ohkura H, Liley K, Raff JW. Hsp90 is required to localise cyclin B and Msps/ch-TOG to the mitotic spindle in Drosophila and humans. J Cell Sci. 2007 Apr 1;120(Pt 7):1278-87.

Bausero MA, Bharti A, Page DT, Perez KD, Eng JW, Ordonez SL, Asea EE, Jantschitsch C, Kindas-Muegge I, Ciocca D, Asea A. Silencing the hsp25 gene eliminates migration capability of the highly metastatic murine 4T1 breast adenocarcinoma cell. Tumour Biol. 2006;27(1):17-26. Epub 2005 Dec 8.

Beere HM, Wolf BB, Cain K, Mosser DD, Mahboubi A, Kuwana T, Tailor P, Morimoto RI, Cohen GM, Green DR. Heat-shock protein 70 inhibits apoptosis by preventing recruitment of procaspase-9 to the Apaf-1 apoptosome. Nature Cell Biology, 2000. 2(8):469-75.

Björkdahl C, Sjögren MJ, Zhou X, Concha H, Avila J, Winblad B, Pei JJ. Small heat shock proteins Hsp27 or alphaB-crystallin and the protein components of neurofibrillary tangles: tau and neurofilaments. J Neurosci Res. 2008 May 1;86(6):1343-52.

Bova MP, McHaourab HS, Han Y, Fung BK. Subunit exchange of small heat shock proteins. Analysis of oligomer formation of alphaA-crystallin and Hsp27 by fluorescence resonance energy transfer and site-directed truncations. J Biol Chem. 2000 Jan 14;275(2):1035-42.

Boyault C, Zhang Y, Fritah S, Caron C, Gilquin B, Kwon SH, Garrido C, Yao TP, Vourc'h C, Matthias P, Khochbin S. HDAC6 controls major cell response pathways to cytotoxic accumulation of protein aggregates. Genes Dev. 2007 Sep 1;21(17):2172-81.

Braines IC, Colas P. Peptide aptamers as guides for small-molecule drug discovery. Drug Discov Today. 2006 Apr;11(7-8):334-41.

Brough PA, Barril X, Borgognoni J, Chene P, Davies NG, Davis B, Drysdale MJ, Dymock B, Eccles SA, Garcia-Echeverria C, Fromont C, Hayes A, Hubbard RE, Jordan AM, Jensen MR, Massey A, Merrett A, Padfield A, Parsons R, Radimerski T, Raynaud FI, Robertson A, Roughley SD, Schoepfer J, Simmonite H, Sharp SY, Surgenor A, Valenti M, Walls S, Webb P, Wood M, Workman P, Wright L. Combining Hit Identification Strategies: Fragment-Based and in Silico Approaches to Orally Active 2-Aminothieno[2,3-d]pyrimidine Inhibitors of the Hsp90 Molecular Chaperone. J Med Chem. 2009 Jul 17. [Epub ahead of print]

Bruey JM, Ducasse C, Bonniaud P, Ravagan L, Susin SA, Diaz-Latoud C, Gurbuxani S, Arrigo AP, Kroemer G, Solary E, Garrido C. Hsp27 negatively regulates cell death by intercting with cytochrome c, Nature Cell Biology, 2000. 2(9):645-52.

Brunet Simioni M, De Thonel A, Hammann A, Joly AL, Bossis G, Fourmaux E, Bouchot A, Landry J, Piechaczyk M, Garrido C. Heat shock protein 27 is involved in SUMO-2/3 modification of heat shock factor 1 and thereby modulates the transcription factor activity. Oncogene. 2009 Sep 17;28(37):3332-44. Epub 2009 Jul 13.

Buccione R, Caldieri G, Ayala I. Invadopodia: specialized tumor cell structures for the focal degradation of the extracellular matrix. Cancer Metastasis Rev. 2009 Jun;28(1-2):137-49.

Bu L, Jin Y, Shi Y, Chu R, Ban A, Eiberg H, Andres L, Jiang H, Zheng G, Qian M, Cui B, Xia Y, Liu J, Hu L, Zhao G, Hayden MR, Kong X. Mutant DNA-binding domain of HSF4 is associated with autosomal dominant lamellar and Marner cataract. Nat Genet. 2002 Jul;31(3):276-8. Epub 2002 Jun 24.

Bukau B, Weissman J, Horwich A. Molecular chaperones and protein quality control. Cell. 2006 May 5;125(3):443-51.

Bunz F, Dutriaux A, Lengauer C, Waldman T, Zhou S, Brown JP, Sedivy JM, Kinzler KW, Vogelstein B. Requirement for p53 and p21 to sustain G2 arrest after DNA damage. Science. 1998 Nov 20;282(5393):1497-501.

Carra S, Sivilotti M, Chávez Zobel AT, Lambert H, Landry J. HspB8, a small heat shock protein mutated in human neuromuscular disorders, has in vivo chaperone activity in cultured cells. Hum Mol Genet. 2005 Jun 15;14(12):1659-69. Epub 2005 May 6.

Carra S, Brunsting JF, Lambert H, Landry J, Kampinga HH. HspB8 participates in protein quality control by a non-chaperone-like mechanism that requires eIF2{alpha} phosphorylation. J Biol Chem. 2009 Feb 27;284(9):5523-32. Epub 2008 Dec 29.

Carra S, Seguin SJ, Lambert H, Landry J. HspB8 chaperone activity toward poly(Q)-containing proteins depends on its association with Bag3, a stimulator of macroautophagy. J Biol Chem. 2008 Jan 18;283(3):1437-44. Epub 2007 Nov 15.

Charrette SJ, Lavoie JN, Lambert H, Landry J. Inhibition of Daxx-Mediated Apoptosis by Heat Shock Protein 27, Molecular and Cellular Biology, 2000. 20(20):7602-12.

Chauhan D, Li G, Auclair D, Hideshima T, Podar K, Mitsiades N et C, Chen LB, Munshi N, Saxena S, Anderson KC. Methoxyestradiol and bortezomib/proteasome-inhibitor overcome dexamethasone-resistance in multiple myeloma cells by modulating Heat Shock Protein-27, Apoptosis, 2004. 9(2):149-55.

Chen J, Kähne T, Röcken C, Götze T, Yu J, Sung JJ, Chen M, Hu P, Malfertheiner P, Ebert MP. Proteome analysis of gastric cancer metastasis by two-dimensional gel electrophoresis and matrix assisted laser desorption/ionization-mass spectrometry for identification of metastasis-related proteins. J Proteome Res. 2004 Sep-Oct;3(5):1009-16.

Chen T, Guo J, Han C, Yang M, Cao X. Heat shock protein 70, released from heat-stressed tumor cells, initiates antitumor immunity by inducing tumor cell chemokine production and activating dendritic cells via TLR4 pathway. J Immunol. 2009 Feb 1;182(3):1449-59.

Cerchietti LC, Lopes EC, Yang SN, Hatzi K, Bunting KL, Tsikitas LA, Mallik A, Robles AI, Walling J, Varticovski L, Shaknovich R, Bhalla KN, Chiosis G, Melnick A. A purine scaffold Hsp90 inhibitor destabilizes BCL-6 and has specific antitumor activity in BCL-6-dependent B cell lymphomas. Nat Med. 2009 Dec;15(12):1369-76. Epub 2009 Nov 22.

Ciupitu AM, Peterson M, Kono K, Charo J, Kiessling R. Immunization with heat shock protein 70 from methylchlantrene-induced sarcomas induces tumor protection correlating with in vitro T cell responses. Cancer Immunoly Immunotherapy. 2002. 51(3):163-70.

Clemons NJ, Buzzard K, Steel R, Anderson RL. Hsp72 inhibits Fas-mediated apoptosis upstream of the mitochondria in type II cells. J Biol Chem. 2005 Mar 11;280(10):9005-12. Epub 2005 Jan 4.

Colas P, Cohen B, Jessen T, Grishina I, McCoy J, Brent R. Genetic selection of peptide aptamers that recognize and inhibit cyclin-dependent kinase 2. Nature. 1996 Apr 11;380(6574):548-50.

Cornford PA, Dodson AR, Parsons KF, Desmond AD, Woolfenden A, Fordham M, Neoptolemos JP, Ke Y, Foster CS. Heat shock protein expression independently predicts clinical outcome in prostate cancer. Cancer Res. 2000 Dec 15;60(24):7099-105.

Da Rocha Dias, S. Frank Friedlo, Yvonne Light, Caroline Springer, Paul Workman and Richard Marais. Activated B-RAF Is an Hsp90 Client Protein That Is Targeted by the Anticancer Drug 17-Allylamino-17-Demethoxygeldanamycin**.** Cancer Research. 65, 10686-10691, December 1, 2005.

Dai C, Whitesell L, Rogers AB, Lindquist S. Heat shock factor 1 is a powerful multifaceted modifier of carcinogenesis. Cell. 2007 Sep 21;130(6):1005-18.

De Jong WW, Leunissen JA, Voorter CE. Evolution of the alpha-crystallin/small heat-shock protein family. Mol Biol Evol. 1993 Jan;10(1):103-26.

Di Tommaso L, Destro A, Seok JY, Balladore E, Terracciano L, Sangiovanni A, Iavarone M, Colombo M, Jang JJ, Yu E, Jin SY, Morenghi E, Park YN, Roncalli M. The application of markers (HSP70 GPC3 and GS) in liver biopsies is useful for detection of hepatocellular carcinoma. J Hepatol. 2009 Apr;50(4):746-54. Epub 2008 Dec 25.

Diaz-Latoud C, Buache E, Javouhey E, Arrigo A.-P. Substitution of the unique cysteine residue of murine Hsp25 interferes with the protective activity of this stress protein through inhibition of dimer formation. Antioxid Redox Signal, 2005. 7, 436-45.

Dix DJ, Allen JW, Collins BW, Poorman-Allen P, Mori C, Blizard DR, Brown PR, Goulding EH, Strong BD, Eddy EM. HSP70-2 is required for desynapsis of synaptonemal complexes during meiotic prophase in juvenile and adult mouse spermatocytes. Development. 1997 Nov;124(22):4595-603.

Dollins DE, Warren JJ, Immormino RM, Gewirth DT. Structures of GRP94-nucleotide complexes reveal mechanistic differences between the hsp90 chaperones. Mol Cell. 2007 Oct 12;28(1):41-56.

Dou F, Netzer WJ, Tanemura K, Li F, Hartl FU, Takashima A, Gouras GK, Greengard P, Xu H. Chaperones increase association of tau protein with microtubules. Proc Natl Acad Sci U S A. 2003 Jan 21;100(2):721-6. Epub 2003 Jan 9.

Eccles SA, Massey A, Raynaud FI, Sharp SY, Box G, Valenti M, Patterson L, de Haven Brandon A, Gowan S, Boxall F, Aherne W, Rowlands M, Hayes A, Martins V, Urban F, Boxall K, Prodromou C, Pearl L, James K, Matthews TP, Cheung KM, Kalusa A, Jones K, McDonald E, Barril X, Brough PA, Cansfield JE, Dymock B, Drysdale MJ, Finch H, Howes R, Hubbard RE, Surgenor A, Webb P, Wood M, Wright L, Workman P. NVP-AUY922: a novel heat shock protein 90 inhibitor active against xenograft tumor growth, angiogenesis, and metastasis. Cancer Res. 2008 Apr 15;68(8):2850-60.

Enari M, Hug H, Nagata S. Involvement of an ICE-like protease in Fas-mediated apoptosis. Nature. 1995 May 4;375(6526):78-81.

Esser C, Scheffner M, Hohfeld J. The chaperone-associated ubiquitin ligase CHIP is able to target p53 for proteasomal degradation, J Biol Chem. 2005.280(29):27443-8.

Evgrafov OV, **Mersiyanova I**, **Irobi J**, **Van Den Bosch L**, **Dierick I**, **Leung CL**, **Schagina O**, **Verpoorten N**, **Van Impe K**, **Fedotov V**, **Dadali E**, **Auer-Grumbach M**, **Windpassinger C**, **Wagner K**, **Mitrovic Z**, **Hilton-Jones D**, **Talbot K**, **Martin JJ**, **Vasserman N**, **Tverskaya S**, **Polyakov A**, **Liem RK**, **Gettemans J**, **Robberecht W**, **De Jonghe P**, **Timmerman V**. Mutant small heat-shock protein 27 causes axonal Charcot-Marie-Tooth disease and distal hereditary motor neuropathy. Nat Genet. 2004 Jun;36(6):602-6. Epub 2004 May 2.

Fan GC, Zhou X, Wang X, Song G, Qian J, Nicolaou P, Chen G, Ren X, Kranias EG. Heat shock protein 20 interacting with phosphorylated Akt reduces doxorubicin-triggered oxidative stress and cardiotoxicity. Circ Res. 2008 Nov 21;103(11):1270-9. Epub 2008 Oct 23**.**

Fields S, Song O. A novel genetic system to detect protein-protein interactions. Nature. 1989.340, 6230, 2456.

García-Morales P, Carrasco-García E, Ruiz-Rico P, Martínez-Mira R, Menéndez-Gutiérrez MP, Ferragut JA, Saceda M, Martínez-Lacaci I. Inhibition of Hsp90 function by ansamycins causes downregulation of cdc2 and cdc25c and G(2)/M arrest in glioblastoma cell lines. Oncogene. 2007 Nov 8;26(51):7185-93. Epub 2007 May 21.

Garrido C, Fomentin A, Bonnotte B, Favre N, Moutet M, Arrigo AP, Melhen P Solary E. Heat shock Protein 27 Enhances the Tumorigenicity of Immunogenic Rat Colon Carcinoma Cell Clones. Cancer Research. 1998. 58(23):5495-9.

Gehrmann M, Marienhagen J, Eichholtz-Wirth H, Fritz E, Ellwart J, Jäättelä M, Zilch T, Multhoff G. Dual function of membrane-bound heat shock protein 70 (Hsp70), Bag-4, and Hsp40: protection against radiation-induced effects and target structure for natural killer cells. Cell Death Differ. 2005 Jan;12(1):38-51.

Gerner C, Frohwein U, Gotzmann J, Bayer E, Gelbmann D, Bursch W, Schulte-Hermann R. The Fas-induced apoptosis analyzed by high throughput proteome analysis. J Biol Chem. 2000 Dec 15;275(50):39018-26.

Golstein P, Kroemer G. A multiplicity of cell death pathways. Symposium on apoptotic and non-apoptotic cell death pathways. EMBO Rep. 2007 Sep;8(9):829-33. Epub 2007 Jul 27.

Gong J, Zhang Y, Durfee J, Weng D, Liu C, Koido S, Song B, Apostolopoulos V, Calderwood SK. A heat shock protein 70-based vaccine with enhanced immunogenicity for clinical use. J Immunol. 2010 Jan 1;184(1):488-96. Epub 2009 Nov 30.

Graw J. Genetics of crystallins: cataract and beyond**.** Exp Eye Res. 2009 Feb;88(2):173-89. Epub 2008 Nov 1.

Guida E, Bisso A, Fenollar-Ferrer C, Napoli M, Anselmi C, Girardini JE, Carloni P, Del Sal G. Peptide aptamers targeting mutant p53 induce apoptosis in tumor cells. Cancer Res. 2008 Aug 15;68(16):6550-8.

Hagemann TL, Boelens WC, Wawrousek EF, Messing A. Suppression of GFAP toxicity by alphaB-crystallin in mouse models of Alexander disease. Hum Mol Genet. 2009 Apr 1;18(7):1190-9. Epub 2009 Jan 7.

Hahn WC, Counter CM, Lundberg AS, Beijersbergen RL, Brooks MW, Weinberg RA. Creation of human tumour cells with defined genetic elements. Nature. 1999 Jul 29;400(6743):464-8.

Hadchity E, Aloy MT, Paulin C, Armandy E, Watkin E, Rousson R, Gleave M, Chapet O, Rodriguez-Lafrasse C. Heat shock protein 27 as a new therapeutic target for radiation sensitization of head and neck squamous cell carcinoma. Mol Ther. 2009 Aug;17(8):1387-94. Epub 2009 May 12.

Hengartner MO, Horvitz HR. Activation of C. elegans cell death protein CED-9 by an amino-acid substitution in a domain conserved in Bcl-2.Nature. 1994 May 26;369(6478):318-20.

Holcik M, Sonenberg N. Translational control in stress and apoptosis. Nat Rev Mol Cell Biol. 2005 Apr;6(4):318-27.

Hostein I, Robertson D, DiStefano F, Workman P, Andrew Clarke P. Inhibition of Signal Transduction by the Inhibitor 17-Allylamino-17-demethoxygeldanamycin Results in Cytostasis and Apoptosis. Cancer Research. 2001. 61(10):4003-9.

Houlihan JL, Metzler JJ, Blum JS. HSP90alpha and HSP90beta isoforms selectively modulate MHC class II antigen presentation in B cells. J Immunol. 2009 Jun 15;182(12):7451-8.

Hu Z, Chen L, Zhang J, Li T, Tang J, Xu N, Wang X. Structure, function, property, and role in neurologic diseases and other diseases of the sHsp22. J Neurosci Res. 2007 Aug 1;85(10):2071-9.

Huang C, Cheng H, Hao S, Zhou H, Zhang X, Gao J, Sun QH, Hu H, Wang CC. Heat shock protein 70 inhibits alpha-synuclein fibril formation via interactions with diverse intermediates. J Mol Biol. 2006 Dec 1;364(3):323-36. Epub 2006 Aug 26.

Hunt C, Morimoto RI. Conserved features of eukaryotic hsp70 genes revealed by comparison with the nucleotide sequence of human hsp70. Proc Natl Acad Sci U S A. 1985 Oct;82(19):6455-9.

Hsu H, Shu HB, Pan MG, Goeddel DV. TRADD-TRAF2 and TRADD-FADD interactions define two distinct TNF receptor 1 signal transduction pathways. Cell. 1996 Jan 26;84(2):299-308.

Hut HM, Kampinga HH, Sibon OC. Hsp70 protects mitotic cells against heat-induced centrosome damage and division abnormalities. Mol Biol Cell. 2005 Aug;16(8):3776-85. Epub 2005 Jun 1.

Jäättelä M, Wissing D, Bauer PA, Li GC. Major heat shock protein hsp70 protects tumor cells from tumor necrosis factor cytotoxicity. EMBO J. 1992 Oct;11(10):3507-12.

Javid B, MacAry PA, Lehner PJ. Structure and function: heat shock proteins and adaptive immunity. J Immunol. 2007 Aug 15;179(4):2035-40.

Jin Z, El-Deiry WS. Distinct signaling pathways in TRAIL- versus tumor necrosis factor-induced apoptosis. Mol Cell Biol. 2006 Nov;26(21):8136-48. Epub 2006 Aug 28.

Kamradt MC, Lu M, Werner ME, Kwan T, Chen F, Stroheckber A, Oshita S, Wilkinson JC, Yu C, Oliver p, Duckett CS, Bchsbaum D, LoBuglio AF , Jordan v, Cryns VL. The small Heat shock Protein αB-crystallin is a novel inhibitor of TRAIL-induced apoptosis that suppresses the activation of c
aspase-3. J Biol Chem. 2005. 280(12):11059-66.

Kantorow M, Piatigorsky J. Phosphorylations of alpha A- and alpha B-crystallin. Int J Biol Macromol. 1998 May-Jun;22(3-4):307-14.

Kanelakis KC, Murphy PJ, Galigniana MD, Morishima Y, Takayama S, Reed JC, Toft DO, Pratt WB. hsp70 interacting protein Hip does not affect glucocorticoid receptor folding by the hsp90-based chaperone machinery except to oppose the effect of BAG-1. Biochemistry. 2000 Nov 21;39(46):14314-21.

Kang BH, Plescia J, Dohi T, Rosa J, Doxsey SJ, Altieri DC. Regulation of tumor cell mitochondrial homeostasis by an organelle-specific Hsp90 chaperone network. Cell. 2007 Oct 19;131(2):257-70.

Karlseder J, Wissing D, Holzer G, Orel L, Sliutz G, Auer H, Jäättelä M, Simon MM. HSP70 overexpression mediates the escape of a doxorubicin-induced G2 cell cycle arrest. Biochem Biophys Res Commun. 1996 Mar 7;220(1):153-9.

Kerr JF, Wyllie AH, Currie AR. Apoptosis: a basic biological phenomenon with wide-ranging implications in tissue kinetics. Br J Cancer. 1972 Aug;26(4):239-57.

Kijima K, Numakura C, Goto T, Takahashi T, Otagiri T, Umetsu K, Hayasaka K. Small heat shock protein 27 mutation in a Japanese patient with distal hereditary motor neuropathy. J Hum Genet. 2005;50(9):473-6. Epub 2005 Sep 10.

Kirkegaard T, Roth AG, Petersen NH, Mahalka AK, Olsen OD, Moilanen I, Zylicz A, Knudsen J, Sandhoff K, Arenz C, Kinnunen PK, Nylandsted J, Jäättelä M. Hsp70 stabilizes lysosomes and reverts Niemann-Pick disease-associated lysosomal pathology. Nature. 2010 Jan 28;463(7280):549-53.

Kim EH, Lee HJ, Lee DH, Bae S, Soh JW, Jeoung D, Kim J, Cho CK, Lee YJ, Lee YS. Inhibition of heat shock protein 27-mediated resistance to DNA damaging agents by a novel PKC delta-V5 heptapeptide. Cancer Res. 2007 Jul 1;67(13):6333-41.

King W. F, Wawrznow A, Hohfed J, Zylicz M. Co-chaperones Bag-1, Hop and Hsp40 regulate Hsc70 and Hsp90 interactions with wild-type or mutant p53, The EMBO Journal, 2001. 20(22):6297-305.

Koga F, Tsutsumi S, Neckers LM. Low dose geldanamycin inhibits hepatocyte growth factor and hypoxia-stimulated invasion of cancer cells. Cell Cycle. 2007 Jun 1;6(11):1393-402.

Kudo T, Kanemoto S, Hara H, Morimoto N, Morihara T, Kimura R, Tabira T, Imaizumi K, Takeda M. A molecular chaperone inducer protects neurons from ER stress. Cell Death Differ. 2008 Feb;15(2):364-75. Epub 2007 Nov 30.

Kwon S, Zhang Y, Matthias P. The deacetylase HDAC6 is a novel critical component of stress granules involved in the stress response. Genes Dev. 2007 Dec 15;21(24):3381-94.

Landry J, Lambert H, Zhou M, Lavoie JN, Hickey E, Weber LA, Anderson. CW.Human HSP27 is phosphorylated at serines 78 and 82 by heat shock and mitogen-activated kinases that recognize the same amino acid motif as S6 kinase II. J Biol Chem. 1992 Jan 15;267(2):794-803.

Lee-Yoon D, Easton D, Murawski M, Burd R, Subjeck JR. Identification of a major subfamily of large hsp70-like proteins through the cloning of the mammalian 110-kDa heat shock protein. J Biol Chem. 1995 Jun 30;270(26):15725-33.

Leu JI, Pimkina J, Frank A, Murphy ME, George DL. A small molecule inhibitor of inducible heat shock protein 70. Mol Cell. 2009 Oct 9;36(1):15-27.

Levine B, Kroemer G. Autophagy in the pathogenesis of disease. Cell. 2008 Jan 11;132(1):27-42.

Levinthal C. Are there pathways for protein folding? J. Chem. Phys. 1968. 65, 44-45.

Li DQ, Wang L, Fei F, Hou YF, Luo JM; Wei-Chen, Zeng R, Wu J, Lu JS, Di GH, Ou ZL, Xia QC, Shen ZZ, Shao ZM. Identification of breast cancer metastasis-associated proteins in an isogenic tumor metastasis model using two-dimensional gel electrophoresis and liquid chromatography-ion trap-mass spectrometry. Proteomics. 2006 Jun;6(11):3352-68.

Li P, Nijhawan D, Budihardjo I, Srinivasula SM, Ahmad M, Alnemri ES, Wang X. Cytochrome c and dATP-dependent formation of Apaf-1/caspase-9 complex initiates an apoptotic protease cascade. Cell. 1997 Nov 14;91(4):479-89.

Lindquist S, Craig EA. The Heat-Shock Proteins, Annual Reviews Genetics, 1988.22:631-77.

Luo X, Budihardjo I, Zou H, Slaughter C,Wang X. Bid, a Bcl2 interacting protein, mediates cytochrome c release from mitochondria in response to activation of cell surface death receptors. Cell. 1998 Aug 21;94(4):481-90.

Ma Z, Izumi H, Kanai M, Kabuyama Y, Ahn NG, Fukasawa K. Mortalin controls centrosome duplication via modulating centrosomal localization of p53. Oncogene. 2006 Aug 31;25(39):5377-90. Epub 2006 Apr 17.

Maizels ET, Peters CA, Kline M, Cutler RE Jr, Shanmugam M, Hunzicker-Dunn M. Heat-shock protein-25/27 phosphorylation by the delta isoform of protein kinase C. Biochem J. 1998 Jun 15;332 (Pt 3):703-12.

Makareeva E, Leikin S. Procollagen triple helix assembly: an unconventional chaperone-assisted folding paradigm. PLoS One. 2007 Oct 10;2(10):e1029.

Martins T, Maia AF, Steffensen S, Sunkel CE. Sgt1, a co-chaperone of Hsp90 stabilizes Polo and is required for centrosome organization. EMBO J. 2009 Feb 4;28(3):234-47. Epub 2009 Jan 8.

Massa C, Guiducci C, Arioli I, Parenza M, Colombo MP, Melani C. Enhanced efficacy of tumor cell vaccines transfected with secretable hsp70. Cancer Res. 2004 Feb 15;64(4):1502-8.

Massa C, Melani C, Colombo MP. Chaperon and Adjuvant Activity of Hsp70: Different Natural Killer Requirement for Cross-Priming of chaperoned and Bystander Antigens. Cancer Research. 2005. 65(17):7942-9.

Massey AJ, Williamson DS, Browne H, Murray JB, Dokurno P, Shaw T, Macias AT, Daniels Z, Geoffroy S, Dopson M, Lavan P, Matassova N, Francis GL, Graham CJ, Parsons R, Wang Y, Padfield A, Comer M, Drysdale MJ, Wood M. A novel, small molecule inhibitor of Hsc70/Hsp70 potentiates Hsp90 inhibitor induced apoptosis in HCT116 colon carcinoma cells. Cancer Chemother Pharmacol. [Epub ahead of print].

Matkovich SJ, Van Booven DJ, Hindes A, Kang MY, Druley TE, Vallania FL, Mitra RD, Reilly MP, Cappola TP, Dorn GW 2nd. Cardiac signaling genes exhibit unexpected sequence diversity in sporadic cardiomyopathy, revealing HSPB7 polymorphisms associated with disease.
J Clin Invest. 2010 Jan;120(1):280-9. doi: 10.1172/JCI39085. Epub 2009 Dec 14.

Matsui Y, Hadaschik BA, Fazli L, Andersen RJ, Gleave ME, So AI. Intravesical combination treatment with antisense oligonucleotides targeting heat shock protein-27 and HTI-286 as a novel strategy for high-grade bladder cancer. Mol Cancer Ther. 2009 Jul 22. [Epub ahead of print].

Mayer MP, Bukau B. Hsp70 chaperones: cellular functions and molecular mechanism. Cell Mol Life Sci. 2005 Mar;62(6):670-84.

Mehlen P, Schulze-Osthoff K, Arrigo AP. Small stress proteins as novel regulators of apoptosis. Heat shock protein 27 blocks Fas/APO-1- and staurosporine-induced cell death. J Biol Chem. 1996 Jul 12;271(28):16510-4.

Mehlen P, Preville X, Chareyron P, Briolay J, Klemenz R, Arrigo AP. Constitutive expression of human hsp27, Drosophila hsp27, or human alpha B-crystallin confers resistance to TNF- and oxidative stress-induced cytotoxicity in stably transfected murine L929 fibroblasts. J Immunol. 1995 Jan 1;154(1):363-74.

Mikolajczyk M, Nelson MA. Regulation of stability of cyclin-dependent kinase CDK11p110 and a caspase-processed form, CDK11p46, by Hsp90. Biochem J. 2004 Dec 15;384(Pt 3):461-7.

Miyata Y. Hsp90 inhibitor geldanamycin and its derivatives as novel cancer chemotherapeutic agents. Curr Pharm Des. 2005;11(9):1131-8.

Miyazaki T, Kato H, Faried A, Sohda M, Nakajima M, Fukai Y, Masuda N, Manda R, Fukuchi M, Ojima H, Tsukada K, Kuwano H. Predictors of response to chemo-radiotherapy and radiotherapy for esophageal squamous cell carcinoma. Anticancer Research. 2005. 25(6C):4439-44.

Morency E, Sabra M, Catez F, Texier P, Lomonte P. A novel cell response triggered by interphase centromere structural instability. J Cell Biol. 2007 Jun 4;177(5):757-68.

Moyano JV, Evans JR, Chen F, Lu M, Werner ME, Yehiely F, Diaz LK, Turbin D, Karaca G, Wiley E, Nielsen TO, Perou CM, Cryns VL. AlphaB-crystallin is a novel oncoprotein that predicts poor clinical outcome in breast cancer. J Clin Invest. 2006 Jan;116(1):261-70.

Muller l, Schaupp A, Walerysch D, Wegele H, Buchner J. Hsp90 Regulates the activity of Wild Type p53 under Physiological and Elevated temperatures, The journal of Biological Chemestry, 2004. 279(47):48846-54.

Murshid A, Gong J, Calderwood SK. Heat-shock proteins in cancer vaccines: agents of antigen cross-presentation. Expert Rev Vaccines. 2008 Sep;7(7):1019-30.

Nagai N, Hosokawa M, Itohara S, Adachi E, Matsushita T, Hosokawa N, Nagata K. Embryonic lethality of molecular chaperone hsp47 knockout mice is associated with defects in collagen biosynthesis. J Cell Biol. 2000 Sep 18;150(6):1499-506.

Narayan V, Eckert M, Zylicz A, Zylicz M, Ball KL. Cooperative regulation of the IRF-1 tumour suppressor protein by core components of the chaperone machinery. J Biol Chem. 2009 Jun 5. [Epub ahead of print]

Nicolaou P, Knöll R, Haghighi K, Fan GC, Dorn GW 2nd, Hasenfub G, Kranias EG. Human mutation in the anti-apoptotic heat shock protein 20 abrogates its cardioprotective effects. J Biol Chem. 2008 Nov 28;283(48):33465-71. Epub 2008 Sep 12.

Nilsen TW. Mechanisms of microRNA-mediated gene regulation in animal cells. Trends Genet. 2007 May;23(5):243-9. Epub 2007 Mar 26.

Nony P, Gaude H, Rossel M, Fournier L, Rouault JP, Billaud M. Stability of the Peutz-Jeghers syndrome kinase LKB1 requires its binding to the molecular chaperones Hsp90/Cdc37. Oncogene. 2003. 22 9165-9175.

Nylansted J, Gyrd-Hansen M, Danielewicz A, Lademann Ulrik, Hoyer-Hansen M, Weber E, Multhoff G, Rohde M, Jaattela M. Heat Schock Protein 70 Promotes Cell Survival by Inhibiting Lysosomal Membrane Permeabilization. Journal of Experimental Medicine. 2004. 200(4):425-35.

O'Callaghan-Sunol C, Gabai VL, Sherman MY. Hsp27 modulates p53 signaling and suppresses cellular senescence. Cancer Res. 2007 Dec 15;67(24):11779-88.

Oh HJ, Chen X, Subjeck JR. Hsp110 protects heat-denatured proteins and confers cellular thermoresistance. J Biol Chem. 1997 Dec 12;272(50):31636-40.

Oltersdorf T, Elmore SW, Shoemaker AR, Armstrong RC, Augeri DJ, Belli BA, Bruncko M, Deckwerth TL, Dinges J, Hajduk PJ, Joseph MK, Kitada S, Korsmeyer SJ, Kunzer AR, Letai A, Li C, Mitten MJ, Nettesheim DG, Ng S, Nimmer PM, O'Connor JM, Oleksijew A, Petros AM, Reed JC, Shen W, Tahir SK, Thompson CB, Tomaselli KJ, Wang B, Wendt MD, Zhang H, Fesik SW, Rosenberg SH. An inhibitor of Bcl-2 family proteins induces regression of solid tumours. Nature. 2005 Jun 2;435(7042):677-81. Epub 2005 May 15.

Omori E, Matsumoto K, Sanjo H, Sato S, Akira S, Smart RC, Ninomiya-Tsuji J. TAK1 is a master regulator of epidermal homeostasis involving skin inflammation and apoptosis. J Biol Chem. 2006 Jul 14;281(28):19610-7. Epub 2006 May 4.

Ostermann J, Horwich AL, Neupert W, Hartl FU. Protein folding in mitochondria requires complex formation with hsp60 and ATP hydrolysis. Nature. 1989 Sep 14;341(6238):125-30.

Pandey P, Farber R , Nakazawa A, Kuman S , Bharti A, Nolin C, Weichseilbaum R, Kufe D, Karbanda S. Hsp27 functions as a negative regulator of cytochrome c dependent activation of procaspase-3. Oncogene. 2000 Apr 13;19(16):1975-81.

Pang Q, Keeble W, Christianson TA, Faulkner GR, Bagby GC. FANCC interacts with Hsp70 to protect hematopoietic cells from IFN-gamma/TNF-alpha-mediated cytotoxicity. EMBO J. 2001 Aug 15;20(16):4478-89.

Panner A, Murray JC, Berger MS, Pieper RO. Heat shock protein 90alpha recruits FLIPS to the death-inducing signaling complex and contributes to TRAIL resistance in human glioma. Cancer Res. 2007 Oct 1;67(19):9482-9.

Parcellier A, Brunet M, Schmitt E, Col E, Didelot C, Hammann A, Nakayama K, Nakayama KI, Khochbin S, Solary E, Garrido C. HSP27 favors ubiquitination and proteasomal degradation of p27Kip1 and helps S-phase re-entry in stressed cells. FASEB J. 2006 Jun;20(8):1179-81. Epub 2006 Apr 26.

Park HS, Cho SG, Kim CK, Hwang HS, Noh KT, Kim MS, Huh SH, Kim MJ, Ryoo K, Kim EK, Kang WJ, Lee JS, Seo JS, Ko YG, Kim S, Choi EJ. Heat shock protein hsp72 is a negative regulator of apoptosis signal-regulating kinase 1. Mol Cell Biol. 2002 Nov;22(22):7721-30.

Paul C, Manero F, Gonin S, Kretz-Remy C, Virot S, Arrigo AP. Hsp27 as a Negative Regulator of Cytochrome c Release, Molecular and Cellular Biology, 2002. 19(16):4310-22.

Peyruchaud O, Winding B, Pécheur I, Serre CM, Delmas P, Clézardin P. Early detection of bone metastases in a murine model using fluorescent human breast cancer cells: application to the use of the bisphosphonate zoledronic acid in the treatment of osteolytic lesions. J Bone Miner Res. 2001 Nov;16(11):2027-34

Petesch SJ, Lis JT. Rapid, transcription-independent loss of nucleosomes over a large chromatin domain at Hsp70 loci. Cell. 2008 Jul 11;134(1):74-84.

Plescia J, Salz W, Xia F, Pennati M, Zaffaroni N, Daidone MG, Meli M, Dohi T, Fortugno P, Nefedova Y, Gabrilovich DI, Colombo G, Altieri DC. Rational design of shepherdin, a novel anticancer agent. Cancer Cell. 2005 May;7(5):457-68.

Prodromou C, Panaretou B, Chohan S, Siligardi G, O'Brien R, Ladbury JE, Roe SM, Piper PW, Pearl LH. The ATPase cycle of Hsp90 drives a molecular 'clamp' via transient dimerization of the N-terminal domains. EMBO J. 2000 Aug 15;19(16):4383-92.

Powers MV, Clarke PA, Workman P. Dual targeting of HSC70 and HSP72 inhibits HSP90 function and induces tumor-specific apoptosis. Cancer Cell. 2008 Sep 9;14(3):250-62.

Queitsch C, Sangster TA, Lindquist S. Hsp90 as a capacitor of phenotypic variation. Nature. 2002 Jun 6;417(6889):618-24. Epub 2002 May 12.

Qian SB, McDonough H, Boellmann F, Cyr DM, Patterson C. CHIP-mediated stress recovery by sequential ubiquitination of substrates and Hsp70. Nature. 2006 Mar 23;440(7083):551-5.

Rajasekaran NS, Connell P, Christians ES, Yan LJ, Taylor RP, Orosz A, Zhang XQ, Stevenson TJ, Peshock RM, Leopold JA, Barry WH, Loscalzo J, Odelberg SJ, Benjamin IJ. Human alpha B-crystallin mutation causes oxido-reductive stress and protein aggregation cardiomyopathy in mice. Cell. 2007 Aug 10;130(3):427-39.

Rane MJ, Pan Y, Singh S, Powell DW, Wu R, Cuminns T, Chen Q, McLeish KR, Klein JB. Heat shock protein 27 controls apoptosis by regulating Akt activation. J Biol Chem. 2003. 278(30):27828-35.

Ravagnan L, Gurbuxani S, Susin SA, Maisse C, Daugas E, Zamzami N, Mak T, Jäättelä M, Penninger JM, Garrido C, Kroemer G. Heat-shock protein 70 antagonizes apoptosis-inducing factor. Nat Cell Biol 2001;3:839–43.

Ribeil JA, Zermati Y, Vandekerckhove J, Cathelin S, Kersual J, Dussiot M, Coulon S, Moura IC, Zeuner A, Kirkegaard-Sørensen T, Varet B, Solary E, Garrido C, Hermine O. Hsp70 regulates erythropoiesis by preventing caspase-3-mediated cleavage of GATA-1. Nature. 2007 Jan 4;445(7123):102-5. Epub 2006 Dec 10.

Rocchi P, Beraldi E, Ettinger S, Fazli L, Vessella RL, Nelson C, Gleave M. Increased Hsp27 after androgen ablation facilitates androgen-independent progression in prostate cancer via signal transducers and activators of transcription 3-mediated suppression of apoptosis. Cancer Res. 2005 Dec 1;65(23):11083-93.

Rohde M, Daugaard M, Jensen MH, Helin K, Nylandsted J, Jäättelä M. Members of the heat-shock protein 70 family promote cancer cell growth by distinct mechanisms. Genes Dev. 2005 Mar 1;19(5):570-82.

Rutherford SL, Lindquist S. Hsp90 as a capacitor for morphological evolution. Nature. 1998 Nov 26;396(6709):336-42.

Shah YM, Basrur V, Rowan BG. Selective estrogen receptor modulator regulated proteins in endometrial cancer cells. Molecular and Cellular Endocrinology. 2004. 219(1-2):127-39.

Sato S, Fujita N, Tsuruo T. Modulation of Akt kinase by binding to HSP90. PNAS. 2000. 7(20):10832-7.

Solit DB, Basso AD, Olshen AB, Scher HI, Rosen N. Inhibition of heat shock protein 90 function down-regulated akt kinase and sensitizes tumors to Taxol. Cancer Research. 2003. 63(9):2139-44.

Schett G, Steiner CW, Gröger M, Winkler S, Graninger W, Smolen J, Xu Q, Steiner G. Activation of Fas inhibits heat-induced activation of HSF1 and up-regulation of hsp70. FASEB J. 1999 May;13(8):833-42.

Scheufler C, Brinker A, Bourenkov G, Pegoraro S, Moroder L, Bartunik H, Hartl FU, Moarefi I. Structure of TPR domain-peptide complexes: critical elements in the assembly of the Hsp70-Hsp90 multichaperone machine. Cell. 2000 Apr 14;101(2):199-210.

Shamovsky I, Ivannikov M, Kandel ES, Gershon D, Nudler E. RNA-mediated response to heat shock in mammalian cells. Nature. 2006 Mar 23;440(7083):556-60.

Shen S, Zhang P, Lovchik MA, Li Y, Tang L, Chen Z, Zeng R, Ma D, Yuan J, Yu Q. Cyclodepsipeptide toxin promotes the degradation of Hsp90 client proteins through chaperone-mediated autophagy. J Cell Biol. 2009 May 18;185(4):629-39. Epub 2009 May 11.

Shi L, Zhang Z, Fang S, Xu J, Liu J, Shen J, Fang F, Luo L, Yin Z. Heat shock protein 90 (Hsp90) regulates the stability of transforming growth factor beta-activated kinase 1 (TAK1) in interleukin-1beta-induced cell signaling. Mol Immunol. 2009 Feb;46(4):541-50. Epub 2008 Oct 31.

Shimizu S, Narita M, Tsujimoto Y. Bcl-2 family proteins regulate the release of apoptogenic cytochrome c by the mitochondrial channel VDAC. Nature. 1999 Jun 3;399(6735):483-7. Erratum in: Nature 2000 Oct 12;407(6805):767.

Shin JH, Kim SW, Lim CM, Jeong JY, Piao CS, Lee JK. AlphaB-crystallin suppresses oxidative stress-induced astrocyte apoptosis by inhibiting caspase-3 activation. Neurosci Res. 2009 Aug;64(4):355-61. Epub 2009 Apr 1.

Shorter J, Lindquist S. Hsp104, Hsp70 and Hsp40 interplay regulates formation, growth and elimination of Sup35 prions. EMBO J. 2008 Oct 22;27(20):2712-24. Epub 2008 Oct 2.

Singh BN, Rao KS, Ramakrishna T, Rangaraj N, Rao ChM. Association of alphaB-crystallin, a small heat shock protein, with actin: role in modulating actin filament dynamics in vivo. J Mol Biol. 2007 Feb 23;366(3):756-67. Epub 2006 Dec 8.

Sliutz G, Karlseder J, Tempfer C, Orel L, Holzer G, Simon MM. Drug resistance against gemcitabine and topotecan mediated by constitutive hsp70 overexpression in vitro: implication of quercetin as sensitiser in chemotherapy. Br J Cancer. 1996 Jul;74(2):172-7.

Smith JR, Clarke PA, de Billy E, Workman P. Silencing the cochaperone CDC37 destabilizes kinase clients and sensitizes cancer cells to HSP90 inhibitors. Oncogene. 2009 Jan 15;28(2):157-69. Epub 2008 Oct 20.

Snoek R, Cheng H, Margiotti K, Wafa LA, Wong CA, Wong EC, Fazli L, Nelson CC, Gleave ME, Rennie PS. In vivo knockdown of the androgen receptor results in growth inhibition and regression of well-established, castration-resistant prostate tumors. Clin Cancer Res. 2009 Jan 1;15(1):39-47.

Song S, Hanson MJ, Liu BF, Chylack LT, Liang JJ. Protein-protein interactions between lens vimentin and alphaB-crystallin using FRET acceptor photobleaching. Mol Vis. 2008 Jul 10;14:1282-7.

Srethapakdi M, Liu Franklin, Tavorath R, Rosen N. Inhibition of Hsp90 Function by Ansamycins Causes Retinoblastoma Gene Production-dependent Arrest. Cancer Research. 2000. 60(14):3940-6.

Steel R, Doherty JP, Buzzard K, Clemons N, Hawkins CJ, Anderson RL. Hsp72 inhibits apoptosis upstream of the mitochondria and not through interactions with Apaf-1. J Biol Chem. 2004. 279(49):51490-9.

Sugiyama Y, Suzuki A, Kishikawa M, Akutsu R, Hirose T, Waye MM, Tsui SK, Yoshida S, Ohno S. Muscle develops a specific form of small heat shock protein complex composed of MKBP/HSPB2 and HSPB3 during myogenic differentiation. J Biol Chem. 2000 Jan 14;275(2):1095-104.

Susin SA, Lorenzo HK, Zamzami N, Marzo I, Snow BE, Brothers GM, Mangion J, Jacotot E, Costantini P, Loeffler M, Larochette N, Goodlett DR, Aebersold R, Siderovski DP, Penninger JM, Kroemer G. Molecular characterization of mitochondrial apoptosis-inducing factor. Nature. 1999 Feb 4;397(6718):441-6.

Takayama S, Reed JC. Molecular chaperone targeting and regulation by BAG family proteins. Nat Cell Biol. 2001 Oct;3(10):E237-41.

Tanabe M, Kawazoe Y, Takeda S, Morimoto RI, Nagata K, Nakai A. Disruption of the HSF3 gene results in the severe reduction of heat shock gene expression and loss of thermotolerance. EMBO J. 1998 Mar 16;17(6):1750-8.

Tanaka Y, Fujiwara K, Tanaka H, Maehata K, Kohno I. Paclitaxel inhibits expression of heat shock protein 27 in ovarian and uterine cancer cells. Int J Gynecol Cancer. 2004 Jul-Aug;14(4):616-20.

Tang D, Khaleque, MA, Jones EL, Theriault JR, Li C, Stevenson MA, Calderwood SK. Expression of heat shock proteins and heat shock protein messenger ribonuceic in human prostate carcinoma in vitro and in tumors in vivo. Cell Stress & Chaperones. 2005. 10(1):46-58.

Taylor RP, Benjamin IJ. Small heat shock proteins: a new classification scheme in mammals. J Mol Cell Cardiol. 2005 Mar;38(3):433-44.

Tomai E, Butz K, Lohrey C, von Weizsäcker F, Zentgraf H, Hoppe-Seyler F. Peptide aptamer-mediated inhibition of target proteins by sequestration into aggresomes. J Biol Chem. 2006 Jul 28;281(30):21345-52. Epub 2006 May 22.

Tian T, Hao J, Xu A, Hao J, Luo C, Liu C, Huang L, Xiao X, He D. Determination of metastasis-associated proteins in non-small cell lung cancer by comparative proteomic analysis. Cancer Sci. 2007 Aug;98(8):1265-74. Epub 2007 May 30.

Venkatakrishnan CD, Tewari AK, Moldovan L, Cardounel AJ, Zweier JL, Kuppusamy P, Ilangovan G. Heat shock protects cardiac cells from doxorubicin-induced toxicity by activating p38 MAPK and phosphorylation of small heat shock protein 27. Am J Physiol Heart Circ Physiol. 2006 Dec;291(6):H2680-91. Epub 2006 Jun 16.

Vicart P, Caron A, Guicheney P, Li Z, Prévost MC, Faure A, Chateau D, Chapon F, Tomé F, Dupret JM, Paulin D, Fardeau M. A missense mutation in the alphaB-crystallin chaperone gene causes a desmin-related myopathy. Nat Genet. 1998 Sep;20(1):92-5.

Voorhees PM, Chen Q, Kuhn DJ, Small GW, Hunsucker SA, Strader JS, Corringham RE, Zaki MH, Nemeth JA, Orlowski RZ. Inhibition of interleukin-6 signaling with CNTO 328 enhances the activity of bortezomib in preclinical models of multiple myeloma. Clin Cancer Res. 2007 Nov 1;13(21):6469-78.

Wang X, Venable J, LaPointe P, Hutt DM, Koulov AV, Coppinger J, Gurkan C, Kellner W, Matteson J, Plutner H, Riordan JR, Kelly JW, Yates JR 3rd, Balch WE. Hsp90 cochaperone Aha1 downregulation rescues misfolding of CFTR in cystic fibrosis. Cell. 2006 Nov 17;127(4):803-15.

Welsh, W. J. and Feramisco, J.R. Purification of the major mammalian heat shock proteins. J Biol Chem. 257 (1982) 14949-59.

Westerheide SD, Anckar J, Stevens SM Jr, Sistonen L, Morimoto RI. Stress-inducible regulation of heat shock factor 1 by the deacetylase SIRT1. Science. 2009 Feb 20;323(5917):1063-6.

Whitesell L , Susan L. Lindquist. HSP90 and the Chaperoning of Cancer: Normal Chaperone Biology. Nat Rev Cancer. 2005;5(10):761-772.

Wickner S, Maurizi MR, Gottesman S. Posttranslational quality control: folding, refolding, and degrading proteins. Science. 1999 Dec 3;286(5446):1888-93.

Willison K, Lewis V, Zuckerman KS, Cordell J, Dean C, Miller K, Lyon MF, Marsh M. The t complex polypeptide 1 (TCP-1) is associated with the cytoplasmic aspect of Golgi membranes. Cell. 1989 May 19;57(4):621-32.

Wolf K, Friedl P. Mapping proteolytic cancer cell-extracellular matrix interfaces. Clin Exp Metastasis. 2009;26(4):289-98. Epub 2008 Jul 4.

Yao H, Zhang Z, Xiao Z, Chen Y, Li C, Zhang P, Li M, Liu Y, Guan Y, Yu Y, Chen Z. Identification of metastasis associated proteins in human lung squamous carcinoma using two-dimensional difference gel electrophoresis and laser capture microdissection. Lung Cancer. 2009 Jul;65(1):41-8. Epub 2008 Dec 5.

Zeng Y, Chen X, Larmonier N, Larmonier C, Li G, Sepassi M, Marron M, Andreansky S, Katsanis E. Natural killer cells play a key role in the antitumor immunity generated by chaperone-rich cell lysate vaccination. Int J Cancer. 2006 Dec 1;119(11):2624-31.

Zhang L, Nephew KP, Gallagher PJ. Regulation of death-associated protein kinase. Stabilization by HSP90 heterocomplexes. J Biol Chem. 2007 Apr 20;282(16):11795-804. Epub 2007 Feb 26.

Zhang Y, Shen X. Heat shock protein 27 protects L929 cells from cisplatin-induced apoptosis by enhancing Akt activation and abating suppression of thioredoxin reductase activity. Clin Cancer Res. 2007 May 15;13(10):2855-64.

Zhao Q, Boschelli F, Caplan AJ, Arndt KT. Identification of a Conserved Motif That Promotes Cdc37 and Cyclin D1 Binding to Cdk4. J Biol Chem. 2004. 279(13):12560-4.